412TW-TIH-19-03

DETERMINING CONVENTIONAL AIRCRAFT TAKEOFF PERFORMANCE AND ADJUSTING THE RESULTS TO A REFERENCE SET OF CONDITIONS

FRANK S. BROWN
Project Engineer

4
1
2
T
W

NOVEMBER 2020

TECHNICAL INFORMATION HANDBOOK

412TH TEST WING
EDWARDS AIR FORCE BASE, CALIFORNIA
AIR FORCE MATERIEL COMMAND
UNITED STATES AIR FORCE

This technical information handbook (412TW-TIH-19-03, *Determining Conventional Aircraft Takeoff Performance and Adjusting the Results to a Reference Set of Conditions*) was submitted under job order number 99800000 by the Commander, 412th Test Wing, Edwards AFB, California 93524-6843.

Prepared by:

Frank S. Brown

FRANK S. BROWN
Project Engineer

This report has been reviewed and is approved for publication: 14 October 2020

John Kok

JOHN KOK
Director
773rd Test Squadron

Charles D. Staley

CHARLES D. STALEY
Director
412th Test Engineering Group

REPORT DOCUMENTATION PAGE

Form Approved
OMB No. 0704-0188

1. REPORT DATE *(DD-MM-YYYY)* 09-11-2020	2. REPORT TYPE Technical Information Handbook	3. DATES COVERED *(From - Through)* N/A

4. TITLE AND SUBTITLE Determining Conventional Aircraft Takeoff Performance and Adjusting the Results to a Reference Set of Conditions	5A. CONTRACT NUMBER 012100 5B. GRANT NUMBER 5C. PROGRAM ELEMENT NUMBER
6. AUTHOR(S) Brown, Franks S., Project Engineer	5D. PROJECT NUMBER 99800000 5E. TASK NUMBER 5F. WORK UNIT NUMBER
7. PERFORMING ORGANIZATION NAME(S) AND ADDRESS(ES) 412th Test Wing Edwards AFB CA 93524-6840	8. PERFORMING ORGANIZATION REPORT NUMBER 412TW-TIH-19-03
9. SPONSORING / MONITORING AGENCY NAME(S) AND ADDRESS(ES) 773d Test Squadron 304 E Popson Ave Edwards AFB, California, 93524-6480	10. SPONSOR/MONITOR'S ACRONYM(S) 11. SPONSOR/MONITOR'S REPORT NUMBER(S)

12. DISTRIBUTION / AVAILABILITY STATEMENT

DISTRIBUTION A. Approved for public release; distribution is unlimited. 412TW-PA-20482

13. SUPPLEMENTARY NOTES

CA: 412th Test Wing Edwards AFB CA   Print this document in COLOR.

14. ABSTRACT

This handbook was prepared to document some of the history of conventional aircraft takeoff performance including test techniques, airborne and ground instrumentation, and data analysis techniques. Emphasis is placed on describing pros and cons of empirical equations used in the past to adjust test day performance to a reference set of conditions as well as the pros and cons of the currently-used modeling and simulation approach. Results from Northrop T-38C tests using the modeling and simulation approach are presented.

15. SUBJECT TERMS

takeoff performance, aircraft performance, modeling and simulation.

16. SECURITY CLASSIFICATION OF: a. REPORT	b. ABSTRACT	c. THIS PAGE	17. LIMITATION OF ABSTRACT	18. NUMBER OF PAGES	19A. NAME OF RESPONSIBLE PERSON
U	U	U	Same as Report	256	John Kok 773 TS Director 19B. TELEPHONE NUMBER (INCLUDE AREA CODE) 661-227-4243

This page was intentionally left blank.

TABLE OF CONTENTS

PURPOSE

The purpose of this handbook is four-fold:

1. Provide proof that takeoffs are not “too dynamic and variable to be analyzed.”
2. Document how to determine test day takeoff performance.
3. Describe how to create or modify aerodynamic and propulsive models to match flight test determined conventional aircraft takeoff performance.
4. Describe how to use models and simulations to adjust the test day takeoff performance results to a common set of reference conditions.

This page was intentionally left blank.

INTRODUCTION

There is a widespread belief within the flight test community that conventional aircraft takeoff performance is too complicated and is “too dynamic and variable to be analyzed.” There are numerous references stating that the majority of the problems are related to the pilot. The authors of these opinions feel that the pilot cannot fly the takeoff as requested and cannot fly the takeoffs in a repeatable manner. Takeoff performance was not important early in the history of conventional aircraft development as the grass fields were square, on the order of 5,000 feet on each side, and typical takeoff distances were less than 1,000 feet. Takeoff criteria were pass or fail.

Tests were performed in the 1920s, and documented in National Advisory Committee for Aeronautics (NACA) technical report (TR), NACA-TR-249, *A Comparison of the Take-off and Landing Characteristics of a Number of Service Airplanes* (reference 1), in various headwinds to quantify the wind effect on ground distance. It wasn’t until the mid-1940s that corrections for wind and gross weight corrections to takeoff distances were proposed. Ground-based camera systems to record the time history of the aircraft were also initially used at this time. The AFFTC Technical Note R-12, *Standardization of Take-off Performance Measurements for Airplanes* (reference 2), published in 1952, and *Standardization of Take-off Performance Measurements for Airplanes Corrigendum to AFFTC Technical Note R12* (reference 3) were used by the AFFTC and others to correct takeoff performance to a reference condition.

National Aerodynamics and Space Administration (NASA) Ames published Technical Memorandum X-62333 in 1973, *Computer Programs for Estimating Aircraft Takeoff and Landing Performance* (reference 4), introducing the NASA TakeOff and LANDing (TOLAND) software. Later, this software was adapted and modified to the AFFTC TOLAND that is now used as the preferred method for analyzing takeoff and landing performance data at the 412th Test Wing (412 TW). See appendix I for a detailed history of the changes in aircraft performance, flight test instrumentation capabilities, and postflight data analysis capabilities. The purpose of this handbook is to provide useful information to the aircraft performance analysis engineer regarding all engines operating takeoff performance testing and analysis at the 412 TW. Historical and current takeoff and analysis techniques are discussed to include:

1. Techniques to determine test day takeoff performance to include types of onboard and external instrumentation.
2. How to create or modify aerodynamic and propulsive models to match flight test determined conventional aircraft takeoff performance.
3. The use of models and simulations to adjust the test day takeoff performance results to a common set of reference conditions.
4. Proof will be provided that takeoff performance analysis can be accomplished with an acceptable degree of accuracy.

There has, in the past, been a widespread belief that conventional aircraft takeoff performance is “too dynamic and variable to be analyzed.” (See appendix H; Published Opinions about Determining Takeoff Performance.) One purpose of this handbook is to show that these opinions, while they may have been valid in the past, are not valid today.

There are many reasons to conduct flight tests for, and analysis of, takeoff performance. Here are a few justifications:

1. Determine an optimum takeoff technique (thrust or power setting, flap setting, rotation speed and rate, initial climb speed, etc.)
2. Determine test day speeds and distances.
3. Adjust test day performance to a common set of reference conditions to:
    a. Compare performance with different external stores.

   b. Compare performance with different engines, engine bleed air, power extraction, etc.
   c. Compare the takeoff performance of different aircraft.
   d. Determine guarantee compliance.
4. Provide information to build an accurate takeoff performance section in the flight manual.

TYPES OF TESTS

Flight testing to determine takeoff performance is a relatively small, but very important, part of most flight test evaluations. Much of the data used for the evaluations come from either wind tunnel testing or from other flight tests. These will not, in general, be addressed in the handbook. This handbook does not address many of the takeoff issues presented in college level textbooks. It does not address:

1. Aircraft design as it relates to optimizing takeoff performance.
2. Federal Aviation Administration (FAA) aircraft design certification requirements and flight test requirements.
3. Selection of rotation speed, liftoff speed, climbout speed, maximum takeoff gross weight (These are normally selected by the airframe manufacturer.)
4. Stall speed determination.
5. Minimum control speed determination on the ground or in the air.
6. Continued takeoff performance after an engine failure.
7. Aborted or rejected takeoff performance after engine failure.
8. Balanced field length determination.
9. Abused takeoff performance including minimum unstick speed determination.
10. Determining Pitot-static position error corrections in ground effect.
11. Landing performance.
12. Vertical takeoff and landing performance.
13. Takeoff performance using thrust vectoring.
14. Amphibian aircraft operations.
15. Contaminated runway operations.
16. Augmented takeoffs using rocket-assisted takeoff (RATO) or jet-assisted takeoff (JATO).

This handbook also does not include the derivation of the equations of motion for the takeoff and climbout of a conventional aircraft. Those derivations are widely available in college textbooks, military handbooks, and industry-published papers available in the open literature.

This handbook does address the following:

1. Determining test day takeoff performance for conventional aircraft via flight test.
2. Modeling takeoff performance.
3. Adjusting test day takeoff performance to a reference set of conditions.

When planning, conducting, and analyzing takeoff performance for an aircraft with more than one engine, consideration must be given to the aircraft performance in the event of an engine failure. This means ground minimum control speeds, airborne minimum control speeds, acceleration with a failed engine, stopping capability, initial climb with a failed engine, and other factors must be tested and analyzed in order to assure the user that the performance in the flight manual or other planning tools are accurate. This, however, is not the purpose of this document. In order to cover the basic techniques of takeoff test and analysis and to show the reader that takeoff performance can be analyzed with an acceptable degree of accuracy and repeatability, only all-engine operating takeoff performance is discussed.

MEASURING TEST DAY TAKEOFF PERFORMANCE

COMPLEXITY OF INSTRUMENTATION AND POSTFLIGHT DATA ANALYSES

It is recognized that the instrumentation and the associated postflight data analyses for aircraft takeoff determination has a wide range of complexity.

<u>Very Simple and Inexpensive:</u>

The most simple and least expensive (and least accurate) method has been used since the late 1920s. An observer positioned near the runway records the ambient air temperature, the ambient air pressure or the pressure altitude, and the wind magnitude and direction. Someone in the aircraft or on the ground records the fuel remaining and the runway number. Other observers with stopwatches record the elapsed time from brake release to mainwheel liftoff (takeoff) and to 50 feet AGL. Observers are positioned next to the runway near the predicted liftoff point spaced maybe every 100 feet from 300 feet short of the predicted liftoff point to 300 feet beyond the predicted liftoff point. After liftoff, the two observers closest to the liftoff point walk to where they think liftoff occurred. The midpoint between those two spots is assumed to be correct and is measured from a reference point. The reference point may be one of a series of traffic cones placed every 50 feet along the runway. The point on the runway above which the aircraft passed 50 feet AGL was determined with another observer looking through a grid like in a flyby tower relative to more traffic cones along the side of the runway. A photographer videotaping the takeoff normally replaces that observer and grid. A reference length in the video is based on two points on the aircraft, e.g., the tip of the propeller spinner and the tip of the vertical stabilizer. The time or video frame for the aircraft passing through 50 feet AGL is determined by the height of the landing gear above the runway compared to the known reference length.

The pilot or an observer in the aircraft records the indicated airspeed and the elapsed time for liftoff and for 50 feet AGL. The liftoff time notated by the aircrew is normally based on a change in the vibration level for small general aviation aircraft. The time for 50 feet AGL recorded in the aircrew notes is normally based on a radio call from a ground-based observer.

The two distances, brake release to takeoff (the ground roll) and takeoff to 50 feet AGL (the air phase), are typically adjusted to a reference set of conditions for:

1. Pressure altitude
2. Ambient air temperature
3. Headwind
4. Runway slope
5. Aircraft gross weight

<u>More Complex and More Expensive:</u>

The other extreme has been used by the military test organizations and by the manufacturers of higher performance (FAA Part 25)[1] aircraft since the 1980s. All of the ground observers are replaced by one person who records the ambient air temperature, the ambient air pressure or the pressure altitude, and the wind

[1] Part 25 is part of the Federal Aviation Regulations (FARs). The FARs are part of Title 14 of the Code of Federal Regulations (CFR). Part 23 contains the airworthiness standards for normal, utility, acrobatic and commuter airplanes. Part 25 contains the airworthiness standards for the transport category airplanes. (A simplified view is that aircraft heavier than 12,500 pounds are covered by Part 25 and Part 23 covers aircraft lighter than 12,500 pounds.) The FARs are maintained by the FAA within the Department of Transportation.

magnitude and direction. (This observer is frequently replaced by the airport weather data and information recorded onboard the aircraft.)

Electronic onboard data recorders record about 75 to 100 parameters for postflight data analyses. The data are typically recorded at 20 to 40 samples per second. Most of the data come from an INS or a GPS or an embedded GPS/INS (EGI), an air data computer, and instrumentation on the engine(s). Data external to the aircraft may include the hand-recorded data from the runway observer and tracking data from phototheodolites.

This much greater amount of collected data can result in the determination of time histories of aircraft position and speed, aircraft control surface positions, and aircraft pitch angles and pitch rates. The data can then be adjusted to a reference set of conditions or they can be compared to a simulation-predicted performance.

TEST DAY VARIABLES

The following is a list of variables related to a test day or test location:

1. Atmospheric parameters
   a. Pressure altitude (or ambient air pressure)
   b. Ambient air temperature
   c. Wind magnitude and direction
   d. Wind variability during takeoff
2. Runway parameters
   a. Runway slope (or runway elevation as a function of position on the runway)
   b. Rolling coefficient of friction
3. Aircraft mass properties
   a. Gross weight
   b. Longitudinal center of gravity

All of these variables can be adjusted for in the postflight data analyses except for the variable wind and the longitudinal center of gravity. Data are normally acquired with either a forward center of gravity, the worst position for performance, or at a production-representative center of gravity for the aircraft configuration being flown.

<u>Test Team Selected Variables:</u>

These variables are related to the desired aircraft configuration:

1. Aircraft mass properties
   a. Gross weight at brake release
   b. Longitudinal center of gravity at brake release
   c. Flap and slat positions
   d. Spoiler/speedbrake position
   e. External fuel tanks and pylons
   f. External stores and racks
   g. Engine power/thrust setting prior to brake release
   h. Tire inflation pressures, tread type, and bias ply or radial design

The atmospheric parameters are affected by the test site and the schedule selected by the test team. Once a test site and a test schedule are selected, the main control the test team has available is the time of day. A takeoff near sunrise will be in the cooler part of the day and should have the lowest magnitude winds for that day. The test site will also determine the test day runway and its characteristics.

The test team selected variables are primarily the aircraft configuration variables. Their selection is driven by the test objectives.

Pilot Technique Related Variables:

These are the results of pilot inputs:

1. Amount of engine thermal stabilization prior to brake release
2. Rate of throttle snap, if required, at brake release
3. Amount of aerodynamic drag created during the control checks after brake release
4. Amount of aerodynamic drag created countering a crosswind during the ground roll
5. Amount of drag produced using the mechanical brakes to counter a crosswind during the ground roll
6. Variation in takeoff trim setting (either intentional or not)
7. Aerodynamic drag caused by control deflections (primarily the elevators or the horizontal stabilizers) prior to the target rotation speed
8. Variability in rotation speed
9. Variability in rotation rate and initial climb pitch angle

It will be shown later that items 2, 8, and 9 can be corrected for in the takeoff performance standardization using modeling and simulation (M&S). The effects of the others (except number 4) can be minimized by the pilot. The effects of the crosswinds can be minimized by executing the performance takeoffs in as light of winds as possible. This can normally be done by performing the takeoffs at sunrise. Mechanical brakes should not be used during the takeoff ground roll for directional control.

For many cases with a new airframe and engine combination, there are contractor suggested but yet to be tested rotation and climbout speeds and techniques. It may be useful to vary rotation speed, pitch rate, and climb pitch angle so the military test pilot can determine what might be most operationally suitable.

SUMMARY

As has been shown, there has been a wide variation in what data are recorded for takeoff performance and in the amount of postflight data analyses. The simple technique only provides two results: the ground roll distance and the air phase distance. Neither result is adjusted for variations in pilot technique. The more complex technique provides far more data and options for more analyses, including adjusting the results for variations in the pilot technique.

Most of this handbook assumes that the reader has the required instrumentation and the data analysis tools to use the more complex approach.

This page was intentionally left blank.

CURRENT METHODS OF TEST DAY TAKEOFF DATA ANALYSIS

This section will assume that the aircraft has a modern instrumentation system with the parameters typically used at the AFFTC since the early 1960s. The aircraft is assumed to have an instrumented INS or at least access to a subset of the data via a data bus.

This section of the handbook summarizes the postflight data processing and data analyses performed in the 1980s through 2010 at the AFFTC to determine the test day aircraft takeoff performance. Although the T-38C Propulsion Modernization Program (PMP) test program is specifically used as an example throughout this section, the methods discussed are general enough to apply to most flight test programs.

Appendix F is provided to give the reader information about the Northrop T-38C aircraft. Appendix F also contains a sensitivity study for the T-38C takeoff performance. The variables addressed include:

1. Pressure altitude
2. Ambient air temperature
3. Aircraft gross weight
4. Rotation speed
5. Headwind
6. Runway slope
7. Aircraft pitch angle in a 3-point attitude
8. Rolling coefficient of friction
9. Aircraft pitch angle for climbout
10. Flap setting
11. Aerodynamic drag
12. Propulsive thrust
13. Change in ground roll distance for a 1.00 KCAS change in airspeed

The first three steps were performed the day of the flight:

1. Aircrew debriefing
    a. Receive aircrew flight cards and notes
    b. Collect aircrew comments
    c. Receive data tape or data cartridge
    d. Receive the head-up display (HUD) video tape
2. Review the HUD video and select time slices for data processing
3. Request engineering unit (EU) data from either the range squadron or the instrumentation group (The data were normally requested at 20 samples per second.)

INSTRUMENTED PARAMETERS

The following parameters are assumed to be available at least 10 to 20 samples per second with the desired instrumentation resolution, table 1.

Table 1 Instrumented Parameters[2]

Parameter	Data Source
Static air pressure or pressure altitude	Instrumented air data computer, data bus, or analog flight test instrumentation
Total air pressure or differential pressure or calibrated airspeed	
Aircraft total air temperature	
Aircraft angle of attack	
Engine total air temperature	Engine fuel controller or data bus
Fuel quantities for each tank and fuel flows	Flight test instrumentation or data bus
Inertial velocities (North, East, and down); pitch, roll, and heading angles; pitch, roll, and yaw rates	Instrumented INS or data bus
Body-mounted, body-axis, accelerations (n_x and n_z)	Flight test instrumentation
Engine parameters required to run the IFTD and the status (cycle) deck	Electronic fuel controller or data bus or flight test instrumentation
Throttle position or the fuel controller feedback position	Flight test instrumentation or electronic fuel controller or data bus
Flight controls: horizontal stabilizer position, rudder position, and wing flaps	Flight control computer or data bus or flight test instrumentation
Radar altimeter	Radar altimeter or data bus
WOW discretes for all three landing gear struts	Flight test instrumentation
Landing gear handle position	Flight test instrumentation
Wheel speeds on the main landing gear	Flight test instrumentation or antiskid system
Time	Flight test instrumentation
Brake line pressures (nice to have)	Flight test instrumentation

QUALITY CONTROL REVIEW OF THE DATA

Prior to About 1995:

When most of the data processing was done at and by the range squadron on their large mainframe computer, they kept the electronic files and the engineers were given paper copies of the selected time slice. A takeoff time slice might be created at 20 samples per second; the paper copy was normally delivered at one sample per second. The data on the paper output became the basis for the Uniform Flight Test Analysis System (UFTAS), *Performance and Flying Qualities Reference Manual* (reference 5) and *Performance and Flying Qualities UFTAS Link 13 User Guide* (reference 6) data request given to the Range Squadron. More information on the UFTAS Link 13 software may be found in a Society of Flight Test Engineers (SFTE) paper, *Fighter Aircraft Dynamic Performance* (reference 7).

Background on the history of UFTAS Link 13 may be found in several technical papers authored by James Olhausen, *The Use of a Navigation Platform for Performance Instrumentation on the YF-16 Flight Test Program, Use of a Navigation Platform for Performance Instrumentation on the YF-16, F-16 Progress in Performance Flight Testing Using an Inertial Navigation Unit* (references 8 through 10). Link 13 was jointly developed by Misters James Olhausen of General Dynamics and Wayne Olsen of the AFFTC.

[2] Abbreviations, acronyms, and symbols in all figures, tables, and plots are defined in appendix L.

The Cyber mainframe computer on Main Base was shut down on 18 December 1995. The Cyber mainframe at South Base was used for a few more years. They were replaced at most combined test forces by IBM compatible PCs.

After About 2005:

There was a gradual transition between 1995 and 2005 concerning how the engineers received their EU data. The T-38C aircraft performance engineers started receiving their EU data as electronic files starting in 2000. The T-38C aircraft performance engineers did not (generally) review the takeoff data in the EU data files. Instead, they ran the UFTAS software for the takeoff maneuver using the time slice from the aircraft HUD video. The output of the UFTAS software was reviewed either on the screen of a desktop personal computer or on a paper copy. The sample rate of the UFTAS output for the T-38C was only five samples per second because that was the refresh rate on the data bus. (A sample rate of 10 to 20 samples per second on the data bus would have been preferred.)

Overall Review of the UFTAS Output:

The first review of the UFTAS output was simply verifying that the correct time slice, (start and stop times), the correct sample rate, the correct UFTAS LINKs in the correct order, and the correct EU data file were used. The UFTAS LINKs for a takeoff are presented in table 2.

Table 2 UFTAS LINKs for a Takeoff

UFTAS LINK	Purpose
SAMPLE	Extract data from the EU files, rename the parameters, perform units conversions, and correct for biases
LINK 11	Calculate aircraft gross weight and longitudinal center of gravity and convert volumetric fuel flows to mass fuel flows
LINK 2	Apply Pitot-static position error corrections and calculate pressure altitude, calibrated airspeed, true airspeed, Mach number, dynamic pressure, ambient and total air temperatures, and aircraft angle of attack
LINK 3A	Calculate energy height, the derivative of energy height, excess thrust, and normal and longitudinal accelerations in the flightpath axis using true airspeed and pressure altitude (the energy method is also known as the airspeed/altitude method)
LINK 9	Calculate gross thrust and propulsive drag using an IFTD
LINK 13	Calculate aircraft lift and drag forces and coefficients, excess thrust, normal and longitudinal acceleration in the flightpath axis, and aircraft angle of attack using the aircraft INS data
LINK 10	Convert INS inertial velocities from North, East, and down to horizontal parallel to the runway heading, horizontal perpendicular to the runway heading, and vertical; and then integrating those velocities to obtain displacements from brake release

Prior to Brake Release.

The following corrections to the test data were based on a review of the data just prior to brake release:

1. Correct the inertial velocities.
2. Correct the body-mounted longitudinal acceleration (nx) and the body-mounted, normal acceleration (nz).
3. Adjust the start time to approximately 1 second prior to brake release.

4. Adjust the assumed fuel quantity (an UFTAS runtime input) based on the sum of all the fuel tanks at the new start time.

Aircraft Inertial Velocity Biases

Prior to brake release, the aircraft should be aligned with the runway heading and completely stopped. The aircrew then performs the aircraft unique pre-takeoff checks. The thrust setting is normally selected based in part on the aircraft brakes ability to hold the aircraft at high thrust settings. The recommended setting may be an engine speed (a fan speed or a core speed), an engine pressure ratio (EPR) or a throttle setting: military power, minimum afterburner or full afterburner (maximum power).

There should be a time period of about 10 to 20 seconds with the aircraft at a complete stop with the inertial velocities from the aircraft INS reading zero. If the recorded inertial velocities are not zero, then either: (1) the pilot did not come to a complete stop or (2) the INS has drifted after it was aligned following engine start. If the pilot did not come to a complete stop, he should have said so in the postflight debrief. If the pilot did not come to a complete stop, the velocities should still be evaluated for biases. The velocities for Edwards AFB runway 22L are equations 1, 2, and 3:

$$V_{grd} = [(V_N)^2 + (V_E)^2]^{0.5} \tag{1}$$

$$V_N = -V_{grd}\,[\sin(270 - 238.32)] \tag{2}$$

$$V_E = -V_{grd}\,[\cos(270 - 238.32)] \tag{3}$$

where:

V_{grd} = groundspeed
V_N = north component of groundspeed
V_E = east component of groundspeed
238.32 = true heading of Edward AFB runway 22L in degrees
270 = true heading (actually ground track) for an aircraft moving to the west
For the case of runway 22L at Edwards AFB, the two velocities should be related as:

$$\begin{aligned}(V_E) / (V_N) &= (\cos 31.68) / (\sin 31.68) \\ &= 1 / (\tan 31.68) \\ &= 1.620\end{aligned}$$

For the case of the aircraft not completely stopped, then either: (1) the aircraft was moving parallel to the runway centerline and (V_E / V_N) = 1.620 or (2) the aircraft was not moving parallel to the runway center with or without biases in the inertial velocities or (3) the aircraft was moving parallel to the runway centerline and one or more of its inertial velocities had biases. This is a case where engineering judgment will have to be used to solve this “problem”.

For the case where there was a time period with the aircraft at a complete stop, the three inertial velocities should be adjusted to be equal to zero for that time period.

In the 1970s and the 1980s, with mechanical INSs, the biases just prior to brake release were typically as large as ±3 to 5 feet per second. The introduction of ring laser gyro INSs in the 1980s reduced the typical biases to less than ±0.6 feet per second. The embedded GPS/ring laser gyro INS known as an EGI reduced the typical velocity biases since 2000 to less than ±0.03 feet per second.

The assumed velocity biases were removed in UFTAS subroutine sample. A residual bias of 0.03 feet per second integrated over a 33-second duration takeoff ground roll would introduce a distance error of approximately 1 foot for the test day ground roll.

Body-mounted Accelerometer Biases

The body-mounted accelerometer biases were determined using the aircraft pitch angle just prior to brake release. The body axis accelerations (actually the load factors) should be equal to the sine and the cosine of the pitch angle with the aircraft stationary prior to brake release, equations 4 and 5:

$$(n_x)_{body} = \text{sine of the aircraft pitch angle} \tag{4}$$

$$(n_z)_{body} = \text{cosine of the aircraft pitch angle} \tag{5}$$

The T-38 fuel quantity indicators for each tank were calibrated as a function of pitch angle. In order to determine an equivalent pitch angle on the takeoff roll, the body-mounted accelerometers corrected for biases were used to calculate an equivalent pitch angle. Those equivalent pitch angles were used for accurate fuel tank quantity readings during the takeoff roll. The equivalent pitch angle was approximated by the arctangent of $[(n_x)/(n_z)]$

Time for Brake Release

The time for brake release was determined by the first change in the aircraft inertial velocities relative to their (zero) values prior to brake release. For most aircraft, a change in the engine operation should have occurred at or shortly after the brake release time. The throttle should move to the takeoff setting if it is not already there and the engine should start accelerating. The time for the engine power change was normally based on either a throttle position change or on a fuel controller feedback signal. Some programs have used one of the following:

1. Increase in fan speed
2. Increase in core speed
3. Increase in fuel flow
4. Change in nozzle exit area

Total Fuel at the Start of the UFTAS Run

The UFTAS software (LINK 11) for the T-38C aircraft calculated the test day aircraft gross weight using two methods: (1) zero fuel weight plus the sum of the fuel in each tank and (2) zero fuel weight plus the sum of the fuel in each tank at the start of the time slice less the integral of the fuel used after the start of the time slice. The zero fuel weight came from the Form F created by the Weight and Balance technicians. The only change for the T-38C zero fuel weight and zero fuel weight moment was to use the actual aircrew weights versus the nominal values on the Form F. For the second method the fuel burned for the T-38C program was calculated by integrating the two mass fuel flows in UFTAS LINK 11.

Larger aircraft -- the tankers, bombers, and the transports -- have typically used one of two other methods for determining their aircraft gross weights. They have used fuel flowmeters that also integrated the fuel used. The output of the flowmeter was either (1) the fuel used or (2) the initial fuel or the initial gross weight minus the fuel used. Those test programs typically weighed their aircraft prior to engine start and after engine shutdown on every performance test flight to evaluate the differences in gross weights from the weighings relative to the differences based on the fuel flow integration.

Ground Roll (Brake Release to Rotation):

In addition to looking for wild points in the data, there are six other considerations during the ground roll prior to rotation:

1. Change in engine thrust while the engine accelerates to takeoff rated thrust
2. Air data computer starting to make Pitot-static position error corrections
3. Variations in the aircraft pitch angle prior to rotation
4. Crosstrack distance calculated by integrating the horizontal inertial velocity perpendicular to the heading selected for the runway
5. Evaluate the Pitot-static position errors in ground effect
6. Evaluate assumed wind speed and direction

Engine Thrust Increase

Engine thrust performance is degraded for engines that have not thermally stabilized because the engine internal components thermally expand at different rates. Very rarely are engines thermally stabilized prior to brake release in operational takeoffs. Modern military engines require approximately 3 minutes to thermally stabilize at maximum power (full afterburner) after operating at idle power. They require about 60 to 90 seconds to stabilize at maximum power following a throttle snap from military power (full throttle except no afterburner operation). Older engines, like the J85 in the T-38 aircraft, required 5 to 10 minutes to thermally stabilize at military power

The AFFTC evaluation of the Northrop T-38C PMP takeoff procedure was to stabilize at military power for 10 to 20 seconds prior to brake release and then snap both throttles to maximum power at brake release. The 10 to 20 seconds were used for the engine health checks and for the determination of inertial velocity biases. The NASA evaluation of their new T-38 inlet did their engine health checks at military power and then light both afterburners (minimum burner) prior to brake release. The NASA selected their procedure to minimize the effects of variabilities in the afterburner lightoff characteristics.

Previous F-15 testing had performed their pre-takeoff engine health checks at 80 to 82 percent core speed. A throttle snap from there to maximum power was made at brake release.

The installed engine thrust models used in digital takeoff simulations are normally a combination of the engine manufacturer's cycle deck and the airframe manufacturer's installation effects. The installation effects normally include:

1. Inlet total pressure recovery
2. Inlet spillage drag
3. Bleed air extraction
4. Power extraction
5. Exhaust nozzle exit drag
6. Other throttle-dependent drag forces

The engine cycle deck is almost always a steady-state simulation. Time variant thrust effects have to be modeled separately.

Historically, there has been a wide range of approaches for modeling the installed thrust of an engine in an accelerating aircraft while the engine is accelerating from one power setting to another. Some of the approaches have included:

1. Ignore the power setting at brake release and just use the takeoff rated thrust model.

2. Use the initial power setting for a short time after brake release (maybe 1 to 3 seconds) and then instantaneously switch to the takeoff rated thrust model.
3. Start with the initial power setting at brake release and then linearly increase the thrust to the takeoff thrust level over a relatively short period of time (maybe 3 to 10 seconds).
4. Start with the initial power setting at brake release and then increase the thrust non-linearly to the takeoff thrust level.

The differences between the first and the fourth option are relatively small when looking at a distance from brake release as a function of airspeed. However, the differences can be significant for the speeds and distances at a given elapsed time after brake release. The selection of how complex to make the thrust model should be based on the required accuracy of the simulation. In most cases, the fourth option is not difficult to create with sufficient accuracy for most applications.

The installed thrust stand at Edwards AFB (Pad 18) can be used to spot check the steady-state, installed thrust model (the status deck) at ground level, static conditions. Information on the AFFTC installed thrust stand may be found in AFFTC-TIH-76-05, *AFFTC Aircraft Horizontal Thrust Stand Evaluation and Operation Update* (reference 11). This spot check will lead to one of several outcomes:

1. The thrust model adequately predicts the ground-level, static, measured thrust on the thrust stand.
2. The thrust model output can be multiplied by a constant to adequately match the measured thrust.
3. The engine manufacturer's uninstalled thrust model or the airframe manufacturer's installation effects model or both need to be improved.
4. A decision to create a thrust model from flight test data is made (assumed aerodynamic drag and excess thrust plus the thrust stand results).

Obviously, the first outcome is the preferred one. The second potential outcome is more typical. The third potential outcome will result in one of several programmatic decisions:

1. Fund a development effort by both contractors and delay/cancel the flight test program.
2. Change the flight test program test objective to collecting data to support the contractor model development.
3. Select option four (above) as the solution.

Using the thermodynamic-based cycle deck is the preferred option for several reasons:

1. It should model the effects of pressure altitude (ambient air pressure), airspeed (ambient and total air pressures), Mach number (shock waves), ambient and total air temperatures, and engine operation and operating schedules and limits correctly.
2. Developing a flight test derived engine model is very expensive and time consuming.
3. An empirical model is usually only valid over the range of the variables that it was developed from.

An expansion of the third reason (above) was made using the T-38C propulsion modernization program (PMP), 2001 to 2010, as an example:

1. Installed thrust stand runs were made at Edwards AFB with ambient air temperatures between approximately 25 and 110 degrees F.
2. Takeoffs were performed at four different bases to get a range of pressure altitudes: (1) Edwards AFB (2,000 to 2,500 feet pressure altitude), (2) Naval Air Station (NAS) Lemoore (approximately sea level), (3) Marine Corps Air Station (MCAS) Yuma (approximately sea level), and Holloman AFB (approximately 4,000 feet pressure altitude).
3. Takeoffs were performed over a wide range of ambient air temperatures ranging from approximately 30 degrees F at Edwards AFB to approximately 120 degrees F at MCAS Yuma.

4. Maximum power, level accelerations were flown between 5,000 and 40,000 feet pressure altitude from approximately 200 KCAS to 0.95 to 0.99 Mach number.
5. Sawtooth climbs were flown between 8,000 and 11,000 feet pressure altitude between 145 and 230 KCAS with either both engines at maximum power or with one at maximum power and the other at idle power or shutdown and windmilling.

These tests were adequate to develop an installed takeoff thrust and fuel flow model valid over the range:

1. Sea level to 8,000 feet pressure altitude
2. 0 and 50 degrees C, 32 and 122 degrees F
3. 0 to 240 KCAS

This approach worked for the J85 engine installed in the T-38C aircraft because the J85 was a relatively simple 1950s vintage turbojet with a hydro-mechanical fuel control and very little variable geometry.

After the steady-state engine model is selected, the non-steady-state addition must be created. Two approaches are presented based (again) on the T-38C PMP flight test program. The first approach is to:

1. Use the TOLAND batch simulation to predict flightpath acceleration or excess thrust for several takeoffs.
2. Compare the "measured" accelerations or excess thrusts to the predicted ones.
3. Adjust the predicted thrust model to match (on average) the accelerations or excess thrusts between 10 seconds after brake release and rotation speed.
4. Develop a thrust multiplicative factor as a function of time after brake release to multiply with the refined thrust model from the previous step for the first 10 seconds after brake release.
5. Spot check results and refine, if required, based on additional takeoffs.

The first approach uses the differences between the predictions and the measured acceleration to determine the required changes in thrust. This approach assumes that the excess thrust is equal to the net thrust less the aerodynamic drag and the rolling friction. The thrust multiplicative factor is adjusted until the TOLAND and the UFTAS aircraft acceleration outputs match within an acceptable level.

A second, simpler approach may be acceptable for a high thrust-to-weight ratio aircraft. If you assume that the thrust is much greater than the aerodynamic drag and the rolling friction at low speeds (less than 50 KCAS); then, equation 6:

$$\frac{Thrust_{net,req}}{Thrust_{net,modeled}} = \frac{longitudinal\ acceleration_{measured}}{longitudinal\ acceleration_{modeled}} \tag{6}$$

Air Data Computer Online

Most air data computers do limited calculations at low airspeeds when the magnitudes of the measured static and total air pressures are similar. This is done to minimize the chances of the measured total air pressure:measured ambient air pressure ratio being less than or equal to one. An air data computer typically does not start applying Pitot-static position error corrections until approximately 60 to 65 KCAS or approximately 0.09 to 0.10 Mach number. The time that the air data computer comes online is important if the data from that takeoff is going to be used to calculate or spot check the Pitot-static position errors in ground effect. There will be a discontinuity in the flight test determined position error correction curve at that indicated Mach number.

Variations in Aircraft Pitch Angle

Setting takeoff trim in most aircraft will normally result in either a nearly constant pitch angle during the acceleration from brake release to rotation or in a slightly increasing (noseup) pitch angle. The pitch angle change is normally less than 2 degrees. The generic TOLAND software assumes a constant pitch angle prior to rotation. The TOLAND users normally select the pitch angle just prior to rotation for the simulation. The TOLAND output prior to rotation is fairly insensitive to small changes in the pitch angle. If using the constant pitch angle from brake release to rotation speed and then a constant pitch rate to a constant pitch angle option in TOLAND, then the selected pitch angle for prior to the rotation speed is very important for matching the mainwheel liftoff speed (takeoff speed) and the ground roll distance. The pitch angle just prior to rotation should be used in most cases.

A third and fourth option for the pitch angle prior to the start of rotation for the test day predicted simulation run are available. The four options are:

1. Use the average angle between brake release and the start of rotation.
2. Use the pitch angle at the start of rotation.
3. Use an "average" angle biased to the time closer to the start of rotation.
4. Use a fictitious start time at or after brake release and before the real start of rotation.

The fourth option requires farther explanation. The first version of the AFFTC TOLAND software, developed from the NASA TOLAND software (reference 4), only had one option for modeling the pitch angle time history for rotation:

1. constant pitch angle from brake release until rotation, then
2. constant pitch rate to a target pitch angle, then
3. constant pitch angle or a switch to a constant climbout airspeed.

The updated AFFTC TOLAND software, AFFTC-TIH-96-02, *AFFTC TOLAND User's Guide* (reference 12), had a second option for modeling the rotation and climbout. The new option was:

1. a constant pitch angle from brake release until rotation, then
2. a table lookup with a pitch angle time history.

The pitch angle time history was either the actual test day time history or a reference time history of a nominal pitch angle at the start of rotation (incremental time zero) followed by a nominal pitch rate to a target pitch angle.

Selected Runway Heading

The aircraft ground track may not be parallel to the assumed runway heading. This is particularly true in the case of a crosswind. The pilot may allow the aircraft to drift downwind (across the runway) during the ground roll. Alternatively, the pilot may vary his crab into the crosswind to maintain his ground track during the acceleration and climbout. The UFTAS LINK 10 software calculates the distance that the aircraft "drifts" left or right of an assumed runway heading. This option was created for ground minimum control speed testing and is not required for normal takeoff or landing tests. It can, however, point to potential aircraft responses to changes in the magnitude or the direction of the wind. If the aircraft is smoothly drifting to one side, then the assumed runway heading can be changed to better match the test day results. The angular change can be estimated by the arctangent of the ratio of the crosstrack distance to the downtrack distance at the rotation speed.

Pitot-statics in Ground Effect

There are two primary methods that may be used to determine the Pitot-static position error corrections in ground effect: (1) an altitude method and (2) an airspeed method. They are both described in 412TW-TIH-19-02, *Determining Pitot Static Position Error Corrections in Ground Effect*, (reference 13). The altitude method assumes there is no error in the measurement of the total (Pitot) pressure. The airspeed method assumes that the wind magnitude and direction are known and are constant. Both methods assume that there are no pneumatic lags in the system.

Ambient Air Pressure and Temperature at the Surface

The ambient air pressure at the reference starting point should be obtained just prior to brake release using the static air pressure or the pressure altitude from the aircraft instrumentation system. A portable pressure sensor carried by the wind kit operator should also be used to record ambient air pressure and temperature as a backup. The measured ambient air temperature is one of the top two sources of error for the airspeed method of determining true airspeed for takeoff performance. The ambient air temperature can be obtained either from the airfield weather station, a wind kit, or various sources on the aircraft. Potential sources on the aircraft include: a flight test total air temperature probe, a production total air temperature probe, or a temperature probe in an engine inlet. Usually the most accurate source for ambient air temperature is the on-aircraft flight test total air temperature measurement. Ambient air temperature is calculated from the total air temperature and the aircraft Mach number in the area of rotation to 50 feet AGL in the initial climb, table 3.

Table 3 Change in Total Air Temperature with Increasing Mach Number

	Total Air Temperature (deg R)			
	Ambient Air Temperature (deg F)			
Mach Number	0	32	59	100
0.00	459.67	491.67	518.67	559.67
0.02	459.71	491.71	518.71	559.71
0.04	459.82	491.83	518.84	559.85
0.06	460.00	492.02	519.04	560.07
0.08	460.26	492.30	519.33	560.39
0.10	460.59	492.65	519.71	560.79
0.12	460.99	493.09	520.16	561.28
0.14	461.47	493.60	520.70	561.86
0.16	462.02	494.19	521.33	562.54
0.18	462.65	494.86	522.03	563.30
0.20	463.35	495.60	522.82	564.15
0.22	464.12	496.43	523.69	565.09
0.24	464.97	497.33	524.65	566.12
0.26	465.88	498.32	525.68	567.24
0.28	466.88	499.38	526.80	568.45
0.30	467.94	500.52	528.01	569.74
0.32	469.08	501.74	529.29	571.13
0.34	470.30	503.04	530.66	572.61
0.36	471.58	504.41	532.11	574.18
0.38	472.95	505.87	533.65	575.83
0.40	474.38	507.40	535.27	577.58

Notes:
1. T(deg R) = T(deg F) + 459.67
2. (total air temperature) = (ambient air temperature) $(1 + 0.2M^2)$

Wind Magnitude and Direction

The major source of error when using the airspeed method to determine the in-ground effect position error corrections is the need to assume that the wind is known and is constant in both magnitude and direction for the duration of the takeoff, from brake release through the aircraft reaching approximately 50 feet AGL. The wind speed and wind direction with respect to true north can be obtained from a portable wind kit positioned near the runway. Because it is not possible to measure the winds over the entire horizontal distance the aircraft will travel during a takeoff or landing maneuver, the wind kit should be positioned adjacent to the estimated takeoff liftoff point or landing touchdown point, since the takeoff and landing calibrated airspeeds are the most critical airspeeds to determine.

Data from analyzing hundreds of takeoffs at Edwards AFB has shown that light surface winds (less than 10 knots) vary about 0.5 to 1.5 knots and winds of 10 to 20 knots vary by about 0.5 to 2 knots during the approximate 30 seconds it takes to perform a takeoff. The ideal situation is to limit takeoff performance flight testing to calm or nearly calm days (less than 2 knots), supplemented by wind kits adjacent to the runway.

The recorded wind direction is the direction the wind is coming FROM. Aviation surface winds, such as those reported by the control tower, are with respect to magnetic north, whereas flight test analysis requires winds with respect to true north. The wind kits can be set to indicate with respect to true north, but other wind data may need to be corrected from magnetic to true using the known magnetic deviation for the flight test locale.

Tables 4 and 5 present historical magnetic deviation (also known as magnetic declination) data for Edwards AFB. Table 3 was created using DoD data from DoD Flight Information Publication (FLIP) (Terminal), Low Altitude, Southern California, United States documents published by the National Geospatial – Intelligence Agency in St. Louis, Missouri. Table 5 was created using FAA National Aeronautical Navigation Services, Los Angeles Sectionals published in Silver Spring, Maryland. The magnetic deviation values from the Los Angeles Sectionals required an interpolation between two isogonic lines separated by 0.5 degree magnetic deviation. The two isogonic lines on the sectionals were approximately 12 inches apart. Both sets of data show that the magnetic deviation at Edwards AFB has been decreasing in magnitude during the last 25 years. These changes are the result of the magnetic north pole's movement to the northwest from its current location in northeastern Canada.

Based on the data in tables 4 and 5, a heading with respect to true north would be approximately 13 degrees more than one with respect to magnetic north.

Table 4 Magnetic Deviations at Edwards AFB from DoD Flight Information Publications (Terminal) Low Altitude, Southern California, United States

Effective Date	Magnetic Deviation (date)	Magnetic Deviation (deg)	Annual Rate of Change (deg/year)
30 March 1995	February 1995	13.9 E	0.0
30 November 2000	August 2000	13.8 E	0.0
1 November 2001	August 2000	13.8 E	0.0
27 December 2001	August 2000	13.8 E	0.0
3 October 2002	March 2002	13.8 E	0.0
5 July 2007	September 2005	13.3 E	0.1 W
20 December 2007	September 2005	13.3 E	0.1 W
25 September 2008	June 2008	13.0 E	0.1 W
7 May 2009	May 2009	12.9 E	0.1 W
22 October 2009	August 2009	12.9 E	0.2 W
17 December 2009	August 2009	12.9 E	0.2 W
11 February 2010	August 2009	12.9 E	0.2 W
3 June 2010	August 2009	12.9 E	0.2 W
26 August 2010	August 2009	12.9 E	0.2 W
15 December 2011	October 2011	12.6 E	0.1 W
31 May 2012	January 2012	12.6 E	0.1 W
10 January 2013	November 2012	12.6 E	0.1 W
10 December 2015	September 2014	12.4 E	0.1 W
31 March 2016	September 2014	12.4 E	0.1 W
7 December 2017	November 2016	12.2 E	0.1 W
19 July 2018	November 2016	12.2 E	0.1 W
8 November 2018	November 2016	12.2 E	0.1 W
28 February 2019	November 2016	12.2 E	0.1W

Table 5 Magnetic Deviations at Edwards AFB from FAA Los Angeles Sectionals

Edition	Date		Magnetic Deviation (deg)
	Chart	Magnetic Model	
36	17 January 1985	1980	14.4 E
41	30 July 1987	1985	14.3 E
52	7 January 1993	1990	14.1 E
56	5 January 1995	1990	14.1 E
57	20 July 1995	1990	14.1 E
58	4 January 1996	1990	14.1 E
59	18 July 1996	1995	14.1 E
61	17 July 1997	1995	14.1 E
66	30 December 1999	1995	14.1 E
67	13 July 2000	1995	14.1 E
68	28 December 2000	1995	14.1 E
69	12 July 2001	1995	14.1 E
70	27 December 2001	2000	13.8 E
71	11 July 2002	2000	13.8 E
72	26 December 2002	2000	13.8 E
74	25 December 2003	2000	13.8 E
76	23 December 2004	2000	13.8 E
77	7 July 2005	2000	13.8 E
78	22 December 2005	2000	13.8 E
79	6 July 2006	2000	13.8 E
80	21 December 2006	2005	13.4 E
81	5 July 2007	2005	13.4 E
82	20 December 2007	2005	13.4 E
83	3 July 2008	2005	13.4 E
84	18 December 2008	2005	13.4 E
86	17 December 2009	2005	13.4 E
87	1 July 2010	2005	13.4 E
88	16 December 2010	2005	13.4 E
90	15 December 2011	2010	12.9 E
91	28 June 2012	2010	12.9 E
103	21 June 2018	2015	12.3 E
105	20 June 2019	2015	12.3 E
106	5 December 2019	2015	12.3 E

Many test programs at Edwards AFB and contractor test programs at other facilities have used wind speed and direction determined from onboard sensors (INS groundspeed, ground track, and air data computer true airspeed). These results have proven to be more accurate than those measured by a wind kit, references 14 through 25, table 6.

Table 6 Reference Number and Title

Reference Number	Title
14	*YC-15 STOL Performance Flight Test Methods and Results*
15	*Takeoff Performance Data Using Onboard Instrumentation*
16	*A Procedure for Determining Flight Path Wind Components During Takeoff and Landing Tests*
17	*Evaluation of Take-off and Landing Facility*
18	*Comparison of Takeoff Performance from Measurements with ASKANIA Cameras and an Inertial Navigation System*
19	*A Method for Measuring Take-off and Landing Performance of Aircraft, Using an Inertial Sensing System*
20	*Use of On-board Inertial Navigation System Data Instead of ASKANIA Data for Takeoff Performance Determination*
21	*Use of Onboard Data for Takeoff Performance Determination*
22	*T-38C Aircraft Performance Evaluation*
23	*T-38C Takeoff Flap Evaluation*
24	*T-38C/J85-GE-5S Synthetic Paraffinic Kerosene/JP-8 Fuel Blend (SJ-8) Aircraft Performance Testing*
25	*T-38C Propulsion Modernization Program (PMP) Engine Bay Overheat Resolution Aircraft Performance Evaluation*

The assumed wind magnitude and direction for the T-38C testing came from one of two potential sources: (1) the Base Weather Office or the control tower via the aircrew flight cards or (2) a calculated value based on previous UFTAS runs for the same time slice. The UFTAS LINK 13 (reference 6) either calculates a wind speed and direction assuming the sideslip angle is zero, or calculates a true airspeed and sideslip angle given a wind magnitude and direction. The true airspeed using the second option is calculated using the inertial velocities and the assumed wind. The UFTAS LINK 13 true airspeeds can be compared to the true airspeeds calculated in UFTAS LINK 2. The true airspeeds from UFTAS LINK 2 used the static and total pressure (or the pressure altitude and the calibrated airspeed from the air data computer) and the total air temperature to calculate the true airspeed. If the wind was constant and equal to the assumed magnitude and direction, and if the Pitot-static position error corrections were correct, then the two sets of calculated true airspeeds would be identical. If the calculated true airspeeds were not the same then one of four options were true:

1. The assumed wind speed or direction or both were wrong.
2. The assumed Pitot-static position error corrections in ground effect were wrong.
3. There was an uncorrected error in the Pitot (total) pressure.
4. There was an uncorrected Pitot-static lag error.

The last three potential sources of error would occur on every takeoff if they existed. An error in the total air pressure was not found in takeoff data on any version of the F-15 aircraft with or without the flight test noseboom, on the T-38C, or on the E-8A Joint Surveillance Target Attack Radar System (Joint-STARS) aircraft. Pitot-static lags on large aircraft use to be fairly common in the 1950s and the 1960s. Reducing the volumes of the lines between the ports and the transducers have significantly reduced the occurrences and magnitudes of Pitot-static lags.

The three most common errors in the assumed winds are:

1. The correct magnitude but the wrong direction in light winds, usually less than 3 knots.
2. The correct direction but the wrong magnitude in the strong winds, usually 10 knots or higher.
3. Winds of less than 3 knots when reported as calm or light and variable.

If the UFTAS LINK 13 data shows a light wind with a slightly erroneous magnitude and/or direction, then engineering judgment is used and one of the two following changes is made:

1. If the assumed wind magnitude and the true airspeed differences are consistent and small and the wind direction is primarily a headwind or a tailwind, then adjust the wind magnitude as required and make it a pure headwind or tailwind.
2. If the assumed wind magnitude is small and primarily a crosswind or the wind is high (greater than eight knots) from any direction, then use the reported wind direction and adjust the magnitude as required.

A wind reported as calm or light and variable can be more difficult. Two methods have been used with some success:

1. Run UFTAS LINK 13 with the wind magnitude set to zero.
2. Run UFTAS LINK 13 to calculate the wind magnitude and direction assuming the aircraft sideslip angle was zero.

If a constant error in true airspeed results from the first method, then it becomes the headwind or tailwind. If in the second method, the wind magnitude and direction look reasonable just prior to rotation; then use those values and rerun the takeoff time slice.

The two most challenging winds for flight test modeling of takeoffs are:

1. Variable winds (variable magnitude) right at mainwheel liftoff (takeoff).
2. Light and variable winds that start as a small (maybe 2-knots) headwind through takeoff and then change to a small (maybe 2-knot) tailwind during the air phase

There is not much that can be done for the first case (the data may be useful for brake release through rotation speed and for part of the air phase.). The second challenge is unfortunately not uncommon at Edwards AFB. The best solution is normally to use two different winds, one from brake release through the ground phase and another for the air phase.

The following results are presented to give the reader a sense of what is achievable with good instrumentation and “flight test winds”. Within the flight test community, “flight test winds” normally refer to the light winds that normally only exist at sunrise. The winds are normally reported as either calm or light and variable with magnitudes less than 5 knots. The “truth source” for the evaluation of the wind magnitude and direction is the variations in the true airspeeds calculated in LINK 2 and LINK 13 of UFTAS. The externally measured headwind was initially used to calculate groundspeed = onboard Pitot-static calculated true airspeed – headwind speed. This was done incrementally throughout the takeoff. The headwind speed was assumed a constant and was modified to make the difference in groundspeed from onboard inertial data and the true airspeed calculated from the onboard Pitot-statics minus the headwind a minimum through the takeoff. A demonstrated quality for low wind conditions based on hundreds of T-38C and F-15 takeoffs is:

1. the differences in calculated true airspeeds from 60 KCAS through mainwheel liftoff (takeoff) were within ±0.8 knot for 95 percent of the takeoffs,
2. within ±0.5 knot for 80 percent of the takeoffs, and
3. within ±0.3 knot for 50 percent of the takeoffs.

The variability of the calculated winds for T-38C test sorties flown in the late morning or in the afternoon were ±1 to 2 knots for reported winds of 20 to 30 knots. The above differences in both the low and higher wind conditions most likely reflect real wind variability and not limitations in the postflight data processing software.

Rotation Through Mainwheel Liftoff (Takeoff):

This is the start of the more dynamic part of the takeoff. There are a number of test day results that need to be collected:

1. Event time for the start of the rotation
2. Rotation speed
3. Ground roll distance from brake release to the start of rotation
4. Pitch angle just prior to the start of rotation
5. Pitch angle time history from the start of rotation through 50 feet AGL
6. Nosewheel liftoff based on its weight-on-wheels/weight-off-wheels (WOW) discrete
7. Airspeed at nosewheel liftoff
8. Ground roll distance from brake release to nosewheel liftoff
9. Event times for the mainwheel strut extensions based on their WOW discretes
10. Event times for the mainwheel liftoffs for the main gear based on wheelspeed sensors
11. Mainwheel liftoff (takeoff) speed
12. Ground roll distance from brake release to mainwheel liftoff
13. Aircraft pitch angle at mainwheel liftoff
14. Dynamic pressure, aircraft gross weight, and total gross thrust at mainwheel liftoff

Rotation.

Takeoff rotation can (and has) been defined based on several different aircraft parameters:

1. Aft stick pressure or force
2. Aft stick movement
3. Control surface (elevator or horizontal stabilizer) movement
4. Significant increase in aircraft noseup pitch rate
5. Significant increase in aircraft noseup pitch angle

There are small, but measurable, differences in the timing of the five events. The decision on what criterion to use for analyzing the data is usually made based on either availability, monetary, schedule, or political reasons. It should be remembered, however, that the definition of rotation speed to the pilot is that speed aft stick or wheel force is applied. If one parameter is instrumented and the others are not, then the additional money and time required to instrument another parameter must be considered. If all five parameters are instrumented, then the airframe manufacturer or the customer tester may have a strong preference concerning which parameter to use based on good or bad experiences on previous test programs.

A factor that must be considered is the time delay between the pilot's input and the time the aircraft nose starts to move. If the pilot attempts to rotate early in a heavy weight aircraft with a forward center of gravity, the aircraft may not respond until either more control input is applied or more dynamic pressure (airspeed) is achieved. The author has historically used the control surface position (when available) and has compared that event time with the time for a significant change in the aircraft noseup pitch angle. The word "significant" is hard to define (and defend) in this case. A working definition might be: The first increase in the aircraft pitch angle after the control input that is greater than the data scatter in the pitch angle signal prior to the control input.

Once an event time has been selected for the start of rotation, four other test results are obtained from the data: (1) rotation speed, (2) ground roll distance from brake release to the start of rotation, (3) the aircraft pitch angle just prior to the start of rotation, and (4) a time history table of aircraft pitch angle as a function of elapse time after the start of rotation. The pitch angle time history data will become an input into the test day predicted TOLAND run.

Nosewheel Liftoff.

Nosewheel liftoff is an event between the start of rotation and the mainwheel liftoff (takeoff). Nosewheel liftoff is normally established based on the change in a WOW discrete signal from the nose strut. The WOW discrete normally switches value when the strut is almost fully extended. "Almost fully extended" is usually 0.5 to 1.5 inches from full extension. Takeoff test programs that used external phototheodolites, like the AFFTC ASKANIA system, defined nosewheel liftoff based on postflight analyses of the film. The event was defined to have occurred halfway between the first frame in which the tire is clearly off the runway and the previous frame of film. A third method has been used when the WOW discrete signal failed or when it was installed on only one of the two test aircraft. The aircraft pitch angle (2.8 degrees noseup for example) has been used after the value was determined based on previous takeoffs in the same or similar aircraft.

After the event time has been established for nosewheel liftoff, the airspeed and the ground roll distance from brake release are obtained. Some aircraft flight manuals include the calibrated airspeeds and ground roll distances for nosewheel liftoff.

Takeoff.

The first task is to find the event times for the two WOW switch discretes (one on each of the two main struts). These establish the earliest that the takeoff could have occurred. Like the nosewheel WOW discrete, the change in the discrete indicates that the strut is almost fully extended.

When available, the wheelspeed sensors were used to determine when the tires actually left the runway surface, figure 1. They are the best source for determining mainwheel liftoff. The aircraft is airborne after the last mainwheel tire leaves the runway.

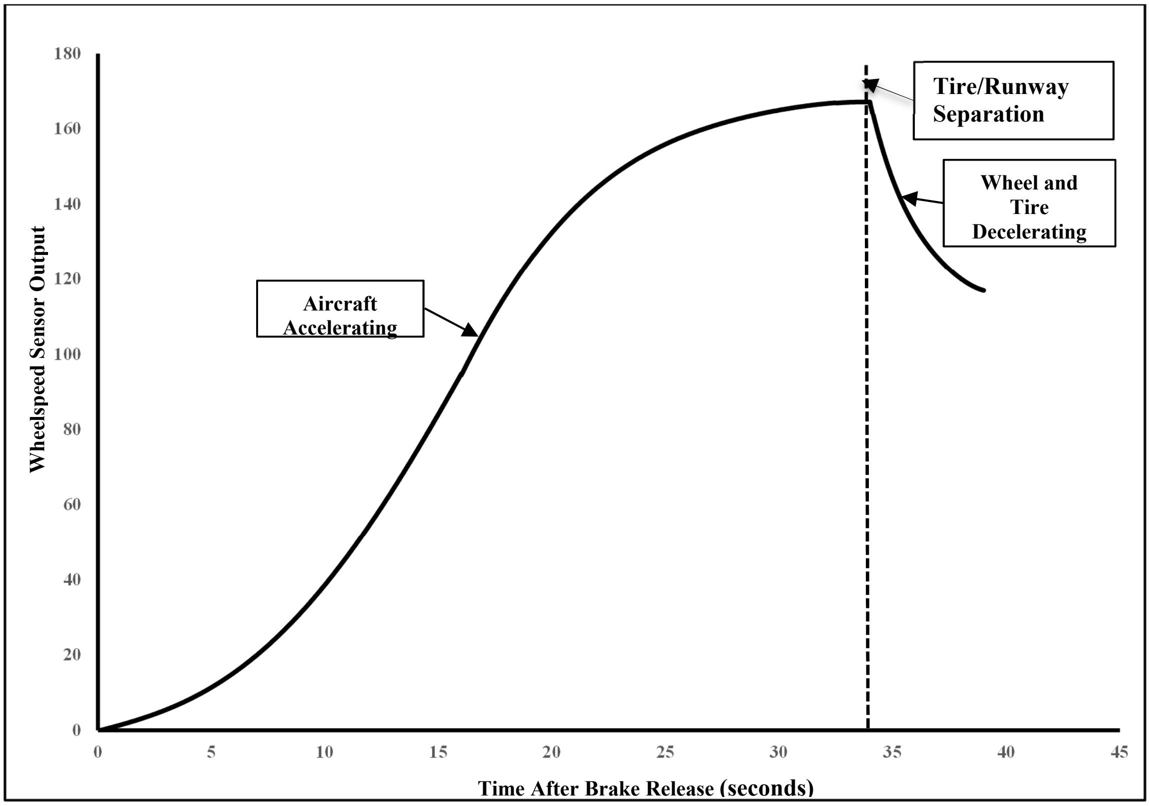

Figure 1 Notional Time History of a Wheelspeed Sensor Output

After determining the event time for the last mainwheel liftoff, the airspeed and the ground roll distance from brake release are determined. Finally, data are acquired to calculate the aircraft lift coefficient just after it became airborne. The aircraft pitch angle, dynamic pressure, aircraft gross weight, and total gross thrust are obtained from the UFTAS output and used to calculate the aircraft lift coefficient, equation 7:

$$C_L = \frac{\{n_z W - F_g[sin(a + i_T)]\}}{qS} \tag{7}$$

where:

C_L = aircraft lift coefficient
n_z = flightpath axis normal acceleration (assumed to be unity)
W = aircraft gross weight
F_g = total gross thrust
α = aircraft angle of attack (assumed to be equal to the aircraft pitch angle with the flightpath angle equal to zero)
i_T = thrust incidence angle (positive noseup from the waterline)
q = incompressible dynamic pressure
S = wing aerodynamic reference area

Air Phase Through 50 Feet AGL:

The final takeoff segment for most military aircraft is the air phase, the initial climbout from mainwheel liftoff through 50 feet AGL. Civilian transport aircraft certified under the CFR Part 25 also consider the second segment of the air phase with the landing gear retracted for all engines operating through

35 feet AGL. With one engine inoperative, a third and fourth segment are also defined by FAA rules: A level acceleration at 400 feet AGL and a climb from 400 to 1,500 feet AGL.

The TOLAND simulation was designed to predict performance for all four segments. However, it is normally used for the first segment with the potential to change from a target pitch angle to a target airspeed during the segment.

The UFTAS output is used to establish when certain events occurred during the climbout. Some of the events of interest are:

1. Start of landing gear retraction
2. Start of wing flap retraction
3. Power (thrust) reduction
4. Change in aircraft bank angle/ground track
5. Aircraft passing through 50 feet AGL

Landing Gear Retraction

The position of the landing gear handle in the cockpit is normally instrumented on aircraft with retractable landing gear. The discrete signal identifies the handle's position as either gear extended or gear retracted. The time required for the movement of the landing gear varies from aircraft to aircraft. However, it is usually between 3 and 20 seconds and, in most aircraft, it is between 6 and 10 seconds. Operationally, the landing gear for most aircraft are fully extended ("down and locked") during a takeoff until the aircraft is above the 35 or 50 foot AGL "obstacle". Pilots in high performance, fighter-type aircraft typically start the landing gear retraction sequence before reaching 50 feet AGL to avoid exceeding the landing gear in transition airspeed limit. There are normally two gear limit speeds: (1) for the landing gear extended and the landing gear doors closed and (2) with the landing gear or the gear doors in transition. During dedicated performance takeoffs in the flight test program, pilots can leave the landing gear extended through 50 feet AGL if it is a heavyweight, high-drag aircraft configuration taking off on a "warm" day. The pilot must take some action to avoid overspeeding the gear on an aircraft with a lot of test day excess thrust. Possible pilot actions include: (1) retracting the gear early, (2) reducing the thrust early, or (3) increasing the aircraft pitch angle to convert more of the excess thrust into potential energy (altitude) and less into kinetic energy (airspeed).

The test team has three options with regard to the landing gear in the air phase: (1) only do dedicated performance takeoffs when the predicted climbout performance allows takeoffs without raising the landing gear early or reducing the thrust early or changing the target pitch angle, or (2) use a more operationally representative procedure of initiating the gear retraction as soon as the aircraft is clearly airborne with a positive rate of climb, or (3) let the pilot on a takeoff-by-takeoff basis use his judgment on how to avoid overspeeding the gear. Ideally, the postflight data processing/data analyses would be robust enough to correct for the pilot actions if one of the last two options was selected. The TOLAND simulation could, for example, initiate the gear retraction at the test day altitude AGL for the test day predicted run and at 50 feet AGL or at some other target altitude for the reference day predicted run, 5 or 10 feet for example.

If the engineer wants to model the landing gear retraction in TOLAND, they have to provide an angle of attack increment at a constant lift coefficient or a lift coefficient increment at a constant angle of attack plus a drag increment as a function of time for the landing gear retraction (including during the doors opening and closing). The engineer has several options:

1. Switch from the gear extended curves to the gear retracted curves instantaneously when the gear handle moved.
2. Switch instantaneously x seconds after the gear handle moved.

3. Linearly transition from gear extended to gear retracted in x seconds.
4. Delay the start of the transition for y seconds and then linearly transition over the last z seconds.
5. Use airframe manufacturer models based on computational fluid dynamics runs.

The aircraft design will significantly affect the shapes and the magnitudes of the increments. For example:

1. Landing gear retracts into the wing of a low-wing aircraft versus into the fuselage of a high-wing aircraft.
2. The main landing gear retracts directly into the fuselage versus rotating 90 degrees then retracting.

The lift coefficient or angle of attack increments are normally more critical to the modeling effort than are the drag increments. The flightpath angle (and therefore the rate of climb) changes with the differences between the pitch angle and the required aircraft angle of attack.

Wing Flap / Slat Retraction

The positions of the wing trailing edge flaps and the leading edge flaps (slats) are normally instrumented. The wing flaps, like the landing gear, have airspeed limits, which must not be exceeded. Most of the comments on modeling for the landing gear retraction also apply to the flap retraction.

Power (Thrust) Reduction.

Power reduction is normally the pilot's first action to avoid overspeeding the landing gear or the flaps on a high-performance aircraft. Cancelling the afterburner and continuing the climbout at military power is typical. The TOLAND software has the required software to accommodate this power change from maximum to military.

Change in Ground Track

The software is not built into TOLAND to account for any heading change prior to achieving 50 feet AGL. However, in almost every case, the pilot will have started the landing gear and the flap retraction (and maybe the power reduction) prior to starting the turn. The air phase of the takeoff is not used for the final technical reports in these cases.

50 Feet Above Ground Level

The final event to be found is when the aircraft passes through 50 feet AGL[3]. There are normally four independent sources for identifying this event:

1. Radar altimeter
2. Integration of the INS vertical inertial velocity since brake release
3. GPS altitude
4. Ground-based phototheodolites.

The output of the radar altimeter is normally the secondary source for 50 feet AGL. Its output has normally not been calibrated. On some aircraft the output represents the height of the transmitting and receiving antennas on the lower surface of the fuselage. It might have a value of 3 feet with the aircraft in a 3-point attitude with the landing gear on the ground. Others have a bias introduced into the output such

[3] AGL, in this context, refers to height above the takeoff point.

that the output will be zero on the ground or zero with the main gear on the ground and the nose pitched up 5 to 15 degrees representing a takeoff mainwheel liftoff or a mainwheel touchdown on landing.

Using the postflight integration of the inertial vertical velocity has its own challenges:

1. Runway slope
2. Aircraft pitch angle at mainwheel liftoff
3. Aircraft pitch angle at 50 feet AGL

The integrated vertical velocity just prior to rotation should be equal to the tangent of the runway slope times the horizontal distance traveled from brake release. For runway 22L at Edwards AFB the slope is 0.08 degree or 21 feet vertically in 15,000 feet horizontally. If the aircraft travels 3,000 feet prior to rotation, then the integrated vertical velocity should be approximately 4 feet. In most cases the inertial navigation system (INS) is installed ahead of the main landing gear. It will move vertically upward while the aircraft is rotating. If the INS is 20 feet ahead of the main gear and the aircraft rotates upward by 7 degrees, then the INS will move 2.44 feet upward due to the rotation. At mainwheel liftoff the INS will have moved vertically due to the sum of these two effects.

If the aircraft's pitch angle at 50 feet AGL is approximately the same as it was at mainwheel liftoff, then the integrated vertical velocity would be 50 feet greater than it was at liftoff. If the pitch angle has changed, then trigonometry can be used to adjust the integrated distances for the pitch angle differences.

The third option as a data source is the GPS altitude. It is normally not used because of its one sample per second update rate and it's typically large, 3 feet for example, resolution.

After the time for 50 feet AGL is determined, the following test results are obtained:

1. Horizontal distance from brake release
2. Horizontal distance from the mainwheel liftoff
3. Calibrated airspeed
4. Aircraft pitch angle
5. Elapsed time since mainwheel liftoff

Summary:

This completes the determination of the test day takeoff performance. At this point the engineer has several options. Those options will be addressed in the remainder of this handbook.

This page was intentionally left blank.

ADDITIONAL ANALYSES

This section addresses what is done with the test day results. These results and takeoff conditions include:

1. Aircraft gross weight at brake release
2. Pressure altitude
3. Ambient air temperature
4. Headwind component
5. Runway slope
6. Runway surface (this may affect the rolling coefficient of friction)
7. Aircraft configuration
8. Power (thrust) setting
9. 3-point pitch angle prior to rotation
10. Rotation speed
11. Average rotation rate
12. Test day pitch angle for the climbout
13. Pitch angle time history from rotation speed through 50 feet AGL
14. Elapsed time from brake release to mainwheel liftoff (takeoff)
15. Calibrated and true airspeed at mainwheel liftoff
16. Horizontal distance from brake release to mainwheel liftoff
17. Aircraft pitch angle at mainwheel liftoff
18. Elapsed time from brake release through 50 feet AGL
19. Calibrated and true airspeed at 50 feet AGL
20. Horizontal distance from brake release through 50 feet AGL
21. Aircraft pitch angle at 50 feet AGL

The additional analysis of the takeoff data depend on the reason for performing the takeoffs, the quality of the data, and the availability, or lack thereof, of models and simulation software. Some of the analysis that might be performed include:

1. An adjustment for takeoff speed
2. An adjustment for the speed at 50 feet AGL
3. A quantitative comparison of test day takeoff performance to the flight manual/pilot operating handbook takeoff performance predictions
4. A qualitative or quantitative comparison of test day takeoff performance to a flight simulator takeoff performance predictions
5. Using aircraft characterization methods for takeoff performance
6. Using empirical methods developed by Ken Lush for takeoff data standardization to a reference set of conditions
7. Using M&S methods, including TOLAND, developed for takeoff data standardization to a reference set of conditions
8. Using M&S methods to calculate test day distances and speeds to compare to actual test takeoffs

ADJUSTMENT FOR TAKEOFF SPEED

This adjustment is not normally made. However, it will make an improvement (a reduction) in the data scatter if used in combination with Ken Lush's equations.

The two major factors affecting the takeoff speed for an aircraft of a fixed aerodynamic configuration, gross weight, ambient air temperature, pressure altitude, and wind are the aircraft pitch angle and calibrated (or equivalent) airspeed. The pitch angle (or angle of attack) establishes the aerodynamic lift coefficient.

The airspeed establishes the dynamic pressure. If the pilot starts the rotation early or pulls to too high of a pitch angle, then the aircraft will generate enough aerodynamic lift to lift off earlier (slower) than expected. Conversely, if the pilot starts the rotation late or does not pull to the target pitch angle; the aircraft will not generate enough aerodynamic lift until the aircraft is faster than expected.

If the engineer is willing to ignore the variations in the aerodynamic drag coefficient with aircraft pitch angle variations during the takeoff ground roll and the variations in the engine inlet efficiencies, then the following simplistic method will provide some reduction in data scatter. This approach assumes that enough takeoffs have been analyzed to establish what the takeoff speed "should" be.

The engineer can go into a tabular time history listing that includes calibrated airspeed and horizontal distance from brake release and select the distance corresponding to the desired takeoff speed versus the actual takeoff speed. A graphical solution could be obtained by plotting the horizontal distance against the calibrated airspeed over a speed range encompassing the speed range of interest. The graphical solution may give a more accurate solution in the presence of significant data scatter. A nonlinear curve fit will be required. A plot of horizontal distance against the calibrated airspeed squared will produce a less nonlinear curve fit.

ADJUSTMENT FOR THE SPEED AT 50 FEET AGL

This is another adjustment that is not normally made. However, this adjustment should provide some reduction in the data scatter for the air phase if used in combination with Ken Lush's equations.

The pilot's control (or lack thereof) in the pitch axis determines how much of the energy from the excess thrust goes into potential energy (altitude) versus kinetic energy (airspeed). The following method assumes that the "desired" airspeed at 50 feet AGL is known, equations 8 through 16.

$$TE = PE + KE \tag{8}$$

$$PE = Wh \tag{9}$$

$$KE = \frac{WV^2}{2g} \tag{10}$$

$$TE_{desired} = 50W + \frac{WV_{50}^2}{2g} \tag{11}$$

$$TE_{actual} = Wh + \frac{WV^2}{2g} \tag{12}$$

$$\text{for } TE_{actual} = TE_{desired} \tag{13}$$

$$Wh + \frac{WV^2}{2g} = 50W + \frac{WV_{50}^2}{2g} \tag{14}$$

$$h + \frac{V^2}{2g} = 50 + \frac{V_{50}^2}{2g} \tag{15}$$

$$h = 50 + \left[\frac{V_{50}^2}{2g} - \frac{V^2}{2g}\right] \tag{16}$$

where:

TE	=	total energy, foot pounds
PE	=	potential energy, foot pounds
KE	=	kinetic energy, foot pounds

W	=	aircraft gross weight, pounds
h	=	height above the liftoff point, feet
g	=	acceleration due to gravity, feet per second squared
$(TE)_{desired}$	=	total energy at 50 feet AGL at the desired airspeed, foot pounds
V_{50}	=	desired true airspeed at 50 feet AGL, feet per second
$(TE)_{actual}$	=	instantaneous total energy, foot pounds
V	=	instantaneous true airspeed, feet per second

The solution is the combination of a height and a true airspeed that have the same total energy as the desired value. The solution can be found by trial and error using a tabular listing of height above the liftoff point, calibrated airspeed, and true airspeed. That approach is time consuming. A faster approach is to include a column of test day total energy in the tabular time history listing. A graphical solution could be obtained by plotting test day total energy versus either height or airspeed. The adjusted airspeed and horizontal distance from brake release can then be used versus the actual values at 50 feet AGL.

This page was intentionally left blank.

OTHER METHODS OF TEST DAY TAKEOFF DATA ANALYSIS

FLIGHT MANUAL COMPARISON

A common test objective is to validate or “spot check” the airplane flight manual takeoff performance charts. The charts normally have the ground roll distance and the horizontal distance from brake release to 35 or to 50 feet AGL. Separate tables or charts (appendix K) provide takeoff speed and the speed at 50 feet AGL. The inputs to the charts include:

1. Ambient air temperature
2. Pressure altitude
3. Aircraft gross weight
4. Headwind component
5. Aircraft configuration (including flap setting)
6. Power (thrust) setting

Some flight manuals also have runway slope and runway surface as inputs.

The flight manual comparison is simply comparing the distances predicted by the flight manual to the test day values from the flight test program or the adjusted values from the two previous sections. If the runway had a significant slope and the flight manual did not have a slope correction, then the slope correction from *Standardization of Take-off Performance Measurements for Airplanes* (reference 2), by Kenneth Lush, could be used prior to making the flight manual comparison.

The flight manual charts could also be used twice to adjust the flight test data to a reference set of conditions. The reference set of conditions could be:

1. Sea level pressure altitude
2. 59 degrees F or 15 degrees C ambient air temprature
3. No wind
4. Flat runway, no slope
5. Maximum takeoff gross weight

Or the flight manual charts can be used at some non-standard atmospheric conditions, such as 5,000 feet pressure altitude and 100 degrees F. The flight manual charts are not normally used for data standardization because of their relatively poor resolution, approximately 100 feet in many cases.

Some airframe manufacturers use the models that were used to create the flight manual charts to compare against the test day takeoff performance results. (This is the equivalent of comparing the test day takeoff performance results to the TOLAND test day predicted results.) This avoids the resolution concern with the flight manual charts. If the contractor finds a consistent difference, then they can adjust their models to more accurately match the flight test results.

FLIGHT SIMULATOR COMPARISON

The comparison of the flight test takeoff performance to the flight simulator results is usually more qualitative than quantitative. It is used as more of a flight-by-flight clearance early in a flight test program for a new aircraft. However, some companies use the flight simulator software in a batch mode versus in a man-in-the-loop mode to acquire data for comparison against the test day flight test data.

AIRCRAFT TAKEOFF CHARACTERIZATION METHODS

Preliminary design textbooks utilize charts to predict takeoff performance for early design trade studies. There are small variations between texts but the charts are generally similar. The plots usually have a takeoff distance on the y-axis and a takeoff parameter (TOP) on the x-axis. Lines representing horizontal distances from brake release to rotation, to mainwheel liftoff (ground roll), and to 35 or 50 feet are presented. One form of the takeoff factor is, equation 17:

$$TOF = \frac{W}{S}\left(\frac{1}{C_L}\right)\left(\frac{1}{T/W}\right)\frac{1}{\sigma} \quad (17)$$

where:

TOF	=	takeoff factor, pounds per square foot
W	=	aircraft gross weight, pounds
S	=	aerodynamics reference area, square feet
C_L	=	lift coefficient, non-dimensional
T	=	net thrust, pounds
σ	=	ambient air density ratio, non-dimensional

The lift coefficient could be:

1. An out of ground effect maximum trimmed lift coefficient
2. An out of ground effect trimmed lift coefficient for the aircraft pitch angle at mainwheel liftoff (takeoff)
3. An in ground effect maximum trimmed lift coefficient limited by the tail strike angle
4. An in ground effect trimmed lift coefficient at a typical pitch angle for mainwheel liftoff

The thrust could be:

1. An uninstalled, sea level, static, standard day takeoff rated thrust
2. An uninstalled , sea level, standard day takeoff rated thrust at the mainwheel liftoff speed
3. An installed, sea level, static, standard day takeoff rated thrust
4. An installed, sea level, standard day takeoff rated thrust at the mainwheel liftoff speed

Most of the preliminary design textbooks have plots that could be used to predict both test day and reference day takeoff performance. Thus, the plots could be used to adjust the test day results to a reference set of conditions. This approach is acceptable for preliminary design, but it is rarely used for flight test efforts.

ADJUSTING THE RESULTS TO A REFERENCE SET OF CONDITIONS

KEN LUSH'S EMPIRICAL EQUATIONS

Ken Lush's empirical equations were a logical evolution from the equations used by the United States Army Air Forces during World War II and documented in Army Air Forces Technical Report Number 5069, *Performance Flight Testing Methods in Use by the Flight Section* (reference 26). Ken's equations were summarized in references 2 and 3). The various aircraft used as a basis for these empirical analyses in references 2 and 3 are discussed in appendix J.

Ken's equations were evaluated by Lieutenant Thomas Twisdale in 1971 using data generated by an analog simulation for a Northrop F-5B aircraft. His results are documented in the Flight Test Technology Branch Office Memorandum, *Take-off Standardization* (reference 27). He proposed some minor changes based on his analyses. They are included in this handbook.

Although not a part of references 2 and 3, the adjustments for takeoff speed and for the speed at 50 feet AGL discussed earlier have been used in connection with Ken Lush's equations. The next two adjustments, which are part of reference 2, are for the wind and the runway slope.

<u>Wind Adjustment:</u>

The adjustment to the test day ground roll for the test day wind is equation 18:

$$S_g = S_{gw}\left[1 + \left({}^{V_W}\!/_{V_T}\right)\right]^{1.85} \tag{18}$$

where:

S_g = no wind ground roll
S_{gw} = test day ground roll with wind
V_w = wind speed (positive for a headwind and negative for a tailwind)
V_T = test day true airspeed at mainwheel liftoff

Lieutenant Tom Twisdale found that an exponent of 1.88 matched his Northrop F-5B data better than the 1.85 exponent.

The adjustment for the air phase is equation 19:

$$S_a = S_{atw} + V_W(\Delta t_{at}) \tag{19}$$

where:

S_a = no wind air phase distance
S_{atw} = test day air phase distance with wind
V_w = wind speed (positive for a headwind and negative for a tailwind)
Δt_{at} = elapsed time from mainwheel liftoff to 50 feet AGL

Runway Slope Adjustment:

The adjustment to the test day ground roll for the test day runway slope is equation 20:

$$S_{gto} = \frac{S_g}{\left\{1+\left[\frac{2gS_g}{V_T^2}\right]\sin\theta\right\}} \tag{20}$$

where:

- S_{gto} = test day ground roll distance adjusted for headwind and for runway slope
- S_g = test day ground roll distance adjusted for headwind
- g = acceleration due to gravity
- V_T = test day true airspeed
- sin = trigonometric function sine
- θ = runway slope (positive uphill)

There is no runway slope adjustment required for the air phase.

Ground Roll Distance Adjustments:

Fixed Pitch Propellers.

The adjustment for fixed pitch propeller powered aircraft running at a constant engine speed is equation 21:

$$S_{gs} = S_{gto}\left(\frac{W_s}{W_t}\right)^{2.4}\left(\frac{\sigma_s}{\sigma_t}\right)^{-2.4} \tag{21}$$

or, for the engine running at full throttle, equation 22:

$$S_{gs} = S_{gto}\left[\left(\frac{W_s}{W_t}\right)^{2.4}\left(\frac{\sigma_s}{\sigma_t}\right)^{-2.4}\left(\frac{T_{as}}{T_{at}}\right)^{-0.7}\right] \tag{22}$$

NOTE: The final exponent, -0.7 for the temperature ratio, was changed in reference 3. It had been 0.5 in reference 2.

where:

- S_{gs} = ground roll distance after adjustments for aircraft gross weight, ambient air density, and ambient air temperature
- S_{gto} = ground roll distance after headwind and runway slope adjustments
- W_s = reference aircraft gross weight
- W_t = test day aircraft gross weight
- σ_s = ambient air density ratio at the reference conditions
- σ_t = ambient air density ratio at the test day conditions
- T_{as} = reference day ambient air temperature in absolute units
- T_{at} = test day ambient air temperature in absolute units

Constant Speed Propellers.

The adjustment for aircraft with constant speed propellers is equation 23:

$$S_{gs} = S_{gto}\left[\left(\frac{W_s}{W_t}\right)^{2.6}\left(\frac{\sigma_s}{\sigma_t}\right)^{-1.7}\left(\frac{N_s}{N_t}\right)^{-0.7}\left(\frac{P_s}{P_t}\right)^{-0.9}\right] \tag{23}$$

where:

N_s = reference day engine speed
N_t = test day engine speed
P_s = reference day brake power to propellers
P_t = test day brake power to the propellers

Turbojet Aircraft.

The adjustment to the ground roll distance for a turbojet-powered aircraft is equation 24:

$$S_{gs} = S_{gto}\left[\left(\frac{W_s}{W_t}\right)^{2.3}\left(\frac{\sigma_t}{\sigma_s}\right)^{1.0}\left(\frac{F_s}{F_t}\right)^{-1.3}\right] \tag{24}$$

where:

F_s = mean thrust for the reference conditions
F_t = mean thrust for the test day conditions

Lieutenant Twisdales' equivalent equation from reference 27 is equation 25:

$$S_{gs} = S_{gto}\left[\left(\frac{W_s}{W_t}\right)^{2.14}\left(\frac{\sigma_t}{\sigma_s}\right)^{0.93}\left(\frac{F_s}{F_t}\right)^{-1.24}\right] \tag{25}$$

Air Phase Distance Adjustments:

Fixed Pitch Propellers.

The adjustment for fixed pitch propeller powered aircraft running at a constant engine speed is equation 26:

$$S_{as} = S_a\left[\left(\frac{W_s}{W_t}\right)^{2.2}\left(\frac{\sigma_s}{\sigma_t}\right)^{-2.2}\right] \tag{26}$$

Or, for the engine running at full throttle, equation 27:

$$S_{as} = S_a\left[\left(\frac{W_s}{W_t}\right)^{2.2}\left(\frac{\sigma_s}{\sigma_t}\right)^{-2.2}\left(\frac{T_{as}}{T_{at}}\right)^{-0.9}\right] \tag{27}$$

NOTE: The final exponent, -0.9 for the temperature ratio, was changed in reference 3. It had been 0.6 in reference 2.

Constant Speed Propellers.

The adjustment for aircraft with constant speed propeller is:

For lightweight aircraft, equation 28:

$$S_{as} = S_a \left[\left(\frac{W_s}{W_t}\right)^{2.3} \left(\frac{\sigma_s}{\sigma_t}\right)^{-1.2} \left(\frac{N_s}{N_t}\right)^{-0.8} \left(\frac{P_s}{P_t}\right)^{-1.1} \right] \tag{28}$$

For heavy weight aircraft, equation 29:

$$S_{as} = S_a \left[\left(\frac{W_s}{W_t}\right)^{2.6} \left(\frac{\sigma_s}{\sigma_t}\right)^{-1.5} \left(\frac{N_s}{N_t}\right)^{-0.8} \left(\frac{P_s}{P_t}\right)^{-1.1} \right] \tag{29}$$

Turbojet Aircraft.

The adjustment to the air phase distance for a turbojet aircraft is:

For a lightweight aircraft, equation 30:

$$S_{as} = S_a \left[\left(\frac{W_s}{W_t}\right)^{2.0} \left(\frac{\sigma_t}{\sigma_s}\right)^{0.4} \left(\frac{F_s}{F_t}\right)^{-1.6} \right] \tag{30}$$

NOTE: The gross weight exponent, 2.0, was 2.6 in reference 2. The ambient air density exponent, 0.4, was 1.0 in reference 2. They were both changed in reference 3.

For a heavy weight aircraft, equation 31:

$$S_{as} = S_a \left[\left(\frac{W_s}{W_t}\right)^{2.3} \left(\frac{\sigma_t}{\sigma_s}\right)^{0.7} \left(\frac{F_s}{F_t}\right)^{-1.6} \right] \tag{31}$$

The equivalent equation from reference 7 is equation 32:

$$S_{as} = S_a \left[\left(\frac{W_s}{W_t}\right)^{1.06} \left(\frac{\sigma_t}{\sigma_s}\right)^{0.54} \left(\frac{F_s}{F_t}\right)^{-0.55} \right] \tag{32}$$

This technical approach to takeoff data reduction, Ken Lush’s equations, was state of the art within the industry from the 1940s through the 1960s. It remained the recommended approach at the AFFTC until 1980 when it was replaced by an M&S approach using the NASA TOLAND software. There were some exceptions, notably the C-5A Combined Category I/II Flight Test Program in the 1968 to 1971 timeframe, where an M&S approach was used.

Notice that Ken Lush’s equations make no adjustments for variations in the pilot’s inputs.

MODELING AND SIMULATION

Technology in the 1970s was significantly advanced relative to that available in the 1940s. Several key advances led to a change from using Ken Lush’s empirical equations to using M&S techniques to adjust the test day takeoff performance to account for the day-to-day and takeoff-to-takeoff variations.

Some of the advances were:

1. Large mainframe, digital computers
2. Onboard tape recorders
3. Electronic inflight thrust decks (IFTD)
4. Electronic engine cycle or status decks
5. Aerodynamic math models in an electronic format
6. Production aircraft data buses
7. Production INSs
8. Improved flight test instrumentation systems

For the AFFTC, the introduction to using M&S versus Ken Lush's equations came from meetings with the airframe manufacturers. This was followed by a 1973 NASA Ames Research Center Technical Memorandum X-62333 document, *Computer Programs for Estimating Takeoff and Landing Performance* (reference 4).

NASA TOLAND:

TOLAND refers to TakeOff and LANDing. The original NASA TOLAND software is described in reference 4. The NASA TOLAND program was developed by NASA Ames as a design tool, not as a flight test tool. Its original inputs were desired aircraft performance such as takeoff ground roll and takeoff air phase distance.

Wayne Olson and Dave Nesst of the AFFTC modified the program to make it more useful as a flight test tool. It was initially run on the Range Squadron's CYBER mainframe computer and was transferred to desktop PCs when the CYBER was retired. Its first use at the AFFTC was in support of the McDonnell Aircraft Company (McAir) F-15C flight tests flown from May 1979 through September of 1980. The results were published in AFFTC-TR-81-18, *F-15C Limited Takeoff and Landing Evaluation,* (reference 28). After the AFFTC Technical Report was published in 1981, the AFFTC version of the NASA TOLAND software became the preferred method of standardizing takeoff and landing performance at the AFFTC. Some of the flight test programs that used this new approach included:

1. Rockwell B-1B
2. Northrop B-2A
3. Boeing B-52G/H (minimum interval takeoff (MITO) evaluation)
4. Northrop-Grumman (Joint STARS) E-8A
5. McAir F-15C/E/I/S
6. Lockheed F-16 (brake evaluations)
7. Boeing KC-135A/E/R (MITO evaluation)
8. Douglas KC-10 (MITO Evaluation)
9. Northrop T-38A (single engine takeoff speed evaluation in 1993)
10. Northrop T-38C PMP

AFFTC TOLAND:

The modified NASA TOLAND software was used as the preferred approach until a new version of the software was created by Kent Standley of the AFFTC in 1996. His software was documented in AFFTC-TIH-96-02, *AFFTC TOLAND User's Guide,* (reference 12). The major changes from Wayne Olson and Dave Nesst's version to Kent Standley's version were:

1. More efficient (faster) software
2. Optimized for use on IBM PC
3. A new option for the rotation/climbout phase
4. Additional options for modeling landing performance

The third change significantly improved the ability of the software to match the actual test day takeoff performance. The Dave Nesst version modeled the aircraft takeoff rotation and initial climbout as:

1. Constant aircraft pitch angle from brake release to rotation speed
2. Constant aircraft pitch rate from rotation speed until achieving a target pitch angle
3. Constant pitch angle until reaching an altitude at which the aircraft will continue to fly at a constant pitch angle or it will transition to a constant speed (also a runtime input)

The challenge for the flight test engineer was when the rotation pitch rate was not a constant and the target pitch angle was not maintained. The flight test engineer, when using the Dave Nesst version of TOLAND, had to use his best engineering judgment when selecting the test day rotation rate and target pitch angle inputs. He would typically generate a time history plot of pitch angle versus time for the period from just prior to rotation through the aircraft passing 50 feet AGL. Generally, the average pitch rate was simply, equation 33:

$$\dot{\theta} = \frac{\theta_{MWLO} - \theta_{RS}}{t_{MWLO} - t_{RS}} \tag{33}$$

where:

$\dot{\theta}$ = Average pitch rate
θ_{MWLO} = Pitch angle at mainwheel liftoff
θ_{RS} = pitch angle at the selected rotation speed
t_{MWLO} = time at mainwheel liftoff
t_{RS} = time selected for the rotation speed

The advantage of using this approach for the average pitch rate was that it created the correct pitch angle for mainwheel liftoff.

The selection of the input for the test day target climbout pitch angle was more subjective. Since the initial part of the air phase typically still had an increasing pitch angle, the selection of the target pitch angle was biased towards the end of the climbout. The value might be the average value of the test day pitch angles while the aircraft was climbing between 40 and 50 feet AGL. Sometimes the pitch angle at the 50 feet AGL was used. In many cases, the selection of the inputs for the pitch rate and the target pitch angle were questionable at best. Some questioned the selections and criticized them as the values required to get the answers the engineer wanted. Kent Standley's version of TOLAND eliminated this problem.

The engineer using Kent Standley's version of TOLAND had two options for modeling rotation and climbout:

1. Dave Nesst's method, using a pitch angle from brake release to rotation followed by an average pitch rate to a target pitch angler
2. A pitch angle from brake release to rotation followed by a table look-up using the actual test day pitch angles as a function of time after the start of rotation

The second option, the table look-up option, was used for the test day predicted TOLAND runs. The first option, the average pitch rate and target pitch angle, was used for the reference day predicted TOLAND runs. The average pitch rate for the reference day predicted runs was either:

1. an average of the test day values observed during the flight test program, or
2. the pitch rate used to create the flight manual charts.

The target pitch angle for the referenced day predicted runs was the flight manual recommended value.

Although rarely used, the software would allow the software rotation speed to be zero (brake release) or any time prior to the real start of rotation. This would allow the engineer to have a pitch angle at brake release that varied until the transition to an airspeed during the climbout. This option would be used for an aircraft with a significant variation in the pitch angle prior to the pilot commanded rotation.

The 1996 version of the AFFTC TOLAND software was a significant improvement over the earlier (1979) version in its ability to model variations in the pilots' inputs. These variations included:

1. Varying pitch angles between brake release and the test day rotation speed
2. Differences between the actual and the target rotation speed (handled by both software versions)
3. Varying the rotation rate vice a constant pitch rate
4. Variations in the actual pitch angle vice the constant target pitch angle

Accounting for these variations in pilot technique significantly reduced the takeoff-to-takeoff variability in the "standardized" results. The most significant source of data scatter when using the 1996 version of the AFFTC TOLAND is variations in the test day wind speed and/or direction.

The standardized flight test results were simply the actual test day values plus the difference between the outputs of the two TOLAND runs, equation 34.

$$S_{std} = S_t + [S'_{std} - S'_t] \tag{34}$$

where:

S_{std} = standardized airspeed or distance
St = actual test day airspeed or distance
S'_t = TOLAND test day predicted airspeed or distance
S'_{std} = TOLAND standard or reference day predicted airspeed or distance

Kent Standley's version of TOLAND has been the AFFTC (presently the 412th Test Wing) preferred method of takeoff performance data standardization since 1996. Some of the flight test programs that have used this approach include: McAir F-15I/S, Northrop T-38A/C PMP from 1999 through 2010, and the Northrop Grumman RQ-4B Global Hawk.

This page was intentionally left blank.

SOME CONSIDERATIONS IN CHOOSING A TAKEOFF ANALYSIS METHOD

Table 7 presents a list of variables that will affect the test day takeoff performance. The test team has some to extensive control over some of the variables:

1. Aircraft gross weight
2. Aircraft longitudinal center of gravity
3. External aircraft configuration (the load out)
4. Pressure altitude
5. Ambient air temperature
6. Wind
7. Runway slope

Table 7 Test Day Takeoff Variable Adjustment Capability

Variable	Can be Adjusted by	
	Ken Lush's Equations	AFFTC TOLAND
Aircraft gross weight	YES	YES
Aircraft longitudinal center of gravity	NO	NO
Pressure altitude	YES	YES
Ambient air temperature	YES	YES
Headwind/tailwind	YES	YES
Crosswind	NO	NO
Runway slope	YES	YES
Wrong external aircraft configuration	NO	MAYBE
Wrong flap setting	NO	MAYBE
Takeoff trim not set correctly	NO	YES
Power/thrust application at brake release	NO	YES
Wrong thrust setting	NO	MAYBE
Number and amplitude of directional control inputs during the flight controls checks after brake release	NO	NO
Use of nosewheel steering, differential braking, or rudder deflection for crosswinds	NO	NO
Control surface deflections between brake release and rotation	NO	NO
Early application of aft stick well before rotation speed	NO	MAYBE
Wrong rotation speed	MAYBE	YES
Wrong magnitude of aft stick input/wrong pitch rate	MAYBE	YES
Wrong or variable pitch angle/did not capture the target Pitch angle	NO	YES
Cancelled the afterburner before reaching 50 feet AGL	NO	MAYBE
Started flap retraction before reaching 50 feet AGL	NO	MAYBE
Started landing gear retraction before reaching 50 feet AGL	NO	MAYBE

The pressure altitude will typically have variations of less than ±1,000 feet for a given test location. (See appendix A for information concerning Edwards AFB surface weather.) However, the pressure altitude can be changed by going to a different test site. Some options in the Southwestern part of the United States for different field elevations are listed in table 8 and appendices B and C.

Table 8 Field Elevation

Airport	Field Elevation (ft)
El Centro NAF (El Centro, California)	-42
Point Mugu NAS (Ventura, California)	13
Moffett Federal Airfield (Mountain View, California)	32
Travis AFB (Fairfield, California)	62
McClellan Airfield (Sacramento, California)	77
Sacramento Mather Airfield (Sacramento, California)	99
Beale AFB (Marysville, California)	113
Yuma MCAS/Yuma International (Yuma, Arizona)	213
Lemoore NAS (California)	232
Vandenberg AFB (Lompoc, California)	350
Miramar MCAS (San Diego, California)	477
Palm Springs International Airport (Palm Springs, California)	477
Luke AFB (Phoenix, Arizona)	1085
Phoenix-Mesa Gateway (Phoenix, Arizona) (formerly Williams AFB)	1382
Nellis AFB (Las Vegas, Nevada)	1870
Edwards AFB (Rosamond, California)	2310
Davis-Monthan AFB (Tucson, Arizona)	2704
Fallon NAS (Fallon, Nevada)	3934
El Paso International Airport/Biggs Army Airfield (El Paso, Texas)	3962
Holloman AFB (Alamogordo, New Mexico)	4093
Cannon AFB (Clovis, New Mexico)	4295
Hill AFB (Ogden, Utah)	4789
Reno-Stead (Reno, Nevada)	5050
Kirtland AFB (Albuquerque, New Mexico)	5355
South Lake Tahoe (Lake Tahoe, California)	6264
Big Bear City (Big Bear, California)	6752
Taos Regional Airport (Taos, New Mexico)	7095
Mammoth Yosemite (Mammoth Lakes, California)	7135
Telluride Regional Airport (Telluride, Colorado)	9070
Lake County Airport (Leadville, Colorado)	9934

Test programs using Ken Lush’s equations should test near the pressure altitudes and ambient air temperatures that are requested by the customer. Historically, a large number of test programs have found that data collected near sea level and adjusted with Ken Lush’s equations did not produce adequate data for the United States Air Force Academy. The academy at Colorado Springs, Colorado has a field near 6,000 feet. More significantly, its density altitude can be over 10,000 feet during the summer months.

The surface ambient air temperatures at Edwards AFB vary by about 20 to 30 degrees F on a daily basis. The ambient air temperatures at the surface at sunrise typically vary from about 30 degrees in the winter to about 65 degrees in the summer. In most cases the temperature at sunrise is the important one because of the surface winds after sunrise. If higher temperatures than about 65 degrees are required, then either you have to takeoff from Edwards AFB later in the day or go to another test site. Potential high ambient air temperature sites include:

1. El Centro NAS
2. Yuma MCAS

3. Luke AFB
4. Phoenix-Mesa Gateway (formerly Williams AFB)
5. Davis-Monthan AFB
6. El Paso International Airport/Biggs Army Airfield

The test team can “control” the winds by scheduling performance takeoffs for sunrise and by “cancel-weather” if the winds are more than 10 knots total or more than 5 knots of crosswind.

The rest of the variables in table 7 are under the pilot’s control. This is where the M&S approach is much more effective than Ken Lush’s empirical equations at adjusting for the pilot’s inputs.

This page was intentionally left blank.

ADVANTAGES AND DISANDVANTAGES OF USING KEN LUSH'S EQUATIONS

Ken Lush's equations and their United States Army Air Forces precursors were the state of the art for several decades, the 1940s through the 1960s. They remain in widespread use because the method is well known, it does not require aerodynamic or propulsive models, it requires a minimum amount of test day data, and it provides a quick answer. The method is documented in many aircraft design and flight test books and is still taught at the United States Air Force Test Pilot School and at the United States Navy Test Pilot School. The following data are required for a turbojet aircraft:

1. Aircraft gross weight at brake release
2. Pressure altitude
3. Ambient air temperature
4. Headwind or tailwind component
5. Runway slope
6. Ground roll distance from brake release
7. Air phase or total distance from brake release to 50 feet AGL
8. Airspeed at mainwheel liftoff
9. Elapsed time from mainwheel liftoff to achieving 50 feet AGL
10. Mean thrust for the test day conditions
11. Mean thrust for the reference day conditions

The first nine items are relatively easy to acquire. (However, they are challenging to acquire accurately.) The last two, the mean thrust values, are more difficult to obtain without access to an installed engine model. In the absence of an installed engine model some engineers have used one or more of the following assumptions:

1. Created a crude installed engine model using the 412 TW installed thrust stand to obtain ground level static, installed thrust and fuel flow data as a function of ambient air temperature and then assumed that the installed thrust for a given ambient air temperature was equal to $(F_N/\delta)\ \delta$ where the F_N/δ came from the installed thrust stand (and assume that the mean thrust was equal to the static thrust)
2. Used the thrust stand data from above but created a relationship for (F_N/σ) as a function of the ambient air density ratio, σ
3. Used uninstalled thrust data from the engine manufacturer
4. Assumed F_N/δ was independent of ambient air temperature (a very poor assumption)

These approaches introduced significant errors for aircraft with the old "dumb turbojets" even though these early turbojet engines had very simple mechanical or hydro-mechanical fuel controls with very little or no variable geometry. This approach is really not appropriate for modern turbojets or turbofan engines with a lot of variable geometry and very complex, full authority, digital engine controls (FADECs). Modern jet engines operate very differently to variations in flight conditions from the turbojets of the 1940s and 1950s. Anyone considering using Ken Lush's equations for an aircraft with modern, high-bypass ratio turbofans and variable geometry should do so with caution.

Besides the above thrust uncertainty there are four major disadvantages of using Ken Lush's equations versus an M&S approach:

1. The approach was not intended for use making large adjustments particular when standardizing to higher altitudes and/or hotter ambient air temperatures (lower aircraft performance).
2. There are limited adjustments available to correct for variations in pilot technique.

3. The exponents in the equations may not be appropriate for modern digital fuel controllers, engines with a lot of variable geometry, and/or high-bypass ratio turbofan engines.
4. The equations are not adaptable to use in analyzing takeoff performance with the loss of thrust in one engine.

These equations were developed to adjust for the day-to-day variations in pressure altitude, ambient air temperature, and aircraft gross weight. The assumption was that the test team would collect the test day data near the conditions that were desired. For example, they might test at a base near sea level, at Edwards AFB (near 2,000 feet elevation), at Holloman AFB (near 4,000 feet elevation), and at South Lake Tahoe, California (near 6,000 feet elevation).

Ken Lush's equations were developed and refined in the era of slide rules and paper spreadsheets. This was well before the introduction of large mainframe, digital computers, inflight thrust and status decks, refined aerodynamic models, INSs, and onboard tape recorders. The equations were developed to make relatively small adjustments to the test day results. They were never intended to be used for large corrections.

The following is from page 27 of reference 2 in 1952:

> *"It should be noted that these formulae should not be used to correct for big differences between test and standard conditions if the take-off acceleration is very low (for example if ($V_T^2/2g\ S_g$) is less than 0.1 in consistent units). For such cases any general method of standardization other than one based on interpolation between test data is liable to be inaccurate, and care should be taken either to make tests under near standard conditions or to cover a large enough range of test conditions to permit reliable interpolation or extrapolation."*

A similar warning is on page 2 of reference 3 from 1982:

> *"The methodology of R12, which is older than most of the authors children, has survived quite well. It is, however, characteristic of take offs that when takeoff performance is critical (marginal performance) the approximate corrections of R12 are least reliable. It is therefore imperative that the formulas not be used to extrapolate substantially in the direction of worsening performance. This is a general principle of performance standardization which is particularly important for takeoffs."*
>
> *"A further point is that with the present, much improved computer capability available use of simulation to standardize take offs is much easier. This is a much more reliable approach when takeoff performance is marginal and has, of course, been used fairly extensively by the Flight Dynamics Division."*

This technical approach to takeoff data reduction, Ken Lush's equations, was state of the art within the industry from the 1940s through the 1960s. It remained the recommended approach at the AFFTC until 1980 when it was replaced by a modeling and simulation approach using the NASA TOLAND software.

ADVANTAGES AND DISADVANTAGES OF USING MODELING AND SIMULATION

Using an M&S approach like AFFTC TOLAND has four major advantages relative to using Ken Lush's equations:

1. The range of validity for AFFTC TOLAND should be the same as for its aerodynamic models and propulsive models.
2. The engine status decks with installation effects should properly model the control logic of the modern, digital fuel controllers.
3. AFFTC TOLAND can adjust the data for most variations in pilot technique.
4. An M&S approach like TOLAND can be adapted to model one engine inoperative takeoff performance, which is the basis for all multi-engine flight manual takeoff capabilities.

Most flight test programs of modern aircraft have access to aerodynamic models including variations of skin friction drag with changes in Reynolds number and propulsive models with installation effects.

There are four disadvantages of using an M&S approach like AFFTC TOLAND versus Ken Lush's equations:

1. The M&S requires aerodynamic and propulsive models.
2. The M&S requires more test day data and more complex and expensive instrumentation.
3. The M&S requires more post-test data processing and data analyses.
4. The M&S requires more calendar time.

The required aerodynamic and propulsive models are normally available for a modern test aircraft. Most of the required instrumentation and data analyses tools are available because they are also used for other test points. If the models, the instrumentation, and the data analyses tools are not available; then additional work must be done to use AFFTC TOLAND or a different technical approach must be used. However, if the required data and tools are available, then an M&S approach will produce better results (less data scatter).

This page was intentionally left blank.

HOW GOOD IS THE MODELING AND SIMULATION METHOD?

Two evaluations of the takeoff performance of a Northrop T-38C aircraft were made and documented in the following pages and in appendix G. The first used the AFFTC TOLAND software and looked at the differences in airspeed or distance for a given takeoff adjusted to a reference set of conditions relative to the average of the adjusted airspeeds or distances. The differences were summarized in “data bins” based on the magnitudes of the differences.

The second evaluation used the data from the first evaluation. The root mean square (RMS) of the differences were summarized. The second evaluation also used the test day data and Ken Lush’s equations to re-standardize the data. Those results were also used to determine RMS values for the differences between the standardized airspeeds and distances and the averages of the differences. The RMS values for Ken Lush’s equations and AFFTC TOLAND could be compared.

The results in this section are from a series of flight tests flown between 2001 and 2010 as part of the Northrop T-38C PMP. Each takeoff was standardized to sea level, 15-degree C day, no runway slope, and a standard aircraft gross weight of 12,800 pounds. The standardized distance or speed was determined by equation 34.

The results are divided into five categories:

1. Distance from brake release to the rotation speed
2. Distance from brake release to mainwheel liftoff (takeoff ground roll)
3. Horizontal distance from brake release to 50 feet AGL
4. Airspeed at mainwheel liftoff
5. Airspeed at 50 feet AGL

The Northrop T-38C takeoff data were divided into data sets for this handbook. The data sets are defined in table G1. It should be noted a number of these takeoffs were performed in wind conditions higher than the accepted cutoff for good consistent data purposes of 5 to 10 knots headwind, no tailwind, and 5 knots crosswind. The engines were trimmed slightly different for each evaluation. Therefore the comparisons presented were the standardized values relative to the average standardized values for the appropriate data set.

DISTANCE TO ROTATION

The following summarizes the 147 standardized distances from brake release to rotation relative to the average standardized distance for the appropriate data set:

24 of 147 (16 percent) within ±10 feet
61 of 147 (41 percent) within ±25 feet
73 of 147 (50 percent) within ±32 feet
103 of 147 (70 percent) within ±50 feet
122 of 147 (82 percent) within ±75 feet
19 of 147 (13 percent) greater than 100 feet
4 of 147 (3 percent) greater than 150 feet

The standardized distances from brake release to rotation for 73 of the 147 takeoffs (50 percent) were within ±32 feet of the averages of the standardized distances. All 19 of the takeoffs with distance differences greater than 100 feet were from data sets one and three. Many of those takeoffs were flown in high and/or gusty winds. Even so, they only represented 13 percent of the 147 takeoffs.

The standardized rotation distances for 73 of the 147 takeoffs were within ±32 feet of the model predicted distance at the standard conditions. To put this in perspective, the length of the T-38C aircraft was 46 feet.

GROUND ROLL DISTANCE

The following summarizes the 147 standardized ground roll distances for brake release to mainwheel liftoff, takeoff, relative to the average standardized distance for the appropriate data set:

26 of 147 (18 percent) within ±10 feet
51 of 147 (35 percent) within ±25 feet
73 of 147 (50 percent) within ±40 feet
80 of 147 (54 percent) within ±50 feet
93 of 147 (63 percent) within ±75 feet
105 of 147 (71 percent) within ±100 feet
42 of 147 (29 percent) greater than ±100 feet
31 of 147 (21 percent) greater than ±125 feet
16 of 147 (11 percent) greater than ±150 feet
10 of 147 (7 percent) greater than ±175 feet
7 of 147 (5 percent) greater than ±200 feet
5 of 147 (3 percent) greater than ±225 feet
5 of 147 (3 percent) greater than ±250 feet

Almost all, except one value in data set number eight, of the standardized distances that varied by more than 100 feet from the average distances, were from data sets one, two and three: the data sets with the high/gusty winds. Even with those distances included in the summary, half (73 of 147) of the differences were within ±40 feet of the average values.

The following summarizes the 49 standardized ground roll distances relative to the average standardized distance for their appropriate data set for data sets four through nine, those with the lighter/less gusty winds:

15 of 49 (31 percent) within ±10 feet
23 of 49 (47 percent) within ±18 feet
25 of 49 (51 percent) within ±19 feet
29 of 49 (59 percent) within ±25 feet
43 of 49 (88 percent) within ±50 feet
47 of 49 (96 percent) within ±75 feet
48 of 49 (98 percent) within ±100 feet
49 of 49 (100 percent) within ±175 feet

Half of the distances for this reduced set were within ±19 feet of the average standardized distance for their appropriate data set. The 19 feet is significantly less than the length of the T-38 fuselage, 46 feet, and is less than 1 percent of the TOLAND predicted takeoff distance for the T-38 on a sea level standard day, 2,657 feet.

TOTAL TAKEOFF DISTANCE TO 50 FEET AGL

The following summarize the 147 standardized distances from brake release to 50 feet AGL relative to the average standardized value for the appropriate data set:

25 of 147 (17 percent) within ±25 feet
50 of 147 (34 percent) within ±50 feet
69 of 147 (47 percent) within ±75 feet
73 of 147 (50 percent) within ±77 feet
88 of 147 (60 percent) within ±100 feet
106 of 147 (72 percent) within ±150 feet
114 of 147 (78 percent) within ±200 feet
119 of 147 (81 percent) within ±250 feet
123 of 147 (84 percent) within ±300 feet

Sixty percent, 88 of 147, of the distances from brake release to 50 feet AGL were within ±100 feet for all 147 takeoffs, all nine data sets. Eighty-four percent, 41 of 49, of the distances were within ±100 feet for data sets 4 through 9.

The following summarizes the 49 standardized distances from brake release to 50 feet AGL relative to the average standardized distance for their appropriate data set for data sets four through nine, those with the lighter/less gusty winds:

14 of 49 (29 percent) within ±25 feet
24 of 49 (49 percent) within ±43 feet
26 of 49 (53 percent) within ±44 feet
28 of 49 (57 percent) within ±50 feet
37 of 49 (76 percent) within ±75 feet
41 of 49 (84 percent) within ±100 feet
46 of 49 (94 percent) within ±125 feet
46 of 49 (94 percent) within ±150 feet
48 of 49 (98 percent) within ±175 feet
48 of 49 (98 percent) within ±200 feet
49 of 49 (100 percent) within ±210 feet

Half the distances for this reduced set were within ±44 feet of the average standardized distance for their appropriate data set. This is approximately the length of the T-38 fuselage, 46 feet. It is less than 1 percent of the TOLAND predicted distance to 50 feet AGL, 4,758 feet.

AIRSPEED AT MAINWHEEL LIFTOFF (TAKEOFF)

The following summarizes the 147 standardized airspeeds at mainwheel liftoff (takeoff) relative to the average standardized value for the appropriate data set:

44 of 147 (30 percent) within ±0.5 KCAS
73 of 147 (50 percent) within ±1.0 KCAS
90 of 147 (61 percent) within ±1.5 KCAS
112 of 147 (76 percent) within ±2.0 KCAS
131 of 147 (89 percent) within ±3.0 KCAS
139 of 147 (95 percent) within ±4.0 KCAS
145 of 147 (99 percent) within ±5.0 KCAS

All of the standardized airspeeds at mainwheel liftoff that differed by more than ±4.0 KCAS from their appropriate average standardized airspeed were from data sets one, two, or three: the data sets with high/gusty winds. Half of the values were within ±1.0 KCAS even when those high/gusty wind flights were included. The average standardized airspeed at mainwheel liftoff for all 147 takeoffs was 0.5 knot less than the TOLAND model predicted airspeed for the reference day conditions.

The following summarizes the 49 standardized airspeeds at mainwheel liftoff (takeoff) relative to the average standardized airspeed for their appropriate data set for data sets four through nine, those with the lighter/less gusty winds.

26 of 49 (53 percent) within ±0.5 KCAS
37 of 49 (76 percent) within ±1.0 KCAS
44 of 49 (90 percent) within ±1.5 KCAS
47 of 49 (96 percent) within ±2.0 KCAS
48 of 49 (98 percent) within ±3.0 KCAS
49 of 49 (100 percent) within ±4.0 KCAS

Over half of the standardized airspeeds at mainwheel liftoff were within ±0.5 KCAS of the average standardized airspeeds for their appropriate data set using the reduced data set. Ninety-six percent were within ±2.0 KCAS and 100 percent were within ±4.0 KCAS. The standardized takeoff speed compared to the TOLAND predicted speed was considered acceptable accuracy.

AIRSPEED AT 50 FEET AGL

The following summarizes the 147 standardized airspeeds at 50 feet AGL relative to the average standardized value for the appropriate data set:

31 of 147 (21 percent) within ±0.5 KCAS
58 of 147 (39 percent) within ±1.0 KCAS
72 of 147 (49 percent) within ±1.2 KCAS
78 of 147 (53 percent) within ±1.3 KCAS
84 of 147 (57 percent) within ±1.5 KCAS
100 of 147 (68 percent) within ±2.0 KCAS
117 of 147 (80 percent) within ±2.5 KCAS
124 of 147 (84 percent) within ±3.0 KCAS
134 of 147 (91 percent) within ±4.0 KCAS
141 of 147 (96 percent) within ±5.0 KCAS
142 of 147 (97 percent) within ±6.0 KCAS

All of the standardized airspeeds at 50 feet AGL that differed by more than ±5.0 KCAS from their appropriate average standardized airspeed were from data sets one, two, or three: the data sets with high/gusty winds. Half of the values were within ±1.3 KCAS even when those high/gusty wind flights were included. The average standardized speed at 50 feet AGL was 1 knot higher than the TOLAND model predicted speed at standardized conditions.

The following summarizes the 49 standardized airspeeds at 50 feet AGL relative to the average standardized airspeed for their appropriate data set for data sets four through nine, those with the lighter/less gusty winds:

11 of 49 (22 percent) within ±0.5 KCAS
18 of 49 (37 percent) within ±1.0 KCAS
25 of 49 (51 percent) within ±1.5 KCAS
32 of 49 (65 percent) within ±2.0 KCAS
38 of 49 (78 percent) within ±2.5 KCAS
42 of 49 (86 percent) within ±3.0 KCAS
48 of 49 (98 percent) within ±4.0 KCAS
49 of 49 (100 percent) within ±5.0 KCAS

Over half of the standardized airspeeds at 50 feet AGL were within ±1.5 KCAS of the standardized average for their appropriate data set using this reduced data set. Sixty-five percent were within ±2.0 KCAS and 100 percent were within ±5.0 KCAS.

SUMMARY

These results, although specifically for the T-38C aircraft, show the reader the data scatter that should be expected in their standardized data using software similar to the AFFTC TOLAND software. The instrumentation of the T-38C test aircraft was typical of that used on military test aircraft at Edwards AFB. The one exception was the five samples per second update rate for the EGI on the data bus. Refresh rates of 10 to 20 samples per second are more typical. The higher update rates would have reduced the data scatter.

This page was intentionally left blank.

COMPARISON OF RESULTS USING BOTH TOLAND AND KEN LUSH'S EQUATIONS

TEST DAY DATA

Test day data from data sets four through nine, table G1, were standardized using Ken Lush's equations: Equations 18 through 20, 24, and 30. The test day data were divided into data sets because of aircraft and/or engine differences. The J85-GE-5 engines required several hardware component changes during the test programs that required retrimming the engines. The significant difference for data set four was the use of a different trailing edge flap deflection, 27 versus 20.25 degrees (60 versus 45 percent).

STANDARDIZED DATA

The test day ground roll distances and air phase distances, mainwheel liftoff to 50 feet AGL, were standardized to:

1. Sea level pressure altitude
2. Standard day ambient air temperature, 59 degrees F or 15 degrees C
3. No wind
4. Flat runway (no slope)
5. 12,800 pounds aircraft gross weigh at brake release
6. 1 degree noseup aircraft pitch angle until rotation speed
7. 140 KCAS rotation speed
8. Rotate to 7.50 degrees aircraft pitch angle at 1.66 degrees per second
9. Maintain 7.50 degrees aircraft pitch angle through 50 feet AGL
10. Rolling coefficient of friction of 0.015

<u>Ground Roll Distance:</u>

The average standardized ground roll distances were summarized in table 9 for each data set for both data processing methods. The differences in the averages for each data set varied from 25 feet for data set five to 267 feet for date set seven.

Table 9 Average Standardized Ground Roll Distances

Data Set	Number of Takeoffs	Average Standardized Ground Roll Distance (ft)		
		TOLAND	Lush	Difference
4	6	2,618	2,427	-191
5	15	2,676	2,651	-25
6	8	2,739	2,792	53
7	4	2,673	2,940	267
8	11	2,698	2,596	-102
9	5	2,701	2,791	90

Notes: 1. The takeoffs for data set four used 60 percent (27 degrees) trailing edge flaps. The takeoffs for the other data sets used 45 percent (20.25 degrees) trailing edge flaps.
2. The difference column is the Lush distance less the TOLAND distance.

Most of the differences originated in the averages using the Ken Lush equations.

The average of the 43 standardized ground roll distances obtained using TOLAND was 2,696 feet for data sets five through nine. (Data set four was not included in this average because its takeoffs used a different flap setting.) The averages obtained using TOLAND for the individual data sets varied from 2,673 feet (data set seven) to 2,739 feet (data set six). Those two averages were within 43 feet of the average for all five data sets obtained using TOLAND, 2,696 feet.

The average of the 43 standardized ground roll distances obtained using Ken Lush's equations was 2,706 feet for data sets five through nine. That was only 10 feet more than the average using TOLAND. The averages were similar but the Ken Lush results had more data scatter. The averages for the Ken Lush derived standardized ground roll distances ranged from 2,596 feet for data set eight to 2,940 feet for data set seven. Those corresponded to 110 feet shorter to 234 feet longer than the average for all 43 takeoff ground rolls.

Table 10 shows the data scatter within each data set for the standardized ground roll distances of each takeoff relative to the average distance for its data set. The values are root-mean-square (RMS) values. The individual differences were squared, the squared values were added together, the sum was divided by the number of takeoffs within the data set, and the RMS value was the square root. The RMS values for the TOLAND data were approximately 30 feet, 18 to 59 feet. The corresponding RMS values for the Ken Lush results were much larger, 112 to 642 feet.

Table 10 Data Scatter Relative to the Data Set Averages for the Standardized Ground Roll Distances

Data Set	Number of Takeoffs	Difference (RMS) from the Data Set Average Standardized Ground Roll Distance (ft)	
		TOLAND	Lush
4	6	43	112
5	15	24	148
6	8	34	156
7	4	18	133
8	11	59	187
9	5	22	642

The large RMS value for data set nine using Ken Lush's equations, 642 feet, was primarily from flight number 564. The standardized ground roll distances for flight number 564 were 2,713 feet using TOLAND and 4,036 feet using Ken Lush's equations. The standardized ground roll distances using Ken Lush's equations for data set number 9 ranged from a low of 2,240 feet (flight number 561) to a high of 4,036 feet (flight number 564) with an average for the five takeoffs of 2,791 feet. The equivalent distances using TOLAND ranged from a low of 2,667 feet (flight number 561) to a high of 2,733 feet (flight number 562) with an average for the five takeoffs of 2,701 feet.

The larger variability of the standardized distances obtained with Ken Lush's equations were primarily two-fold: They did not correct for variations in the rotation speed or for variations in the pitch rate during rotation. (The aircraft normally lifted off before achieving the target pitch angle for climbout.)

Air Phase Distance:

The average standardized air phase distances were summarized in table 11 for each data set for both data processing methods. The differences in the averages for each data set varied from 99 feet for data set nine to 530 feet for data set five. Again most of the differences originated in the averages using the Ken Lush equations.

Table 11 Average Standardized Air Phase Distances

Data Set	Number of Takeoffs	Standardized Air Phase Distance (ft)		
		TOLAND	Lush	Difference
4	6	1,969	1,863	-106
5	15	2,240	1,710	-530
6	8	2,311	1,940	-371
7	4	2,280	1,840	-440
8	11	2,250	1,953	-297
9	5	2,231	2,132	-99

Notes: 1. The takeoffs for data set four used 60 percent (27 degrees) trailing edge flaps. The takeoffs for the other data sets used 45 percent (20.25 degrees) trailing edge flaps.
2. The difference column is the Lush distance less the TOLAND distance.

The average of the 43 standardized air phase distances using TOLAND was 2,258 feet for data sets five through nine. The averages for the individual data sets varied from 2,231 feet (data set nine) to 2,311 feet (data set six). Those two averages were within 53 feet of the average for all five data sets, 2,258 feet.

The average of the 43 standardized air phase distances obtained using Ken Lush's equations was 1,876 feet for data sets five through nine. That distances was 382 feet shorter than the one determined with the TOLAND software. The most likely cause of the shorter distance with Ken Lush's equations versus using TOLAND was that the Ken Lush equations did not correct for variations in the aircraft pitch angle during climbout. The pilots almost always overshot the target of 7.50 degrees.

Table 12 shows the data scatter within each data set for the standardized air phase distances of each takeoff relative to the average distance for its data set. The RMS values for the TOLAND data were approximately 70 feet, 49 to 91 feet. The corresponding RMS values for the Ken Lush results were much larger, 167 to 583 feet.

Table 12 Data Scatter Relative to the Data Set Averages for the Standardized Air Phase Distances

Data Set	Number of Takeoffs	Difference (RMS) from the Data Set Average Standardized Ground Roll Distance (ft)	
		TOLAND	Lush
4	6	62	221
5	15	75	239
6	8	72	167
7	4	91	234
8	11	49	583
9	5	82	279

Note: The takeoffs for data set four used 60 percent (27 degrees) trailing edge flaps. The takeoffs for the other data sets used 45 percent (20.25 degrees) trailing edge flaps.

The larger variability of the standardized distances obtained with Ken Lush's equations were primarily due to the flight-to-flight variability in the pilot's ability to rotate to and maintain the target pitch angle of 7.50 degrees. The TOLAND-based data processing corrected for the pitch angle variability. Ken Lush's equations did not.

APPLICABILITY OF KEN LUSH'S EQUATIONS

The method known as Ken Lush's equations evolved in the 1930s and 1940s to make small corrections to test day takeoff results. It was intended to correct for day-to-day variations at a given airfield. The variables it corrected for are:

1. Pressure altitude
2. Ambient air temperature
3. Headwind/tailwind components
4. Runway slope
5. Aircraft gross weight

The equations were never intended to correct for large variations. If you wanted data at sea level, you tested near sea level. If you wanted data at 5,000 feet pressure altitude and 100 degrees F, you tried to test there.

The modern high bypass ratio turbofans with digital electronic fuel controllers are significantly different than the "dumb turbojets" of the 1940s and early 1950s. In general, the performance of the newer engines do not collapse when normalized. An engine thermodynamic-based cycle deck is required to model their performance. The results using Ken Lush's equations presented in this handbook for J85-GE-5 turbojets installed in a Northrop T-38C aircraft are not typical of what would be expected with a modern turbofan or turbojet engine with a digital electronic fuel controller.

The most significant limitation when using the equations to make relatively small adjustments is the inability to correct for the pilot-to-pilot and flight-to-flight variabilities in the aircraft rotation speed and pitch angle time histories Those test day variabilities are easily handled with the TOLAND software.

CONCLUSIONS

There is still a significant percentage of the engineers, managers, and pilots within the flight test community who believe that "takeoffs are too dynamic to be analyzed". While that may be true using handheld data and Ken Lush's equations for data standardization, it is certainly not true if one uses a modern, instrumented aircraft and a modeling and simulation approach, like TOLAND, for data standardization.

The Air Force Flight Test Center (AFFTC), now the Air Force Test Center (AFTC), at Edwards AFB has used the TOLAND simulation since the late 1970s. It has been the AFFTC preferred method for takeoff data standardization since the early 1980s. It has successfully stood the test of time.

One criticism of using TOLAND is that the engineer needs in and out of ground effect aerodynamic models plus an installed propulsive model. These are almost always available for a modern aircraft. The engineer can create models if they are not available to get started. As flight test data becomes available, the models can then be refined.

Bottom line: The M&S approach for standardizing takeoff data has been successfully used on a wide variety of aircraft at the AFFTC for over 35 years. It produces significantly better results than Ken Lush's equations and should continue to be used.

This page was intentionally left blank.

REFERENCES

1. Carroll, Thomas, *A Comparison of the Take-off and Landing Characteristics of a Number of Service Airplanes*, National Advisory Committee for Aeronautics (NACA) Report number 249, NACA-TR-249, Langley Memorial Aeronautical Laboratory, 1927.
2. Lush, Kenneth J., *Standardization of Take-off Performance Measurements for Airplanes*, AFFTC Technical Note R-12, AFFTC, Edwards AFB, California, 1952.
3. Lush, Kenneth J., *Standardization of Take-off Performance Measurements for Airplanes Corrigendum to AFFTC Technical Note R12*, AFFTC, Edwards AFB, California, May 1982.
4. Bowles, Jeff V. and Thomas L. Galloway, *Computer Programs for Estimating Takeoff and Landing Performance*, NASA Technical Memo (TM) X-62333, NASA Ames Research Center, Moffett Field, California, October 1973.
5. *Performance and Flying Qualities UFTAS Reference Manual*, Computer Sciences Branch, AFFTC, Edwards AFB, California, October 1984.
6. *Performance and Flying Qualities UFTAS Link 13 User Guide*, Computer Sciences Branch, AFFTC, Edwards AFB, California, March 1991.
7. Olson, Wayne M., and Yvonne L. Sell, *Fighter Aircraft Dynamic Performance*, presented at the SFTE Fourteenth Annual Symposium, Newport Beach, California, 15 through 19 August 1983.
8. Olhausen, J.N., *The Use of a Navigation Platform for Performance Instrumentation on the YF-16 Flight Test Program*, Presented at the American Institute of Aeronautics and Astronautics (AIAA) Thirteen Aerospace Sciences meeting in Pasadena, California, January 1975. Also published as AIAA Paper 75-32.
9. Olhausen, J.N., *Use of a Navigation Platform for Performance Instrumentation on the YF-16*, AIAA Journal of Aircraft, Volume 13, Number 4, April 1976.
10. Olhausen, James N., *F-16 Progress in Performance Flight Testing Using an Inertial Navigation Unit*, presented at the Eighth Annual Symposium in Washington, D.C., August 1977.
11. Mahlum, Ron W., *AFFTC Aircraft Horizontal Thrust Stand Evaluation and Operation Update*, AFFTC-TIH-76-05, AFFTC, Edwards AFB, California, August 1977.
12. Standley, Kent, *AFFTC TOLAND User's Guide*, AFFTC-TIH-96-02, AFFTC, Edwards AFB, California, October 1996.
13. Brown, Frank S., *Determining Pitot Static Position Error Corrections in Ground Effect*, 412TW-TIH-19-02, 412th Test Wing, Edwards AFB, California, to be published.
14. Cheney, H.K., *YC-15 STOL Performance Flight Test Methods and Results*, presented at the SFTE Eighth Annual Symposium in Washington, D.C., August 1977.
15. Cheney, H.K., *Takeoff Performance Data Using Onboard Instrumentation*, presented at the SFTE Fourteenth Annual Symposium in Newport Beach, California, August 1983.
16. Cheney, H.K., *A Procedure for Determining Flight Path Wind Components During Takeoff and Landing Tests*, AIAA-83-2741, presented at the 2nd Flight Testing Conference, Las Vegas, Nevada, November 1983.

17. Taylor, Albert E., *Evaluation of Take-off and Landing Facility*, AFFTC Technical Memorandum FTFF-TM-58-12, AFFTC, Edwards AFB, California, April 1958.

18. Eichhorst, Ingo B., *Comparison of Takeoff Performance from Measurements with ASKANIA Cameras and an Inertial Navigation System*, Flight Test Technology Branch Office Memorandum, 412 TW, AFFTC, Edwards AFB, California, April 1973.

19. Pool, A., J.L. Simons, G.J.H. Wensink, and A.J.L. Willekens, *A Method for Measuring Take-off and Landing Performance of Aircraft, Using an Inertial Sensing System*, presented at the NATO Advisory Group for Aeronautical Research and Development (AGARD) Flight Mechanics Panel Symposium on Subsystems Testing and Flight Test Instrumentation, Geilo, Norway, 27-30 October 1980.

20. Brown, Frank, *Use of On-board Inertial Navigation System Data Instead of ASKANIA Data for Takeoff Performance Determination*, AFFTC-TLR-88-06, AFFTC, Edwards AFB, California, 26 January 1989.

21. Brown, Frank S., *Use of Onboard Data for Takeoff Performance Determination*, presented at the SFTE Twentieth Annual Symposium, Reno, Nevada, 18-21 September 1989.

22. Woolf, Reagan K. and Benjamin J. Reid, *T-38C Aircraft Performance Evaluation*, AFFTC-TR-03-18, AFFTC, Edwards AFB, California, September 2004.

23. Haubelt, Lane C., First Lieutenant (USAF) and Roger J. Tanner, *T-38C Takeoff Flap Evaluation*, AFFTC-TR-07-10, AFFTC, Edwards AFB, California, October 2007.

24. To, Lan, *T-38C/J85-GE-5S Synthetic Paraffinic Kerosene/JP-8 Fuel Blend (SJ-8) Aircraft Performance Testing*, AFFTC-TR-09-45, AFFTC, Edwards AFB, California, October 2009.

25. Tanner, Nicholas A. and Mark A. Sherrier, *T-38C Propulsion Modernization Program (PMP) Engine Bay Overheat Resolution Aircraft Performance Evaluation*, AFFTC-TR-10-52, AFFTC, Edwards AFB, California, May 2011.

26. Bikle, Paul F., *Performance Flight Testing Methods in Use by the Flight Section*, Army Air Forces Technical Report Number 5069, War Department, Army Air Forces Material Command, Dayton, Ohio, 15 January 1944.

27. Twisdale, Thomas R., Lieutenant (USAF), *Take-off Standardization*, Flight Test Technology Branch Office Memo, AFFTC, Edwards AFB, California, June 1971.

28. Batt, James T., *F-15C Limited Takeoff and Landing Evaluation*, AFFTC-TR-81-18, AFFTC, Edwards AFB, California, September 1981.

29. Summerell, C.J., MSgt, *The Weather at AFFTC Climatological Data – 1943 – 1980*, AFFTC Technical Memorandum 81-1, Detachment 21, 2d Weather Squadron (MAC), AFFTC, Edwards AFB, California, March 1981.

30. Rarick, Bradley A., SSgt, *The Weather at AFFTC Climatological Data – 1943 – 1983*, AFFTC Technical Information Memorandum 84-2, Detachment 21, 2nd Weather Squadron (MAC), AFFTC, Edwards AFB, California, March 1984.

31. Keates, Gregory D., MSgt, *The Weather at AFFTC Climatological Data – September 1943 – December 1986*, AFFTC Technical Memorandum 87-1, Detachment 21, 2nd Weather Squadron (MAC) AFFTC, Edwards AFB, California, August 1987.

32. Hamlin, Benson, *Flight Testing Conventional and Jet-propelled Airplanes*, the Macmillan Company, New York, New York, 1946.

33. Perkins, Courtland D. and Robert E. Hage, *Airplane Performance Stability and Control*, John Wiley & Sons, New York, New York, 1949.

34. Herrington, Russel M., Major USAF, Paul E. Shoemaker, Captain USAF, Eugene P. Bartlett, First Lieutenant USAF, and Everett W. Dunlap, *Flight Test Engineering Handbook*, Air Force Technical Report Number 6273, AFFTC, Edwards AFB, California, May 1951, corrected and revised June 1964.

35. *Flight Test Manual Volume I Performance*, NATO AGARD, January 1956.

36. *Performance Flight Test Techniques*, FTC-TIH-64-2006, USAF Aerospace Research Pilot School, Edwards AFB, California, 1965.

37. Kimberlin, Ralph D., *Performance Flight Testing Lecture Notes*, University of Tennessee Space Institute, Tullahoma, Tennessee, 1966.

38. *Performance Volume II of III Performance Flight Testing Theory*, FTC-TIH-70-1001, USAF Test Pilot School, Edwards AFB, California, revised January 1973.

39. *Performance Volume III of III Performance Flight Test Techniques*, FTC-TIH-70-1001, USAF Test Pilot School, Edwards AFB, California, revised January 1973.

40. *Flight Dynamics Division Volume I Performance*, 6520th Test Group, AFFTC, Edwards AFB, California, January 1982.

41. *Volume 1 Aircraft Performance*, Chapter 8, Takeoff and Landing Performance, USAF Test Pilot School, Edwards AFB, California, July 1987.

42. *Volume I Performance Phase*, Chapter 8, Takeoff & Landing Performance, USAF Test Pilot School, Edwards AFB, California, January 1993.

43. *Aircraft Performance*, Chapter 3, Takeoff & Landing Performance, Performance Branch, USAF Test Pilot School, Edwards AFB, California, December 2002.

44. Kimberlin, Ralph D., *Flight Testing of Fixed-wing Aircraft*, AIAA., Reston, Virginia, 2003.

45. Ward, Don, Thomas Strganac, and Rob Niewoehner, *Introduction to Flight Test Engineering*, third edition, Kendall/Hunt Publishing Company, Dubuque, Iowa, 2006.

46. *Full Flight Performance Testing*, The Bulletin of the Airplane Engineering Department U.S.A., War Department, Bureau of Aircraft Production, Airplane Engineering Department, McCook Field, Dayton, Ohio, Volume I, number 2, July 1918.

47. Norton, F.H., and E.P. Warner, *Preliminary Report on Free Flight Tests*, NACA-TR-70, Government Printing Office, Washington, D.C., 1920.

48. Carroll, T., *A Study of Taking Off and Landing an Airplane*, NACA-TR-154, Langley Memorial Aeronautical Laboratory, Washington, D.C., 1923.

49. Diehl, Walter S. and E.P. Lesley, *The Reduction of Airplane Flight Test Data to Standard Atmosphere Conditions*, NACA-TR-216, Government Printing Office, Washington, D.C., 1925.

50. Proll, A., *Take-off Distance for Airplanes*, NACA Technical Memorandum (TM) NACA-TM-381, Government Printing Office, Washington, D.C., September 1926.

51. Reid, Elliott G. and Thomas Carroll, *A Warning Concerning the Take-off with Heavy Load*, NACA-TN-258, Washington D.C., July 1927.

52. Wieselsberger, C., *Wing Resistance Near the Ground*, NACA-TM-77, Washington, D.C., April 1922.

53. Reid, Elliott G., *A Full-scale Investigation of Ground Effect*, NACA-TR-265, Government Printing Office, Washington, D.C., 1927.

54. Von Baumhauer, A.G., *Photographic Time Studies of Airplane Paths*, NACA-TM-345, Washington, D.C., January 1926.

55. Hall, Donald A., *Technical Preparation of the Airplane "Spirit of St. Louis*", NACA-TN-257, Washington D.C., July 1927.

56. Lindbergh, Charles A., *The Spirit of St. Louis*, Charles Scribner's Sons, New York, New York, 1953, reprinted by Avon Books, New York, New York, 1985 as a paperback book.

57. Lachmann, G., *Experiments with Slotted Wings*, NACA-TN-71, Washington, D.C., November 1921.

58. Lachmann, G., *Results of Experiments with Slotted Wings*, NACA-TM-282, Washington, D.C., 1924.

59. Weick, Fred E. and Joseph A. Shortal, *The Effect of Multiple Fixed Slots and a Trailing Edge Flap on the Lift and Drag of a Clark Y Airfoil*, NACA-TR-427, Washington, D.C., 1932.

60. Weick, Fred E. and Robert C. Platt, *Wind-Tunnel Tests of the Fowler Variable-Area Wing*, NACA-TN-419, Washington, D.C., May 1932.

61. Wetmore, J.W., *Calculated Effect of Various Types of Flap on Take-off Over Obstacles*, NACA TN-568, Washington, D.C., May 1936.

62. Diehl, Walter, S., *The Calculation of Take-off Run*, NACA-TR-450, Washington, D.C., 1934.

63. Hartman, Edwin P., *Considerations of the Take-off Problem*, NACA-TN-557, Washington, D.C., February 1936.

64. Wetmore, J.W., *The Transition Phase in the Take-off of an Airplane*, NACA-TR-626, Washington, D.C., January 1938.

65. Proll, A., *Take-off of Heavily Loaded Airplanes*, NACA-TM-460, Washington, D.C., April 1928.

66. Breguet, Louis, *On the Take-off of Heavily Loaded Airplanes*, NACA-TM-489, Washington, D.C., November, 1928.

67. Diehl, Walter S., *The Reduction of Observed Airplane Performance to Standard Conditions*, NACA-TR-297, Washington, D.C., 1929.

68. Schrenk, Martin, *Take-off and Propeller Thrust*, NACA-TM-703, Washington, D.C., April 1933.

69. Shoemaker, James M. and John R. Dawson, *The Effect of Trim Angle on the Take-off Performance of a Flying Boat*, NACA-TN-486, Washington, D.C., January 1934.

70. Thompson, F.L., W.C Peck, and A.P. Beard, *Air Conditions Close to the Ground and the Effect on Airplane Landings*, NACA-TR-489, Washington, D.C., 1935.

71. Platt, Robert C. *Aerodynamic Characteristics of a Wing with Fowler Flaps Including Flap Loads, Downwash, and Calculated Effect on Take-off*, NACA-TR-534, Washington, D.C., 1935.

72. Le Sueur, Maurice, *Ground Effect on the Take-off and Landing of Airplanes*, NACA-TM-771, Washington, D.C., July 1935.

73. Wetmore, J.W., *The Rolling Friction of Several Airplane Wheels and Tires and the Effect of Rolling Friction on Take-off*, NACA-TR-583, Washington, D.C, 1937.

74. Rockefeller, W.C., *General Airplane Performance*, NACA-TR-654, Washington, D.C., 1939.

75. Rosengarten, Nathan Robert, Major, Air Corps, *Performance Flight Testing Methods on Jet Propelled Aircraft as used by the Flight Section*, Army Air Forces Technical Report Number 5239, Flight Research Branch, Flight Section, Wright Field, Ohio, 22 June 1945.

76. Turner, L. Richard, *Consideration of Auxiliary Jet Propulsion for Assisting Take-off*, NACA Advance Confidential Report (Wartime Report), NACA-WR-E-49, Washington, D.C., May 1940.

77. Bond, Aleck C. and Joseph G. Thibodaux, Jr., *Flight Test of the Aerojet 7KS-6000 T-27 JATO Rocket Motor*, NACA-RM-SL9L 13a, Washington, D.C., 20 December 1949.

78. Rollins, Francis W. and Corporal Leonard Friedman, *Discussion of Recent Takeoff and Landing Performance Test Development*, Army Air Forces Technical Report Number 5172, War Department Army Air Forces Air Technical Service Command, Dayton, Ohio, 25 November 1944.

79. Kiehle, M.H. and A. Vantine, *A Consideration of Calculated Versus Flight Test Take-off Performance*, Journal of the Aeronautical Sciences, volume 12, number 3, July 1945, pages 263-272.

80. Bohanon, H.R. and E. C. Wilcox, *Theoretical Investigation of Thrust Augmentation of Turbojet Engines by Tail-pipe Burning*, NACA RM Number E6L02, Washington, D.C., January 28, 1947.

81. Hall, Eldon W. and E. Clinton Wilcox, *Theoretical Comparison of Several Methods of Thrust Augmentation for Turbojet Engines*, NACA RM Number E8H11, Washington, D.C., October 27, 1948.

82. Jackson, G. and J. K. Lush, *The Reduction to Standard Conditions of Take-off Measurements on Turbo-jet Aircraft*, Reports and Memoranda Number 2890, British Aeronautical Research Council, London, England, June 1951 (republished in 1957).

83. Serebrisky, Y.M. and S.A. Biachuev, *Wind-tunnel Investigation of the Horizontal Motion of a Wing Near the Ground*, NACA-TM-1095, Washington, D.C., September 1946.

84. Gasich, Welco, E., *Experimental Verification of Two Methods for Computing the Take-off Ground Run of Propeller-driven Aircraft*, NACA-TN-1258, Washington, D.C., June 1947.

85. Weick, Fred E., L.E. Flanagan, Jr., and H.H. Cherry, *An Analytical Investigation of Effect of High-lift Flaps on Take-off of Light Airplanes*, NACA-TN-2404, Washington, D.C., 1951.

86. Horton, Elmer A., Laurence K. Loftin, Jr., Stanley F. Racisz, and John H. Quinn, Jr., *Analysis of the Effects of Boundary-layer Control on the Take-off and Power-off Landing Performance Characteristics of a Liaison Type of Airplane*, NACA-TR-1057, Washington, D.C., 1951.

87. Hall, Albert W., *Take-off Distances of a Supersonic Transport Configuration as Affected by Airplane Rotation During the Take-off Run*, NASA TN D-982, Washington, D.C., October 1961.

88. Alias, Guiscardo S., *Notes on the Ground-run of Jet-propelled Aircraft During Landing and Takeoff*, AGARD Report 82, Paris, France, August 1956.

89. P. deBenque D'Augt, H. Riebeck, and A. Pool, *AGARD Flight Test Instrumentation Series Volume 16 on Trajectory Measurements for Take-off and Landing Tests and Other Short-range Applications*, AGARD-AG-160, Volume 16, January 1985.

90. Mindell, David A., *Digital Apollo*, MIT Press, Cambridge, Massachusetts, 2011.

91. Larson, Terry J. and William G. Schweikhard, *A Simplified Flight-Test Method for Determining Aircraft Takeoff Performance that Includes Effects of Pilot Technique*, NASA-TN D-7603, Washington, D.C., February 1974.

92. T.O. 1T-38C-1, USAF Series T-38C Aircraft Flight Manual, OO-ALC/558 ACSD/ENF, Hill AFB, Utah, 15 June 2008.

This page was intentionally left blank.

APPENDIX A - EDWARDS AFB SURFACE TEMPERATURES AND SURFACE PRESSURES

The purpose of the tables in this appendix is to provide the reader with:

1. An idea of the extreme ranges of pressure altitude that might occur on the runways
2. An idea of the "normal" low and high ambient air temperatures at the surface
3. An idea of the extreme ambient air temperatures at the surface

This information may be useful during the test planning phase of a test program. Can the required data be obtained at Edwards AFB or must the team deploy to a remote site?

The pressure altitude at Edwards AFB tends to be higher than the field elevation, 2,310 feet above sea level. A "normal" pressure altitude is typically between 2,300 and 2,500 feet.

Tables A1 and A2 present ambient air pressures at the surface from the minute-by-minute Base Weather observations recorded from their website. Data were also obtained from their half-hourly, daily observations. The half-hourly observations were recorded at 25 and at 55 minutes after the hour. Low surface pressures corresponded to pressure altitudes as high as 2,700 feet or higher. High surface pressures corresponded to pressure altitudes as low as 1,700 feet or lower.

Ambient air temperatures for "normal" low temperatures, typically near sunrise, and "normal" high temperatures, typically in the mid to late afternoon (1500 to 1600 local), are presented in tables A3 through A14. The "normal" air temperatures were identified by the Base Weather Office and were obtained from minute-by-minute surface observations. The "extreme" high and low ambient air temperatures were obtained from multiple Base Weather sources:

1. AFFTC Technical Memorandum 81-1, *The Weather at AFFTC Climatological Data–1943–1980* (reference 29)
2. AFFTC Technical Memorandum 84-2, *The Weather at AFFTC Climatological Data–1943–1983* (reference 30)
3. AFFTC Technical Memorandum 87-1, *The Weather at AFFTC Climatological Data-– September 1943 – December 1986* (reference 31)
4. Record MAX/MIN temperature climatology, (released semi-annually)
5. Daily climatic summary for Edwards AFB, California (released monthly)
6. Minute-by minute surface observations prior to 14 May 2014, (no longer available on the Base Weather website)

When inconsistences were found between the ambient air temperature data sources, the data from the daily climatic summaries were assumed to be correct.

In general, the extreme ambient air temperatures were approximately 15 and 110 degrees F for the time period between September 1943 and October 2019.

Table A1 Low Ambient Air Surface Pressures Recorded by the Edwards AFB Weather Office

Date (DDMMMYYYY)	Time (Z) (HH:MM)	Surface Pressure (in Hg)	Equivalent Pressure Altitude (ft)	Calculated Altimeter Setting (in Hg)
21 JAN 2010	21:55	26.679	3,139	29.02
22 JAN 2010	08:25	26.856	2,960	29.21
22 MAY 2008	01:25	27.038	2,777	29.41
07 DEC 2009	22:55	27.050	2,765	29.42
22 MAY 2008	21:02	27.080	2,735	29.45
20 JAN 2010	22:48	27.085	2,730	29.46
23 MAY 2008	11:25	27.100	2,715	29.47
31 JAN 2016	21:58	27.100	2,715	29.47
28 FEB 2014	22:32	27.154	2,661	29.54
19 JAN 2010	20:32	27.171	2,644	29.55
25 MAY 2012	01:53	27.171	2,644	29.56
19 JAN 2010	22:25	27.172	2,643	29.55
29 DEC 2010	21:56	27.174	2,641	29.56
30 NOV 2007	05:25	27.175	2,640	29.56
20 MAR 2011	02:54	27.182	2,633	29.57
14 APR 2009	23:25	27.185	2,630	29.56
17 MAR 2012	23:46	27.185	2,630	29.57
11 MAR 2006	11:55	27.187	2,628	29.56
01 DEC 2007	08:25	27.187	2,628	29.57
21 MAY 2008	02:25	27.191	2,624	29.57
20 FEB 2013	09:55	27.203	2,612	29.59
08 APR 2013	22:47	27.207	2,608	29.60
18 MAR 2012	09:55	27.211	2,604	29.60
23 MAY 2012	03:45	27.213	2,602	29.60
18 JAN 2010	20:25	27.214	2,601	29.59
25 MAY 2012	08:25	27.215	2,600	29.60
27 FEB 2010	21:25	27.223	2,592	29.60
03 OCT 2009	00:25	27.224	2,591	29.61
04 JUN 2008	00:55	27.225	2,590	29.61
10 MAR 2006	07:55	27.228	2,587	29.61
19 FEB 2013	07:55	27.228	2,587	29.62
04 OCT 2009	08:25	27.230	2,585	29.61
25 DEC 2008	21:25	27.232	2,583	29.61
15 NOV 2013	21:55	27.232	2,583	29.62
15 NOV 2016	21:55	27.232	2,583	29.62
29 MAY 2011	10:55	27.233	2,582	29.62
21 MAR 2011	08:25	27.235	2,580	29.63
28 APR 2004	01:55	27.237	2,578	29.62
21 SEP 2010	00:25	27.242	2,573	29.63
09 OCT 2013	22:19	27.242	2,573	29.63
13 FEB 2008	00:25	27.244	2,571	29.63

Table A1 Low Ambient Air Surface Pressures Recorded by the Edwards AFB Weather Office (Continued)

Date (DDMMMYYYY	Time (Z) (HH:MM)	Surface Pressure (in Hg)	Equivalent Pressure Altitude (ft)	Calculated Altimeter Setting (in Hg)
25 DEC 2003	23:55	27.246	2,569	29.63
21 APR 2010	23:55	27.250	2,565	29.63
19 DEC 2013	13:55	27.251	2,564	29.64
10 MAR 2006	00:57	27.252	2,563	29.63
04 MAY 2013	22:54	27.252	2,563	29.64
03 DEC 2013	23:28	27.252	2,563	29.64
28 MAY 2011	06:47	27.253	2,562	29.65
27 OCT 2009	17:25	27.254	2,561	29.64
14 SEP 2006	22:55	27.256	2,559	29.64
19 JUN 2009	00:55	27.256	2,559	29.64
26 FEB 2011	21:55	27.256	2,559	29.65
10 OCT 2008	23:55	27.257	2,558	29.64
06 MAR 2012	21:51	27.257	2,558	29.65
09 MAR 2006	03:55	27.261	2,554	29.64
14 APR 2013	00:53	27.262	2,553	29.65
27 OCT 2004	10:25	27.264	2,551	29.65
04 NOV 2011	00:16	27.265	2,550	29.66
22 APR 2010	11:25	27.266	2,549	29.65
07 JUN 2004	21:09	27.267	2,548	29.65
29 DEC 2004	11:55	27.267	2,548	29.65
30 AUG 2008	00:55	27.267	2,548	29.65
28 OCT 2013	10:25	27.267	2,548	29.66
25 SEP 2013	02:07	27.269	2,546	29.66
03 APR 2009	21:25	27.274	2,541	29.66
13 APR 2012	00:25	27.275	2,540	29.67
26 APR 2014	11:25	27.276	2,539	29.67
02 JUN 2013	23:53	27.278	2,537	29.67
08 APR 2011	23:56	27.279	2,536	29.67
28 MAY 2013	23:11	27.281	2,534	29.67
23 JUN 2003	00:55	27.282	2,533	29.67
20 OCT 2004	11:25	27.282	2,533	29.67
26 OCT 2004	00:55	27.282	2,533	29.67
22 SEP 2010	21:55	27.283	2,532	29.68
16 OCT 2006	23:25	27.284	2,531	29.67
16 JUN 2011	00:03	27.284	2,531	29.68
19 OCT 2004	04:55	27.285	2,530	29.67
03 FEB 2008	23:25	27.285	2,530	29.68
14 APR 2012	07:06	27.285	2,530	29.68
05 DEC 2009	22:55	27.286	2,529	29.67
30 APR 2013	22:46	27.286	2,529	29.68
08 DEC 2009	08:25	27.287	2,528	29.67
23 JAN 2010	08:25	27.289	2,526	29.68

Table A1 Low Ambient Air Surface Pressures Recorded by the Edwards AFB Weather Office (Concluded)

Date (DDMMMYYYY)	Time (Z) (HH:MM)	Surface Pressure (in Hg)	Equivalent Pressure Altitude (ft)	Calculated Altimeter Setting (in Hg)
07 APR 2011	22:25	27.289	2,526	29.68
31 AUG 2008	23:55	27.290	2,525	29.68
02 JUL 2010	00:55	27.291	2,524	29.69
27 OCT 2013	07:55	27.291	2,524	29.69
24 AUG 2007	00:31	27.292	2,523	29.68
13 DEC 2008	20:55	27.292	2,523	29.68
18 MAY 2011	17:24	27.292	2,523	29.69
06 JUN 2004	01:25	27.293	2,522	29.68
26 MAY 2006	23:55	27.293	2,522	29.68
22 SEP 2010	22:55	27.293	2,522	29.69
19 JUN 2011	01:12	27.293	2,522	29.69
21 MAY 2007	00:55	27.294	2,521	29.69
23 AUG 2007	00:25	27.294	2,521	29.68
28 AUG 2010	00:55	27.294	2,521	29.69
14 SEP 2013	00:55	27.294	2,521	29.69
13 APR 2013	02:29	27.295	2,520	29.69
16 DEC 2006	21:25	27.296	2,519	29.69
22 JUN 2009	01:25	27.296	2,519	29.68
18 FEB 2011	05:45	27.296	2,519	29.69
29 MAY 2013	01:55	27.296	2,519	29.69
03 JUN 2008	06:25	27.297	2,518	29.68
09 NOV 2008	13:25	27.297	2,518	29.68
10 APR 2009	23:25	27.297	2,518	29.68
20 JUN 2009	08:25	27.297	2,518	29.68
15 APR 2013	01:22	27.297	2,518	29.69
20 SEP 2010	00:25	27.298	2,517	29.69
13 DEC 2012	01:22	27.298	2,517	29.69
21 MAY 2006	02:55	27.299	2,516	29.68
29 MAR 2009	03:55	27.299	2,516	29.69
09 JUN 2012	01:01	27.299	2,516	29.69

Notes:
1. Most data were obtained between 01 JAN 2006 and 31 OCT 2013.
2. Pressure altitudes were calculated from the recorded surface pressures.
3. The field elevation at Edwards AFB was 2,302 feet prior to the opening of runway 04L/22R on 19 May 2008. The field elevation has been 2,310 feet since then.
4. The altimeter setting was calculated by the Base Weather Office software and is presented for reference only.

Table A2 High Ambient Air Surface Pressures Recorded by the Edwards AFB Weather Office

Date (DDMMMYYYY)	Time (Z) (HH:MM)	Surface Pressure (in Hg)	Equivalent Pressure Altitude (ft)	Calculated Altimeter Setting (in Hg)
10 JAN 2009	17:55	28.146	1,683	30.59
03 DEC 2007	17:38	28.145	1,684	30.60
30 NOV 2006	16:25	28.116	1,712	30.56
07 JAN 2007	17:25	28.116	1,712	30.57
03 DEC 2006	16:55	28.107	1,721	30.55
05 JAN 2006	16:25	28.103	1,725	30.54
23 DEC 2011	17:52	28.103	1,725	30.56
11 JAN 2009	08:25	28.083	1,744	30.52
22 OCT 2007	17:10	28.080	1,747	30.53
16 DEC 2004	17:55	28.079	1,748	30.52
17 DEC 2004	18:25	28.073	1,754	30.51
04 JAN 2006	07:25	28.073	1,754	30.51
22 DEC 2007	17:25	28.070	1,757	30.52
14 JAN 2014	17:09	28.069	1,758	30.52
15 JAN 2013	17:29	28.062	1,764	30.51
08 JAN 2007	17:25	28.061	1,765	30.51
01 JAN 2008	17:55	28.059	1,767	30.50
30 NOV 2010	16:55	28.058	1,768	30.51
02 DEC 2007	06:25	28.056	1,770	30.50
03 FEB 2011	17:00	28.052	1,774	30.50
16 DEC 2003	17:25	28.049	1,777	30.49
24 DEC 2011	17:45	28.048	1,778	30.50
13 JAN 2014	18:24	28.047	1,779	30.50
09 JAN 2009	07:55	28.042	1,784	30.48
10 DEC 1997	17:55	28.035	1,791	30.48
16 DEC 2003	16:22	28.035	1,791	30.47
28 DEC 2003	17:25	28.035	1,791	30.47
29 NOV 2006	06:55	28.032	1,794	30.47
04 DEC 2007	08:25	28.031	1,795	30.47
06 FEB 2004	18:03	28.029	1,797	30.47
26 NOV 2011	17:19	28.027	1,799	30.47
29 NOV 2004	17:46	28.026	1,800	30.46
16 JAN 2013	17:07	28.026	1,800	30.47
29 NOV 2010	07:25	28.025	1,801	30.47
27 NOV 2011	17:52	28.022	1,803	30.47
27 JAN 2009	05:55	28.017	1,808	30.45
23 DEC 2007	16:55	28.016	1,809	30.46
02 DEC 2006	07:25	28.013	1,812	30.45
04 JAN 2012	17:22	28.011	1,814	30.46
06 JAN 2007	16:25	28.009	1,816	30.45
15 JAN 2007	17:25	28.009	1,816	30.45
31 DEC 2007	07:25	28.009	1,816	30.45
25 DEC 2011	17:29	28.007	1,818	30.45

Table A2 High Ambient Air Surface Pressures Recorded by the Edwards AFB Weather Office (Concluded)

12 NOV 2010	15:55	28.006	1,819	30.45
09 DEC 2013	18:13	28.006	1,819	30.45
18 DEC 2004	17:25	28.002	1,823	30.44
15 JAN 2005	17:55	28.002	1,823	30.44
14 DEC 2013	17:25	28.001	1,824	30.45
10 DEC 2008	15:17	28.000	1,825	30.44
22 DEC 2011	07:55	28.000	1,825	30.45
23 DEC 2013	17:46	28.000	1,825	30.44

Notes:
1. Most data were obtained between 01 JAN 2006 and 31 OCT 2013.
2. Pressure altitudes were calculated from the recorded surface pressures.
3. The field elevation at Edwards AFB was 2,302 feet prior to the opening of runway 04L/22R on 19 MAY 2008. The field elevation has been 2,310 feet since then.
4. The altimeter setting was calculated by the Base Weather Office software and is presented for reference only.

Table A3 Ambient Air Surface Temperatures Recorded by the Edwards AFB Weather Office in January

Date	Low Temperatures		Normal Low Temperature (deg F)	Normal High Temperature (deg F)	High Temperatures	
	Year	Temperature (deg F)			Year	Temperature (deg F)
1	1976	13	28	56	1959	72
	2016	13			2001	66
	2015	16			2018	65
	2013	19			2012	64
					2014	64
2	1976	11	29	55	1946	70
	1960	13			2001	70
	1974	15			2018	69
	2013	17			1981	68
3	1970	12	28	54	1996	74
	1976	12			2018	73
	1974	13			2007	72
	2013	15			1981	71
	2019	19			2001	70
4	1949	12	27	54	2018	73
	1970	12			1996	70
	2013	13			2014	69
	1976	17			2001	68
	1990	17			2007	68
	1999	17			2012	68
	2004	17				
5	1949	10	28	55	2018	73
	1973	14			1981	67
	1970	15			2012	66
	1972	16			2006	63
	2013	16			2014	62
6	1973	11	30	56	2018	72
	1970	12			1948	69
	2007	18			2003	69
	1999	19			2012	69
	2000	21				
7	1973	11	30	56	1969	76
	1950	12			1999	75
	2000	19			2009	71
	2007	23			2003	69
8	1961	15	30	57	1948	73
	2000	15			2003	72
	1999	23			2015	67
	2007	23			1999	65
	2013	24				

Table A3 Ambient Air Surface Temperatures Recorded by the Edwards AFB Weather Office in January (Continued)

Date	Low Temperatures		Normal Low Temperature (deg F)	Normal High Temperature (deg F)	High Temperatures	
	Year	Temperature (deg F)			Year	Temperature (deg F)
9	1964	15	30	57	1996	73
	2000	22			1948	70
	1999	24			2002	69
	2007	24				
	2012	24				
10	1949	18	31	57	1948	73
	2006	23			2000	70
	2012	24			2002	70
	1999	25			2007	68
	2004	25			2014	66
	2007	26				
11	1994	20	31	57	2014	74
	1976	21			1999	73
	2012	24			2012	71
	2002	25			1947	70
	2004	25			2000	70
	2006	25				
12	1963	7	32	57	2012	73
	2013	15			1999	71
	2007	20			1956	69
	2012	21			2009	68
	2002	23			2010	68
13	1963	4	30	57	1945	71
	2007	8			1956	71
	2013	10			1999	68
	2012	16			2000	68
	2016	24			2018	68
14	2007	7	30	58	1945	72
	1963	9			2002	71
	2013	9			2000	68
	2012	17			2004	68
	2002	22			2014	68
15	2007	9	30	58	1943	83
	1963	13			1996	78
	2013	15			1999	72
	2012	19			1956	72
	2002	22			2002	71
					2000	70
16	2007	10	32	58	2014	72
	1963	18			1965	70
	2013	19			1976	70
	2006	23			2009	66
	2014	24			2016	66

Table A3 Ambient Air Surface Temperatures Recorded by the Edwards AFB Weather Office in January (Continued)

Date	Low Temperatures Year	Low Temperatures Temperature (deg F)	Normal Low Temperature (deg F)	Normal High Temperature (deg F)	High Temperatures Year	High Temperatures Temperature (deg F)
17	2007	10	31	59	1999	73
	2012	17			2001	73
	1987	18			2011	73
	2002	18			1965	72
	2013	19			2018	69
	1963	20			2003	68
18	2007	11	31	59	1959	75
	2013	18			1999	72
	2002	19			2000	72
	2012	19			2018	72
	1967	20			2003	70
	2008	21			2012	69
					2011	68
19	1943	11	32	59	1971	73
	2007	14			2000	72
	2002	17			2012	71
	2013	17			2003	69
	1962	21			2011	69
20	1963	12	31	58	1971	82
	2007	16			2012	73
	2013	17			2003	70
	2002	19			1999	68
	2006	19			2019	65
21	1963	16	32	57	1950	74
	1987	16			2003	71
	2013	17			2005	68
	2006	18			2002	67
	2002	20			2013	67
22	1966	17	33	58	1948	72
	2013	17			1999	69
	2006	21			2014	69
	2007	21			2005	68
	2004	24			2011	66
23	2002	16	32	59	1947	78
	1958	17			1999	69
	2007	18			2005	67
	2004	21			2014	67
	2006	22			2003	66
					2016	64

Table A3 Ambient Air Surface Temperatures Recorded by the Edwards AFB Weather Office in January (Concluded)

Date	Low Temperatures		Normal Low Temperature (deg F)	Normal High Temperature (deg F)	High Temperatures	
	Year	Temperature (deg F)			Year	Temperature (deg F)
24	2002	18	33	59	1948	77
	1949	21			2003	71
	2007	21			2000	70
	2018	22			2015	69
	2006	23			2006	66
	2011	24			2007	66
25	1966	20	33	59	1946	75
	2002	20			1975	75
	2007	23			2003	72
	2012	28			2015	71
	2019	28			2014	69
26	1949	15	33	58	2012	74
	2007	21			1951	73
	2004	22			1971	73
	2002	24			2003	73
					1975	71
27	1950	16	32	58	1971	73
	2009	23			2003	71
	2018	24			2014	68
	2016	26			2012	66
	2011	27			2019	66
28	1957	14	31	57	2018	73
	1999	22			1976	70
	2009	23			2003	67
	2000	25			2006	66
	2012	25			2014	66
					2019	66
29	1975	15	31	58	2014	76
	2012	20			2016	74
	1999	22			2018	73
	2000	25			1953	71
	2004	26			1984	71
30	1970	15	31	58	2014	76
	2002	19			2003	74
	2012	20			1965	72
	1999	25			2006	72
31	1972	14	31	58	2003	80
	1975	17			1965	75
	2002	18			2018	71
	2008	23			2012	68

Table A4 Ambient Air Surface Temperatures Recorded by the Edwards AFB Weather Office in February

Date	Low Temperature Year	Low Temperature Temperature (deg F)	Normal Low Temperature (deg F)	Normal High Temperature (deg F)	High Temperature Year	High Temperature Temperature (deg F)
1	1946	19	32	60	2003	78
	2002	19			1954	73
	2004	24			2018	72
	2011	25			2009	70
	2014	26				
2	2002	19	32	59	1995	77
	1946	20			1959	75
	2014	21			2018	74
	2016	22			2000	72
	2007	23				
3	1972	14	31	60	2018	77
	2011	16			1995	73
	2002	20			1963	72
	2007	21			2006	72
	2016	21			2009	72
	2012	23			2015	71
	1999	24			2000	69
4	1955	19	32	61	2018	75
	1985	20			2001	74
	2003	20			2015	73
	2012	21			1954	72
	2002	22			2009	72
5	1985	20	34	61	2001	81
	2008	21			2018	76
	2012	21			1963	75
	1955	22			2007	75
	2002	22			2015	75
	2003	23			2013	73
	2016	26			2006	72
6	2003	15	34	61	1963	76
	2002	20			2007	75
	2012	23			2018	75
	1949	24			2015	74
	1985	24			2000	71
7	1974	20	34	61	1951	80
	2006	22			2011	75
	2002	23			2000	73
	2005	25			2018	73
	2003	27			2002	72
	2019	27			2016	72
8	1965	20	34	60	1951	77
	2006	21			2015	75
	2003	22			2016	75
	2001	23			2006	74
	2004	25			2018	74
	2019	25			2014	72

Table A4 Ambient Air Surface Temperatures Recorded by the Edwards AFB Weather Office in February (Continued)

Date	Low Temperature Year	Low Temperature Temperature (deg F)	Normal Low Temperature (deg F)	Normal High Temperature (deg F)	High Temperature Year	High Temperature Temperature (deg F)
9	2003	20	35	60	2018	79
	1949	22			1951	78
	2004	23			2006	78
	2006	27			2017	76
	2001	28			2014	74
	2008	28			2016	74
10	1974	21	34	61	2012	78
	2013	22			1951	76
	2003	24			2006	74
	2006	27			2016	73
	2011	27			2007	72
	2009	28			2015	71
11	1965	20	34	60	1971	78
	2011	20			2015	76
	2002	21			2006	73
	2004	22			2016	73
	2013	24			2008	70
12	1965	14	34	61	2014	79
	2013	18			1991	78
	1999	19			1971	75
	2002	21			2015	74
	2019	23			2006	73
	2011	24			2016	73
13	1948	15	35	61	2014	83
	1999	21			1957	80
	2004	22			2015	76
	2013	22			2016	76
	2011	25			2006	74
	2009	27				
14	1949	16	35	62	2014	85
	2004	25			1971	78
	2013	25			2015	76
	2001	28			2006	74
	2002	29			2016	74
15	1990	19	34	61	2014	84
	1964	20			2015	78
	2007	27			1957	77
	2009	27			2016	77
16	2006	19	36	62	2015	83
	1965	21			2016	77
	2018	23			1957	76
	2008	25			2014	76

Table A4 Ambient Air Surface Temperatures Recorded by the Edwards AFB Weather Office in February (Continued)

Date	Low Temperature		Normal Low Temperature (deg F)	Normal High Temperature (deg F)	High Temperature	
	Year	Temperature (deg F)			Year	Temperature (deg F)
17	1956	20	36	62	1996	78
	2012	22			1985	77
	2006	24			2014	77
	2008	25			1958	76
	2013	27			2015	75
18	1975	18	36	62	1950	78
	2006	26			2015	76
	2012	29			1999	75
	2013	29			2014	73
					2010	72
19	1955	24	36	61	1981	81
	2019	27			2015	79
	2009	28			1999	67
	2006	29				
20	2018	15	35	61	1977	80
	1953	20			2002	75
	1955	20			2015	75
	2006	20				
21	1953	18	35	62	2002	76
	2012	23			1965	75
	2006	25			2015	74
					2016	72
22	1975	19	36	62	1991	78
	2006	20			1954	77
	1999	24			2002	75
	2013	25			2012	75
	2011	26			2016	73
23	1975	21	35	62	1989	79
	2006	22			1947	77
	1999	25			2012	77
	2018	25			2002	74
	2019	25			2014	74
24	2018	16	35	63	1986	79
	1960	20			1954	76
	2006	23			1999	76
	2007	25			2014	76
					2009	72
25	2013	21	37	63	1989	84
	1974	22			1954	80
	2018	23			2002	77
					2014	75
26	1964	24	37	63	1986	82
	1971	25			1954	77
	2012	28			2016	76
	2018	28			2002	73

Table A4 Ambient Air Surface Temperatures Recorded by the Edwards AFB Weather Office in February (Concluded)

Date	Low Temperature		Normal Low Temperature (deg F)	Normal High Temperature (deg F)	High Temperature	
	Year	Temperature (deg F)			Year	Temperature (deg F)
27	1971	16	37	63	1986	81
	2013	26			2016	80
	2018	28			1968	76
	2011	31			2002	75
	2008	32			2008	75
28	1964	17	36	62	1999	83
	2013	23			1986	81
	2018	24			1972	80
	2002	29			2002	78
	2011	29			2016	78
29	1996	29	37	62	2016	80
	2004	30			2008	77
	1984	31			1984	72
	1948	34			1968	69
	2012	34				

Table A5 Ambient Air Surface Temperatures Recorded by the Edwards AFB Weather Office in March

Date	Low Temperatures		Normal Low Temperature (deg F)	Normal High Temperature (deg F)	High Temperatures	
	Year	Temperature (deg F)			Year	Temperature (deg F)
1	1997	20	37	62	2016	83
	1964	23			1967	80
	2007	25			1999	77
	2011	29			2013	75
2	1971	19	38	61	2016	83
	2002	24			1999	81
	2007	27			1959	77
3	1971	19	37	61	1994	81
	2002	20			2016	80
	2012	21			1959	79
	2017	27			1999	73
4	2002	17	36	62	1994	80
	1966	22			1972	79
	2012	27			2016	78
	2006	28			2012	74
	2008	28			2013	71
5	1963	23	36	63	1972	83
	2015	26			2012	80
	2006	28			2002	77
	2010	28			1999	72
	2002	29			2007	72
	2003	29			2014	72
6	2008	23	38	63	1972	86
	1977	25			2007	81
	2018	25			2015	74
	2015	28			2014	73
	2000	31			2002	70
					2011	70
7	1971	22	37	65	1972	81
	2009	28			2007	77
	2000	32			2015	77
	2008	32			2004	76
	2012	32			2005	72
	2017	32			2014	71
8	1964	22	37	67	1972	82
	2012	24			2004	81
	2009	27			2007	81
	2003	32			2015	80
	2016	32			2005	77
9	1961	24	38	67	1972	83
	1965	24			2004	81
	2002	25			2005	80
	2012	26			2015	78
	2008	32			2017	78
	2003	33			2007	77
	2011	33			2018	77

Table A5 Ambient Air Surface Temperatures Recorded by the Edwards AFB Weather Office in March (Continued)

Date	Low Temperatures		Normal Low Temperature (deg F)	Normal High Temperature (deg F)	High Temperatures	
	Year	Temperature (deg F)			Year	Temperature (deg F)
10	1958	27	39	66	1972	82
	2009	27			2004	81
	2013	27			2005	80
	2000	32			2016	80
	2008	32			2007	79
	2012	32			2012	79
	2006	33			2015	79
	2015	33			2011	77
					2017	77
11	1988	25	39	65	1997	85
	2009	26			2007	82
	1964	27			2005	80
	2010	28			2004	79
	2013	28			2017	79
12	1988	23	38	66	2007	84
	1977	25			2004	82
	1999	25			2005	82
	2006	29			2012	82
	2009	32			2017	81
	2010	32			2002	80
	2013	32				
13	1954	23	38	65	2007	90
	1999	25			2017	84
	2006	28			2013	83
	2009	30			1994	81
	2011	33			2004	81
14	1988	23	38	66	2013	87
	1969	27			2007	86
	2006	27			2017	85
	2010	28			2004	83
	2009	32			2015	82
15	2002	24	38	66	2007	88
	1962	26			2013	88
	2005	28			1994	84
	2019	30			2002	84
	2010	31			2017	84
16	1999	28	39	66	2007	90
	1956	30			2004	83
	2019	32			2015	83
	2005	33			2017	83
17	1955	30	40	67	2007	88
	1975	30			1972	83
	1999	31			2004	83
	2008	32			2017	82
	2012	34			2016	81

Table A5 Ambient Air Surface Temperatures Recorded by the Edwards AFB Weather Office in March (Continued)

Date	Low Temperatures		Normal Low Temperature (deg F)	Normal High Temperature (deg F)	High Temperatures	
	Year	Temperature (deg F)			Year	Temperature (deg F)
18	1988	27	39	67	2004	86
	1968	28			2017	83
	2011	28			1947	82
	1999	31			1972	82
	2002	31			2016	82
					2007	81
19	2002	24	39	67	2004	88
	1968	27			1997	86
	2014	31			2016	83
	2006	32			2001	81
	2018	32			2007	81
	1999	35			2009	81
	2003	35			2017	81
	2012	35				
20	1971	25	39	67	1997	90
	2006	29			2004	90
	2012	29			1972	82
	2002	31			2001	82
	1999	34			2015	82
21	1968	25	39	67	2004	90
	1999	33			1972	83
	2006	33			2015	81
22	1999	28	40	68	2004	90
	2006	28			1990	85
	1968	33			1971	81
	2008	36			2012	80
	2011	36				
23	1957	26	41	68	1956	83
	2016	31			2004	81
	2006	32			2001	79
					2007	79
24	2009	26	40	68	1956	86
	1996	29			2001	81
	1968	31			2008	81
	1999	32			2014	81
25	1964	25	41	67	1988	85
	2002	30			1980	84
	2009	32			2007	81
					2014	81
26	1995	26	41	68	1988	85
	1964	30			2015	84
	2002	33			1960	82
	2005	35			1986	82

Table A5 Ambient Air Surface Temperatures Recorded by the Edwards AFB Weather Office in March (Concluded)

Date	Low Temperatures		Normal Low Temperature (deg F)	Normal High Temperature (deg F)	High Temperatures	
	Year	Temperature (deg F)			Year	Temperature (deg F)
27	1975	28	42	68	2015	88
	2012	33			1986	83
	2002	35			1953	82
	2005	35			2001	79
28	1972	27	41	67	2015	88
	2009	30			1986	84
	2010	31			2001	83
	2007	34			1969	80
29	1944	29	40	69	2015	87
	1945	30			2002	85
	1976	30			2004	84
	2007	30			1969	84
30	1975	27	41	69	2015	88
	2007	32			2002	87
	2009	33			2004	85
	2003	35			1969	84
					2018	84
31	2009	28	41	70	2002	88
	1977	29			1966	87
	2005	33			2011	87
	2016	34			2007	84

Table A6 Ambient Air Surface Temperatures Recorded by the Edwards AFB Weather Office in April

Date	Low Temperatures		Normal Low Temperature (deg F)	Normal High Temperature (deg F)	High Temperatures	
	Year	Temperature (deg F)			Year	Temperature (deg F)
1	1988	29	42	69	1966	89
	1971	30			2002	89
	1999	31			2011	89
	2005	31			2007	86
	2010	36				
2	1971	29	42	69	1966	92
	1975	29			2002	89
	2005	30			2000	85
	1999	31			2017	82
	2012	33			2007	81
	2006	37			2016	81
	2010	37				
3	1945	27	42	70	1961	94
	2014	32			2000	90
	2012	35			2007	88
	2015	35			2002	87
4	1945	29	41	71	1961	93
	2009	29			2000	90
	1999	37			2002	84
	2003	37			2007	84
	2005	37			2018	84
	2008	37				
	2015	37				
5	1945	30	42	71	1960	91
	2009	30			2016	87
	2005	31			2000	86
	2011	37			2007	86
6	2010	29	44	71	1989	93
	1975	30			1960	89
	2009	32			2007	88
	2012	34			2016	88
	2006	35			2000	85
7	2012	25	43	71	1989	95
	1969	32			2000	89
	2010	32			1985	87
	1999	33			1977	86
	2003	33				
8	2012	29	43	71	1989	94
	1975	31			1964	88
	2011	32			1985	88
	2003	33			2000	87
					2014	87
9	2011	30	43	72	1989	93
	1945	32			1960	90
	1967	32			2014	89
	2017	32			2002	86

Table A6 Ambient Air Surface Temperatures Recorded by the Edwards AFB Weather Office in April (Continued)

Date	Low Temperatures		Normal Low Temperature (deg F)	Normal High Temperature (deg F)	High Temperatures	
	Year	Temperature (deg F)			Year	Temperature (deg F)
10	1999	26	44	72	1989	95
	1945	31			1951	90
	2011	33			2018	89
	2005	35			2014	88
	2017	35				
11	1953	32	44	72	1989	89
	2005	34			2002	88
	2011	38			1949	86
	2017	38			2014	86
12	2006	34	43	73	1985	94
	1953	35			2000	88
	2009	35			2002	88
	2012	39			1962	86
13	1945	33	43	74	1985	96
	2001	34			2002	93
	2018	34			1962	89
	2007	36			2008	86
14	1972	30	45	73	1985	101
	2005	30			2002	94
	2011	35			1947	92
					2008	88
15	1976	30	44	74	1947	93
	1970	31			2014	84
	2005	33			1999	81
	2012	35			2017	80
16	1998	30	44	75	1947	93
	1967	31			1954	93
	2002	36			2014	88
	2005	36			2001	85
	2008	36			2005	85
17	1976	31	46	74	1954	95
	2013	35			2001	88
	2008	36			1999	86
	2009	36			2014	85
	2015	37			2005	83
18	1968	29	46	72	1954	93
	2006	31			1999	93
	2018	32			2019	88
	2013	38			2015	85
					2016	85
19	2007	32	45	73	1950	94
	1972	33			1999	92
	2002	35			2019	89
	2006	35			2016	88
	2013	35			2009	87

Table A6 Ambient Air Surface Temperatures Recorded by the Edwards AFB Weather Office in April (Continued)

Date	Low Temperatures		Normal Low Temperature (deg F)	Normal High Temperature (deg F)	High Temperatures	
	Year	Temperature (deg F)			Year	Temperature (deg F)
20	1966	30	45	74	1950	94
	2002	36			2009	92
	2006	37			2012	91
	2003	38			2014	88
	2005	38				
21	1957	34	45	74	2012	94
	1972	34			1950	92
	2005	35			2009	92
	2002	36			2013	90
	2010	36			2014	88
22	1963	31	45	74	1949	96
	2001	33			1969	96
	2010	34			2012	96
23	1968	30	46	75	1949	97
	2010	35			2018	90
	2005	36			2012	89
	2001	38			2019	88
24	1988	35	47	74	1946	94
	1980	36			2019	91
	2007	39			2018	89
	2010	40			2001	87
25	1964	34	46	74	2019	93
	2008	37			1946	92
	2006	39			2001	90
					2018	90
26	1998	33	46	75	1996	97
	1964	36			2004	94
	1967	36			1946	93
	2005	38			2000	93
27	1984	30	47	77	2004	95
	1976	33			1992	92
	1963	35			2000	91
	2015	44			2007	91
	2009	45			2013	91
	2002	45			2019	91
28	1963	35	47	76	2007	97
	2015	41			2013	95
	2002	42			1992	92
	2009	43			2008	91

Table A6 Ambient Air Surface Temperatures Recorded by the Edwards AFB Weather Office in April (Concluded)

Date	Low Temperatures		Normal Low Temperature (deg F)	Normal High Temperature (deg F)	High Temperatures	
	Year	Temperature (deg F)			Year	Temperature (deg F)
29	1967	35	47	77	2013	95
	1970	35			1981	94
	2003	37			2007	93
	2002	42			2006	92
	2014	43			2015	91
30	1970	36	48	78	1981	96
	1975	36			2001	92
	2011	39			2006	91
	2017	41			2007	91
	2000	42			2013	90
	2001	43			2015	90

Table A7 Ambient Air Surface Temperatures Recorded by the Edwards AFB Weather Office in May

Date	Low Temperatures		Normal Low Temperature (deg F)	Normal High Temperature (deg F)	High Temperatures	
	Year	Temperature (deg F)			Year	Temperature (deg F)
1	1967	32	48	78	1947	97
	2011	32			2000	93
	1999	39			2006	92
	2008	41			2001	90
	2010	41			2017	89
2	1988	35	49	79	1947	98
	2011	35			2004	95
	1953	39			2014	95
	2008	39			2000	92
	2002	43			2017	92
3	1983	37	49	80	1947	100
	2010	42			2004	99
	2011	42			2017	94
	2002	43			2014	93
	2001	14			2000	89
4	2001	38	50	78	1947	97
	1964	39			2004	97
	2002	45			2017	97
	2007	46			2000	93
5	1999	38	49	79	1947	94
	1964	39			1954	94
	2003	46			2011	93
	2008	46			2017	91
	2011	46			2018	91
	2007	48			2001	90
	2012	48			1999	83
6	1975	36	50	78	1990	96
	1978	36			1954	94
	2012	42			2001	93
	1999	45			1999	91
					2011	91
7	1968	37	50	79	2001	97
	2017	39			1954	94
	2015	40			2018	92
	2010	42			2006	90
8	1965	37	50	78	2001	99
	2017	38			1974	97
	2015	41			2018	96
	2003	43			2009	92
	2005	46			2006	89
	2007	46			2012	89

Table A7 Ambient Air Surface Temperatures Recorded by the Edwards AFB Weather Office in May (Continued)

Date	Low Temperatures		Normal Low Temperature (deg F)	Normal High Temperature (deg F)	High Temperatures	
	Year	Temperature (deg F)			Year	Temperature (deg F)
9	1948	42	50	78	2001	100
	1965	42			2018	99
	2003	42			1960	93
	2011	44			2009	93
	2015	46			2012	93
	2005	49			2006	91
	2017	49			2007	91
10	2003	35	50	79	1960	99
	1979	41			2001	97
	2011	43			2009	94
	2010	46			2006	93
	2015	46				
11	1983	35	50	80	1996	99
	2003	40			2001	99
	2005	40			1960	98
	2010	41			2006	97
12	2000	37	50	81	1996	102
	1983	38			2006	97
	2010	40			2013	96
	2005	41			1984	95
	2002	42			1973	94
	2014	42			2016	94
13	1967	36	50	83	1997	100
	2000	41			2013	99
	2005	44			2012	96
	2008	44			2002	95
	2001	46			2016	95
14	1967	39	52	81	2006	98
	2005	43			1976	94
	2017	45			2007	93
	2010	46			2001	92
	2008	48			2002	92
15	1968	36	52	81	2006	96
	2011	43			1973	95
	2015	43			2009	95
	1999	46			2014	95
	2017	46			2005	94

Table A7 Ambient Air Surface Temperatures Recorded by the Edwards AFB Weather Office in May (Continued)

Date	Low Temperatures		Normal Low Temperature (deg F)	Normal High Temperature (deg F)	High Temperatures	
	Year	Temperature (deg F)			Year	Temperature (deg F)
16	2011	39	51	83	2009	100
	1944	41			2006	99
	1984	41			2012	98
	1953	42			2014	97
17	1962	42	52	84	2009	102
	1981	42			1954	100
	2011	44			2006	100
	1999	46			2008	100
	2005	50			2014	97
	2010	50			2012	96
	2015	50			2002	95
18	1998	36	53	83	2008	104
	1974	39			1954	102
	2019	41			2006	101
	2017	42			2009	96
19	1974	41	53	83	2008	102
	2003	44			1954	98
	2011	44			2006	97
	2017	46			2001	93
	2019	47			2005	93
20	1974	37	53	84	2001	100
	2002	44			1947	99
	2019	44			2000	96
	2011	46				
21	1975	39	53	83	2000	101
	2002	42			2003	99
	2016	46			2012	99
	1999	47			1967	98
	2019	48			2001	98
22	1957	41	53	84	2000	105
	1948	42			1984	101
	1975	42			2001	101
	2010	44			1967	100
	2016	48			2003	100
23	1960	41	54	83	2000	105
	2010	43			2001	103
	2006	48			2017	100
	2007	48			2003	99
	2008	48			1967	97
					2005	97

Table A7 Ambient Air Surface Temperatures Recorded by the Edwards AFB Weather Office in May (Concluded)

Date	Low Temperatures		Normal Low Temperature (deg F)	Normal High Temperature (deg F)	High Temperatures	
	Year	Temperature (deg F)			Year	Temperature (deg F)
24	2008	41	54	84	2001	103
	1953	42			2000	101
	1960	42			1951	97
	2010	44			2003	96
25	1980	40	54	85	1951	103
	2010	42			2001	99
	2008	45			2005	98
	2012	49			2014	96
26	1953	40	54	85	1951	103
	1980	40			2014	100
	2012	44			1999	98
	2008	46			2005	97
27	1953	41	55	84	1984	102
	2019	44			2000	102
	2008	45			2003	101
	2006	48			1957	100
	2012	48			2014	99
28	1953	43	54	85	2003	108
	2019	44			1984	102
	2006	45			2000	101
	2008	48			1983	100
	2010	48			1999	97
	2012	48			2009	96
29	2010	40	55	85	2003	104
	1953	43			1984	100
	2006	43			2002	99
	2011	49			1973	98
	2008	50			2000	98
	2019	50			2001	98
30	2011	43	55	86	2002	104
	2010	44			2001	103
	1985	46			1950	102
					1985	102
31	1988	42	56	86	2001	106
	2011	42			1950	105
	1971	46			2002	101
	2006	49			2012	100

Table A8 Ambient Air Surface Temperatures Recorded by the Edwards AFB Weather Office in June

Date	Low Temperatures		Normal Low Temperature (deg F)	Normal High Temperature (deg F)	High Temperatures	
	Year	Temperature (deg F)			Year	Temperature (deg F)
1	1971	42	57	87	2001	106
	1967	43			1960	103
	2011	48			2012	102
	2017	51			2016	102
2	1967	41	56	87	2016	103
	2011	46			1957	102
	1999	48			2003	101
	2014	52			2007	99
	2018	52			2013	98
3	1967	42	57	89	1996	105
	2011	42			1957	103
	1999	47			2018	102
					2016	102
4	1958	44	57	89	1996	105
	1999	48			1957	105
	2009	48			2006	103
					2016	102
5	1998	45	58	87	1996	105
	1999	46			2002	104
	1967	47			1981	102
	2011	47			2013	101
6	2012	43	58	86	2002	107
	1943	46			2013	104
	1954	46			1981	101
	2011	48			2016	100
7	1950	44	57	87	2013	107
	2007	45			1996	104
	2011	49			2001	104
	2012	49			1978	103
	2005	50			1985	103
8	1995	42	57	87	2013	109
	1950	46			1973	106
	2007	48			2014	105
	2008	50			2016	104
9	1979	47	56	87	2014	107
	2000	50			2001	104
	2004	51			1996	102
10	2002	45	57	88	1994	105
	1953	46			1985	104
	2012	51			1949	102
	2000	55			2014	100

Table A8 Ambient Air Surface Temperatures Recorded by the Edwards AFB Weather Office in June (Continued)

Date	Low Temperatures		Normal Low Temperature (deg F)	Normal High Temperature (deg F)	High Temperatures	
	Year	Temperature (deg F)			Year	Temperature (deg F)
11	1964	44	57	89	1985	104
	2002	48			1977	102
	2012	50			2019	101
	2017	53			2013	100
12	1943	46	58	90	1985	106
	1952	48			1979	105
	2017	48			2018	102
	2008	52			2019	101
13	1943	46	58	90	2000	106
	1952	50			1960	103
	1960	50			2015	102
	2017	50				
14	1967	48	59	91	2000	108
	2017	48			1960	105
	2001	50			1999	105
					2005	104
15	1944	46	59	91	2000	111
	1964	46			1961	106
	1962	48			2015	103
	2009	55				
16	1944	45	60	92	1961	108
	1995	45			2000	107
	1981	48			2015	102
	2016	52			2017	102
17	1995	42	59	93	1961	106
	1965	48			2017	105
	2018	53			2000	104
					2003	104
18	1995	48	60	93	2017	109
	1965	50			1985	107
	2005	51			2001	104
	2018	54			2015	104
19	2005	44	60	94	2017	110
	1974	49			1961	106
	2014	55			2015	105
					2016	105
20	2005	49	61	94	1961	111
	1975	50			2016	110
	1999	56			2017	109
	2010	56			2015	107

Table A8 Ambient Air Surface Temperatures Recorded by the Edwards AFB Weather Office in June (Concluded)

Date	Low Temperatures		Normal Low Temperature (deg F)	Normal High Temperature (deg F)	High Temperatures	
	Year	Temperature (deg F)			Year	Temperature (deg F)
21	1995	47	61	94	1954	112
	1975	52			1961	112
	2005	52			2016	108
	2003	56			2017	107
	2009	56			2018	107
22	1944	42	61	95	1954	111
	2009	50			2017	107
	1945	53			2006	105
	2003	55			2018	105
23	1943	51	62	95	2017	110
	1945	52			1954	109
	2009	54			2006	105
	2005	55			2002	102
24	1944	47	62	94	2017	111
	1963	49			1957	107
	2003	52			1961	107
					2006	106
25	1943	50	61	94	1994	107
	1965	50			2006	107
	2005	50			1957	106
	2003	51			2017	106
26	1965	46	62	95	2016	107
	2005	54			1994	106
	2003	55			1973	105
	2012	56			2015	105
27	1965	45	62	96	1994	111
	2005	54			1956	110
	2012	54			2016	109
28	1996	50	62	96	1956	112
	1964	52			2013	109
	2008	57			2003	106
	2001	58			2009	105
	2005	58			2010	105
29	1952	50	62	96	1994	113
	1969	50			2013	110
	2005	55			1950	108
	2004	56			1999	107
30	1970	48	62	97	1994	113
	2011	51			2013	112
	2004	58			1972	110
	2005	59			1999	110

Table A9 Ambient Air Surface Temperatures Recorded by the Edwards AFB Weather Office in July

Date	Low Temperatures		Normal Low Temperature (deg F)	Normal High Temperature (deg F)	High Temperatures	
	Year	Temperature (deg F)			Year	Temperature (deg F)
1	1997	48	63	97	2001	110
	1982	55			1950	109
	2011	55			2013	107
	2004	57			1999	106
	2005	63			2002	106
	2008	63			2014	106
2	1979	50	63	97	2001	112
	2004	58			2011	108
	1998	60			1967	107
	2002	60			2013	106
3	1975	52	64	98	1991	112
	1997	52			2001	112
	2004	61			2013	109
	2016	61			2011	108
	1998	62			1973	107
	1999	62			2007	106
	2000	62			2008	104
4	1978	52	64	98	1991	112
	1998	56			1985	109
	2000	59			2007	109
	2018	61			2013	108
	1999	62			1973	107
5	1948	51	64	98	2007	115
	1999	53			1989	112
	1998	56			1984	111
	2018	59			2017	107
	2000	61			1970	105
6	1998	51	65	98	1984	110
	1978	52			2007	109
	2000	58			1945	108
					2017	108
					2018	108
7	1969	50	65	99	1989	111
	2000	59			2017	110
	2010	61			2007	108
	2012	63			2018	107
	2006	64			1984	106
	2008	64			1951	105
8	1959	55	65	98	2008	111
	1978	55			1994	109
	2000	58			2018	109
	2010	58			2002	108
	2012	61			1985	106
	2019	61			2013	105

Table A9 Ambient Air Surface Temperatures Recorded by the Edwards AFB Weather Office in July (Continued)

Date	Low Temperatures		Normal Low Temperature (deg F)	Normal High Temperature (deg F)	High Temperatures	
	Year	Temperature (deg F)			Year	Temperature (deg F)
9	1983	53	65	98	2002	114
	2003	55			2008	109
	2000	56			1969	108
	2004	57			2003	108
	2010	59			2012	106
	2015	60			2013	106
10	1983	47	65	98	2002	111
	2000	57			1961	110
	2015	58			2003	110
	2019	61			2008	109
	1998	62			2012	108
	2004	63			2010	105
11	1983	53	65	99	1961	113
	2005	58			2003	111
	2015	59			2012	110
	2000	60			2002	104
	1998	62			2005	104
	2004	62			1998	103
	2016	62				
12	1974	53	66	99	2002	109
	2000	56			1961	107
	1998	57			2003	107
	2015	60				
13	1995	52	65	99	1972	108
	1965	55			1979	108
	2001	55			2002	108
	2000	59			2005	108
14	1995	54	66	100	1972	113
	1956	57			2005	110
	2011	60			2002	108
	2000	61			2003	108
15	1966	57	67	100	1972	111
	2011	57			2005	111
	1998	59			2003	109
	2012	59			2006	109
16	1943	56	67	99	1998	112
	2012	56			2005	110
	1994	57			1979	109
	2011	57			2003	109
	1956	58			2006	109
					2017	109

Table A9 Ambient Air Surface Temperatures Recorded by the Edwards AFB Weather Office in July (Continued)

Date	Low Temperatures		Normal Low Temperature (deg F)	Normal High Temperature (deg F)	High Temperatures	
	Year	Temperature (deg F)			Year	Temperature (deg F)
17	1943	55	66	99	1998	113
	1995	55			1979	112
	2011	55			2005	110
					2009	109
18	1987	52	66	100	1998	115
	1957	55			2005	112
	2011	55			1960	111
	2012	57			2009	110
	2000	59			2000	106
	2013	60			2010	106
19	1987	51	67	100	1968	112
	1983	57			2005	110
	1999	60			2000	107
	2000	61			2009	107
					2013	107
20	1987	52	67	99	1959	108
	1983	57			2000	107
	2000	60			2009	106
21	1972	55	67	99	2000	108
	1999	57			2009	107
	2002	59			1980	106
	2000	60			2005	106
					2006	106
22	1957	51	67	99	1942	108
	1999	52			2006	108
	2002	61			1953	107
	2001	63			1980	107
					2005	107
23	1972	54	67	100	1942	110
	2001	59			2000	108
	1999	61			2016	108
24	1957	56	67	100	1996	110
	1983	56			2018	110
	1999	59			2000	109
	2008	59			1980	108
25	1944	57	67	101	1959	110
	1948	57			1975	110
	1999	57			2006	110
	2012	61			2018	110

Table A9 Ambient Air Surface Temperatures Recorded by the Edwards AFB Weather Office in July (Concluded)

Date	Low Temperatures		Normal Low Temperature (deg F)	Normal High Temperature (deg F)	High Temperatures	
	Year	Temperature (deg F)			Year	Temperature (deg F)
26	1944	55	67	101	1945	112
	1957	55			2018	110
	1999	57			1998	107
	2012	61			2006	107
	2005	64			2016	107
27	1965	55	67	101	1995	111
	1999	58			1998	109
	2012	61			2018	109
	2002	63			2001	108
	2010	63			2016	108
28	1965	52	67	101	1995	112
	2012	59			2016	109
	2015	60			1980	108
	2000	61			1998	108
	2002	63			2003	108
	2004	64			2018	108
	2010	64			2019	108
29	2012	55	68	100	1995	114
	1983	58			2016	110
	2015	63			2000	108
	2002	64			1980	107
30	1979	59	68	100	2000	111
	2001	63			1982	109
	1999	64			2002	108
31	1975	56	67	100	1982	111
	2004	61			2017	108
	1998	62			2000	107

Table A10 Ambient Air Surface Temperatures Recorded by the Edwards AFB Weather Office in August

Date	Low Temperatures		Normal Low Temperature (deg F)	Normal High Temperature (deg F)	High Temperatures	
	Year	Temperature (deg F)			Year	Temperature (deg F)
1	1975	55	67	100	1993	110
	1998	57			1995	110
	1985	59			1974	109
	1999	60			1996	109
					2000	109
2	1976	53	66	100	1979	111
	1985	58			1995	109
	1999	59			1980	106
	2019	59			2008	106
3	1956	54	66	100	1998	109
	2004	55			1969	107
	1985	57			1986	107
	1998	60			2007	106
	2013	60			2018	106
4	1944	56	66	99	1998	110
	1953	56			1969	107
	1956	56			1986	107
	2004	58			1994	104
					2000	104
					2007	104
5	1956	52	65	100	1966	112
	1991	54			1998	111
	2006	54			1994	110
	2003	59			2000	105
					2005	105
					2019	105
6	1999	55	66	99	1997	111
	1950	56			1996	110
	2006	59			1994	110
	2004	61			1998	110
	2007	61			1995	107
7	1950	55	66	99	1997	111
	1956	55			1981	110
	2006	57			1994	109
	1999	58			1998	107
	2004	58			2001	107
8	1976	54	65	100	1981	111
	1999	54			1980	107
	2002	56			1995	107
	2009	56			2012	107

Table A10 Ambient Air Surface Temperatures Recorded by the Edwards AFB Weather Office in August (Continued)

Date	Low Temperatures		Normal Low Temperature (deg F)	Normal High Temperature (deg F)	High Temperatures	
	Year	Temperature (deg F)			Year	Temperature (deg F)
9	1976	54	65	99	2004	109
	1999	56			1980	108
	2006	57			2012	108
	2010	57			1981	107
10	1949	51	66	99	2004	109
	1973	59			2012	109
	2010	59			1970	108
					1971	108
					1996	108
					2002	108
11	1988	51	65	99	1980	111
	1949	52			2002	110
	1973	53			2004	109
	2010	55			2001	108
	2016	55			1994	107
					1996	107
12	1949	55	66	99	2002	112
	1999	56			1994	107
	1985	57			2000	107
	2015	58			2001	107
	2019	59			1980	106
					2012	106
13	1954	54	66	99	2002	111
	2006	56			1996	109
	1985	58			1998	107
	1999	58			2000	106
	2013	60			1979	105
					2012	105
14	2006	55	66	98	2002	111
	1968	56			1962	109
	2005	58			1996	108
	1999	59			1998	108
15	1954	54	65	97	2002	112
	1999	58			1994	110
	2006	58			1996	107
	1980	59			1951	106
					2000	106
					2015	106

Table A10 Ambient Air Surface Temperatures Recorded by the Edwards AFB Weather Office in August (Continued)

Date	Low Temperatures		Normal Low Temperature (deg F)	Normal High Temperature (deg F)	High Temperatures	
	Year	Temperature (deg F)			Year	Temperature (deg F)
16	1976	52	65	97	1994	111
	2009	53			2002	109
	1999	54			2015	108
	1980	57			1966	107
					2001	107
17	1976	51	64	98	2002	110
	2005	56			1950	108
	2009	56			2001	108
	2011	56			2014	105
					2015	105
18	1978	47	64	97	1950	111
	2005	55			2001	109
	2019	55			2003	107
	2006	56			2002	106
					2015	106
19	1978	51	64	96	1950	110
	2005	56			2015	106
	1998	57			2018	106
	1980	58			1995	103
	2006	58			2009	103
					2012	103
20	1976	52	63	96	1950	109
	1985	53			2015	106
	1998	55			2009	103
	2005	55			2012	103
21	1959	48	62	96	1950	105
	1985	53			2007	104
	2005	55			2019	104
22	1968	52	62	96	1945	106
	2002	53			1998	106
	1998	55			1999	104
	2000	55			1996	103
					2006	103
23	1968	48	62	96	1998	108
	1980	53			1945	106
	1985	53			1999	104
	2005	54			2011	104
24	1973	50	62	96	1945	106
	1980	52			1985	106
	2005	55			2010	106
	2001	56			2011	105

Table A10 Ambient Air Surface Temperatures Recorded by the Edwards AFB Weather Office in August (Concluded)

Date	Low Temperatures		Normal Low Temperature (deg F)	Normal High Temperature (deg F)	High Temperatures	
	Year	Temperature (deg F)			Year	Temperature (deg F)
25	1943	50	63	96	2010	107
	1963	52			1985	106
	1980	54			2011	106
	1995	55				
26	1943	49	63	96	2001	108
	1954	53			2017	106
	1955	53			1994	105
	1973	54			1999	105
					2010	105
					2011	105
27	1973	49	62	96	2001	108
	2002	55			2011	107
	2004	55			2017	107
	2012	56			1981	106
					2005	106
28	1973	47	62	97	2017	108
	1996	53			1981	107
	2004	56			1998	107
	2010	56			2005	107
	1995	58				
29	1942	51	62	96	1998	109
	1973	51			1950	108
	2010	56			2017	108
	1999	58			1981	106
					1996	106
					2011	106
30	1942	49	62	96	1998	110
	1947	52			1996	109
	1994	55			1950	107
	2002	55			2017	107
	2010	55			1995	105
					2016	105
31	1957	47	61	96	1948	108
	2000	53			1996	108
	2010	53			2004	105
	1999	55			2019	105
	2001	55			1995	104
					2007	104

Table A11 Ambient Air Surface Temperatures Recorded by the Edwards AFB Weather in September

Date	Low Temperatures		Normal Low Temperature (deg F)	Normal High Temperature (deg F)	High Temperatures	
	Year	Temperature (deg F)			Year	Temperature (deg F)
1	1957	48	61	96	1950	108
	2011	52			1958	108
	1999	53			2007	106
	2000	55			1995	105
	2010	55			2019	105
	1978	56			2004	104
	2001	56			2002	103
	2005	56			2017	103
2	1964	45	62	96	1950	109
	1973	51			2002	107
	2005	52			2017	107
	1999	53			2007	106
	2008	54			1995	103
	2012	54			2006	102
	2000	55			2009	102
3	1964	45	62	96	1955	106
	2005	50			1995	104
	1999	52			2002	104
	1973	53			2007	104
4	2004	47	62	95	1955	106
	1961	48			2019	103
	1973	50			2002	102
	2005	50			2010	102
5	1953	49	62	95	1955	109
	1973	49			1995	102
	2004	49			2006	102
	1992	51			2013	101
	1995	51				
6	2000	44	61	95	1955	109
	1970	48			2006	102
	1985	50			2008	102
	2004	50			2013	102
	2015	51			1979	100
7	1964	47	61	95	1955	109
	1973	51			1979	105
	2005	51			1990	103
	2000	52			2008	102
8	1978	48	60	94	1955	105
	2002	48			1979	105
	2005	51			2018	104

Table A11 Ambient Air Surface Temperatures Recorded by the Edwards AFB Weather in September (Continued)

Date	Low Temperatures Year	Low Temperatures Temperature (deg F)	Normal Low Temperature (deg F)	Normal High Temperature (deg F)	High Temperatures Year	High Temperatures Temperature (deg F)
9	2002	47	60	94	1944	107
	1973	50			1990	107
	2006	51			1979	104
	2010	51			2012	102
	1978	53			2018	102
10	2010	46	59	93	1944	106
	1961	49			1948	105
	2002	49			1979	104
	1985	50			1971	102
11	2000	46	58	93	1944	106
	1985	47			1979	105
	1965	48			1971	103
	1999	49			1990	103
	2010	49				
12	1985	40	59	93	1948	106
	2005	48			1971	105
	1998	50			1979	104
	2019	51			1990	101
	1978	52			1995	101
13	1985	40	58	93	1948	107
	2005	48			1971	106
	1978	50			1979	105
	2019	52			2000	105
	2001	53			1990	102
	2016	53				
14	2016	44	57	92	1948	106
	1993	45			1971	106
	1958	46			1995	104
	1970	50			1979	102
	2005	50			2014	102
15	1970	44	56	91	1971	104
	2005	47			1995	103
	2016	47			2000	102
	1978	49			2002	102
					2014	101
16	1970	45	57	89	2000	105
	2006	47			1951	103
	2016	49			1971	102
	2010	51			2014	101

Table A11 Ambient Air Surface Temperatures Recorded by the Edwards AFB Weather in September (Continued)

Date	Low Temperatures Year	Low Temperatures Temperature (deg F)	Normal Low Temperature (deg F)	Normal High Temperature (deg F)	High Temperatures Year	High Temperatures Temperature (deg F)
17	2006	41	57	88	2000	105
	1970	48			1956	100
	1977	48			2014	100
	2002	48			1979	97
	1973	49			2009	97
18	1993	41	56	88	1979	101
	2006	46			2000	101
	1950	47			2009	99
	2018	50			1995	97
19	1978	42	55	88	2000	104
	1971	45			1958	100
	2005	46			2009	100
	1998	49			1979	99
	1992	50			1995	99
					2016	99
20	1965	43	55	87	2000	105
	1978	47			1995	101
	1999	47			1949	100
	2004	47			2015	98
21	1978	39	54	88	1949	104
	1986	39			1992	100
	2004	44			2002	99
	2007	45			2009	99
					2015	99
22	1968	41	54	88	1948	106
	1978	41			1949	106
	2004	41			2002	100
	2017	45			2003	100
23	1970	42	54	89	1949	104
	2017	43			2003	102
	1971	45			2011	100
	2004	45				
24	1993	40	55	89	1947	101
	2017	42			2002	101
	1968	43			2015	100
	2006	44			2001	99
25	1993	40	55	89	2002	101
	1958	42			1953	100
	2017	42			2009	99
	2000	43			2010	99
					2015	99

Table A11 Ambient Air Surface Temperatures Recorded by the Edwards AFB Weather in September (Concluded)

Date	Low Temperatures		Normal Low Temperature (deg F)	Normal High Temperature (deg F)	High Temperatures	
	Year	Temperature (deg F)			Year	Temperature (deg F)
26	1948	34	54	90	1947	100
	1970	43			1960	100
	2007	43			1999	100
	2017	45			2009	100
27	1948	39	54	89	2010	101
	2013	39			1947	100
	1970	43			2003	100
	1973	43			2009	100
28	1971	39	55	88	2010	102
	2013	40			2003	100
	1943	43			1992	99
	2004	45			2018	97
29	1986	40	54	87	1992	100
	1971	41			1980	98
	2013	44			2011	98
	1973	45				
30	1982	37	52	87	2001	101
	2019	39			1980	99
	2007	41			1992	98
	1995	42			2003	97
	1999	45			2010	97
	2014	48			2012	97

Table A12 Ambient Air Surface Temperatures Recorded by the Edwards AFB Weather Office in October

Date	Low Temperatures		Normal Low Temperature (deg F)	Normal High Temperature (deg F)	High Temperatures	
	Year	Temperature (deg F)			Year	Temperature (deg F)
1	1971	37	53	87	1980	101
	1982	37			1999	99
	1995	44			2000	99
	2009	44			1991	98
	1985	45			2012	98
	1989	45			2001	97
	2019	45			2008	95
2	1971	35	52	86	1980	102
	2009	37			2012	99
	2019	37			1991	98
	2002	42			2000	96
	1995	44			1999	95
	2007	45			2001	95
3	2002	36	52	85	1980	101
	1973	37			1991	99
	1971	38			2001	97
	2019	39			1995	96
	2014	42			2000	94
	1995	45			2012	94
4	1973	38	51	84	1980	100
	2017	38			1991	98
	2002	39			2014	95
	1989	40			1999	94
	1998	41			2001	93
5	1969	33	51	83	1991	99
	2017	37			1980	98
	2009	40			1996	94
	2019	41			2014	94
	1998	42				
6	2009	32	50	83	1980	97
	1946	36			1991	96
	1969	36			1996	95
	1995	37			2000	94
	2007	37			2014	94
					2004	92
7	2011	38	50	82	1996	100
	1969	39			1980	98
	1998	40			1991	95
	2005	40			2014	94
					2002	91
					2004	91

Table A12 Ambient Air Surface Temperatures Recorded by the Edwards AFB Weather Office in October (Continued)

Date	Low Temperatures		Normal Low Temperature (deg F)	Normal High Temperature (deg F)	High Temperatures	
	Year	Temperature (deg F)			Year	Temperature (deg F)
8	1975	36	49	83	1996	100
	2007	37			1980	97
	1999	39			1991	93
					2002	93
9	1949	37	49	83	1996	99
	1998	38			1980	98
	1970	39			2015	95
	2007	39			1991	94
					2002	94
10	1961	29	49	82	1991	96
	2017	35			1989	95
	1990	37			1999	93
	2013	39			1971	92
	1995	43			1980	92
	2005	43			1996	92
	2009	43			2015	92
11	1973	35	48	81	1950	95
	1998	37			1954	95
	2006	39			1999	93
	2008	39			2015	93
12	2019	31	48	81	1950	96
	1969	32			2015	95
	2008	32			1971	92
	1997	36			1999	92
	1998	41			2010	91
	1990	42			2014	91
13	1986	34	47	81	1950	99
	2019	34			1971	96
	1956	38			1999	93
	2017	38			2004	93
	2000	39			2011	93
14	2017	32	47	81	1991	95
	1975	36			1950	94
	2013	38			1999	94
	2000	39			2011	94
	2008	39			2010	90
15	1966	29	47	81	1991	96
	1985	32			2001	93
	2008	37			1958	92
	2013	37			2010	91
	2017	37			2011	91

Table A12 Ambient Air Surface Temperatures Recorded by the Edwards AFB Weather Office in October (Continued)

Date	Low Temperatures		Normal Low Temperature (deg F)	Normal High Temperature (deg F)	High Temperatures	
	Year	Temperature (deg F)			Year	Temperature (deg F)
16	2018	32	46	80	1991	96
	1984	34			1959	91
	1985	35			2011	91
	1971	36			2001	90
	1984	37			2009	90
	2017	37			2010	90
17	1966	28	46	79	1958	94
	1971	32			1991	94
	1980	36			2017	92
	1998	36			2009	90
					2011	90
18	1998	29	45	78	1991	93
	1966	31			1995	91
	1999	33			1958	90
	1980	35			2003	90
	1984	35			2009	89
19	1969	30	46	79	1947	91
	1971	32			1991	91
	2006	35			1995	91
	1998	36			2003	90
	1999	36			2011	88
20	1949	33	45	78	2003	93
	1971	33			1995	91
	1996	34			2001	91
	1998	36			1974	89
	2013	36			2000	89
					1991	88
21	1948	33	45	77	2003	93
	1949	33			1954	89
	1996	33			1995	88
	1971	37			1999	88
	1999	37			1991	87
					2001	87
22	1996	25	44	77	2003	95
	1966	34			1959	88
	1984	34			2011	88
	1971	35			2016	88
23	1961	32	44	77	1959	93
	1968	32			2017	91
	1996	34			2003	90
	1975	35			2011	87

Table A12 Ambient Air Surface Temperatures Recorded by the Edwards AFB Weather Office in October (Continued)

Date	Low Temperatures		Normal Low Temperature (deg F)	Normal High Temperature (deg F)	High Temperatures	
	Year	Temperature (deg F)			Year	Temperature (deg F)
24	1995	29	43	77	1959	93
	1975	31			2017	90
	1984	35			2003	88
	1996	36				
25	1975	29	43	76	1959	95
	1971	32			2003	89
	1995	33			1990	88
	1997	37			2017	88
	2008	37				
26	1997	30	44	76	1959	90
	1989	32			2017	89
	1956	33			2019	89
	1995	35			1990	86
	1996	36			2008	86
	1998	36			2013	86
27	1997	30	44	74	2018	90
	2006	30			1995	87
	2011	31			1990	86
	1989	32			2003	86
	2012	34			2008	86
					2017	86
28	1970	27	42	73	2018	90
	1991	29			2003	89
	2011	29			2017	88
	1975	31			1990	87
	1997	31			2008	86
29	1970	26	42	72	2008	88
	1971	26			2017	87
	2009	31			1949	86
	1991	27			1990	86
	2011	31			2014	84
	1980	32				
30	1971	20	41	71	1955	83
	1989	30			1965	83
	1970	31			2012	83
	2009	32			1985	82
	2013	32			1990	82
	2011	34			1995	82

Table A12 Ambient Air Surface Temperatures Recorded by the Edwards AFB Weather Office in October (Concluded)

Date	Low Temperatures		Normal Low Temperature (deg F)	Normal High Temperature (deg F)	High Temperatures	
	Year	Temperature (deg F)			Year	Temperature (deg F)
31	2019	21	41	71	1966	83
	1991	26			1997	83
	1972	27			2012	83
	1989	30			1970	82
	2013	31			2011	82
	1999	33			2015	82
	2000	33			1999	80

Table A13 Ambient Air Surface Temperatures Recorded by the Edwards AFB Weather Office in November

Date	Low Temperatures		Normal Low Temperature (deg F)	Normal High Temperature (deg F)	High Temperatures	
	Year	Temperature (deg F)			Year	Temperature (deg F)
1	1991	2828	40	72	2015	87
	1989	29			1949	84
	1971	30			1999	80
	2000	32			2009	80
	2013	32			2011	80
2	1996	23	40	72	1949	83
	1971	26			1960	83
	1989	27			2010	83
	2002	29				
3	1990	23	39	73	2010	85
	2000	26			1949	84
	1971	28			1959	84
	1989	28			1980	83
	2011	28			2009	83
4	1956	24	39	72	1980	87
	1994	24			2018	84
	1990	26			2010	81
	2003	27			2012	81
	2002	28			2016	81
5	1946	28	40	72	1980	84
	1956	28			2012	83
	2015	28			1999	82
	1995	30			2007	82
	2003	30			2016	82
	2013	30			2018	82
6	1947	26	39	71	1980	84
	1959	26			2007	84
	2013	28			1991	83
	2002	29			2012	83
7	1959	26	39	70	1980	86
	1996	29			1991	86
	2011	29			2012	85
	2015	30			2006	83
8	2011	25	39	70	2006	86
	2000	27			1950	83
	1959	28			1991	83
	2015	28			2016	83
9	2011	24	38	69	1980	83
	1948	26			2016	83
	1998	30			2014	82
	2010	30			1991	80
	2018	30			1995	79

Table A13 Ambient Air Surface Temperatures Recorded by the Edwards AFB Weather Office in November (Continued)

Date	Low Temperatures		Normal Low Temperature (deg F)	Normal High Temperature (deg F)	High Temperatures	
	Year	Temperature (deg F)			Year	Temperature (deg F)
10	2018	21	38	68	1980	86
	1948	24			2014	81
	1998	26			2016	81
	2011	29			1990	78
11	1950	20	38	66	1973	79
	2012	23			1989	78
	2015	25			2016	78
	2018	26				
12	2000	21	38	66	1989	81
	2012	22			1999	80
	2015	22			1981	78
	2018	22			1996	78
13	2000	20	37	67	1956	85
	2012	21			1999	82
	2015	24			1989	80
	2018	25			1995	80
14	1968	23	38	65	1995	82
	2012	24			1999	81
	1980	25			2008	81
	1981	25			1967	80
15	1994	21	37	65	2016	82
	1956	22			1995	81
	1971	26			2017	81
	2000	28			1975	80
16	1956	21	36	65	2006	82
	2009	22			1995	81
	1958	23			2008	81
	2000	23			1981	79
	1991	27			2007	79
17	1958	18	37	64	2006	82
	2000	22			1977	79
	2009	23			2008	79
	2015	23			1990	77
	1971	24			1995	77
18	1958	16	35	64	1995	81
	1980	22			1949	80
	2000	22			1996	78
	2009	25			2006	77
	2014	27			2007	77
19	1964	13	34	64	1996	81
	2000	20			2007	81
	1998	22			1949	80
	2009	23			1996	80

Table A13 Ambient Air Surface Temperatures Recorded by the Edwards AFB Weather Office in November (Continued)

Date	Low Temperatures		Normal Low Temperature (deg F)	Normal High Temperature (deg F)	High Temperatures	
	Year	Temperature (deg F)			Year	Temperature (deg F)
20	1964	15	33	63	2002	78
	2000	20			1996	77
	1998	23			2003	77
	2009	23			2008	77
21	1964	18	34	62	1995	81
	1980	24			1950	80
	1998	26			1989	78
	2018	27			2001	77
22	1983	21	34	63	2007	81
	1956	22			1950	77
	2007	23			1998	76
	1999	25			1995	74
	2009	25			2006	73
23	1947	18	33	64	2017	80
	1999	20			1981	79
	2003	22			1995	78
	2007	23			1998	77
24	1999	19	33	64	2017	86
	2003	21			1949	81
	2007	21			1995	75
	1974	22			2005	73
25	2010	19	35	64	1947	81
	2016	23			1949	81
	1956	24			2017	79
	1966	24			1995	78
	1999	24			2005	78
	2014	25			2012	78
26	2010	17	33	63	2017	83
	2016	21			1949	81
	1955	22			1977	81
	1980	24				
27	2010	18	32	63	1949	80
	2005	22			1999	74
	1974	24			1991	73
28	1968	21	32	61	1950	78
	1990	21			2014	74
	2005	23			2002	72
	2001	24			1980	70
	2015	24			2000	70

Table A13 Ambient Air Surface Temperatures Recorded by the Edwards AFB Weather Office in November (Concluded)

Date	Low Temperatures		Normal Low Temperature (deg F)	Normal High Temperature (deg F)	High Temperatures	
	Year	Temperature (deg F)			Year	Temperature (deg F)
29	1958	16	32	61	2014	76
	2010	18			1949	74
	2015	19			2000	73
	1989	21			1980	72
					1995	72
30	2015	15	31	61	1980	74
	2004	16			1949	73
	1957	17			1999	72
	1958	17			1995	71
	2010	17			2011	71

Table A14 Ambient Air Surface Temperatures Recorded by the Edwards AFB Weather Office in December

Data	Low Temperatures Year	Low Temperatures Temperature (deg F)	Normal Low Temperature (deg F)	Normal High Temperature (deg F)	High Temperatures Year	High Temperatures Temperature (deg F)
1	2004	16	31	61	1995	78
	1958	17			1949	76
	2006	19			2005	74
	1976	20			1980	72
	2015	20			2017	69
2	2004	18	32	61	2008	75
	1957	20			1949	74
	2006	20			1980	72
	1990	21			2017	71
3	1996	19	31	60	1958	76
	1973	21			1977	70
	1990	21			2012	69
	2004	21			2000	67
	2009	22			2017	67
4	2006	14	31	59	1958	84
	2011	16			2003	68
	1968	17			1976	66
	2004	19			2016	65
5	2006	14	32	59	1958	78
	1968	16			2012	75
	2011	19			2007	72
	1999	20			2000	69
	2005	20				
6	1959	17	31	59	1977	77
	2005	17			2003	70
	2011	17			2012	70
	2006	18			2007	68
7	1978	14	32	58	1950	73
	2011	14			2000	70
	1998	15			2006	70
	2006	19			2001	68
8	1978	14	31	58	1950	73
	1998	17			2000	67
	2011	18			2006	66
	1976	20			2015	66
	1990	20			2017	66
9	1956	9	31	58	2015	76
	1994	12			2010	72
	1978	13			1993	71
	2013	18			1979	70
	2011	19			2016	68
	2009	21			2017	67

Table A14 Ambient Air Surface Temperatures Recorded by the Edwards AFB Weather Office in December (Continued)

Data	Low Temperatures Year	Low Temperatures Temperature (deg F)	Normal Low Temperature (deg F)	Normal High Temperature (deg F)	High Temperatures Year	High Temperatures Temperature (deg F)
10	1956	12	31	58	1975	73
	2013	14			2016	71
	1998	16			2015	70
	1978	18			2010	67
	2011	18			2002	64
11	1972	10	30	58	1977	72
	1998	16			1990	72
	2013	16			2016	69
	1999	19			2017	69
	2011	20			2010	66
12	1972	13	30	58	1950	77
	2017	15			2016	70
	2007	19			2008	68
	1998	21			2004	66
	2013	21			2010	66
13	1968	14	29	58	1950	72
	2017	20			2016	71
	1976	21			2002	67
	1978	22			2004	67
	2001	22			2005	67
					2017	67
14	1972	16	29	57	1977	76
	2007	19			2016	74
	1976	22			2017	73
	1978	22			2010	72
15	1972	16	29	57	1981	75
	1990	17			1998	74
	2015	17			1980	72
	1978	18			2006	70
	1999	19			2016	69
16	1975	14	29	58	1998	78
	2015	16			1980	76
	2005	17			1976	65
	2001	20			2000	65
	2007	21			2017	65
17	1990	18	30	58	1998	74
	2003	18			1980	70
	2015	18			1999	68
	1976	19			2000	64
	2001	20			2013	64

Table A14 Ambient Air Surface Temperatures Recorded by the Edwards AFB Weather Office in December (Continued)

Data	Low Temperatures		Normal Low Temperature (deg F)	Normal High Temperature (deg F)	High Temperatures	
	Year	Temperature (deg F)			Year	Temperature (deg F)
18	1968	16	30	57	1980	75
	2016	16			1999	74
	2008	18			1998	70
	1990	19			1990	63
	2004	20			2003	63
	2015	20			2018	63
19	2006	16	30	57	1981	76
	2016	17			1999	70
	1996	19			1980	69
	2015	19			2017	68
20	2016	13	30	57	1969	72
	2012	15			1980	67
	2006	16			1999	67
	1973	19			2004	66
21	1968	13	30	56	2018	73
	1998	13			1969	72
	2012	14			1999	71
	1990	15			2000	68
22	1990	4	31	56	2005	77
	1968	7			1955	73
	1998	8			2000	71
	2017	14			1980	67
	1976	15			2014	67
23	1998	9	30	56	1969	73
	2011	15			2005	70
	1956	16			1980	69
	2006	19			1999	67
24	1998	5	29	56	2005	72
	2011	15			1964	71
	1976	16			2018	68
	2009	19			1999	67
25	1998	13	29	57	2005	73
	1953	15			1969	71
	2011	18			2013	66
	2004	18			1999	64
26	1990	14	28	56	1964	68
	1962	17			2017	67
	2011	17			1999	65
	1998	19			2000	62
	2013	21			2013	62

Table A14 Ambient Air Surface Temperatures Recorded by the Edwards AFB Weather Office in December (Concluded)

Data	Low Temperatures		Normal Low Temperature (deg F)	Normal High Temperature (deg F)	High Temperatures	
	Year	Temperature (deg F)			Year	Temperature (deg F)
27	1962	8	29	55	1989	69
	1990	14			1980	67
	2015	14			2017	66
	2011	17			1999	65
28	1962	10	30	55	1980	73
	1990	14			1998	69
	2015	14			2013	68
	2003	17			2017	66
	2012	17			1999	65
29	1962	14	30	56	1980	74
	1967	14			2017	67
	2015	17			1998	65
	2018	19			2000	65
					2011	65
30	2015	13	29	56	2011	75
	1962	15			1950	74
	2006	19			1980	74
	1978	22			1998	70
	1999	22			2005	67
	2013	22				
31	1969	16	30	55	1980	68
	2015	16			2017	68
	2012	18			1998	67
	2000	21			2001	67
	2013	22			2011	66

APPENDIX B - EXAMPLES OF LOW-FIELD ELEVATION AIRPORTS

Table B1 Examples of Low-Field Elevation Airports

Number	Airport Name	Airport Designator	Field Elevation (ft)	Latitude (deg)	Longitude (deg)
1	Minhat Hashnayim Airfield (Sedom or Sdom or Sodom), Israel	SED	-1301	31.2 N	35.4E
2	I Bar Yehuda (AKA Dead Sea)(Metzada or Masada), Israel	LLM/MTZ	-1266	31.3 N	35.4 E
3	Turpan Jiaohe, China	ZWTP/TLQ	-505	43.0 N	89.2 E
4	Furnace Creek (Death Valley), California	L06	-210	36.5 N	116.9 W
5	Cliff Hatfield Memorial Airport (Calipatria), California	CLR	-182	33.1 N	115.5 W
6	Brawley Municipal Airport, California	BWC	-128	33.0 N	115.5 W
7	Jacqueline Cochran Regional Airport, (Thermal), California	TRM	-115	33.6 N	116.2 W
8	O'Connell (private airport) Salton Sea, California	N/A	-99	33.0 N	115.5 W
9	Salton Sea, California	SAS	-84	33.2 N	116.0 W
10	Ramsar, Iran	OINR/RZR	-70	36.9 N	50.7 E
11	Noshahr, Iran	OINN/NSH	-61	36.7 N	51.5 E
12	Imperial County (Imperial), California	IPL	-54	32.8 N	115.6 W
13	El Centro NAF (El Centro), California	KNJK	-42	32.8 N	115.7 W
14	Rasht, Iran	OIGG/RAS	-40	37.3 N	49.6 E
15	Schiphol (Amsterdam), Netherlands	EHAM/AMS	-11	52.3 N	4.8 E
16	Desert Air (private gliderport) Salton Sea, California	N/A	0	33.5 N	115.9 W
17	New Orleans NAS JRB (AKA Alvin Callender Field) New Orleans, Louisiana	KNBG	3	29.8 N	90.3 W
18	Louis Armstrong International Airport (New Orleans), Louisiana	MSY	4	30.0 N	90.3 W
19	Oakland International Airport, California	OAK	6	37.7 N	122.2 W
20	Stovepipe Wells (Death Valley), California	L09	25	36.6 N	117.2 W
21	Moffett Federal Airfield (Mountain View), California	NUQ	32	37.4 N	112.0 W
22	Yuma MCAS/Yuma International, Arizona	KNYl	213	32.7 N	114.6 W
23	Palm Springs International Airport, California	KPSP	477	33.8 N	116.5 W
24	Borrego Valley Airport (Borrego Springs), California	L08	520	33.3 N	116.3 W

Notes: 1. Field elevation is the height above mean sea level of the highest point on a runway or taxiway.
2.The elevation of the approach end of runway 04/22 at New Orleans NAS in New Orleans, Louisiana is -1 foot.
3. The elevation of the approach end of runway 15 at Oakland International in Oakland, California is -1 foot.

This page was intentionally left blank.

APPENDIX C - EXAMPLES OF HIGH-FIELD ELEVATION AIRPORTS

Table C1 Examples of High-Field Elevation Airports Outside the United States

Number	Airport Name	ICAO Airport Designator	IATA Airport Designa	Field Elevation (ft)	Latitude (deg)	Longitude (deg)
1	Nagqu Dagring, Tibet	N/A	N/A	14,554	N/A	N/A
2	San Rafael, Peru	SPRF	N/A	14,422	14.3 S	70.5 W
3	Qambo Bangda, (AKA Changdu Bangda), Tibet	ZUBD	BPX	14,219	30.6 N	97.1 E
4	Kangding, Tibet	N/A	N/A	14,040	N/A	N/A
5	Ali Kunsha (AKA Ngari Gunsa and Elikunsha), Tibet	N/A	N/A	14,020	N/A	N/A
6	El Alto (La Paz), Bolivia	SLLP	LPB	13,325	16.5 S	68.2 W
7	Ventilla, Peru	SPNP	N/A	13,123	15.8 S	70.1 W
8	Yauri, Peru	SPIY	N/A	12,972	14.8 S	71.4 W
9	Captain Nicolas Rojas (Postosi), Bolivia	SLPO	POI	12,913	19.5 S	65.7 W
10	Yushu Batang, China	ZLYS	YUS	12,762	32.8 N	97.1 E
11	Copacabana, Bolivia	SLCC	N/A	12,591	16.2 S	69.1 W
12	Inca Manco Capac (Juliaca), Peru	SPJL	JUL	12,552	15.5 S	70.2 W
13	Coposa, Chile	SCKP	N/A	12,468	20.8 S	68.7 W
14	Xigaze Peace (AKA Shigatse), Tibet	N/A	N/A	12,405	N/A	N/A
15	Juan Mendoza (Oruro), Bolivia	SLOR	ORU	12,146	18.0 S	67.1 W
16	Laja, Bolivia	SLLJ	N/A	12,103	16.5 S	68.3 W
17	Lhasa Gonggar (Lhasa), Tibet	ZULS	LXA	11,712	29.3 N	90.9 E
18	Jiuzhai Huanglong (AKA Jiuzhaigou and Jiuhuang), China	ZUJZ	JZH	11,311	32.9 N	103.7 E
19	Andahuaylas, Peru	SPHY	ANS	11,300	13.7 S	73.4 W
20	Jauja, Peru	SPJJ	JAU	11,034	11.8 S	75.5 W
21	Alejandro Velasco Astete (Cuscu), Peru	SPZO	CUZ	10,860	13.5 S	71.9 W
22	Deqen Shangri-La, Tibet	ZPDQ	DIG	10,761	27.8 N	99.7 E
23	Leh, India	VILH	IXL	10,682	34.1 N	77.5 E
24	San Luis (Ipiales), Colombia	SKIP	IPI	9765	0.9 N	77.7 W
25	Nyingchi (AKA Linzhi), Tibet	ZUNZ	LZY	9670	29.3 N	94.3 E
26	Teniente Coronel Luis a Mantilla (Tulcan), Ecuador	SETU	TUA	9649	0.8 S	77.7 W
27	Juana Azurduy de Padilla (Sucre), Bolivia	SLSU	SRE	9527	19.0 S	65.3 W
28	Tenzing-Hillary (Lukla), Nepal	VNLK	LUA	9337	27.7 N	86.7 E

Table C1 Examples of High-Field Elevation Airports Outside the United States (Continued)

Number	Airport Name	ICAO Airport Designator	IATA Airport Designa	Field Elevation (ft)	Latitude (deg)	Longitude (deg)
29	Golmud, China	ZLGM	GOQ	9333	36.4 N	94.8 E
30	Mariscal Sucre (Quito), Ecuador	SEQU	UIO	9228	0.1 S	78.5 W
31	Cotopaxi (Latacunga), Ecuador	SELT	LTX	9205	0.9 S	78.6 W
32	Comandante FAP German Arias Graziani (Huaraz), Peru	SPHZ	ATA	9097	9.3 S	77.6 W
33	Yongphulla (AKA Yonphula), Bhutan	VQTY	N/A	9000	27.3 N	91.5 E
34	Coronel FAP Alfredo Mendivil Duarte (Ayacucho), Peru	SPHO	AYP	8917	13.2 S	74.2 W
35	Bathpalathang (AKA Bumthang), Bhutan	VQBT	N/A	8856	27.6 N	90.7 E
36	Jomsom, Nepal	VNJS	JMO	8800	28.8 N	83.7 W
37	Major General FAP Armando Revoredo Iglesias (Cajamarca), Peru	SPJR	CJA	8781	7.1 S	78.5 W
38	Chachoan (Ambato), Ecuador	SEAM	ATF	8502	1.2 S	78.6 W
39	Licenciado Adolfo Lopez Mateos (Toluca), Mexico	MMTO	TLC	8466	19.3 N	99.6 W
40	Rodriguez Ballon (Arequipa), Peru	SPQU	AQP	8405	16.3 S	71.6 W
41	Guaymaral (Bogota), Colombia	SKGY	GAA	8390	4.8 N	74.1 W
42	Bamyan, Afghanistan	OABN	BIN	8367	34.8 N	67.8 E
43	El Dorado (Bogota), Colombia	SKBO	BOG	8361	4.7 N	74.1 W
44	Jorge Wilsterman (Cochabamba), Bolivia	SLCB	CBB	8360	17.4 S	66.2 W
45	Chachapoyas, Peru	SPPY	CHH	8333	6.2 S	77.9 W
46	Major Justino Marino Cuesto (Madrid), Colombia	SKMA	N/A	8325	4.7 N	74.3 W
47	Mariscal Lamar (Cuenca), Ecuador	SECU	CUE	8306	2.9 S	79.0 W
48	Mariscal Sucre International Airport, (Tababela/Quito),Equador	SEQM	UIO	7910	0.1S	78.4W
49	Bole (Addis Ababa), Ethiopia	HAAB	ADD	7656	9.0 N	38.8 E
50	Matekane Air Strip, Lesotho	FXME	N/A	7544	29.9 S	27.8 E
51	Chaghcharan, Afghanistan	OACC	CNN	7383	34.5 N	65.3 E
52	Paro, Bhutan	VQPR	PBH	7332	27.4 N	89.4 E
53	Licenciado Benito Juarez (Mexico City), Mexico	MMMX	MEX	7316	19.4 N	99.1 W
54	Semonkong, Lesotho	FXSM	SOK	7200	29.8 S	28.1 E
55	Dali (AKA Dali Huangcaoba), China	ZPDL	DLU	7050	25.7 N	100.3 E
56	Jose Maria Cordova (Medellin), Colombia	SKRG	MDE	7027	6.2 N	75.4 W
57	Sardeh Band, Afghanistan	OADS	SBF	6971	33.3 N	68.6 E
58	Kunming Changshui International Airport, China	ZPPP	KMG	6900	25.1N	102.9 E

Table C1 Examples of High-Field Elevation Airports Outside the United States (Concluded)

Number	Airport Name	ICAO Airport Designator	IATA Airport Designa	Field Elevation (ft)	Latitude (deg)	Longitude (deg)
59	Sheghnan (AKA Shughnan), Afghanistan	OASN	N/A	6750	37.5 N	71.5 E
60	Shahrekord, Iran	OIFS	CQD	6723	32.3 N	50.8 E
61	La Nubia (Manizales), Colombia	SKMZ	MZL	6690	5.0 N	75.7 W
62	King Khalid Air Base (Khamis Mushait) Saudi Arabia	OEKM	KMX	6663	18.3 N	42.8 E
63	Courchevel Airport, France	LGLJ	CVF	6588	45.4 N	6.6 E
64	Capitan Oriel Lea Plaza (Tarija), Bolivia	SLTJ	TJA	6084	21.6 S	64.7 W
65	Alferez FAP David Figueroa Fernandini (Huanuco), Peru	SPNC	HUU	6070	9.9 S	76.2 W
66	Antonio Narino (Pasto), Colombia	SKPS	PSO	5951	1.4 N	77.3 W
67	Yasuj, Iran	OISY	YES	5939	30.7 N	51.5 E
68	Hamid Karzai International Airport, Kabul, Afghanistan	OAKB	KBL	5877	34.6 N	69.2 E
69	Hamadan, Iran	OIHH	HDM	5755	34.9 N	48.6 E
70	Kerman, Iran	OIKK	KER	5741	30.3 N	57.0 E
71	Guillermo Leon Valencia (Popayan), Colombia	SKPP	PPN	5687	2.5 N	76.6 W
72	Samedan (AKA Engadin Airport) St. Moritz, Switzerland	LSZS	SMV	5600	46.5 N	9.9 E
73	OR Tambo (AKA Johannesburg and Jan Smuts), South Africa	FAJS	JNB	5558	26.1 S	28.2 E
74	Moshoeshoe I International Airport (Maseru), Lesotho	FXMM	MSU	5348	29.5 S	27.6 E
75	Jomo Kenyatta International Airport, Nairobi, Kenya ()	HKJK	NBO	5327	1.3 S	36.9 E
76	Rafsanjan, Iran	OIKR	RJN	5298	30.3 N	56.1 E
77	Ricardo Garcia Posada (El Salvador), Chile	SCES	ESR	5240	26.3 S	69.8 W
78	Peyresourde, France	LFIP	N/A	5193	42.8N	0.4 E
79	Xichang Qingshan, China	ZUXC	XIC	5112	28.0 N	102.2 E
80	Mejametalana (Maseru), Lesotho	FXMU	N/A	5105	29.3 S	27.5 E
81	Isfahan, Iran	OIFM	IFN	5059	32.8 N	51.9 E
82	Bagram, Afghanistan	OAIX	OAI	4895	34.9 N	69.3 E
83	Tribhuvan (Kathmandu), Nepal	VNKT	KTM	4390	27.7 N	85.4 E
84	Kandahar International Airport, Kandahar, Afghanistan	OAKN	KDH	3330	31.5 N	65.9 E
85	Toncontin (Tegucigalpa) , Honduras	MHTG	TGU	3294	14.1 N	87.2 W

Note: Field elevation is the height above mean sea level of the highest point on a runway or a taxiway.

Table C2 Examples of High Field Elevation Airports in the United States

Number	Airport Name	City	State	FAA Airport Designator	Field Elevation (ft)	Latitude (deg)	Longitude (deg)
1	Lake County Airport	Leadville	Colorado	LXV	9934	39.2 N	106.3 W
2	Telluride Regional	Telluride	Colorado	TEX	9070	38.0 N	107.9 W
3	Mineral County Memorial	Creede	Colorado	C24	8680	37.8 N	106.9 W
4	Angel Fire	Black Lake	New Mexico	AXX	8380	36.4 N	105.3 W
5	Silver West	Westcliffe	Colorado	CO8	8290	38.0 N	105.4 W
6	Granby-Grand County	Granby	Colorado	GNB	8207	40.1 N	105.9 W
7	Walden-Jackson County	Walden	Colorado	33V	8154	40.8 N	106.3 W
8	Astronaut Kent Rominger	Del Norte	Colorado	8V1	7949	37.7 N	106.4 W
9	Central Colorado Regional	Buena Vista	Colorado	AEJ	7946	38.8 N	106.1 W
10	Saguache Municipal	Saguache	Colorado	O4V	7850	38.1 N	106.2 W
11	Aspen-Pitkin County/Sardy Field	Aspen	Colorado	ASE	7820	39.2 N	106.9 W
12	Blanca	Blanca	Colorado	O5V	7720	37.4 N	105.6 W
13	Questa Municipal NR2	Cerro	New Mexico	N24	7700	36.8 N	105.6 W
14	Jewett Mesa	Apache Creek	New Mexico	13Q	7681	34.0 N	108.7 W
15	Gunnison-Crested Butte Regional Airport	Gunnison	Colorado	GUC	7680	38.5 N	106.9 W
16	Stevens Field	Pagosa Springs	Colorado	PSO	7664	37.3 N	107.1 W
17	Monte Vista Municipal	Monte Vista	Colorado	MVI	7611	37.5 N	106.0 W
18	Leach	Center	Colorado	1V8	7598	37.8 N	106.0 W
19	Bryce Canyon	Bryce Canyon	Utah	BCE	7590	37.7 N	112.1 W
20	Alamosa/San Luis Valley Regional/Bergman Field	Alamosa	Colorado	ALS	7539	37.4 N	105.9 W
21	Harriet Alexander Field	Salida	Colorado	ANK	7523	38.5 N	106.0 W
22	McElroy Airfield	Kremmling	Colorado	20V	7411	40.1 N	106.4 W
23	Laramie Regional Airport	Laramie	Wyoming	LAR	7284	41.3 N	105.7 W
24	Lindrith Airpark	Lindrith	New Mexico	E32	7202	36.3 N	107.1 W
25	Los Alamos	Los Alamos	New Mexico	LAM	7171	35.9 N	106.3 W
26	Cuchara Valley at La Veta	La Veta	Colorado	O7V	7153	37.5 N	105.0 W
27	Evanston-Uinta County Burns Field	Evanston	Wyoming	EVW	7143	41.3 N	111.0 W
28	Mammoth Yosemite	Mammoth Lakes	California	MMH	7135	37.6 N	118.8 W
29	Taos Regional Airport	Taos	New Mexico	SKX	7095	36.5 N	105.7 W
30	Springerville Municipal	Springerville	Arizona	D68	7055	34.1 N	109.3 W

Table C2 Examples of High Field Elevation Airports in the United States (Continued)

Number	Airport Name	City	State	FAA Airport Designator	Field Elevation (ft)	Latitude (deg)	Longitude (deg)
31	Fort Bridger	Fort Bridger	Wyoming	KFBR	7034	41.4 N	110.4 W
32	Cold Meadows USFS	N/A	Idaho	KU81	7030	45.3 N	114.9 W
33	Wayne Wonderland	Loa	Utah	38U	7029	38.4 N	111.6 W
34	Flagstaff Pulliam	Flagstaff	Arizona	FLG	7014	35.1 N	111.7 W
35	Saratoga/ Shively Field	Saratoga	Wyoming	SAA	7012	41.5 N	106.8 W
36	Dove Creek	Dove Creek	Colorado	8V6	6975	37.8 N	108.9 W
37	Monticello	Monticello	Utah	U64	6966	37.9 N	109.3 W
38	Big Piney/ Miley Memorial Field	Big Piney	Wyoming	BPI	6990	42.6 N	110.1 W
39	Mesa View Ranch	Craig	Colorado	5C07	6978	40.8 N	107.5 W
40	Steamboat Springs/Bob Adams Field	Steamboat Springs	Colorado	SBS	6882	40.5 N	106.9 W
41	Las Vegas Municipal	Las Vegas	New Mexico	LVS	6877	35.7 N	105.1 W
42	Meadow Lake	Falcon	Colorado	FLY	6874	38.9 N	104.6 W
43	Sweetwater	Wellington	Nevada	NV72	6837	38.5 N	119.2 W
44	Sierra Blanca Regional Airport	Ruidoso	New Mexico	SRR	6814	33.5 N	105.5 W
45	Rawlins Municipal/ Harvey Field	Rawlins	Wyoming	RWL	6813	41.8 N	107.2 W
46	Lee Vining	Lee Vining	California	O24	6802	38.0 N	119.1 W
47	Rock Springs-Sweetwater County	Rock Springs	Wyoming	RKS	6764	41.6 N	109.1 W
48	Panguitch Municipal	Panguitch	Utah	U55	6763	37.8 N	112.4 W
49	Big Bear City	Big Bear	California	L35	6752	34.3 N	116.9 W
50	Window Rock	Window Rock	Arizona	RQE	6742	35.7 N	109.1 W
51	Magdalena	Magdalena	New Mexico	N29	6727	34.1 N	107.3 W
52	Crownpoint	Crownpoint	New Mexico	OE8	6696	35.7 N	108.2 W
53	H.A. Clark Memorial Field	Williams	Arizona	CMR	6691	35.3 N	112.2 W
54	Durango-La Plata County	Oxford	Colorado	DR0	6685	37.2 N	107.8 W
55	Animas Air Park	Durango	Colorado	OOC	6684	37.2 N	107.9 W
56	West Yellowstone/ Yellowstone	West Yellowstone	Montana	WYS	6644	44.7 N	111.1 W
57	Grand Canyon	Grand Canyon	Arizona	GCN	6609	35.9N	112.1W
58	Yampa Valley	Hayden	Colorado	HDN	6606	40.5N	107.2W
59	USAF Academy Airfield	Colorado Springs	Colorado	KAFF	6572	39.0N	104.8W

Table C2 Examples of High Field Elevation Airports in the United States (Continued)

Number	Airport Name	City	State	FAA Airport Designator	Field Elevation (ft)	Latitude (deg)	Longitude (deg)
60	Dutch John	Dutch John	Utah	K33U	6561	40.9N	109.4W
61	Eagle County Regional Airport	Eagle	Colorado	EGE	6548	39.6N	106.9W
62	Grants – Milan Municipal Airport	Grants	New Mexico	GNT	6537	35.2N	107.9W
63	Mountainair Municipal Airport	Mountainair	New Mexico	M1O	6492	34.5N	106.2W
64	Navajo Dam	Navajo Lake	New Mexico	1VO	6475	36.8N	107.7W
65	Bryant Field	Bridgeport	California	O57	6472	38.3N	119.2W
66	Gallup Municipal Airport	Gallup	New Mexico	GUP	6472	35.5N	108.8W
67	Crawford	Crawford	Colorado	99V	6470	38.7N	107.6W
68	Black Rock	Zuni Pueblo	New Mexico	ZUN	6454	35.1N	108.8W
69	Jackson Hole	Jackson	Wyoming	JAC	6451	43.6N	110.7W
70	Calhan	Calhan	Colorado	5V4	6450	39.0N	104.3W
71	Meeker	Meeker	Colorado	EEO	6426	40.0N	107.9W
72	Show Low Regional Airport	Show Low	Arizona	SOW	6415	34.3N	110.0W
73	Stevens – Crosby	North Fork	Nevada	O8U	6397	41.5N	115.9W
74	Bruce Meadows	Stanley	Idaho	KU63	6370	44.4N	115.3W
75	Santa Fe Municipal Airport	Santa Fe	New Mexico	SAF	6350	35.6N	106.1W
76	South Lake Tahoe	South Lake Tahoe	California	TVL	6269	38.9N	120.0W
77	Ely Airport/Yelland Field	Ely	Nevada	KELY	6259	39.3N	114.8W
78	Afton Municipal Airport	Afton	Wyoming	KAFO	6201	42.7N	110.9W
79	Moriarty	Moriarty	New Mexico	OEO	6199	35.0N	106.0W
80	City of Colorado Springs Municipal Airport	Colorado Springs	Colorado	COS	6187	38.8N	104.7W
81	Manila	Manila	Utah	4OU	6179	41.0N	109.7W
82	Cheyenne Regional Airport/ Jerry Olson Field	Cheyenne	Wyoming	CYS	6159	41.2N	104.8W
83	Colorado Springs East	Ellicott	Colorado	A5O	6145	38.9N	104.4W
84	Whiskey Creek	Whiskey Creek	New Mexico	94E	6126	32.8N	108.2W
85	Junction	Junction	Utah	U13	6069	38.3N	112.2W
86	Spanish Peaks Airfield	Walsenburg	Colorado	4V1	6056	37.7N	104.8W
87	USAF Academy Bullseye Auxiliary Airstrip	Colorado Springs	Colorado	CO9O	6036	38.8N	104.3W
88	Fort Ruby Ranch	Ruby Valley	Nevada	16U	6006	40.1N	115.5W

Table C2 Examples of High Field Elevation Airports in the United States (Continued)

Number	Airport Name	City	State	FAA Airport Designator	Field Elevation (ft)	Latitude (deg)	Longitude (deg)
89	Valle	Valle	Arizona	4OG	5999	35.7N	112.1W
90	Kirkeby Ranch	Ely	Nevada	O4U	5980	38.9N	114.4W
91	Geyser Ranch	Ely	Nevada	O3U	5977	38.7N	114.6W
92	Eureka	Eureka	Nevada	O5U	5958	39.6N	116.0W
93	Carbon County Regional Airport/ Buck Davis Field	Price	Utah	PUC	5957	39.6N	110.8W
94	Kingston	Kingston	Nevada	N15	5950	39.2N	117.1W
95	Hopkins Field	Nucla	Colorado	AIB	5940	38.2N	108.6W
96	Parowan	Parowan	Utah	K1L9	5930	37.9N	112.8W
97	Bear Lake Country Airport	Paris	Idaho	K1U7	5928	42.3N	111.3W
98	Vaughn	Vaughn	New Mexico	N17	5928	34.6N	105.2W
99	Cortez Municipal Airport	Cortez	Colorado	CEZ	5918	37.3N	108.6W
100	Glenwood Springs Municipal Airport	Glenwood Springs	Colorado	GWS	5916	39.5N	107.3W
101	Huntington Municipal Airport	Huntington	Utah	69V	5915	39.4N	110.9W
102	Truckee – Tahoe	Truckee	California	TRK	5901	39.3N	120.1W
103	Springer Municipal Airport	Springer	New Mexico	S42	5891	36.3N	104.6W
104	Denver Centennial Airport	Denver	Colorado	APA	5885	39.6N	104.9W
105	Aztec Municipal Airport	Aztec	New Mexico	N19	5882	36.8N	108.0W
106	Blanding Municipal Airport	Blanding	Utah	BDG	5868	37.6N	109.5W
107	Alpine County Airport	Markleeville	California	M45	5867	38.7N	119.8W
108	Beaver Municipal Airport	Beaver	Utah	U52	5863	38.2N	112.7W
109	Butts Army Air Field	Fort Carson	Colorado	KFCS	5838	38.7N	104.8W
110	Albuquerque / Double Eagle II	Albuquerque	New Mexico	AEG	5837	35.1N	106.8W
111	Mount Pleasant	Mount Pleasant	Utah	43U	5830	39.5N	111.5W
112	Duchesne Municipal Airport	Duchesne	Utah	KU69	5826	40.2N	110.4W
113	Taylor	Taylor	Arizona	TYL	5823	34.5N	110.1W
114	North Fork Valley	Paonia	Colorado	7V2	5798	38.8N	107.6W
115	Wells Municipal / Harriet Field	Wells	Nevada	LWL	5769	41.1N	114.9W
116	Chamberlain USFS	Chamberlain	Idaho	KU79	5765	45.4N	115.2W

Table C2 Examples of High Field Elevation Airports in the United States (Continued)

Number	Airport Name	City	State	FAA Airport Designator	Field Elevation (ft)	Latitude (deg)	Longitude (deg)
117	Perry Stokes	Trinidad	Colorado	TAD	5762	37.3N	104.3W
118	Montrose Regional Airport	Montrose	Colorado	MTJ	5759	38.5N	107.9W
119	Round Mountain	Hadley	Nevada	NV76	5744	38.7N	117.1W
120	St Johns Industrial Air Park	St Johns	Arizona	SJN	5737	34.5N	109.4W
121	Austin	Austin	Nevada	TMT	5735	39.5N	117.2W
122	Escalante Municipal Airport	Escalante	Utah	K1L7	5733	37.7N	111.6W
123	Pinon Canyon Army Air Field	Pinon Canyon	Colorado	OCD5	5698	37.5N	104.1W
124	Kayenta	Kayenta	Arizona	OV7	5688	36.7N	110.2W
125	Doctors Mesa	Eckert/Orchard City	Colorado	EOO	5680	38.9N	108.0W
126	Denver / Rocky Mountain Metropolitan Airport	Denver	Colorado	BJC	5673	39.9N	105.1W
127	Buckley AFB	Aurora	Colorado	KBKF	5664	39.7N	104.8W
128	Heber City Municipal / Russ McDonald Airport	Heber City	Utah	K36U	5637	40.5N	111.4W
129	Cedar City Regional Airport	Cedar City	Utah	CDC	5622	37.7N	113.1W
130	Hunt Field	Lander	Wyoming	KLND	5586	42.8N	108.7W
131	Polacca	Polacca	Arizona	P1O	5573	35.8N	110.4W
132	Butte/Bert Mooney	Butte	Montana	BTM	5550	46.0N	112.5W
133	Chinle Municipal Airport	Chinle	Arizona	E91	5550	36.1N	109.6W
134	Tonopah Test Range	Tonopah	Nevada	KTNX	5550	37.8N	116.8W
135	Garfield County Regional Airport	Rifle	Colorado	RIL	5537	39.5N	107.7W
136	Riverton Regional Airport	Riverton	Wyoming	RIW	5528	43.1N	108.5W
137	Denver / Front Range	Denver	Colorado	FTG	5512	39.8N	104.5W
138	Farmington / Four Corners Regional Airport	Farmington	New Mexico	FMN	5506	36.7N	108.2W
139	Manti-Ephraim	Manti-Ephraim	Utah	41U	5500	39.3N	111.6W
140	Grant County Airport	Silver City	New Mexico	SVC	5446	32.6N	108.2W
141	Fremont County Airport	Canon City	Colorado	1V6	5442	38.4N	105.1W
142	Denver International Airport	Denver	Colorado	DEN	5432	39.9N	104.7W
143	Tonopah	Tonopah	Nevada	TPH	5430	38.1N	117.1W
144	Glenwood – Catron County Airport	Glenwood	New Mexico	E94	5428	33.3N	108.9W

Table C2 Examples of High Field Elevation Airports in the United States (Continued)

Number	Airport Name	City	State	FAA Airport Designator	Field Elevation (ft)	Latitude (deg)	Longitude (deg)
145	Grand Canyon Caverns	Peach Springs	Arizona	L37	5386	35.5N	113.3W
146	Owyhee	Owyhee	Nevada	1OU	5377	42.0N	116.2W
147	Limon Municipal Airport	Limon	Colorado	LIC	5374	39.3N	103.7W
148	Carrizozo Municipal Airport	Carrizozo	New Mexico	F37	5371	33.6N	105.9W
149	Albuquerque International Sunport	Albuquerque	New Mexico	ABQ	5355	35.0N	106.6W
150	Casper/Natrona County International Airport	Casper	Wyoming	CPR	5350	42.9N	106.5W
151	Arco Butte County Airport	Arco	Idaho	KAOC	5332	43.6N	113.3W
152	Friedman Memorial Airport	Hailey	Idaho	KSUN	5318	43.5N	114.3W
153	Richfield Municipal Airport	Richfield	Utah	KRIF	5301	38.7N	112.1W
154	Boulder Municipal Airport	Boulder	Colorado	BDU	5288	40.0N	105.2W
155	Blue Canyon - Nyack	Emigrant Gap	California	BLU	5284	39.3N	120.7W
156	Rangely	Rangely	Colorado	4VO	5278	40.1N	108.8W
157	Vernal Regional Airport	Vernal	Utah	VEL	5278	40.4N	109.5W
158	Shiprock Airstrip	Shiprock	New Mexico	5V5	5270	36.7N	108.7W
159	Holbrook Regional Airport	Holbrook	Arizona	KP14	5262	34.9N	110.1W
160	Dillon	Dillon	Montana	DLN	5241	45.3N	112.6W
161	Seligman	Seligman	Arizona	P23	5235	35.3N	112.9W
162	Jackpot Hayden Field	Jackpot	Nevada	KO6U	5213	42.0N	114.7W
163	Alexander Municipal Airport	Belen	New Mexico	E8O	5194	34.6N	106.8W
164	Blake Field	Delta	Colorado	AJZ	5193	38.8N	108.1W
165	Currant Ranch	Currant	Nevada	K9U7	5181	38.7N	115.5W
166	Roosevelt Municipal Airport	Roosevelt	Utah	74V	5176	40.3N	110.1W
167	Salina – Gunnison	Salina	Utah	44U	5159	39.0N	111.8W
168	Payson	Payson	Arizona	PAN	5157	34.3N	111.3W
169	Whiteriver	Whiteriver	Arizona	E24	5153	33.8N	110.0W
170	Elko Regional Airport	Elko	Nevada	EKO	5140	40.8N	115.8W
171	Duckwater	Duckwater	Nevada	O1U	5133	38.9N	115.6W
172	Erie Municipal Airport	Erie	Colorado	EIK	5130	40.0N	105.0W
173	Susanville	Susanville	California	1Q2	5116	40.7N	120.8W
174	Cody / Yellowstone Regional Airport	Cody	Wyoming	COD	5098	44.5N	109.0W

Table C2 Examples of High Field Elevation Airports in the United States (Continued)

Number	Airport Name	City	State	FAA Airport Designator	Field Elevation (ft)	Latitude (deg)	Longitude (deg)
175	Powell Municipal Airport	Powell	Wyoming	POY	5092	44.9N	108.8W
176	Challis	Challis	Idaho	KLLJ	5072	44.5N	114.2W
177	Vance Brand	Longmont	Colorado	LMO	5055	40.2N	105.2W
178	Reno/Stead	Reno	Nevada	RTS	5050	39.7N	119.9W
179	Prescott/Ernest A. Love Field	Prescott	Arizona	PRC	5045	34.7N	112.4W
180	Milford Municipal Ben and Judy Briscoe Field	Milford	Utah	KMLF	5039	38.4N	113.0W
181	Cibecue	Cibecue	Arizona	Z95	5037	34.0N	110.4W
182	McCall Municipal Airport	McCall	Idaho	KMYL	5024	44.9N	116.1W
183	Nephi Municipal Airport	Nephi	Utah	U14	5022	39.7N	111.9W
184	Morgan County Airport	Morgan	Utah	42U	5020	41.1N	111.8W
185	Fort Collins – Loveland Municipal Airport	Fort Collins/Loveland	Colorado	FNL	5016	40.5N	105.0W
186	Westwinds	Westwinds	Colorado	D17	5000	38.8N	108.1W
187	Fillmore Municipal Airport	Fillmore	Utah	FOM	4985	39.0N	112.4W
188	Sierraville Dearwater	Sierraville	California	O79	4984	39.6N	120.4W
189	Clayton Municipal Airport	Clayton	New Mexico	CAO	4970	36.4N	103.2W
190	Buffalo/Johnson County	Buffalo	Wyoming	BYG	4968	44.4N	106.7W
191	Platte Valley Airport	Hudson	Colorado	18V	4965	40.1N	104.7W
192	Lusk Municipal Airport	Lusk	Wyoming	KLSK	4964	42.8N	104.4W
193	Flagger Aerial Spraying Inc.		Colorado	COOO	4945	39.3N	103.1W
194	Winslow – Lindbergh Regional Airport	Winslow	Arizona	INW	4941	35.0N	110.7W
195	Parker Carson	Parker	Nevada	2Q5	4939	39.2N	119.7W
196	Fort Collins Downtown	Fort Collins	Colorado	3V5	4935	40.6N	105.0W
197	Douglas / Converse County	Douglas	Wyoming	DGW	4933	42.8N	105.4W
198	Kimball Municipal/Robert E. Arraj Field	Kimball	Nebraska	KIBM	4926	41.2N	103.7W
199	Stallion Army Air Field	Socorro	New Mexico	K95E	4925	33.8N	106.6W
200	Nervino	Beckwourth	California	O82	4900	39.8N	120.4W
201	Parker Carson	Carson City	Nevada	2Q5	4900	39.2N	119.7W
202	Dyer	Dyer	Nevada	2Q9	4899	37.6N	118.0W
203	Socorro Municipal Airport	Socorro	New Mexico	ONM	4875	34.0N	106.9W

Table C2 Examples of High Field Elevation Airports in the United States (Continued)

Number	Airport Name	City	State	FAA Airport Designator	Field Elevation (ft)	Latitude (deg)	Longitude (deg)
204	Colorado City Municipal Airport	Colorado City	Arizona	AZC	4874	37.0N	113.0W
205	Kanab Municipal Airport	Kanab	Utah	KNB	4868	37.0N	112.5W
206	Camp W.G. Williams Total Force Field	Riverton	Utah	UTO8	4860	40.4N	111.9W
207	Grand Junction Regional Airport	Grand Junction	Colorado	GJT	4858	39.1N	108.5W
208	Rexburg – Madison County Airport	Rexburg	Idaho	RXE	4858	43.8N	111.8W
209	Schafer United States Forest Service	Schafer	Montana	K8U2	4855	48.1N	113.3W
210	Truth or Consequences Municipal Airport	Truth or Consequences	New Mexico	TCS	4853	33.2N	107.3W
211	Oljato	Oljato	Utah	O5UT	4838	37.0N	110.3W
212	Mid Valley Airpark	Los Lunas	New Mexico	E98	4836	34.8N	106.7W
213	Lincoln County	Panaca	Nevada	1L1	4831	37.8N	114.4W
214	Sedona	Sedona	Arizona	SEZ	4830	34.8N	111.8W
215	Grand Canyon West	Peach Springs	Arizona	1G4	4825	36.0N	113.8W
216	Easton (Valley View)	Greeley	Colorado	11V	4820	40.3N	104.6W
217	Rosaschi Air Park	Smith	Nevada	N59	4809	38.8N	119.3W
218	Santa Rosa Route 66	Santa Rosa	New Mexico	SXU	4791	34.9N	104.6W
219	Hill AFB	Ogden	Utah	KHIF	4789	41.1N	112.0W
220	Crescent Valley	Crescent Valley	Nevada	U74	4787	40.4N	116.6W
221	Bisbee Municipal Airport	Bisbee	Arizona	KPO4	4780	31.4N	109.9W
222	Delta Municipal Airport	Delta	Utah	DTA	4759	39.4N	112.5W
223	Idaho Falls Regional Airport	Idaho Falls	Idaho	IDA	4744	43.5N	112.0W
224	Tombstone Municipal Airport	Tombstone	Arizona	P29	4743	31.7N	110.0W
225	Lakeview/Lake County	Lakeview	Oregon	LKV	4733	42.2 N	120.4W
226	Pueblo Memorial Airport	Pueblo	Colorado	PUB	4729	38.3N	104.5W
227	Preston	Preston	Idaho	KU1O	4728	42.1N	111.9W
228	Mack Mesa	Mack Mesa	Colorado	CO7	4724	39.3N	108.9W
229	Minden/Minden-Tahoe	Minden	Nevada	MEV	4722	39.0N	119.8W
230	Fort Huachuca-Sierra Vista/ Sierra Vista Municipal-Libby Army Airfield	Sierra Vista	Arizona	KFHU	4719	31.6N	110.3W
231	Colorado Plains Regional Airport	Akron	Colorado	AKO	4716	40.2N	103.2W

Table C2 Examples of High Field Elevation Airports in the United States (Continued)

Number	Airport Name	City	State	FAA Airport Designator	Field Elevation (ft)	Latitude (deg)	Longitude (deg)
232	Carson	Carson City	Nevada	CXP	4705	39.2N	119.7W
233	Gabbs	Gabbs	Nevada	GAB	4700	38.9N	118.0W
234	Greeley-Weld County	Greeley	Colorado	GXY	4697	40.4N	104.6W
235	Lida Junction	Goldfield	Nevada	OL4	4684	37.5N	117.2W
236	Coaldale	Coaldale Junction	Nevada	2Q6	4664	38.0N	117.9W
237	Mission Field	Livingston	Montana	KLVM	4656	45.7N	110.4W
238	Cedarville	Cedarville	California	059	4623	41.6N	120.2W
239	Salt Lake City/South Valley Regional Airport	Salt Lake City	Utah	U42	4607	40.6N	112.0W
240	Fort Bidwell	Fort Bidwell	California	A28	4602	41.9N	120.1W
241	Spanish Springs	Spanish Springs	Nevada	N86	4600	39.7N	119.7W
242	Hot Springs County Thermopolis Municipal Airport	Thermopolis	Wyoming	KTHP	4592	43.7N	108.2W
243	Fort Morgan Municipal Airport	Fort Morgan	Colorado	FMM	4569	40.3N	103.8W
244	Moab/Canyonlands Field	Moab	Utah	CNY	4555	38.8N	109.8W
245	Mina	Mina	Nevada	3QO	4552	38.4N	118.1W
246	Battle Mountain	Battle Mountain	Nevada	BAM	4536	40.6N	116.9W
247	Rogers Field	Chester	California	005	4534	40.3N	121.2W
248	Spanish Fork Springville	Springville	Utah	KU77	4529	40.1N	111.7W
249	Tuba City	Tuba City	Arizona	T03	4513	36.1N	111.4W
250	Gebauer	Akron	Colorado	5V6	4509	40.2N	103.1W
251	Malad City	Malad City	Idaho	KMLD	4503	42.2N	112.3W
252	Provo Municipal Airport	Provo	Utah	PVU	4497	40.2N	111.7W
253	McCarley Field	Blackfoot	Idaho	KU02	4488	43.2N	112.4W
254	Bluff	Bluff	Utah	66V	4476	37.1N	109.6W
255	Bozeman/Gallatin Field	Bozeman	Montana	BZN	4473	45.8N	111.2W
256	Ogden-Hinckley	Ogden	Utah	OGD	4473	41.2N	112.0W
257	Las Cruces International Airport	Las Cruces	New Mexico	LRU	4457	32.3N	106.9W
258	Logan-Cache	Logan	Utah	LGU	4457	41.8N	111.9W
259	Pocatello Regional Airport	Pocatello	Idaho	PIH	4452	42.9N	112.6W
260	Hanksville	Hanksville	Utah	HVE	4444	38.4N	110.7W

Table C2 Examples of High Field Elevation Airports in the United States (Continued)

Number	Airport Name	City	State	FAA Airport Designator	Field Elevation (ft)	Latitude (deg)	Longitude (deg)
261	American Falls	American Falls	Idaho	KU01	4419	42.8N	112.8W
262	Reno/Tahoe International Airport	Reno	Nevada	RNO	4415	39.5N	119.8W
263	Dayton Valley Airpark	Dayton/Carson City	Nevada	A34	4414	39.2N	119.6W
264	Guernsey/Camp Guernsey	Guernsey	Wyoming	7V6	4400	42.3N	104.7W
265	California Pines	California Pines	California	A24	4398	41.4N	120.7W
266	Springfield Municipal Airport	Springfield	Colorado	8V7	4390	37.5N	102.6W
267	Cal Black Memorial Airport	Halls Crossing	Utah	U96	4388	37.4N	110.6W
268	Yerington Municipal Airport	Yerington	Nevada	043	4382	39.0N	119.2W
269	Alturas Municipal Airport	Alturas	California	AAT	4378	41.5N	120.6W
270	Gillette-Campbell County	Gillette	Wyoming	GCC	4365	44.4N	105.5W
271	Michael Army Air Field	Dugway Proving Ground	Utah	KDPG	4350	40.2N	112.9W
272	Tiger Field	Fernley	Nevada	N58	4346	39.6N	119.2W
273	Bolinder Field-Tooele Valley	Tooele	Utah	TVY	4322	40.6N	112.4W
274	Christmas Valley	Christmas Valley	Oregon	K62S	4317	43.2N	120.7W
275	Page Municipal Airport	Page	Arizona	PGA	4316	36.9N	111.4W
276	Deming Municipal Airport	Deming	New Mexico	DMN	4314	32.3N	107.7W
277	Sidney Municipal/Lloyd W. Carr Field	Sidney	Nebraska	SNY	4313	41.1N	103.0W
278	Winnemucca	Winnemucca	Nevada	WMC	4308	40.9N	117.8W
279	Cannon AFB	Clovis	New Mexico	KCVS	4295	34.4N	103.3W
280	Lordsburg Municipal Airport	Lordsburg	New Mexico	LSB	4289	32.3N	108.7W
281	Brush Municipal Airport	Brush	Colorado	7V5	4280	40.3N	103.6W
282	Silver Springs	Silver Springs	Nevada	B08	4269	39.4N	119.3W
283	Melon Field	Rocky Ford	Colorado	1C05	4260	38.0N	103.7W
284	Eads Municipal Airport	Eads	Colorado	9V7	4245	38.5N	102.8W
285	Butte Valley	Dorris	California	A32	4243	41.9N	122.0W
286	Wendover	Wendover	Utah	ENV	4237	40.7N	114.0W
287	Skypark	Bountiful	Utah	BTF	4234	40.9N	111.9W
288	Brigham City	Brigham City	Utah	BMC	4230	41.6N	112.1W
289	Conchas Lake	Conchas Dam	New Mexico	E89	4230	35.4N	104.2W

Table C2 Examples of High Field Elevation Airports in the United States (Continued)

Number	Airport Name	City	State	FAA Airport Designator	Field Elevation (ft)	Latitude (deg)	Longitude (deg)
290	La Junta Municipal Airport	La Junta	Colorado	LHX	4229	38.1N	103.5W
291	Salt Lake City International Airport	Salt Lake City	Utah	SLC	4227	40.8N	112.0W
292	Worland Municipal Airport	Worland	Wyoming	WRL	4227	44.0N	108.0W
293	Green River Municipal Airport	Green River	Utah	KU34	4225	39.0N	110.2W
294	Mountain Valley	Tehachapi	California	L94	4220	35.1N	118.4W
295	Kit Carson County	Burlington	Colorado	ITR	4219	39.2N	102.3W
296	Clovis Municipal Airport	Clovis	New Mexico	CVN	4216	34.4N	103.1W
297	Hawthorne Industrial	Hawthorne	Nevada	KHTH	4215	38.5N	118.6W
298	Torrington Municipal Airport	Torrington	Wyoming	TOR	4205	42.1N	104.2W
299	Denio Junction	Denio Junction	Nevada	E85	4202	42.0N	118.6W
300	Alamogordo-White Sands Regional Airport	Alamogordo	New Mexico	ALM	4200	32.8N	106.0W
301	Cochise County	Willcox	Arizona	P33	4187	32.2N	109.9W
302	Bagdad	Bagdad	Arizona	E51	4183	34.6N	113.2W
303	Douglas Municipal Airport	Douglas	Arizona	DGL	4173	31.3N	109.5W
304	Lewistown Municipal Airport	Lewistown	Montana	LWT	4170	47.1N	109.5W
305	Bullfrog Basin	Glen Canyon National Recreational Area	Utah	U07	4167	37.5N	110.7W
306	Fort Sumner Municipal Airport	Fort Sumner	New Mexico	FSU	4165	34.5N	104.2W
307	Sunriver	Sunriver	Oregon	S21	4164	43.9N	121.5W
308	Southard Field	Bieber	California	O55	4158	41.1N	121.1 W
309	Twin Falls/Joslin Field-Magic Valley Regional Airport	Twin Falls	Idaho	TWF	4154	42.5N	114.5W
310	Douglas-Bisbee/Bisbee-Douglas International Airport	Douglas Bisbee	Arizona	DUG	4151	31.5N	109.6W
311	Burley Municipal Airport	Burley	Idaho	BYI	4150	42.6N	113.8W
312	Susanville Municipal Airport	Susanville	California	SVE	4149	40.3N	120.6W
313	Burns Municipal Airport	Burns	Oregon	BNO	4148	43.6N	119.0W
314	Yuma Municipal Airport	Yuma	Colorado	2V6	4136	40.1N	102.7W
315	Eastern Sierra Regional Airport	Bishop	California	BIH	4124	37.4N	118.4W

Table C2 Examples of High Field Elevation Airports in the United States (Concluded)

Number	Airport Name	City	State	FAA Airport Designator	Field Elevation (ft)	Latitude (deg)	Longitude (deg)
316	Cochise College	Douglas	Arizona	P03	4124	31.4N	109.7W
317	Joseph State	Joseph State	Oregon	K4S3	4121	45.4N	117.3W
318	Dona Ana County at Santa Teresa	Santa Teresa	New Mexico	K5T6	4112	31.9N	106.7W
319	Grand Canyon Bar Ten Airstrip	Whitmore	Arizona	1Z1	4100	36.3N	113.2W
320	Klamath Falls	Klamath Falls	Oregon	LMT	4095	42.2N	121.7W
321	Holloman AFB	Alamogordo	New Mexico	KHMN	4093	32.9N	106.1W
322	Hatch Municipal Airport	Hatch	New Mexico	E05	4080	32.7N	107.2W
323	Portales Municipal Airport	Portales	New Mexico	PRZ	4078	34.1N	103.4W
324	Tucumcari Municipal Airport	Tucumcari	New Mexico	TCC	4065	35.2N	103.6W
325	Herlong	Herlong	California	H37	4055	40.1N	120.2W
326	Jerome County	Jerome	Idaho	JER	4053	42.7N	114.5W
327	Fort Harrison Army Air Field	Fort William Harrison	Montana	MT15	4050	46.6N	112.1W
328	Tulelake	Tulelake	California	O81	4044	41.9N	121.4W
329	Lemhi County	Salmon	Idaho	KSMN	4043	45.1N	113.9W
330	Sterling Municipal Airport	Sterling	Colorado	STK	4038	40.6N	103.3W
331	Haxtun Municipal Airport	Haxtun	Colorado	17V	4035	40.6N	102.3W
332	Sheridan County	Sheridan	Wyoming	SHR	4021	44.8N	107.0W
333	Amedee Army Air Field	Sierra Army Depot, Herlong	California	AHC	4012	40.3N	120.2W
334	Tehachapi Municipal Airport	Tehachapi	California	TSP	4001	35.1N	118.4W

Note: Field elevation is the height above mean sea level of the highest point on a runway or a taxiway.

This page was intentionally left blank.

APPENDIX D - RUNWAY PROFILE FOR EDWARDS AFB RUNWAY 04R/23L

Table D1 Variation of Runway Elevation with Distance for
Edwards AFB Runway 04R/22L

Distance from the East End (1,000 ft)	Orthometric Elevation (EGM 96) (ft)
0	2281.9
1	2283.3
2	2284.7
3	2286.1
4	2287.5
5	2288.9
6	2290.2
7	2291.6
8	2293.0
9	2294.4
10	2295.8
11	2297.2
12	2298.5
13	2299.9
14	2301.3
15	2302.7
15,024	2302.7

Note: The average slope over the entire 15,024 feet is 0.001382 (feet/feet), 0.0793 (degree), or 20.8 feet of elevation change in 15,024 feet.

This page was intentionally left blank.

APPENDIX E - RUNWAY PROFILES FOR USAF PLANT 42

Table E1 Variation of Runway Elevation with Distance for Plant 42 Runway 04/22

Station Name	Latitude (WGS 84) (DD MM SS.SSSSS)	Longitude (WGS 84) (DDD MM SS.SSSSS)	Ellipsoid Elevation (WGS 84) (ft)	Orthometric Elevation (EGM 96) (ft)	Slope Distance (ft)
RW 04	N 34 37 00.87310	W118 05 29.85183	2437.19	2543.75	0.00
R0401	N 34 37 06.99111	W118 05 20.45211	2430.95	2537.51	1000.03
R0402	N 34 37 13.10748	W118 05 11.05120	2424.70	2531.25	2000.02
R0403	N 34 37 19.22426	W118 05 01.64990	2419.13	2525.67	3000.04
R0404	N 34 37 25.34035	W118 04 52.24815	2413.79	2520.31	4000.04
R0405	N 34 37 31.45530	W118 04 42.84493	2407.77	2514.28	5000.05
R0406	N 34 37 37.57119	W118 04 33.44390	2401.61	2508.11	5999.97
R0407	N 34 37 43.68695	W118 04 24.04083	2397.30	2503.79	6999.99
R0408	N 34 37 49.80185	W118 04 14.63659	2394.56	2501.04	8000.01
R0409	N 34 37 55.91673	W118 04 05.23168	2392.26	2498.73	9000.06
R0410	N 34 38 02.03310	W118 03 55.82748	2389.90	2496.36	10000.14
R0411	N 34 38 08.14646	W118 03 46.42421	2387.60	2494.04	10999.97
RW 22	N 34 38 14.18069	W118 03 37.13936	2385.38	2491.82	11987.05

Table E2 Variation of Runway Elevation with Distance for Plant 42 Runway 07/25

Station Name	Latitude (WGS 84) (DD MM SS.SSSSS)	Longitude (WGS 84) (DDD MM SS.SSSSS)	Ellipsoid Elevation (WGS 84) (ft)	Orthometric Elevation (EGM 96) (ft)	Slope Distance (ft)
RW 07	N 34 37 50.13195	W118 06 47.06392	2434.77	2541.28	0.00
R0701	N 34 37 50.79103	W118 06 35.12627	2429.81	2536.32	999.97
R0702	N 34 37 51 44861	W118 06 23.18545	2424.92	2531.42	2000.16
R0703	N 34 37 52.10607	W118 06 11.24848	2420.06	2526.55	3000.04
R0704	N 34 37 52.76309	W118 05 59.31006	2415.15	2521.64	4000.02
R0705	N 34 37 53.42029	W118 05 47.37123	2410.20	2516.69	5000.05
R0706	N 34 37 54.07761	W118 05 35.43160	2405.75	2512.24	6000.13
R0707	N 34 37 54.73311	W118 05 23.49337	2403.10	2509.59	7000.07
R0708	N 34 37 55.39014	W118 05 11.55504	2400.41	2506.89	8000.03
R0709	N 34 37 56.04519	W118 04 59.61557	2397.63	2504.11	9000.08
R0710	N 34 37 56.70128	W118 04 47.67600	2396.15	2502.63	10000.12
R0711	N 34 37 57.35650	W118 04 35.73733	2394.69	2501.16	11000.09
RW 25	N 34 37 58.00895	W118 04 23.81560	2393.08	2499.55	11998.63

This page was intentionally left blank.

APPENDIX F - NORTHROP T-38C TAKEOFF PERFORMANCE SENSITIVITY STUDIES

PURPOSE

The purpose of this appendix is to provide the reader with a sense of the magnitudes of the effects on takeoff performance of variations in takeoff related variables for a Northrup T-38C aircraft powered by two General Electric J85-GE-5R afterburning turbojet engines. The selected variables are presented in table F1.

Some of the sensitivity studies used a flap setting of 45 percent (20.25 degrees) while others used 60 percent (27.00 degrees). Within a given study, a constant flap setting was used.

These sensitivity studies were created over an eight-year period between 2003 and 2010. There were small, less than 2 percent, changes in the baseline thrust models during that time period. Within a given study a constant thrust model was used.

Northrop T-38C Aircraft:

The Northrop T-38C aircraft was an advanced trainer used by the USAF. The T-38C had been updated by the Boeing Company with modern avionics including an embedded GPS/INS known as an EGI. The T-38C also had a radar altimeter. A later update added NASA-designed inlets. The NASA inlet was optimized for ground level static operation. The original Northrop T-38A inlet was optimized for operation at transonic Mach numbers.

The T-38C had a wingspan of 25.25 feet and a reference wing area of 170 square feet, resulting in a wing aspect ratio of 3.75. The wingtips were approximately 4.0 feet off the runway prior to rotation. The General Electric J85-GE-5R engines produced approximately 3,700 and 3,400 pounds of maximum power thrust at standard day, sea level, static conditions for uninstalled and installed engines, respectively. For a brake release aircraft gross weight of 12,800 pounds, that corresponded to an installed thrust-to-weight ratio of 0.53 and a wing loading of 75.3 pounds per square foot.

AFFTC TOLAND DIGITAL BATCH SIMULATION

The AFFTC (now the 412th Test Wing) TOLAND simulation was used to create the data for these sensitivity studies.

TOLAND Models:

The TOLAND software required information unique to the type of aircraft being modeled. The required models for predicting takeoff performance included five aerodynamic models and two to four propulsive models. The five aerodynamic models were:

1. In ground effect lift curve, trimmed lift coefficient as a function of aircraft angle of attack
2. In ground effect drag polar, trimmed drag coefficient as a function of trimmed lift coefficient
3. Out of ground effect trimmed lift curve
4. Out of ground effect trimmed drag polar
5. Interpolation scheme to determine lift coefficient and drag coefficient after the tires have left the runway and before the wing is at least one-half of a wingspan length off the runway.

The four propulsive models for the Northrop T-38C were:

1. Maximum power (full afterburner), installed, net thrust
2. Maximum power, installed, airflow used to calculate propulsive ram drag
3. Maximum power, installed, fuel flow
4. Engine thrust spoolup curve for an installed engine snap from military power (full power except no afterburner operation) to maximum power (a thrust multiplicative factor as a function of time after throttle snap to be multiplied with the maximum power thrust and fuel flow models

T-38C Aerodynamic Models:

In Ground Effect Lift Curves.

The in ground effect lift curves were created from a combination of the out of ground effect lift curves and data acquired at mainwheel liftoff during the flight test program. The flight test determined, in ground effect lift curves were linear based on two points. First, the aircraft angle of attack for a trimmed lift coefficient of zero from the out of ground effect lift curves. second, a point (a trimmed lift coefficient and an aircraft angle of attack) determined from the "average" of one flight test determined point from each takeoff.

In Ground Effect Drag Polars.

Northrop-generated models for the in ground effect drag polars were used in TOLAND. The contractor drag models were also used with the flight test determined excess thrusts to calculate net thrusts to develop propulsive models.

Out of Ground Effect Trimmed Lift Curves.

Sawtooth climbs and descents were flown near 10,000 feet pressure altitude to create out of ground effect trimmed lift curves for the T-38C with its landing gear extended, the landing gear doors closed, and the two flap settings, 45 and 60 percent flap deflection.

Out of Ground Effect Trimmed Drag Polars.

The same sawtooth climbs and descents provided the information required to create the out of ground effect drag polars.

Ground Effect Interpolation Scheme.

The interpolation scheme for the T-38C program was a modified version of one created by the AFFTC for the McAir F-15E. The in ground effect curves were used when the tires were on the runway. The out of ground effect curves were used when the aircraft wingtips were at least one-half of a wingspan above the runway.

For the T-38C:

1. Wing semispan = 25.25/2 = 12.63 (feet)
2. Height of the wingtips with the tires on the ground = 4.0 (feet)
3. Height of the tires above the runway with the wingtips one wing semispan above the runway = (12.6 – 4.0) = 8.6 (feet)
4. An empirical relationship was developed for the interpolation scheme:

For HAGL less than or equal to 8.6 (feet), equation F1:

$$SRATIO = 1 - (HAGL/8.6)^{0.75} \tag{F1}$$

where:

HAGL= height of the tires above the runway, (feet)
For HAGL greater than 8.6, set SRATIO to zero

For a given angle of attack and HAGL, equation F2:

$$C_L = (C_L)_{OGE} + SRATIO[(C_L)_{IGE} - (C_L)_{OGE}] \tag{F2}$$

-or equation F3-

$$C_D = (C_D)_{OGE} + SRATIO[(C_D)_{IGE} - (C_D)_{OGE}] \tag{F3}$$

where:

C_L = lift coefficient
C_D = drag coefficient

T-38C Propulsive Models:

Maximum Power, Installed, Net Thrust.

A maximum power, installed, net thrust model for the T-38C was created using flight test data from installed thrust stand runs, takeoffs, sawtooth climbs, and maximum power level accelerations. The model was for net thrust versus for gross thrust because it was developed from measured (calculated) excess thrusts and assumed aerodynamic drags.

Maximum Power, Installed, Airflow.

A General Electric curve for corrected airflow as a function of corrected engine speed was used to calculate actual airflow. The airflow and true airspeed were used to calculate propulsive ram drag.

Installed gross thrust was approximated by adding net thrust and propulsive ram drag. The approximated gross thrust was used to calculate the aerodynamic lift force and lift coefficient, equations F4 and F5.

$$n_z W = L + F_g[\sin(\alpha + i_T)] \tag{F4}$$

$$L = n_z W - F_g[\sin(\alpha + i_T)] \tag{F5}$$

where:

n_z = normal load factor in the wind axis
W = aircraft gross weight
F_g = gross propulsive thrust

α = aircraft angle of attack
i_T = thrust incidence angle with respect to the aircraft waterline (i_T = 0.5 degree for the T-38C)

The added complexity of estimating gross thrust and using equation (F5) could have been avoided by using equation (F6) versus the more complex and accurate equation (F5).

$$L = n_{zW} \tag{F6}$$

A quick sensitivity check shows what is lost by ignoring the thrust component in equation (F5). Given:

n_z = 1
W = 12,800 (pounds)
F_g = 6,784 (pounds)
α = 7.5 (degrees)
i_T = 0.5 (degrees)

The gross thrust component perpendicular to the velocity vector is 944 pounds. This reduces the required aerodynamic lift by 7.4 percent, 11,856 versus 12,800 pounds.

Maximum Power, Installed, Fuel Flow.

The maximum power, installed fuel flow model was created from data acquired with flight test fuel flowmeters. The model was developed as fuel flow per engine divided by the ambient air pressure ratio as a function of ambient air temperature and Mach number. In TOLAND the fuel flow model was used to reduce the aircraft's gross weight during the takeoff. For the T-38C, a typical total fuel flow during takeoff was 16,000 pounds per hour or approximately 4.5 pounds per second. During a 20-second ground roll from brake release to takeoff, the aircraft's gross weight would decrease by approximately 90 pounds or 0.7 percent for a 12,800 pound aircraft at brake release.

The decrease in gross weight was predicted to reduce the total distance from brake release to 50 feet AGL by approximately 70 feet and to increase the speed at 50 feet AGL by 0.4 KCAS relative to a constant weight of 12,800 pounds.

Engine Thrust Spoolup Curve.

The brakes on the T-38C, like those on most high performance jet aircraft, were not capable of holding the aircraft at their takeoff thrust settings. The pilots typically checked the engine health at a specified engine speed or at military power prior to brake release. The pilot then advanced the throttle to the takeoff setting at brake release. In multi-engine aircraft with afterburners, the pilot normally advanced both engines to military power and then slowly light one afterburner at a time as the aircraft accelerated. This operational procedure was not very repeatable. A different procedure was normally used for flight test to get more repeatable results for modeling and simulation.

The flight test procedure for the F-15 was to come to a full stop on the active runway, advance the engines to 80 to 82 percent of core speed, perform the engine health checks, and then snap both throttles to full afterburner (maximum power) simultaneously with brake release. The NASA flight test procedure for the T-38 with the large NASA inlets was similar to the F-15 procedure except that the engine health checks were performed at military power and the engines were then stabilized at minimum afterburner operation prior to brake release. The NASA pilots snapped both throttles from minimum afterburner to full afterburner at brake release. The procedure used by the AFFTC during the T-38C evaluation with the NASA inlets was the same as the NASA procedure except that the engines were snapped from military power (no afterburner operation) to full afterburner at brake release. The NASA procedure minimized the engine-to-engine and flight-to-flight variations during the initial afterburner lights. The NASA procedure was not used by the AFFTC because it was less operationally representative than was the AFFTC flight test procedure.

A time history of a multiplicative factor for the maximum power thrust model, a spoolup curve for thrust, was created starting with approximately 70 percent for military power at brake release to 100 percent, maximum power, approximately 8 seconds later. The nonlinear curve was created such that the TOLAND predicted aircraft accelerations "matched" those of the real aircraft during the first part of the ground roll.

T-38C SENSITIVITIES

The takeoff related variables used in these sensitivity studies were summarized in Table F1. The results were compared to a reference set of conditions, which were also summarized in Table F1. The reference flap setting was either 45 or 60 percent of 45 degrees (100 percent flap deflection).

Table F1 T-38C Takeoff Performance Variables

Variable	Units	Range	Reference Value
pressure altitude	1,000 feet	0 to 8	0 (sea level)
ambient air temperature	degrees C	-20 to +50	15
aircraft gross weight	pounds	11,000 to 13,250	12,800
rotation speed	KCAS	130 to 150	140
headwind	knots	0 to 10	0 (calm)
runway slope	degrees	-2 to +2	0 (flat)
aircraft pitch angle in a 3-point attitude	degrees	0 to 2	1.00
rolling coefficient of friction	non-dimensional	0.000 to 0.030	0.015
aircraft pitch rate during rotation	degrees per second	not applicable	1.66
aircraft pitch angle for climbout	degrees	5 to 12	7.50
flap setting	percent of 45 degrees	45 and 60	45 or 60
aerodynamic drag	percent of actual drag	0 to 200	100
propulsive thrust	percent of actual thrust	98 to 107	100
change in ground roll distance for a 1.00 KCAS change in airspeed	feet	not applicable	not applicable

Pressure Altitude:

The pressure altitudes evaluated were from sea level through 8,000 feet. This sensitivity study also allowed the ambient air temperatures to decrease by approximately 2 degrees C for each 1,000-foot increase in pressure altitude. The appropriate ambient air temperature from the 1976 U.S. Standard Atmosphere was used.

Table F2 summarizes the ambient air pressure, temperature, and density ratios for the pressure altitudes in the study.

Table F2 Pressure Altitudes

Pressure Altitude (1,000 ft)	Ambient Air Pressure Ratio (n/d)	Ambient Air Temperature Ratio (n/d)	Ambient Air Density Ratio (n/d)
0	1.0000	1.0000	1.0000
1	0.9644	0.9931	0.9711
2	0.9298	0.9862	0.9428
4	0.8637	0.9725	0.8881
6	0.8014	0.9587	0.8359
8	0.7428	0.9450	0.7860

Note: The ambient air temperature ratios and the ambient air density ratios are for the 1976 U.S. Standard Atmosphere model.

Increasing the pressure altitude relative to sea level resulted in lower thrust levels and therefore lower accelerations and longer ground rolls and air distances, table F3.

Table F3 Variations in the Ground Roll Distance to Rotation and to Takeoff and the Total Distances to 50 Feet Above Ground Level with Changes to the Pressure Altitudes

Pressure Altitude (1,000 ft)	Horizontal Distances from Brake Release (ft)		
	to Rotation	to Takeoff	to 50 ft AGL
0	1,879	2,657	4,758
1	1,995	2,795	5,013
2	2,117	2,943	5,293
4	2,389	3,268	5,935
6	2,705	3,640	6,711
8	3,070	4,066	7,656

Notes:
1. 1975 U.S. Standard Atmosphere
2. calm (no wind)
3. flat runway – no runway slope
4. Northrop T-38C aircraft with General Electric J85-GE-5R engines
5. 12,800 pounds gross weight
6. 60 percent flaps
7. rolling coefficient of friction = 0.015
8. aircraft pitch angle = 1.00 degree prior to rotation
9. 140 KCAS rotation speed
10. 1.66 degrees/second rotation rate after rotation speed
11. 7.50 degrees target pitch angle for climbout

All of the TOLAND predictions used a rotation speed of 140 KCAS. At rotation, the aircraft rotated at 1.66 degrees per second from a pitch angle of 1 degree to a pitch angle of 7.50 degrees. Mainwheel liftoff, takeoff, occurred at a combination of pitch angle (aerodynamic lift coefficient) and airspeed (dynamic pressure) such that the aerodynamic lift plus a component of gross thrust equaled the aircraft gross weight. The aircraft lifted off at lower airspeeds and at higher pitch angles as the pressure altitudes increased, table F4. This was due to the slower acceleration rates at the higher altitudes. The lower excess thrusts also resulted in slower airspeeds and longer horizontal distances for 50 feet AGL.

Table F4 Variations in the Takeoff Speed, the Speed at 50 Feet Above Ground Level, and the Pitch Angle at Mainwheel Liftoff with Changes to the Pressure Altitude

Pressure Altitude (1,000 ft)	Takeoff Speed (KCAS)	Speed at 50 ft AGL (KCAS)	Aircraft Pitch Angle at Mainwheel Liftoff (deg)	Elapsed Time from Rotation to Mainwheel Liftoff (sec)
0	163.2	201.7	6.05	3.03
1	162.5	200.6	6.13	3.08
2	161.7	199.5	6.22	3.14
4	160.3	197.7	6.47	3.26
6	158.9	196.1	6.60	3.38
8	157.5	194.7	6.89	3.51

Notes: 1. 1976 U.S. Standard Atmosphere
2. Northrop T-38C aircraft with General Electric J85-GE-5R engines
3. 12,800 pounds gross weight
4. 60 percent flaps

Ambient Air Temperature:

Increasing the ambient air temperature at a constant pressure altitude will have two effects on takeoff performance. First, the air density will decrease resulting in higher true airspeeds and groundspeeds for a given calibrated or equivalent airspeed. Second, the engine thrust and therefore excess thrust will decrease resulting in longer takeoff distances, table F5, and lower airspeeds at 50 feet AGL, table F6.

Table F5 Variations in the Ground Roll Distances to Rotation, to Takeoff, and the Total Distances to 50 Feet Above Ground Level with Changes to the Ambient Air Temperature

Ambient Air Temperature		Horizontal Distances from Brake Release (ft)		
(deg C)	(deg F)	To Rotation	To Takeoff	To 50 ft AGL
-20	-4	1,414	2,079	3,734
-15	5	1,472	2,153	3,858
-10	14	1,532	2,228	3,987
-5	23	1,596	2,307	4,124
0	32	1,661	2,387	4,269
5	41	1,732	2,476	4,422
10	50	1,804	2,563	4,585
15	59	1,879	2,657	4,758
20	68	1,960	2,754	4,942
25	77	2,043	2,854	5,142
30	86	2,133	2,960	5,356
35	95	2,226	3,072	5,588
40	104	2,324	3,189	5,840
45	113	2,428	3,311	6,114
50	122	2,539	3,440	6,413

Notes: 1. pressure altitude = 0 (sea level)
2. Northrop T-38C aircraft with General Electric J85-GE-5R engines
3. 12,800 pounds gross weight
4. 60 percent flaps

Table F6 Variations in the Takeoff Speed, the Speed at 50 Feet Above Ground Level, and the Pitch Angle at Mainwheel Liftoff with Changes to the Ambient Air Temperature

Ambient Air Temperature		Takeoff Speed	Speed at 50 ft	Aircraft Pitch Angle at Mainwheel Liftoff	Elapsed Time from Rotation to Mainwheel
(deg C)	(deg F)	(KCAS)	AGL (KCAS)	(deg)	Liftoff (sec)
-20	-4	167.1	209.6	5.55	2.73
-15	5	166.6	208.4	5.62	2.77
-10	14	166.0	207.2	5.68	2.81
-5	23	165.4	206.0	5.75	2.85
0	32	164.8	204.9	5.81	2.89
5	41	164.3	203.8	5.90	2.94
10	50	163.7	202.8	5.96	2.98
15	59	163.2	201.7	6.05	3.03
20	68	162.6	200.7	6.12	3.07
25	77	162.0	199.8	6.20	3.12
30	86	161.4	198.9	6.27	3.16
35	95	160.9	198.0	6.35	3.21
40	104	160.3	197.2	6.43	3.26
45	113	159.7	196.4	6.51	3.31
50	122	159.1	195.7	6.59	3.36

Notes:
1. pressure altitude = 0 (sea level)
2. Northrop T-38C aircraft with General Electric J85-GE-5R engines
3. 12,800 pounds gross weight
4. 60 percent flaps

Aircraft Gross Weight:

The sensitivity to gross weight also has a variation to the rotation speed associated with it. The T-38C recommended rotation speeds were used versus holding a constant rotation speed of 140 KCAS, table F7.

Table F7 T-38C Flight Manual Recommended Rotation Speeds

Aircraft Gross Weight (lb)	Flight Manual Recommended Rotation Speed (KCAS)
11,000	123.0
11,500	128.0
12,000	133.0
12,250	133.5
12,500	138.0
12,750	140.5
13,000	143.0
13,250	145.5

Note: Over the gross weight range of 11,000 to 13,250 pounds, the flight manual recommended rotation speed may be approximated by the equation F7:

$$V_{ROT} = 141+[0.01(W- 12,800)] \quad \text{(F7)}$$

As would be expected, the aircraft performance was degraded with increasing gross weight, Table F8 and table F9. The aircraft pitch angle at liftoff and the elapsed time from the start of rotation until liftoff were almost independent of variations in the gross weight because of the increases in rotation speed with increases in the aircraft gross weights.

Table F8 Variations in the Ground Roll Distances to Rotation, to Takeoff, and the Total Distances to 50 Feet AGL with Changes to the Aircraft Gross Weight

Aircraft Gross Weight (lb)	Rotation Speed (KCAS)	Horizontal Distances from Brake Release (ft)		
		To Rotation	To Takeoff	To 50 ft AGL
11,000	123.0	1,224	1,920	3,669
11,500	128.0	1,394	2,111	3,953
12,000	133.0	1,578	2,318	4,250
12,250	135.5	1,677	2,427	4,403
12,500	138.0	1,779	2,537	4,560
12,750	140.5	1,886	2,653	4,719
13,000	143.0	1,998	2,773	4,881
13,250	145.5	2,115	2,899	5,046

Notes: 1. 1976 U.S. Standard Atmosphere
2. pressure altitude = 0 (sea level)
3. ambient air temperature = 59 (degrees F)
4. Northrop T-38C aircraft with General Electric J85-GE-5R engines
5. 60 percent flaps
6. Flight Manual recommended rotation speed

Table F9 Variations in the Takeoff Speed, the Speed at 50 feet Above Ground Level, and the Pitch Angle at Mainwheel Liftoff with Changes to the Aircraft Gross Weight

Aircraft Gross Weight (lb)	Takeoff Speed (KCAS)	Speed at 50 ft AGL (KCAS)	Aircraft Pitch Angle at Mainwheel Liftoff (deg)	Elapsed Time from Rotation to Mainwheel Liftoff (sec)
11,000	150.9	193.7	6.00	3.00
11,500	154.4	195.9	6.00	3.00
12,000	158.0	198.2	6.00	3.00
12,250	159.8	199.3	6.00	3.00
12,500	161.6	200.4	5.98	2.99
12,750	163.4	201.6	5.97	2.98
13,000	165.3	202.7	5.94	2.97
13,250	167.2	203.8	5.93	2.96

Notes: 1. 1976 U.S. Standard Atmosphere
2. pressure altitude = 0 (sea level)
3. ambient air temperature = 59 (degrees F)
4. Northrop T-38C aircraft with General Electric J85-GE-5R engines
5. 60 percent flaps
6. Flight Manual recommended rotation speed

Table F10 shows the effect of increasing aircraft gross weight on the acceleration of the aircraft in a 3-point attitude, prior to rotation. The ground roll distances from brake release to a target speed, 120 to 150 KCAS, clearly show the effect of the added mass on the required distances to accelerate from brake release to a target airspeed.

Table F10 Variations in the Ground Roll Distances from Brake Release to a Target Airspeed Due to Changes in Aircraft Gross Weight

Aircraft Gross Weight (lb)	Ground Roll Distance from Brake Release (ft)						
	Target Airspeed (KCAS)						
	120	125	130	135	140	145	150
11,000	1,162	1,266	1,376	1,490	1,611	1,736	1,865
11,500	1,216	1,325	1,439	1,558	1,683	1,816	1,952
12,000	1,270	1,384	1,503	1,628	1,760	1,895	2,040
12,250	1,297	1,413	1,536	1,663	1,798	1,937	2,082
12,500	1,323	1,443	1,568	1,698	1,835	1,977	2,126
12,750	1,352	1,472	1,599	1,733	1,872	2,019	2,171
13,000	1,378	1,502	1,631	1,768	1,910	2,059	2,213
13,250	1,406	1,533	1,664	1,803	1,947	2,098	2,258

Notes:
1. 1976 U.S. Standard Atmosphere
2. pressure altitude = 0 (sea level)
3. ambient air temperature = 59 (degrees F)
4. aircraft pitch angle = 1.00 (degree)
5. flat runway – no runway slope
6. Northrop T-38C aircraft with General Electric J85-GE-5R engines
7. 60 percent flaps
8. rolling coefficient of friction = 0.015

Headwind:

The effect of an increasing headwind is to reduce the groundspeed required for a given calibrated (or true) airspeed. An aircraft accelerating on a calm day from a full stop (groundspeed equal to zero) to an airspeed of 10.0 KCAS would move a relatively short distance, 13 feet for the example in table F11. The same aircraft would have an airspeed of 10.0 KCAS and a groundspeed of zero prior to brake release in a 10.0 knot headwind case.

Table F11 Ground Roll Distances from Brake Release to a Target Calibrated Airspeed Near Brake Release During a Calm (no wind) Takeoff at Sea Level on a Standard Day

Calibrated Airspeed (KCAS)	Ground Roll Distance from Brake Release (ft)
0	0
5	4
10	13
15	28
20	45
25	64
30	87
35	115
40	148
45	185
50	228

Notes:
1. 1976 U.S. Standard Atmosphere
2. pressure altitude = 0 (sea level)
3. ambient air temperature = 59 (degrees F)
4. calm (no wind)
5. flat runway – no runway slope
6. Northrop T-38C aircraft with General Electric J85-GE-5R engines
7. 12,800 pounds gross weight
8. 60 percent flaps
9. rolling coefficient of friction = 0.015

A 10.0 KCAS airspeed difference has a much greater effect at higher airspeeds, 140 KCAS (rotation speed) for example. The ground roll distances from brake release for a calm day are shown in table F12. An airspeed of 130 KCAS requires 273 feet less than that required for 140 KCAS and 150 KCAS requires 300 feet more than that required for 140 KCAS. The differences are even greater at higher airspeeds.

Table F12 Ground Roll Distances from Brake Release to Near Rotation Speed

Calibrated Airspeed (KCAS)	Ground Roll Distance from Brake Release (ft)
120	1355
125	1477
130	1606
132	1657
134	1712
136	1766
138	1822
140	1879
142	1936
144	1996
146	2054
148	2117
150	2179
155	2343
160	2525

Table F12 Ground Roll Distances from Brake Release to Near Rotation Speed (Concluded)

Notes: 1. 1976 U.S. Standard Atmosphere
2. pressure altitude = 0 (sea level)
3. ambient air temperature = 59 (degrees F)
4. calm (no wind)
5. flat runway – no runway slope
6. Northrop T-38C aircraft with General Electric J85-GE-5R engines
7. 12,800 pounds gross weight
8. 60 percent flaps
9. rolling coefficient of friction = 0.015
10. aircraft pitch angle = 1.0 (degree)

The data in table F13, although nonlinear, are approximately 24.3, 29.4, and 40.7 feet per knot for 140.0, 163.2, and 201.7 KCAS respectively (rotation, mainwheel liftoff, and speed at 50 feet AGL). Those average slopes were calculated using a headwind range of 0 to 20 knots. A local slope for 140 KCAS based on headwinds of 8 and 12 knots is 24.8 feet per knot based on the results in table F13.

Table F13 Variations in the Ground Roll Distances to Rotation, to Takeoff, and the Total Distances to 50 Feet AGL with Changes to the Headwind

Headwind (kts)	Horizontal Distances from Brake Release (ft)		
	To Rotation	To Takeoff	To 50 ft AGL
0	1,879	2,657	4,758
1	1,854	2,624	4,716
2	1,829	2,594	4,673
3	1,802	2,564	4,632
4	1,777	2,534	4,590
5	1,752	2,502	4,548
6	1,726	2,470	4,506
7	1,702	2,441	4,465
8	1,678	2,412	4,424
9	1,652	2,383	4,383
10	1,628	2,355	4,342
12	1,579	2,296	4,261
14	1,531	2,237	4,181
16	1,486	2,182	4,101
18	1,439	2,125	4,022
20	1,393	2,069	3,944

Notes: 1. 1976 U.S. Standard Atmosphere
2. pressure altitude = 0 (sea level)
3. ambient air temperature = 59 (degrees F)
4. Northrop T-38C aircraft with General Electric J85-GE-5R engines
5. 12,800 pounds aircraft gross weight at brake release
6. 60 percent flaps
7. the rotation, mainwheel liftoff, and speed at 50 feet AGL were 140.0 , 163.2 and 201.7 KCAS respectively

The effects of headwinds on the ground roll distances are more complicated than simply assuming an initial airspeed equal to the headwind speed at brake release and then using ground roll distance data predicted for a calm day. The TOLAND software has the complexity to perform the necessary calculations.

Runway Slope:

Accelerating up a sloped runway increases the distances required relative to a flat runway or a downward sloping runway. In addition to gaining kinetic energy, the aircraft has to gain potential energy. A 1-degree slope changed the required distance from brake release to 140 KCAS by approximately 70 feet or 3.7 percent. A 2-degree uphill slope increased the required distance by 153 feet, 8.1 percent, relative to a flat, zero slope, runway.

Table F14 Variations in Ground Roll Distances from Brake Release to 140 KCAS due to Changes in Runway Slope

Runway Slope (deg)	Ground Roll Distance from Brake Release to 140 KCAS (ft)
-2.0	1,750
-1.0	1,812
-0.5	1,845
0.0	1,879
0.5	1,915
1.0	1,953
2.0	2,032

Notes:
1. 1976 U.S. Standard Atmosphere
2. pressure altitude = 0 (sea level)
3. ambient air temperature = 59 (degrees F)
4. calm (no wind)
5. Northrop T-38C aircraft with General Electric J85-GE-5R engines
6. 12,800 pounds gross weight
7. a positive slope is uphill and a negative slope is downhill

Rolling Coefficient of Friction:

The rolling coefficient of friction on a smooth, hard surface has relatively little effect on the ground roll distance. For the T-38C at 12,800 pounds, reducing the rolling coefficient of friction from 0.015 to zero reduced the ground roll distance from brake release to 140 KCAS by 67 feet, 3.6 percent, table F15. Doubling the friction increased the distance by 51 feet, 2.7 percent. A more realistic variation in the rolling coefficient of friction, ±0.005, changed the predicted distances by less than 20 feet.

Table F15 Variations in Ground Roll Distances from Brake Release to 140 KCAS due to Changes in the Rolling Coefficient of Friction

Rolling Coefficient of Friction	Ground Roll Distance from Brake Release to 140 KCAS (ft)
0.000	1,832
0.005	1,847
0.010	1,863
0.015	1,879
0.020	1,896
0.025	1,913
0.030	1,930

Notes:
1. 1976 U.S. Standard Atmosphere
2. pressure altitude = 0 (sea level)
3. ambient air temperature = 59 (degrees F)
4. calm (no wind)
5. flat runway – no runway slope
6. Northrop T-38C aircraft with General Electric J85-GE-5R engines
7. 12,800 pounds gross weight
8. 60 percent flaps
9. aircraft pitch angle = 1.00 (degree)

Aircraft Pitch Angle Before Rotation:

Variations in the aircraft pitch angle prior to rotation for the T-38C between zero and 2 degrees have almost no effect on the aircraft's acceleration prior to rotation, table F16. The pitch angle prior to rotation becomes more important as the initial value for the pitch angle during rotation. An error in the pitch angle prior to rotation will affect the mainwheel liftoff speed (takeoff speed) and the ground roll distance if the aircraft rotation is modeled as a pitch angle prior to rotation followed by a pitch rate to a pitch angle. (This is how the AFFTC used TOLAND prior to 1997.) After 1997, the AFFTC used a new version of TOLAND that has two options for modeling takeoff rotations. First, a pitch angle prior to a rotation speed and then a pitch rate until achieving a pitch angle. An example of this option is a pitch angle of 1.00 degree until a 140.0 KCAS rotation speed and then a pitch rate of 1.66 degrees per second from 1.00 degree to 7.50 degrees. The new option after 1997 was a pitch angle to a rotation speed and then a pitch angle time history (table) that represented what the aircraft had actually done.

Table F16 Variations in Ground Roll Distances from Brake Release to a Target Calibrated Airspeed Due to Changes in the Aircraft Pitch Angle Prior to Rotation

Aircraft Pitch Angle (deg)	Ground Roll Distance from Brake Release (ft)			
	Target Airspeed (KCAS)			
	80	100	120	140
0.0	587	929	1,358	1,882
0.5	587	929	1,357	1,881
1.0	587	928	1,357	1,879
1.5	587	927	1,357	1,879
2.0	587	927	1,356	1,879

Notes:
1. 1976 U.S. Standard Atmosphere
2. Pressure altitude = 0 (sea level)
3. Ambient air temperature = 59 (degrees F)
4. Calm (no wind)
5. Flat runway – no runway slope
6. Northrop T-38C aircraft with General Electric J85-GE-5R engines
7. 12,800 pounds gross weight
8. 60 percent flaps
9. Rolling coefficient of friction = 0.015

Aircraft Target Pitch Angle During Climbout:

The T-38C TOLAND simulation was run for the baseline conditions and then with different target pitch angles for rotation and climbout. The baseline inputs associated with the rotation and climbout were: (1) a 1.00 degree aircraft pitch angle prior to rotation, (2) a 140.0 KCAS rotation speed, (3) a 1.66 degree/second rotation rate, and (4) a 7.50 degree target pitch angle. The ground phase predictions were almost identical for all of the runs except for the runs with the three smallest pitch angles: 5.0, 5.5, and 6.0 degrees.

The first three runs, those with the smallest target pitch angles, had faster takeoff speeds and longer ground rolls than those with larger target pitch angles, table F17. A target pitch angle of 6.05 degrees would have resulted in the aircraft lifting off just as the target pitch angle was achieved. Takeoffs with larger target pitch angles had no effect of the ground phases of their takeoffs.

Table F17 Variations in the Mainwheel Liftoff (Takeoff) with Changes to the Target Aircraft Pitch Angle During Rotation

Aircraft Target Pitch Angle During Rotation (deg)	Aircraft Pitch Angle at Mainwheel Liftoff (deg)	Elapsed Time Between Brake Release and Mainwheel Liftoff (sec)	Airspeed at Mainwheel Liftoff (KCAS)	Horizontal Distance from Brake Release to Mainwheel Liftoff (ft)
5.0	5.00	20.70	173.4	3,075
5.5	5.50	19.98	168.2	2,867
6.0	6.00	19.25	163.3	2,663
6.5	6.05	19.23	163.2	2,657

Notes:
1. 1976 U.S. Standard Atmosphere
2. pressure altitude = 0 (sea level)
3. ambient air temperature = 59 (degrees F)
4. calm (no wind)
5. flat runway – no runway slope
6. Northrop T-38C aircraft with General Electric J85-GE-5R engines
7. 12,800 pounds gross weight
8. 60 percent flaps
9. rolling coefficient of friction = 0.015
10. aircraft pitch angle = 1.0 (degree) prior to rotation
11. 140 KCAS rotation speed
12. 1.66 degrees/second rotation rate after rotation speed
13. All takeoffs with target pitch angles greater than 6.05 degrees had the same ground performance as they would have had with a target pitch angle of 6.05 degrees.

The predicted air phases had slower airspeeds at 50 feet AGL and shorter air phase distances with increasing target pitch angles, table F18.

Table F18 Variations in the Air Phase (Climbout After Takeoff) with Changes to the Aircraft Pitch Angle During the Climbout

Aircraft Target Pitch Angle During Climbout (deg)	Speed at 50 ft AGL (KCAS)	Horizontal Distance from Mainwheel Liftoff to 50 ft AGL (ft)	Total Horizontal Distance from Brake Release to 50 ft AGL (ft)	Elapsed Time Between Mainwheel Liftoff And 50 ft AGL (sec)
5.0	231.2	3,210	6,285	9.35
5.5	224.6	3,065	5,932	9.21
6.0	218.4	2,942	5,605	9.11
6.5	212.5	2,638	5,295	8.31
7.0	206.9	2,352	5,009	7.53
7.5	201.7	2,101	4,758	6.82
8.0	197.4	1,896	4,553	6.24
8.5	193.8	1,734	4,391	5.76
9.0	190.7	1,609	4,266	5.39
9.5	188.3	1,510	4,167	5.10
10.0	186.3	1,432	4,089	4.86
10.5	184.7	1,370	4,027	4.67
11.0	183.8	1,321	3,978	4.52
12.0	181.3	1,253	3,910	4.31

Notes:
1. 1976 U.S. Standard Atmosphere
2. pressure altitude = 0 (sea level)
3. ambient air temperature = 59 (degrees F)
4. calm (no wind)
5. flat runway – no runway slope
6. Northrop T-38C aircraft with General Electric J85-GE-5R engines
7. 12,800 pounds gross weight
8. 60 percent flaps
9. Rolling coefficient of friction = 0.015
10. aircraft pitch angle = 1.0 (degree) prior to rotation
11. 140 KCAS rotation speed
12. 1.66 degrees/second rotation rate after rotation speed

This was as expected. At the higher pitch angles, more of the excess thrust was used to increase the potential energy (climb) and less for increasing the kinetic energy (velocity), table F19.

Table F19 Variations in the Aircraft's Kinetic Energy at 50 feet Above Ground Level with Changes to the Aircraft Pitch Angle During Climbout

Aircraft Target Pitch Angle During Climbout (deg)	Aircraft Gross Weight at 50 ft AGL (lb)	Aircraft Kinetic Energy at 50 ft AGL [10^6(ft-lb)]	Average Aircraft Longitudinal Acceleration During the Climbout to 50 ft AGL [ft/(sec)^2]
5.0	12,663	29.972	10.435
5.5	12,667	28.295	10.337
6.0	12,672	26.765	10.210
6.5	12,676	25.346	10.014
7.0	12,679	24.033	9.796

Table F19 Variations in the Aircraft's Kinetic Energy at 50 feet Above Ground Level with Changes to the Aircraft Pitch Angle During Climbout (Concluded)

Aircraft Target Pitch Angle During Climbout (deg)	Aircraft Gross Weight at 50 ft AGL (lb)	Aircraft Kinetic Energy at 50 ft AGL [10^6(ft-lb)]	Average Aircraft Longitudinal Acceleration During the Climbout to 50 ft AGL [ft/(sec)^2]
7.5	12,682	22.846	9.529
8.0	12,685	21.887	9.252
8.5	12,688	21.101	8.968
9.0	12,690	20.435	8.612
9.5	12,691	19.925	8.308
10.0	12,692	19.506	8.023
10.5	12,693	19.174	7.771
11.0	12,694	18.989	7.693
12.0	12,694	18.476	7.089

Notes: 1.1976 U.S. Standard Atmosphere
2. pressure altitude = 0 (sea level)
3. ambient air temperature = 59 (degrees F)
4. calm (no wind)
5. flat runway – no runway slope
6. Northrop T-38C aircraft with General Electric J85-GE-5R engines
7. 12,800 pounds gross weight
8. 60 percent flaps
9. rolling coefficient of friction = 0.015
10. aircraft pitch angle = 1.0 (degree) prior to rotation
11. 140 KCAS rotation speed
12. 1.66 degrees/second rotation rate after rotation speed
13. All takeoffs with target pitch angles greater than 6.05 degrees had the same ground performance as they would have had with a target pitch angle of 6.05 degrees.

Aircraft Flap Setting:

This comparison of the predictions for two T-38C flap settings, table F20, can best be evaluated using three separate comparisons:

1. Ground roll distance from brake release to 140 KCAS rotation speed with 1.00-degree aircraft pitch angle.
2. Ground roll distance from brake release to mainwheel liftoff (takeoff), takeoff speed, and aircraft pitch angle at mainwheel liftoff.
3. Total ground roll distance from brake release to 50 feet AGL and the speed at 50 feet AGL.

Table F20 Variations in the Distances and Airspeeds with Changes to the Trailing Edge Flap Deflection

Variable	Flap Deflection, percent	
	45	60
Distance to Rotation (ft)	1,800	1,825
Ground Roll Distance (ft)	2,675	2,600
Distance to 50 ft AGL (ft)	4,925	4,670
Air Distance (ft)	2,250	2,070
Rotation Speed (KCAS)	140.0	140.0
Takeoff Speed (KCAS)	167.3	163.8
Aircraft Pitch Angle at Takeoff (deg)	6.5	6.0
Airspeed at 50 ft AGL (KCAS)	210.8	203.1

Notes:
1. Sea level pressure altitude
2. Standard day, 59 degrees F
3. Flat runway, no slope
4. No wind, calm
5. 12,800 pounds gross weight at brake release
6. 1.00 degree pitch angle prior to rotation
7. 140 KCAS rotation speed
8. 1.66 degrees per second pitch rate to 7.50 degrees after rotation speed
9. These two takeoff predictions were created using a larger gross thrust model and slightly different aerodynamic models than those used for the other sensitivity studies in this appendix.

The ground roll distances from brake release to rotation, 140 KCAS, were within 25 feet of each other. This was the result of two small and somewhat offsetting effects. The aircraft with the larger flap setting had both more drag and more lift at a given pitch angle and airspeed. The greater aerodynamic lift reduced the weight on the tires and therefore the rolling friction.

The ground roll distances from rotation to takeoff were 875 feet for the smaller flap setting and 775 feet for the larger flap setting. The speeds at takeoff were 167.3 and 163.8 KCAS for the smaller and larger flap settings, respectively. The aircraft with the larger flap setting had more lift at a given pitch angle and airspeed. This allowed the aircraft to take off at a lower airspeed and in a shorter distance.

Since both aircraft used a pitch angle of 7.50 degrees for the climbout and the aircraft with the larger flap deflection required less angle of attack for a given lift coefficient, it was able to climb out at a larger flightpath angle. The larger flightpath angle resulted in a shorter air distance and a slower airspeed at 50 feet AGL.

Aircraft Aerodynamic Drag:

An aeronautical engineer should be able to predict the aerodynamic lift and drag forces and coefficients in ground effect within less than ±20 percent (more likely within ±10 percent) for a fairly conventional aircraft in ground effect (tires on the runway) at low angles of attack (typically -1 to +2 degrees). Table F21 shows the effect of changing the assumed drag by 50 and by 100 percent. The effect becomes more pronounced with increasing airspeed. A 50 percent error in drag changed the predicted ground roll distances from brake release to 80 KCAS by 6 feet, less than a 1 percent error in the distance. The same 50 percent error in drag changed the predicted ground roll distance from brake release to 140 KCAS by approximately 65 feet, approximately 3.5 percent. Reducing the aerodynamic drag errors to 10 percent (from 50 percent) would reduce the calculated distance errors to 1 foot and 13 feet for 80 and 140 KCAS, respectively.

Table F21 Variations in Ground Roll Distances from Brake Release with Changes to the Aircraft Aerodynamic Drag

Aerodynamic Drag Relative to the Baseline (pct)	Ground Roll Distance from Brake Release to XXX KCAS (ft)			
	Final Airspeed (KCAS)			
	80	100	120	140
0	575	897	1,292	1,757
50	581	912	1,323	1,815
100	587	928	1,357	1,879
150	593	944	1,392	1,947
200	599	961	1,430	2,027

Notes:
1. Sea level pressure altitude
2. Standard day, 59 degrees F
3. Flat runway, no slope
4. No wind, calm
5. 12,800 pounds gross weight at brake release
6. 1.0 degree aircraft pitch angle
7. 60 percent flaps
8. The aerodynamic drag was reduced to no drag, half of the actual (baseline) drag, 150 percent of the baseline drag, and double the baseline drag
9. The baseline drag coefficient for 1 degree angle of attack in ground effect was 0.0710 based on an aerodynamic reference area of 170 square feet.

This sensitivity study was based on a T-38C aircraft with a brake release gross weight of 12,800 pounds and an installed gross thrust of 6,800 pounds at brake release. That corresponded to an installed thrust-to-weight ratio of 0.53. These results would not be typical of those for a modern jet fighter with a thrust-to-weight ratio greater than one or for a heavyweight aircraft at a high elevation airport on a hot day.

Thrust:

The thrust sensitivity study varied the installed gross thrust from 98 to 107 percent of the baseline thrust. The effect on the ground roll distance from brake release to 160 KCAS in a 1.00 degree pitch angle acceleration was evaluated, table F22. The effect was slightly nonlinear but was approximately 28 feet for each 1 percent change in thrust. A change of 28 feet was approximately equivalent to a 1.2 percent reduction in the distance for each 1 percent increase in thrust.

Table F22 Variations in Ground Roll Distance from Brake Release to 160 KCAS with changes in the Propulsive Thrust

Propulsive Thrust Relative to the Baseline (pct)	Ground Roll Distance from Brake Release to 160 KCAS (ft)
98	2,441
99	2,413
100	2,384
101	2,357
102	2,330
103	2,304
104	2,276

Table F22 Variations in Ground Roll Distance from Brake Release to 160 KCAS with changes in the Propulsive Thrust (Concluded)

Propulsive Thrust Relative to the Baseline (pct)	Ground Roll Distance from Brake Release to 160 KCAS (ft)
105	2,253
106	2,229
107	2,204

Notes: 1. Sea level pressure altitude
2. Standard day, 59 degrees F
3. Flat runway, no slope
4. No wind, calm
5. 12,800 pounds gross weight at brake release
6. 1.0 degree aircraft pitch angle
7. 45 percent flaps

Notice that a relatively small percentage change in thrust can have the same effect on the ground roll distance as does a relatively large percentage change in aerodynamic drag. This becomes important when trying to change the TOLAND models to match the observed test day takeoff performance. If the TOLAND predicted ground roll distances from brake release to rotation do not match the observed distances, then the thrust model is normally changed versus the aerodynamic model. The choice is less obvious if the distances to rotation “match” but the distances to liftoff and/or 50 feet AGL do not “match”.

Errors in Airspeed:

The purpose of this sensitivity study is to illustrate the errors in the predicted test day ground roll distances caused by using an erroneous test day airspeed. The error in the assumed airspeed could have been due to an error in the Pitot-static position error corrections used in the postflight data processing. The measured test day distances as a function of time would be correct, but the calculated airspeeds as a function of time would be wrong. The TOLAND software would predict a “wrong” distance because it used the “wrong” airspeed. The test day event would be correct because it would have been determined based on a change in aircraft pitch angle or horizontal stabilizer position for rotation or on a wheelspeed sensor or a WOW discrete for mainwheel liftoff, takeoff. The test day distances would be determined using the event times.

The error in the airspeed would propagate into the standardized distance because the test day predicted rotation speed would be wrong while the reference day predicted speed would be correct. The errors would be on the order of 20 to 35 feet, table F23.

Table F23 Variations in Ground Roll Distance from Brake Release with a 1.00 KCAS Change in Calibrated Airspeed

Actual Calibrated Airspeed (KCAS)	Ground Roll Distance Difference (ft)
100	19
110	22
120	24
130	26
140	28
150	30
160	34
170	37

Notes:
1. Sea level pressure altitude
2. Standard day, 59 degrees F
3. Flat runway, no slope
4. No wind, calm
5. 12,800 pounds gross weight at brake release
6. 1.00 degree aircraft pitch angle
7. 60 percent flaps

APPENDIX G - T-38C TAKEOFF TEST RESULTS

The results in this section are from a series of flight tests flown between 2001 and 2010 as part of the Northrop T-38C PMP. The results are divided into five categories:

1. Distance from brake release to the rotation speed
2. Distance from brake release to mainwheel liftoff (takeoff ground roll)
3. Horizontal distance from brake release to 50 feet AGL
4. Airspeed at mainwheel liftoff
5. Airspeed at 50 feet AGL

DISTANCE TO ROTATION

The Northrop T-38C takeoff data were divided into data sets for this handbook. The data sets are defined in table G1. The rotation speed for data standardization was 141 KCAS for data sets one through three and 140 KCAS for all of the others.

<u>Data Set Number One:</u>

The baseline configuration, data set number 1, had 41 takeoffs. Of those, there were no useable data for six of the takeoffs. The remaining 35 takeoffs were analyzed and used in *T-38C Aircraft Performance Evaluation*, AFFTC-TR-03-18 (reference 22). The quality of the results was rather poor: Relative to the average standardized distance, the distances for eight of the takeoffs were more than ±100 feet from the average. The three extremes were 156 feet short of the average and 146 and 131 feet longer than the average.

Three of the four takeoffs with the poorest agreement had strong winds. The tower reported winds for those four takeoffs were: (1) 20 knots gusting to 27 knots, (2) 12 knots, (3) 16 knots gusting to 24 knots, and (4) a 4 knot crosswind. Many of these takeoffs were flown in the late morning or in the afternoon in high and/or gusty winds.

The average of the standardized ground rolls was 37 feet longer than that predicted for the reference day conditions. This was the equivalent of about a 1.7 percent error in the installed thrust model. The following are standardized distances relative to the average standardized distance:

0 of 35 (0 percent) within ±10 feet
6 of 35 (17 percent) within ±25 feet
18 of 35 (51 percent) within ±50 feet
22 of 35 (63 percent) within ±75 feet
27 of 35 (77 percent) within ±100 feet
8 of 35 (23 percent) greater than 100 feet
4 of 35 (11 percent) greater than 125 feet
1 of 35 (3 percent) greater than 150 feet

If the eight takeoffs with the largest differences for their standardized distances from brake release to rotation were eliminated, then the average for the remaining 27 takeoffs would have been 2 feet longer than that for the 35 takeoffs.

Table G1 Northrop T-38C Data Sets

Data Set	Number of Takeoffs Evaluated	Aircraft Inlet (T-38A/PMP)	Aircraft Boattail (T-38A/PMP)	Wing Trailing Edge Flaps (pct)	J85-GE-5R versus J85-GE-5M or J85-GE-5S (-5M/-5R/-5S)	Jet Fuel (JP-8/SJ-8)	PMP Final Engine Bay Configuration (YES/NO)	AFFTC Technical Report Number
1	35	T-38A	T-38A	60	-5M	JP-8	NO	TR-03-18
2	12	T-38A	PMP	60	-5M	JP-8	NO	TR-03-18
3	51	PMP	PMP	60	-5M	JP-8	NO	TR-03-18
4	6	PMP	PMP	60	-5R	JP-8	NO	TR-07-10
5	15	PMP	PMP	45	-5R	JP-8	NO	TR-07-10
6	10	PMP	PMP	45	-5S	JP-8	NO	TR-09-45
7	4	PMP	PMP	45	-5S	SJ-8	NO	TR-09-45
8	11	PMP	PMP	45	-5S	JP-8	NO	TR-10-52
9	5	PMP	PMP	45	-5S	JP-8	YES	TR-10-52

Data Set Number Two:

Data set number two used 12 of 12 takeoffs. Relative to the average of the standardized distances from brake release to rotation (141 KCAS), the extreme differences in distance were 50 and 57 feet longer and 42 feet shorter.

3 of 12 (25 percent) within ±10 feet
6 of 12 (50 percent) within ±25 feet
11 of 12 (92 percent) within ±50 feet
12 of 12 (100 percent) within ±57 feet

While that may sound good, there were two less favorable aspects to the standardized distances. First, the average of the standardized distances was 40 feet longer than the reference day predicted distance. This could have been "fixed" by decreasing the thrust by approximately 2 percent. Changing the thrust would have made the reference day predicted distance equal to the average of the standardized distances.

Second, half (6 of 12) of the standardized distances had significantly more variability relative to the average standardized distance than did the other half. The average distance for the six takeoffs with the least variability relative to the average standardized distance would have been 7 feet shorter than if all 12 takeoffs were used.

One of the reasons that the distances in data set two had less scatter than those in data set one was the relatively light winds for data set two. None of the winds were five knots or greater for data set two.

Data Set Number Three:

Data set number three was 51 takeoffs selected from 101 available takeoffs. Most of these 101 takeoffs were flown in the late mornings or during the afternoons. Approximately half of the available takeoffs were flown in high and/or gusty winds. The primary criterion for eliminating half of the takeoffs was the high winds.

The average of the standardized distances from brake release to rotation speed, 141 KCAS, was 8 feet longer than the reference day predicted distance. Decreasing the modeled thrust by approximately 0.4 percent would have eliminated that difference.

The extremes of the differences between the average of the standardized distances and the standardized value for a given flight were 147 and 141 feet longer than the average and two that were 141 feet shorter than the average standardized distance. Eliminating those four flights and using 47 of the 51 takeoffs would not have significantly changed the average distance. The change in the average distance would have been less than 1 foot.

9 of 51 (18 percent) within ±10 feet
16 of 51 (31 percent) within ±25 feet
25 of 51 (49 percent) within ±40 feet
27 of 51 (53 percent) within ±41 feet
33 of 51 (65 percent) within ±50 feet
43 of 51 (84 percent) within ±100 feet

Data Set Number Four:

The fourth data set was obtained as a spot check of the baseline models using 60 percent flap deflection. Data from all six baseline takeoffs were used.

The standardized distances from brake release to 140 KCAS were all within ±45 feet of both the average standardized distance and the reference day predicted distance for all six takeoffs. The average of six standardized distances from brake release to the rotation speed (140 KCAS) was 8 feet shorter than the reference day predicted distance. The two extremes for the six takeoffs were the distances of 30 feet longer than predicted (flight number 499) and 45 feet shorter than predicted (flight number 502). The following are distances relative to the average standardized distance, 1,818 feet.

2 of 6 (33 percent) within ±10 feet
3 of 6 (50 percent) within ±15 feet
4 of 6 (67 percent) within ±25 feet
6 of 6 (100 percent) within ±38 feet

Data Set Number Five:

Data set number five used 45 percent trailing edge flap deflection versus 60 percent. Data were acquired for 15 takeoffs and all 15 were used.

The average of the 15 standardized distances from brake release to rotation speed (140 KCAS) was 10 feet shorter than the reference day predicted distance. The extreme differences relative to the average standardized distance were 55 feet shorter, 50 feet longer, and 40 feet shorter. The following are distances relative to the average standardized distance:

4 of 15 (27 percent) within ±10 feet
5 of 15 (33 percent) within ±20 feet
9 of 15 (60 percent) within ±25 feet
14 of 15 (93 percent) within ±50 feet
15 of 15 (100 percent) within ±55 feet

Data Set Number Six:

Data set six was 10 takeoffs flown with JP-8 fuel as a baseline to evaluate a new fuel, SJ-8. The standardized distances from brake release to rotation (140 KCAS) were significantly different for two of the ten takeoffs. The standardized distances for those two were 73 and 132 feet shorter than the average of the standardized distances. The tower reported wind for one of those takeoffs was 21 knots with the wind varying by ±5 knots. The cause of the other outlier was not determined.

The average of the eight standardized distances was 1 foot longer than the reference day prediction. The extreme differences between the average of the eight standardized distances and the individual standardized distances were 33 feet shorter and 20 feet longer that the average standardized distance. The following are distances relative to the average standardized distance:

1 of 8 (13 percent) within ±10 feet
4 of 8 (50 percent) within ±12 feet
7 of 8 (88 percent) within ±25 feet
8 of 8 (100 percent) within ±33 feet

Data Set Number Seven:

Data set number seven was four takeoffs flown with SJ-8 fuel. The standardized distances from brake release to rotation (140 KCAS) were relatively close with the extremes being 31 feet shorter and 21 feet longer than the average for the four takeoffs. The following are distances relative to the average standardized distance:

1 of 4 (25 percent) within ±10 feet
2 of 4 (50 percent) within ±20 feet
3 of 4 (75 percent) within ±25 feet
4 of 4 (100 percent) within ±50 feet

The average distance was 31feet shorter than the reference day predicted distance. This was most likely due to both engines having been retrimmed when the fuel was changed from JP-8 to SJ-8.

Data Set Number Eight:

Data set number eight was the baseline for the final PMP engine bay configuration evaluation. There were 11 takeoffs that were standardized to a rotation speed of 140 KCAS. The average of the 11 standardized distances from brake release to rotation was 27 feet longer than the reference day predicted distance. This difference could have been eliminated by decreasing the thrust model by approximately 1.5 percent. The extremes of the differences between the average of the standardized distances and the individual standardized distances were 62 and 57 feet longer and 38 feet shorter than the average distance. The following are distances relative to the average standardized distance:

3 of 11 (27 percent) within ±10 feet
5 of 11 (45 percent) within ±18 feet
6 of 11 (55 percent) within ±23 feet
8 of 11 (73 percent) within ±30 feet
9 of 11 (82 percent) within ±50 feet
11 of 11 (100 percent) within ±62 feet

Data Set Number Nine:

The final data set were from five takeoffs with the final PMP engine bay configuration. The data were standardized to a rotation speed of 140 KCAS. The average of the five standardized distances was 1 foot shorter than the reference day prediction. The extreme differences between the average of the five standardized distances and the individual standardized distances were 20 feet longer and 14 feet shorter than the average standardized distance. The following are distances relative to the average standardized distance:

2 of 5 (40 percent) within ±10 feet
3 of 5 (60 percent) within ±12 feet
5 of 5 (100 percent) within ±20 feet

Summary for the Distance to Rotation:

The following summarizes the 147 standardized distances from brake release to rotation relative to the average standardized distance for the appropriate data set:

24 of 147 (16 percent) within ±10 feet
61 of 147 (41 percent) within ±25 feet
73 of 147 (50 percent) within ±32 feet
103 of 147 (70 percent) within ±50 feet
122 of 147 (82 percent) within ±75 feet
19 of 147 (13 percent) greater than 100 feet
4 of 147 (3 percent) greater than 150 feet

The standardized distances from brake release to rotation for 73 of the 147 takeoffs (50 percent) were within ±32 feet of the averages of the standardized distances. To put that in perspective, the length of the T-38C aircraft was 46 feet.

All 19 of the takeoffs with distance differences greater than 100 feet were from data sets one and three. Many of those takeoffs were flown in high and/or gusty winds. Even so, they only represented 13 percent of the 147 takeoffs.

Potential TOLAND Thrust Model Refinement:

The General Electric J85 turbojet engine in the Northrop T-38C aircraft was a 1950s vintage engine. The engine used a hydromechanical fuel controller and the engine had relatively little variable geometry.

The test engines had a large number of mechanical problems during the flight testing. This resulted in numerous trim checks for the engines. This lead to the creation of nine separate data sets. Each data set had a unique trim level. (Note: all trim levels were within the allowed maintenance technical order trim limits.)

The test day distances from brake release to the start of rotation were used to refine the engine model in the TOLAND software. The engine model for each data set was developed by matching (in general) the distances from brake release to rotation. The thrust adjustment was a multiplicative factor for the modeled gross thrust.

The process was iterative based on the differences in the test day (actual) distance from brake release to rotation relative to the predicted distance from TOLAND. The iteration continued until it converged within an acceptable limit. After adjustments had been made, half of the standardized distances from brake release to rotation for data sets four through nine were less than 30 feet from the reference day predicted distances, table G2.

The potential thrust model changes for an additional iteration ranged from 2.0 percent less thrust for data set two to 1.5 percent more thrust for data set seven. Five of the nine data sets would have had a thrust change of less than 1 percent.

Table G2 Potential Thrust Model Adjustments

Data Set	Sample Size	Data Scatter for 50 pct of the Data (ft)	Distance Difference (ft)	Potential Thrust Model Adjustment (pct)
1	35	50	37 short	1.7 less
2	12	25	40 short	2.0 less
3	51	40	8 short	0.4 less
4	6	15	8 long	0.4 more
5	15	25	10 long	0.5 more
6	8	12	1 short	0
7	4	20	31 long	1.5 more
8	11	20	27 short	1.2 less
9	5	11	1 long	0

Notes:
1. The data sets are defined in table G1.
2. Sample size was the number of takeoffs used for a given data set.
3. The data scatter for 50 percent of the data presents the distance within which one-half of the data points fell.
4. The distance difference is the average difference between the test day (actual) distance for a data set relative to the TOLAND predicted distance. “Short” refers to a predicted distance that is shorter than the test day (actual) distance for the data set. “Long” refers to a predicted distance that is too long.
5. The potential thrust model adjustment is the estimated change to the thrust model to reduce the average difference between the test day (actual) distance and the predicted distance.

GROUND ROLL DISTANCE

Data Set Number One:

Data set number one had data from 35 takeoffs mainly flown in the late morning or in the afternoon. The winds were frequently high and/or gusty.

The average of the standardized ground roll distances was 39 feet longer than the reference day predicted distance. This was the equivalent of about a 1.3 percent error in the thrust model. The extremes between the individual standardized ground rolls and the average of the standardized ground rolls were 262 and 281 feet longer and 214 feet shorter than the average standardized distance. The following are standardized distances relative to the average standardized distance:

3 of 35 (9 percent) within ±10 feet
8 of 35 (23 percent) within ±25 feet
13 of 35 (37 percent) within ±50 feet
17 of 35 (49 percent) within ±75 feet
21 of 35 (60 percent) within ±100 feet
14 of 35 (40 percent) greater than ±100 feet
12 of 35 (14 percent) greater than ±125 feet
7 of 35 (20 percent) greater than ±150 feet
5 of 35 (14 percent) greater than ±175 feet
4 of 35 (11 percent) greater than ±200 feet
2 of 35 (6 percent) greater than ±225 feet
2 of 35 (6 percent) greater than ±250 feet

Data Set Number Two:

The most significant difference between data set number one and data set number two was the high winds for data set one and the light winds for data set two. The winds for all 12 of the data set two takeoffs were less than five knots.

The average of the standardized ground roll distances was 59 feet longer than the reference day predicted distance. This was the equivalent of about a 1.9 percent error in the thrust model. The extremes between the individual standardized ground rolls and the average of the standardized distances were 188, 160, and 125 feet longer and 152 feet shorter than the average standardized distance. The following are standardized ground roll distances relative to the average standardized ground roll distance:

1 of 12 (8 percent) within ±10 feet
2 of 12 (17 percent) within ±25 feet
6 of 12 (50 percent) within ±50 feet
7 of 12 (58 percent) within ±75 feet
8 of 12 (67 percent) within ±100 feet
4 of 12 (33 percent) greater than ±100 feet
3 of 12 (25 percent) greater than ±125 feet
3 of 12 (25 percent) greater than ±150 feet
1 of 12 (8 percent) greater than ±175 feet
0 of 12 (0 percent) greater than ±188 feet

Data Set Number Three:

These data, like those in data set number one, were obtained in windy conditions. However, the average of the standardized ground roll distances to takeoff was only 2 feet longer than the reference day predicted distance.

The extremes of the differences between the average of the standardized ground roll distances and the standardized value for a given flight were 592, 492, and 289 feet longer than the average standardized distance and 191 and 157 feet shorter. The following are standardized ground roll distances relative to the average standardized ground roll:

5 of 51 (10 percent) within ±10 feet
9 of 51 (18 percent) within ±25 feet
17 of 51 (33 percent) within ±50 feet
22 of 51 (43 percent) within ±75 feet
28 of 51 (55 percent) within ±100 feet
23 of 51 (45 percent) greater than ±100 feet
15 of 51 (29 percent) greater than ±125 feet
5 of 51 (10 percent) greater than ±150 feet
4 of 51 (8 percent) greater than ±175 feet
3 of 51 (6 percent) greater than ±200 feet
3 of 51 (6 percent) greater than ±225 feet
3 of 51 (6 percent) greater than ±250 feet
2 of 51 (4 percent) greater than ±300 feet

Data Set Number Four:

Data from six of six available takeoffs were used. The average of the six standardized ground roll distances was 18 feet longer than the reference day predicted distance. This was the equivalent of a thrust error of approximately 0.7 percent.

The extremes of the differences between the average of the standardized ground roll distances and the standardized value for a given flight were 82 feet longer and 53 feet shorter than the average standardized distance. The following are standardized ground roll distances relative to the average standardized ground roll:

2 of 6 (33 percent) within ±10 feet
3 of 6 (50 percent) within ±25 feet
4 of 6 (67 percent) within ±50 feet
5 of 6 (83 percent) within ±75 feet
6 of 6 (100 percent) within ±82 feet

Data Set Number Five:

Data from 15 of 15 available takeoffs were used. The average of the 15 standardized ground roll distances was only 1 foot longer than the reference day predicted distance.

The extremes of the differences between the average of the standardized ground roll distances and the standardized value for a given flight were 46 and 41 feet shorter and 34 feet longer than the average standardized distance. The following are standardized ground roll distances relative to the average standardized ground roll:

5 of 15 (33 percent) within ±10 feet
10 of 15 (67 percent) within ±25 feet
15 of 15 (100 percent) within ±46 feet

Data Set Number Six:

Data set number six had data from 10 takeoffs. Data were used from eight of the 10 takeoffs. The average of the standardized ground roll distances to liftoff was 17 feet longer than the reference day predicted distance. This was the equivalent of a thrust model error of approximately 0.6 percent.

The extremes of the differences between the average of the standardized ground roll distances and the standardized value for a given flight were 61 and 46 feet shorter and 42 feet longer than the average standardized distance. The following are standardized ground roll distances relative to the average standardized ground roll:

2 of 8 (25 percent) within ±10 feet
4 of 8 (50 percent) within ±25 feet
7 of 8 (88 percent) within ±50 feet
8 of 8 (100 percent) within ±61 feet

Data Set Number Seven:

Data set number seven was four takeoffs flown with SJ-8 fuel. All of the actual test day distances were shorter than predicted by TOLAND. The differences were 31, 41, 46, and 79 feet. The average standardized ground roll distance was 49 feet shorter than the reference day predicted distance. This was probably the result of the engine trim performed after changing fuel and was the equivalent of a 1.8 percent deficit in thrust. The following are standardized ground roll distances relative to the average standardized ground roll: 3, 8, 18, and -30 feet.

2 of 4 (50 percent) within ±10 feet
3 of 4 (75 percent) within ±25 feet
4 of 4 (100 percent) within ±30 feet

Data Set Number Eight:

Data set number eight was 11 takeoffs flown as the baseline for the final PMP engine bay configuration. One of the 11 ground roll distances was approximately 100 feet shorter than any of the others. The average of the 11 standardized ground roll distances was 24 feet longer than the reference day predicted distance. This was the equivalent of a thrust model error of approximately 0.9 percent, less thrust than modelled in TOLAND. The extreme differences between the 11 standardized ground roll distances and their average were 167 feet shorter and 55 feet longer than the average distance. The following are standardized ground roll distances relative to the average standardized distance:

5 of 11 (45 percent) within ±10 feet
6 of 11 (55 percent) within ±25 feet
8 of 11 (73 percent) within ±50 feet
10 of 11 (91 percent) within ±75 feet
11 of 11 100 percent) within ±167 feet

Flight number 551 in data set number eight had an actual test day ground roll distance of 2,848 feet and a predicted distance of 2,999 feet, a difference of 151 feet.

Data Set Number Nine:

The final data set was from five takeoffs with the final PMP engine bay configuration. The average of the five standardized ground roll distances was 11 feet longer than the reference day predicted distance. That was the equivalent of an error in the thrust model of approximately 0.4 percent, less thrust than modelled in TOLAND.

The extremes of the differences between the average of the standardized distances and the individual standardized distances were 32 feet longer and 34 feet shorter than the average standardized distance. The following are standardized ground roll distances relative to the average standardized distance:

2 of 5 (40 percent) within ±10 feet
3 of 5 (60 percent) within ±25 feet
5 of 5 (100 percent) within ±34 feet

Summary for the Ground Roll Distance:

The following summarizes the 147 standardized ground roll distances for brake release to mainwheel liftoff, takeoff, relative to the average standardized distance for the appropriate data set:

23 of 147 (16 percent) within ±10 feet
51 of 147 (35 percent) within ±25 feet
73 of 147 (50 percent) within ±40 feet
80 of 147 (54 percent) within ±50 feet
93 of 147 (63 percent) within ±75 feet
105 of 147 (71 percent) within ±100 feet
41 of 147 (28 percent) greater than ±100 feet
30 of 147 (20 percent) greater than ±125 feet
15 of 147 (10 percent) greater than ±150 feet
11 of 147 (7 percent) greater than ±175 feet
8 of 147 (5 percent) greater than ±200 feet
6 of 147 (4 percent) greater than ±225 feet
6 of 147 (4 percent) greater than ±250 feet

All of the standardized distances that varied by more than 100 feet from the average distances (except one, flight number 551 in data set number eight) were from data sets one, two and three; the data sets with the high/gusty winds. Even with those distances included in the summary, half (73 of 147) of the differences were within ±40 feet of the average values.

The following summarizes the 49 standardized ground roll distances relative to the average standardized distance for their appropriate data set for data sets four through nine, those with the lighter/less gusty winds:

15 of 49 (31 percent) within ±10 feet
23 of 49 (47 percent) within ±18 feet
25 of 49 (51 percent) within ±19 feet
29 of 49 (59 percent) within ±25 feet
43 of 49 (88 percent) within ±50 feet
47 of 49 (96 percent) within ±75 feet
47 of 49 (96 percent) within ±100 feet
48 of 49 (98 percent) within ±150 feet
49 of 49 (100 percent within ±151 feet

Half of the distances for this reduced set were within ±19 feet of the average standardized distance for their appropriate data set. Nineteen feet is significantly less than the length of the T-38 fuselage, 46 feet.

Review of Potential Thrust Model Adjustments:

The TOLAND T-38C engine model was refined based on the test day ground roll distances from brake release to rotation. The test day predicted distances were compared with the actual test day distances. A similar comparison was made using the ground roll distances from brake release to mainwheel liftoff (takeoff), table G3. A farther refinement to the engine model was not made in this case.

Table G3 Review of Potential Thrust Model Adjustments

Data Set	Sample Size	Rotation Distance Difference (ft)	Ground Roll Distance Difference to Mainwheel Liftoff (ft)
1	35	37 short	39 short
2	12	40 short	59 short
3	51	8 short	2 short
4	6	8 long	18 short
5	15	10 long	1 short
6	8	1 short	17 short
7	4	31 long	49 long
8	11	27 short	24 short
9	5	1 long	11 short

Notes: 1. The data sets are defined in table G1.
2. Sample size was the number of takeoffs used for a given data set.
3. The distance difference is the average difference between the test day (actual) distance for a data set relative to the TOLAND predicted distance. “Short” refers to a predicted distance that is shorter than the test day (actual) distance for the data set. “Long” refers to a predicted distance that is too long.

TOTAL TAKEOFF DISTANCE TO 50 FEET AGL

Data Set Number One:

Data set number one had data from 35 takeoffs mainly flown in the late morning or in the afternoon. The winds were frequently high and/or gusty.

The average of the standardized horizontal distances to 50 feet AGL were 89 feet longer than the reference day predicted distance. This was the equivalent of about a 1.8 percent error in the thrust model. The extremes between the individual standardized distances and the average standardized distance were 468, 336, and 304 feet longer and 305 and 254 feet shorter than the average standardized distance. The following are standardized distances relative to the average standardized distance:

5 of 35 (14 percent) within ±25 feet
6 of 35 (17 percent) within ±50 feet
15 of 35 (43 percent) within ±75 feet
19 of 35 (54 percent) within ±100 feet
25 of 35 (71 percent) within ±150 feet
29 of 35 (83 percent) within ±200 feet
30 of 35 (86 percent) within ±250 feet
31 of 35 (89 percent) within ±300 feet
34 of 35 (97 percent) within ±350 feet
35 of 35 (100 percent) within ±468 feet

Data Set Number Two:

The average of the standardized distances was 64 feet longer than the reference day predicted distance. This was the equivalent of about a 1.3 percent error in the thrust model. The extremes between the individual standardized distances and the average of the standardized distances were 296 feet longer and 198 feet shorter than the average of the standardized distances. The following are standardized distances from brake release to 50 feet AGL relative to the average standardized distance:

2 of 12 (17 percent) within ±25 feet
2 of 12 (17 percent) within ±50 feet
4 of 12 (33 percent) within ±75 feet
7 of 12 (58 percent) within ±100 feet
10 of 12 (83 percent) within ±150 feet
11 of 12 (92 percent) within ±200 feet
11 of 12 (92 percent) within ±250 feet
12 of 12 (100 percent) within ±296 feet

Data Set Number Three:

These data, like those of data set number one, were obtained in windy conditions. The average of the standardized distances was 21 feet shorter than the reference day predicted distance. This was the equivalent of a thrust error of approximately 0.4 percent.

The extremes of the differences between the average of the standardized distances and the standardized values for a given flight were 629, 517, 443, and 388 feet longer and 1107, 550, 446, and 427 feet shorter than the average distance. The following are standardized distances from brake release to 50 feet AGL relative to the average standardized distance:

4 of 51 (8 percent) within ±25 feet
11 of 51 (22 percent) within ±50 feet
16 of 51 (31 percent) within ±75 feet
21 of 51 (41 percent) within ±100 feet
27 of 51 (53 percent) within ±150 feet
37 of 51 (73 percent) within ±200 feet
41 of 51 (80 percent) within ±250 feet
43 of 51 (84 percent) within ±300 feet

Data Set Four:

Data from six of six available takeoffs were used. The average of the six standardized distances from brake release to 50 feet AGL were 83 feet shorter than the reference day predicted distance. This was the equivalent of a thrust error of approximately 1.8 percent, more thrust than modelled in TOLAND.

The extremes of the differences between the average of the standardized distances and the standardized value for a given flight were 78 feet longer and 92 feet shorter than the average standardized distance. The following are standardized distances from brake release to 50 feet AGL relative to the average standardized distance:

2 of 6 (33 percent) within ±25 feet
3 of 6 (50 percent) within ±50 feet
4 of 6 (67 percent) within ±75 feet
6 of 6 (100 percent) within ±92 feet

Data Set Five:

Data from 15 of 15 available takeoffs were used. The average of the 15 standardized distances was only 10 feet shorter than the reference day predicted distance. The extremes of the differences between the average of the standardized distances and the standardized value for a given flight were 110 feet longer and 210 feet shorter than the average standardized distance. The following are standardized distances from brake release to 50 feet AGL relative to the average standardized distance:

6 of 15 (40 percent) within ±25 feet
9 of 15 (60 percent) within ±50 feet
12 of 15 (80 percent) within ±75 feet
13 of 15 (87 percent) within ±100 feet
14 of 15 (93 percent) within ±150 feet
14 of 15 (93 percent) within ±200 feet
15 of 15 100 percent) within ±210 feet

Data Set Six:

Data set six had data from 10 takeoffs. Data were used from eight of the 10 takeoffs. These were the same eight takeoffs as were used for the distance to rotation and the takeoff ground roll. The average of the standardized distances were only 5 feet longer than the reference day predicted distance.

The extremes of the differences between the average of the standardized distances and the standardized value for a given flight were 102 feet shorter and 89 feet longer than the average standardized distance. The following are standardized distances from brake release to 50 feet AGL relative to the average standardized distance:

2 of 8 (25 percent) within ±25 feet
3 of 8 (38 percent) within ±50 feet
6 of 8 (75 percent) within ±75 feet
7 of 8 (88 percent) within ±100 feet
8 of 8 (100 percent) within ±102 feet

Data Set Number Seven:

Data set number seven was four takeoffs flown with SJ-8 fuel. The average of the standardized distances was 61 feet shorter than the reference day predicted distance. This was equivalent to a thrust model error of approximately 1.2 percent and was probably the result of an engine trim performed after changing fuels. Relative to the average of the four standardized distances, the extremes were 156 feet shorter and 124 feet longer than the average value. The other two standardized distances were 67 feet longer and 35 feet shorter than the average of the four standardized distances. The following are standardized distances from brake release to 50 feet AGL relative to the average standardized distance:

0 of 4 (0 percent) within ±25 feet
1 of 4 (25 percent) within ±50 feet
2 of 4 (50 percent) within ±75 feet
2 of 4 (50 percent) within ±100 feet
3 of 4 (75 percent) within ±125 feet
3 of 4 (75 percent) within ±150 feet
4 of 4 (100 percent) within ±156 feet

Data Set Number Eight:

Data set number eight was 11 takeoffs flown as the baseline for the final PMP engine bay configuration. All 11 takeoffs were used for determining the distance from brake release to 50 feet AGL. The average of the 11 standardized distances was 13 feet longer than the reference day predicted distance. This was the equivalent of a thrust model error of approximately 0.3 percent. The extreme differences between the 11 standardized distances and their average were 50 feet shorter and 74 feet longer than the average distance. The following are standardized distances from brake release to 50 feet AGL relative to the average standardized distance:

3 of 11 (27 percent) within ±25 feet
10 of 11 (91 percent) within ±50 feet
11 of 11 (100 percent) within ±74 feet

Data Set Number Nine:

The final data set was from five takeoffs with the final PMP engine bay configuration. The average of the five standardized distances from brake release to 50 feet AGL were only 3 feet shorter than the reference day predicted distance. The extreme differences between the average of the standardized distances and the individual standardized distances for each flight were 162 feet longer and 112 feet shorter than the average standardized distance. The differences between the average of the standardized distances, 4,932 feet, and the standardized distance for each flight were -112 feet for flight number 561, -109 feet for flight number 565, 15 feet for flight number 563, 44 feet for flight number 564, and 162 feet for flight number 562. The average distance would have been 4,892 versus 4,932 feet if flight number 562 had not been included. Then, the distances for all four flights would have been within ±84 feet of the average and the average would have been 43 feet shorter than the reference day predicted distance of 4,935 feet. The following are standardized distances from brake release to 50 feet AGL relative to the average standardized distance:

1 of 5 (20 percent) within ±25 feet
2 of 5 (40 percent) within ±50 feet
2 of 5 (40 percent) within ±75 feet
2 of 5 (40 percent) within ±100 feet
4 of 5 (80 percent) within ±125 feet
4 of 5 (80 percent) within ±150 feet
5 of 5 (100 percent) within ±162 feet

Summary for the Total Takeoff Distance to 50 feet AGL:

The following summarize the 147 standardized distances from brake release to 50 feet AGL relative to the average standardized value for the appropriate data set:

25 of 147 (17 percent) within ±25 feet
50 of 147 (34 percent) within ±50 feet
69 of 147 (47 percent) within ±75 feet
73 of 147 (50 percent) within ±77 feet
75 of 147 (51 percent) within ±78 feet
88 of 147 (60 percent) within ±100 feet
106 of 147 (72 percent) within ±150 feet
114 of 147 (78 percent) within ±200 feet
119 of 147 (81 percent) within ±250 feet
123 of 147 (84 percent) within ±300 feet

Table G4 summarizes the data scatter for the distances from brake release to 50 feet AGL and the quality of the thrust model. All of the standardized distances from brake release to 50 feet AGL that were different from the average values by more than 165 feet were from data sets one, two and three; the data sets with the high/gusty winds. Even with those data sets included, half of the distances were within 77 feet of the average values.

Table G4 TOLAND Predictions for the Distance to 50 Feet AGL

Data Set	Sample Size	Data Scatter for 50 Percent of the Data (ft)	Distance Difference (ft)
1	35	90	89 short
2	12	90	64 short
3	51	145	21 long
4	6	50	83 long
5	15	40	10 long
6	8	55	5 short
7	4	75	61 long
8	11	30	13 short
9	5	105	3 long

Notes: 1. The data sets are defined in table G1.
2. Sample size was the number of takeoffs used for a given data set.
3. The data scatter for 50 percent of the data presents the distance within which one-half of the data points fell.
4. The distance difference is the average difference between the test day (actual) distance for a data set relative to the TOLAND predicted distance. "Short" refers to a predicted distance that is shorter than the test day (actual) distance for the data set. "Long" refers to a predicted distance that is too long.

The following summarizes the 49 standardized distances from brake release to 50 feet AGL relative to the average standardized distance for their appropriate data set for data sets four through nine, those with the lighter/less gusty winds:

14 of 49 (29 percent) within ±25 feet
24 of 49 (49 percent) within ±43 feet
26 of 49 (53 percent) within ±44 feet
28 of 49 (57 percent) within ±50 feet
37 of 49 (76 percent) within ±75 feet
41 of 49 (84 percent) within ±100 feet
46 of 49 (94 percent) within ±125 feet
46 of 49 (94 percent) within ±150 feet
48 of 49 (98 percent) within ±175 feet
48 of 49 (98 percent) within ±200 feet
49 of 49 (100 percent) within ±210 feet

Half the distances for this reduced set were within ±44 feet of the average standardized distance for their appropriate data set. This is approximately the length of the T-38 fuselage, 46 feet.

AIRSPEED AT MAINWHEEL LIFTOFF (TAKEOFF)

Data Set Number One:

Data set number one had data from 35 takeoffs mainly flown in the late morning or in the afternoon. The winds were frequently high and/or gusty.

The average of the 35 standardized airspeeds at mainwheel liftoff was 1.2 KCAS slower than the reference day predicted value. This could indicate an error in the ground effect lift curve. However, it was probably the result of the large data scatter due to the unfavorable winds.

The extremes between the individual standardized airspeeds and the average standardized airspeed were 5.9, 4.8, and 3.8 KCAS faster and 3.1, 2.8, and 2.7 KCAS slower than the average standardized value. The following are standardized mainwheel liftoff airspeeds relative to the average of the standardized airspeeds:

7 of 35 (20 percent) within ±0.5 KCAS
13 of 35 (37 percent) within ±1.0 KCAS
18 of 35 (51 percent) within ±1.5 KCAS
20 of 35 (57 percent) within ±2.0 KCAS
31 of 35 (89 percent) within ±3.0 KCAS
33 of 35 (94 percent) within ±4.0 KCAS
34 of 35 (97 percent) within ±5.0 KCAS
35 of 35 (100 percent) within ±6.0 KCAS

Data Set Number Two:

The average of the 12 standardized airspeeds at mainwheel liftoff was 0.8 KCAS slower than that for the reference day predicted value. The extremes of the standardized airspeeds relative to the average of the standardized airspeeds were 3.5 KCAS faster and 1.9 KCAS slower than the average of the standardized airspeeds. The following are standardized airspeeds at mainwheel liftoff relative to the average standardized airspeed:

2 of 12 (17 percent) within ±0.5 KCAS
4 of 12 (33 percent) within ±1.0 KCAS
7 of 12 (58 percent) within ±1.5 KCAS
11 of 12 (92 percent) within ±2.0 KCAS
11 of 12 (92 percent) within ±3.0 KCAS
12 of 12 (100 percent) within ±3.5 KCAS

Data Set Number Three:

These data, like those of data set number one, were obtained in windy conditions. The average of the 51 standardized airspeeds was 0.8 KCAS slower than the reference day predicted value.

The extremes of the differences between the average of the 51 standardized airspeeds and the standardized value for a given flight were 10.8, 5.0, and 4.4 KCAS faster and 4.8 (twice) and 4.1 KCAS slower than the average standardized value. The following are standardized airspeeds at mainwheel liftoff relative to the average standardized airspeed:

9 of 51 (18 percent) within ±0.5 KCAS
19 of 51 (37 percent) within ±1.0 KCAS
21 of 51 (41 percent) within ±1.5 KCAS

34 of 51 (67 percent) within ±2.0 KCAS
41 of 51 (80 percent) within ±3.0 KCAS
45 of 51 (88 percent) within ±4.0 KCAS
50 of 51 (98 percent) within ±5.0 KCAS

Data Set Number Four:

Data from six of six available takeoffs were used. The average of the six standardized airspeeds at mainwheel liftoff were 1.0 KCAS faster than the reference day predicted airspeed.

The extremes of the differences between the average of the six standardized airspeeds and the standardized value for a given flight were 0.7 KCAS faster and 0.6 KCAS slower than the average standardized value. The following are standardized airspeeds at mainwheel liftoff relative to the average standardized value:

3 of 6 (50 percent) within ±0.5 KCAS
6 of 6 (100 percent) within ±1.0 KCAS

Data Set Number Five:

Data from 15 of 15 available takeoffs were used. The average of the 15 standardized airspeeds at mainwheel liftoff was only 0.1 KCAS faster than the reference day predicted value. The average if only 14 of the 15 takeoffs were used would have been 0.2 KCAS slower than the reference day predicted value.

The extremes of the differences between the average of the 15 standardized airspeeds and the standardized value for a given flight were 3.4 and 1.2 KCAS faster and 1.2 KCAS slower than the average standardized airspeed. All of the other differences were between 0.5 KCAS faster and 0.9 KCAS slower than the average. The following are standardized airspeeds at mainwheel liftoff relative to the average standardized airspeed:

6 of 15 (40 percent) within ±0.5 KCAS
11 of 15 (73 percent) within ±1.0 KCAS
14 of 15 (93 percent) within ±1.5 KCAS
14 of 15 (93 percent) within ±2.0 KCAS
14 of 15 (93 percent) within ±3.0 KCAS
15 of 15 (100 percent) within ±3.4 KCAS

Data Set Number Six:

Data set number six had data from 10 takeoffs. Data were used from eight of the 10. These were the same eight takeoffs as were used previously. The average of the eight standardized airspeeds at mainwheel liftoff was only 0.1 KCAS slower than the reference day predicted value.

The extremes of the differences between the average of the eight standardized airspeeds at mainwheel liftoff and the standardized values for a given flight were 1.9 KCAS faster and 1.4 KCAS slower than the average standardized airspeed. The following are the standardized airspeeds at mainwheel liftoff relative to the average standardized airspeed:

3 of 8 (38 percent) within ±0.5 KCAS
6 of 8 (75 percent) within ±1.0 KCAS
7 of 8 (88 percent) within ±1.5 KCAS
8 of 8 (100 percent) within ±1.9 KCAS

Data Set Number Seven:

Data set number seven was four takeoffs flown with SJ-8 fuel. The average standardized airspeed at mainwheel liftoff was 1.6 KCAS faster than the reference day predicted value. Relative to the average of the four standardized airspeeds, the extremes were 1.3 KCAS slower and 0.4 KCAS faster than the average value. The following are standardized airspeeds at mainwheel liftoff relative to the average standardized airspeed:

3 of 4 (75 percent) within ±0.5 KCAS
3 of 4 (75 percent) within ±1.0 KCAS
4 of 4 (100 percent) within ±1.3 KCAS

Data Set Number Eight:

Data set number eight was 11 takeoffs flown as the baseline for the final PMP engine bay configuration. All 11 takeoffs were used for determining the airspeed at mainwheel liftoff. The average of the 11 standardized airspeeds was 0.3 KCAS slower than the reference day predicted airspeed at mainwheel liftoff. The extreme differences between the 11 standardized airspeeds and their average were 2.2 KCAS faster and 1.8 KCAS slower than the average value. The following are standardized airspeeds at mainwheel liftoff relative to the average standardized airspeed:

7 of 11 (64 percent) within ±0.5 KCAS
7 of 11 (64 percent) within ±1.0 KCAS
8 of 11 (73 percent) within ±1.5 KCAS
10 of 11 (91 percent) within ±2.0 KCAS
11 of 11 (100 percent) within ±2.2 KCAS

Data Set Number Nine:

The final data set was from five takeoffs with the final PMP engine bay configuration. The average of the five standardized airspeeds at mainwheel liftoff was 0.2 KCAS slower than the reference day predicted value. The extreme differences between the average of the five standardized airspeeds at mainwheel liftoff and the individual standardized airspeed for each flight were 1.5 KCAS slower and 0.7 KCAS faster than the average standardized airspeed. If only four of the five standardized speeds had been used, then all four of the remaining speeds would have been within ±0.3 KCAS of the new average. The new average would be 0.2 KCAS faster than the reference day predicted speed. The following are standardized airspeeds at mainwheel liftoff relative to the average standardized airspeed:

4 of 5 (80 percent) within ±0.5 KCAS
4 of 5 (80 percent) within ±1.0 KCAS
5 of 5 (100 percent) within ±1.5 KCAS

Summary for the Airspeed at Mainwheel Liftoff:

The following summarizes the 147 standardized airspeeds at mainwheel liftoff (takeoff) relative to the average standardized value for the appropriate data set:

44 of 147 (30 percent) within ±0.5 KCAS
73 of 147 (50 percent) within ±1.0 KCAS
90 of 147 (61 percent) within ±1.5 KCAS
112 of 147 (76 percent) within ±2.0 KCAS
131 of 147 (89 percent) within ±3.0 KCAS

139 of 147 (95 percent) within ±4.0 KCAS
145 of 147 (99 percent) within ±5.0 KCAS

All of the standardized airspeeds at mainwheel liftoff that differed by more than ±3.5 KCAS from their appropriate average standardized airspeed were from data sets one, two, or three; the data sets with high/gusty winds. Half of the values were within ±1.0 KCAS even when those high/gusty wind flights were included.

The following summarizes the 49 standardized airspeeds at mainwheel liftoff (takeoff) relative to the average standardized airspeed for their appropriate data set for data sets four through nine, those with the lighter/less gusty winds.

26 of 49 (53 percent) within ±0.5 KCAS
37 of 49 (76 percent) within ±1.0 KCAS
44 of 49 (90 percent) within ±1.5 KCAS
47 of 49 (96 percent) within ±2.0 KCAS
48 of 49 (98 percent) within ±3.0 KCAS
49 of 49 (100 percent) within ±4.0 KCAS

Over half of the standardized airspeeds at mainwheel liftoff were within ±0.5 KCAS of the average standardized airspeeds for their appropriate data set using data sets four through nine. Ninety-six percent were within ±2.0 KCAS and 100 percent were within ±4.0 KCAS.

AIRSPEED AT 50 FEET AGL

Data Set Number One:

Data set number one had data from 35 takeoffs mainly flown in the late morning or in the afternoon. The winds were frequently high and/or gusty. The average of the 35 standardized airspeeds at 50 feet AGL was 0.5 KCAS faster than the reference day predicted airspeed.

The extremes between the individual standardized airspeeds and the average standardized airspeed were 16.5, 6.7, and 4.4 KCAS slower and 6.7 and 4.2 KCAS faster than the average standardized value. The following are standardized airspeeds at 50 feet AGL relative to the average of the standardized airspeeds:

7 of 35 (20 percent) within ±0.5 KCAS
13 of 35 (37 percent) within ±1.0 KCAS
22 of 35 (63 percent) within ±1.5 KCAS
25 of 35 (71 percent) within ±2.0 KCAS
30 of 35 (86 percent) within ±3.0 KCAS
30 of 35 (86 percent) within ±4.0 KCAS
32 of 35 (91 percent) within ±5.0 KCAS
32 of 35 (91 percent) within ±6.0 KCAS

Data Set Number Two:

The average of the 12 standardized airspeeds at 50 feet AGL was 0.4 KCAS slower than the reference day predicted value. The extremes of the airspeeds relative to the average of the standardized airspeeds were 3.9 KCAS slower and 2.4 KCAS faster than the average of the standardized airspeeds. The following are standardized airspeeds at 50 feet AGL relative to the average standardized airspeed:

3 of 12 (25 percent) within ±0.5 KCAS
6 of 12 (50 percent) within ±1.0 KCAS
8 of 12 (67 percent) within ±1.5 KCAS
10 of 12 (83 percent) within ±2.0 KCAS
11 of 12 (92 percent) within ±3.0 KCAS
12 of 12 (100 percent) within ±3.9 KCAS

Data Set Number Three:

These data, like those of data set number one, were obtained in windy conditions. The average of the 51 standardized airspeeds was 0.5 KCAS faster than the reference day predicted value.

The extremes of the differences between the average of the 51 standardized airspeeds and the standardized value for a given flight were 17.5, 14.7, and 4.6 KCAS slower and 6.6, 4.8, and 4.5 (twice) faster than the average value. The following are standardized airspeeds at 50 feet AGL relative to the average standardized airspeed:

10 of 51 (20 percent) within ±0.5 KCAS
21 of 51 (41 percent) within ±1.0 KCAS
29 of 51 (57 percent) within ±1.5 KCAS
33 of 51 (65 percent) within ±2.0 KCAS
41 of 51 (80 percent) within ±3.0 KCAS
44 of 51 (86 percent) within ±4.0 KCAS
48 of 51 (94 percent) within ±5.0 KCAS

Data Set Number Four:

Data from six of the six available takeoffs were used. The average of the six standardized airspeeds at 50 feet AGL were 4.3 KCAS faster than the reference day predicted airspeed.

The extremes of the differences between the average of the six standardized airspeeds and the standardized value for a given flight were 3.7 KCAS faster and 3.5 KCAS slower than the average standardized value. The following are standardized airspeeds at 50 feet AGL relative to the average standardized value:

0 of 6 (0 percent) within ±0.5 KCAS
2 of 6 (33 percent) within ±1.0 KCAS
3 of 6 (50 percent) within ±1.5 KCAS
4 of 6 (67 percent) within ±2.0 KCAS
4 of 6 (67 percent) within ±3.0 KCAS
6 of 6 (100 percent) within ±3.7 KCAS

Data Set Number Five:

Data from 15 of the 15 available takeoffs were used. The average of the 15 standardized airspeeds at 50 feet AGL was 2.8 KCAS faster than the reference day predicted value.

The extremes of the differences between the average of the 15 standardized airspeeds and the standardized value for a given flight were 3.9 and 2.8 KCAS faster and 3.3 and 2.3 KCAS slower than the average standardized airspeed. The following are standardized airspeeds at 50 feet AGL relative to the average standardized value:

2 of 15 (13 percent) within ±0.5 KCAS
3 of 15 (20 percent) within ±1.0 KCAS
6 of 15 (40 percent) within ±1.5 KCAS
10 of 15 (67 percent) within ±2.0 KCAS
13 of 15 (87 percent) within ±3.0 KCAS
15 of 15 (100 percent) within ±3.9 KCAS

Data Set Number Six:

Data set number six had 10 takeoffs and eight of the 10 were used for the airspeed at 50 feet AGL. The average of the eight standardized airspeeds at 50 feet AGL was 1.3 KCAS faster than the reference day predicted value.

The extremes of the differences between the average of the eight standardized airspeeds at 50 feet AGL and the standardized value for a given flight were 5.2 and 3.3 KCAS faster and 3.0 KCAS slower than the average standardized airspeed. The following are standardized airspeeds at 50 feet AGL relative to the average standardized airspeed:

0 of 8 (0 percent) within ±0.5 KCAS
2 of 8 (25 percent) within ±1.0 KCAS
2 of 8 (25 percent) within ±1.5 KCAS
4 of 8 (50 percent) within ±2.0 KCAS
6 of 8 (75 percent) within ±3.0 KCAS
7 of 8 (88 percent) within ±4.0 KCAS
7 of 8 (88 percent) within ±5.0 KCAS
8 of 8 (100 percent) within ±5.2 KCAS

Data Set Number Seven:

Data set number seven was four takeoffs flown with SJ-8 fuel. The average standardized airspeed at 50 feet AGL was 3.4 KCAS faster than the reference day predicted value. Relative to the average of the four standardized airspeeds, the extremes were 3.2 KCAS slower and 2.7 KCAS faster than the average value. The following are standardized airspeeds at 50 feet AGL relative to the average standardized airspeed:

0 of 4 (0 percent) within ±1.5 KCAS
1 of 4 (25 percent) within ±2.0 KCAS
3 of 4 (75 percent) within ±3.0 KCAS
4 of 4 (100 percent) within ±3.2 KCAS

Data Set Number Eight:

Data set number eight was 11 takeoffs flown as the baseline for the final PMP engine bay configuration. All 11 takeoffs were used for determining the standardized airspeed at 50 feet AGL. The average of the 11 standardized airspeeds was 0.4 KCAS faster than the reference day predicted airspeed for 50 feet AGL. The extreme differences between the 11 standardized airspeeds and their average were 1.3 KCAS faster and 1.2 KCAS slower than the average value. The following are standardized airspeeds at 50 feet AGL relative to the average standardized airspeed:

6 of 11 (55 percent) within ±0.5 KCAS
9 of 11 (82 percent) within ±1.0 KCAS
11 of 11 (100 percent) within ±1.3 KCAS

Data Set Number Nine:

The final data set was from five takeoffs with the final PMP engine bay configuration. The average of the five standardized airspeeds at 50 feet AGL was 0.5 KCAS faster than the reference day predicted value. The extreme differences between the average of the five standardized airspeeds at 50 feet AGL and the individual standardized airspeed for each flight were 2.2 KCAS slower and 1.7 KCAS faster than the average standardized airspeed. The following are standardized airspeeds at 50 feet AGL relative to the average standardized airspeed:

1 of 5 (20 percent) within ±0.5 KCAS
3 of 5 (60 percent) within ±1.0 KCAS
3 of 5 (60 percent) within ±1.5 KCAS
4 of 5 (80 percent) within ±2.0 KCAS
5 of 5 (100 percent) within ±2.2 KCAS

Summary for the Airspeed at 50 feet AGL:

The following summarizes the 147 standardized airspeeds at 50 feet AGL relative to the average standardized value for the appropriate data set:

30 of 147 (20 percent) within ±0.5 KCAS
58 of 147 (39 percent) within ±1.0 KCAS
72 of 147 (49 percent) within ±1.2 KCAS
78 of 147 (53 percent) within ±1.3 KCAS
84 of 147 (57 percent) within ±1.5 KCAS
100 of 147 (68 percent) within ±2.0 KCAS
117 of 147 (80 percent) within ±2.5 KCAS
124 of 147 (84 percent) within ±3.0 KCAS
134 of 147 (91 percent) within ±4.0 KCAS
141 of 147 (96 percent) within ±5.0 KCAS
142 of 147 (97 percent) within ±6.0 KCAS

All but one of the standardized airspeeds at 50 feet AGL that differed by more than ±5.0 KCAS from their appropriate average standardized airspeed were from data sets one, two, or three; the data sets with high/gusty winds. For one flight in data set number six the difference was 5.2 KCAS faster than the average for data set number six. Half of the values were within ±1.3 KCAS even when those high/gusty wind flights were included.

The following summarizes the 49 standardized airspeeds at 50 feet AGL relative to the average standardized airspeed for their appropriate data set for data sets four through nine, those with the lighter/less gusty winds:

9 of 49 (18 percent) within ±0.5 KCAS
19 of 49 (39 percent) within ±1.0 KCAS
25 of 49 (51 percent) within ±1.5 KCAS
32 of 49 (65 percent) within ±2.0 KCAS
38 of 49 (78 percent) within ±2.5 KCAS
42 of 49 (86 percent) within ±3.0 KCAS
47 of 49 (96 percent) within ±4.0 KCAS
48 of 49 (98 percent) within ±5.0 KCAS
49 of 49 (100 percent) within ±5.2 KCAS

Over half of the standardized airspeeds at 50 feet AGL were within ±1.5 KCAS of the standardized average for their appropriate data set using this reduced data set. Sixty-five percent were within ±2.0 KCAS and 100 percent were within ±5.2 KCAS.

Summary of the Performance to 50 Feet AGL:

The TOLAND predicted performance, the horizontal distance from brake release to 50 feet AGL and the airspeed at 50 feet AGL, is summarized in table G5. The TOLAND predicted distances were 13 feet shorter to 83 feet longer than the averages of the standardized distances. The TOLAND predicted airspeeds were 0.4 to 4.3 KCAS slower than the averages of the standardized airspeeds.

The results in table G5 show that the TOLAND predicted distances was within two fuselage lengths of the T-38C aircraft relative to the standardized test data and within 5 KCAS for the airspeed at 50 feet AGL. In an effort to consider making “good enough” better, changes to the TOLAND models were considered:

1. Change the out of ground effect lift curve.
2. Change the thrust model between 160 and 210 KCAS.
3. Change the out of ground effect drag polar.
4. Look at the effect of wind shear during the climbout.
5. Do nothing, the models are good enough.

Table G5 TOLAND Predictions for the Speed at 50 Feet AGL

Data Set	Sample Size	Distance Difference (ft)	Airspeed Difference (KCAS)
4	6	83 long	4.3 slow
5	15	10 long	2.8 slow
6	8	5 short	1.3 slow
7	4	61 long	3.4 slow
8	11	13 short	0.4 slow
9	5	3 long	0.5 slow

Notes:
1. The data sets are defined in table G1.
2. Sample size was the number of takeoffs used for a given data set.
3. The distance difference is the average difference between the test day (actual) distance for a data set relative to the TOLAND predicted distance. "Short" refers to a predicted distance that is shorter than the test day (actual) distance for the data set. "Long" refers to a predicted distance that is too long.
4. The airspeed difference is the average difference between the test day (actual) speeds for a data set relative to the TOLAND predicted airspeeds. "Slow" refers to a predicted airspeed slower than the test day (actual) airspeed.
5. The T-38C trailing edge flap deflection was 60 percent for data set number four and 45 percent for data sets five through nine.

Ideally, the changes to the models would reduce the predicted distance from brake release to 50 feet AGL by 15 feet while increasing the airspeed by 2.0 KCAS. These "improvements" should not be allowed to affect the predicted performance from brake release through mainwheel liftoff, takeoff.

Changing the out of ground effect lift curve would change the flightpath angle if the pitch angle is not changed. Increasing the angle of attack for a given lift coefficient and pitch angle would decrease the flightpath angle. Decreasing the flightpath angle would increase the predicted airspeed at 50 feet AGL and increase the predicted air phase distance. That change would improve the predicted airspeed at the expense of the predicted distance. This does not appear to be a good option from a technical perspective. Two other considerations would also need to be considered. First, how good is the existing fit of the data for the lift curve? Could it be changed slightly? Second, is there any evidence that the flaps may be "blowing back" at higher dynamic pressures, higher airspeeds? Maybe the lift curve needs to be function of both angle of attack and dynamic pressure.

Changing the thrust model would need to be done without significantly changing the model for speeds below 160 KCAS. Increasing the thrust in the higher speed range would reduce the predicted horizontal distance to 50 feet AGL and would also increase the predicted airspeed at 50 feet AGL. The physics that would permit this thrust model change would seem to be limited to one of two elements of the engine's operation. First, an engine could have variable geometry or schedules in the fuel controller that could create these thrust changes with increasing total air pressure or total air temperature. The J85 engine did not have these capabilities. Second, the engine model for the T-38C PMP was created from maximum power level accelerations, low altitude sawtooth climbs and descents, and installed ground level static thrust stand runs. These data should have been collected with the engines nearly thermally stabilized. The engines during the takeoffs were not thermally stabilized at brake release but became more so during the acceleration, rotation, and climbout. The modeled thrust in TOLAND was the flight test model with a multiplicative factor intended to account for changes in engine trim. Another multiplicative factor like the engine spoolup curve could be added to the thrust model to account for the time while the engine was being thermally stabilized. The additional multiplicative factor was not developed for the T-38C PMP test program.

The out of ground effect drag polar was developed from flight test data using the flight test developed thrust model. If the curve fit of the drag polar would permit a decrease in the drag at the lower lift coefficients (high airspeeds), then some small decrease in the air phase distance and some small increase in the predicted airspeed at 50 feet AGL might be achievable. This potential change to the out of ground effect drag polar was not made during the T-38C PMP test program.

The wind speeds used for the test day predicted TOLAND runs were either measured by the Base Weather system or determined using onboard aircraft data at about 4 to 6 feet AGL (prior to rotation). The actual winds probably increased with increasing aircraft height during the climbout through 50 feet AGL. The effect of this wind shear was not determined.

The effects of a wind shear during the takeoff climbout are attentuated by minimizing the magnitude of the wind. This leads to the goal of conducting the performance takeoffs at sunrise. The effects of wind shears are also the reason that sawtooth climbs and descents are repeated on reciprocal headings.

The engineers working on the T-38C PMP flight test program considered the four “improvements” identified earlier. They determined that with the time available to publish their results, that their models were “good enough”.

APPENDIX H - PUBLISHED OPINIONS ABOUT DETERMINING TAKEOFF PERFORMANCE

The following paragraphs are from page 78 of *Flight Testing Conventional and Jet-Propelled Airplanes* published in 1946 (reference 32). Mister Hamlin had worked for United Aircraft Corporation, Vega Aircraft Corporation, Boeing Aircraft Company's Flight Test organization, and in 1946 was the Senior Flight Research Engineer at the Bell Aircraft Corporation.

> *"Like rate of climb, take-off is another dynamic flight condition and consequently, the complicated accurate analysis is impractical. This complication is further aggravated by the fact that the take-off performance is largely dependent upon pilot technique. Different pilots will obtain widely different take-off performances with the same airplane, whereas the same pilot will find it extremely difficult to obtain the same results on successive tests.*
>
> *…Another factor involves the fact that the optimum take-off performance conditions of which the airplane is capable are dangerous, since flight at very low velocities, lower than possible without power, near the ground are required. Hence, take-off flight test results are more or less relative and optimum take-off performance is generally impractical."*

Three years later, in 1949, Courtland Perkins and Robert Hage from Princeton University and the Boeing Airplane Company, respectively, published the following on pages 194, 196 and 197 in *Airplane Performance Stability and Control* (reference 33):

> *"Airplane take-off distance is perhaps the most difficult performance item to predict accurately. Most analyses of this problem, although mathematically rigorous, are based on assumptions that are accurate only for special conditions of pilot technique, ground conditions, airplane attitude and drag, and average variations in effective thrust. Experimental data on a given airplane are often widely dispersed as a result of these variables, and an average of several runs is usually used as a basis for correlation with theoretical analyses."*
>
> *"…even a detailed analysis of the take-off problem is at best only as accurate as the accuracy of the assumptions made."*

In 1951, the United States Air Force Technical Report Number 6273, *Flight Test Engineering Handbook,* (reference 34) also known as "Herrington" for one of the authors had the following paragraph from pages 6-7:

> *"The take-off performance of any aircraft is highly dependent on pilot technique. Even with experienced well-qualified pilots it is difficult to make the aircraft take off at the same value of lift coefficient each time. As this is the rule rather than the exception, a rigorous mathematical treatment of reducing observed take-off data to standard conditions is not warranted; therefore, no mathematically exact solutions will be given for reducing data."*

In 1956, the NATO AGARD published its *Flight Test Manual Volume I Performance* (reference 35). It had the following observations on pages 6:41 and 6:42:

> *"The problem of determining the ground distance required to clear a fifty-foot obstacle (or an obstacle of other height) under standard conditions is more complex than determination of standard ground run itself. There are a number of reasons for this with the principal one being the large possible variation in pilot technique. However, provided one is satisfied with reasonable approximations it is possible to correct to standard distance required to clear an obstacle of a given height."*

In 1964, the USAF Test Pilot School, then known as the USAF Aerospace Research Pilot School, published the following observation in their handbook FTC-TIH 64-2006, *Performance Flight Test Techniques* (reference 36), on page 5.1:

> *"More than any other test, takeoffs and landings are affected by factors which cannot be accurately measured and properly compensated. It is only possible to estimate the capabilities of the airplane within rather broad limits, relying on a statistical average of as many takeoff and landing maneuvers as possible to cancel residual errors."*

The following comments were in the 1966 performance short course notes from Professor Ralph D. Kimberlin of the University of Tennessee Space Institute, *Performance Flight Testing Lecture Notes* (reference 37):

> *"Take-off and landing distances are some of the most difficult and costly flight test data to obtain. They are difficult to obtain due to the large number of variables involved with some variables, such as pilot technique, being essentially uncontrollable. They are costly due to the size of the test team required, the amount of specialized test equipment required, and the amount of data reduction involved.*
>
> *Also, take-off and landing data may only be considered to be "ball park" answers due to the large factor which pilot technique plays. This is especially true where less skilled pilots are involved and may be the reason why the FAA does not have a regulatory requirement to collect take-off and landing data for airplanes of less than 6,000 pound gross weight."*

In 1973, the USAF Test Pilot School revised their 1970 handbook on aircraft performance, FTC-TIH-70-1001, *Performance Volume II of III Performance Flight Testing Theory* (reference 38). The first paragraph in Chapter V, Takeoff and Landing, on page 5.1 was:

> *"A very important part of the testing of any aircraft is the takeoff, landing, and operation in close proximity to the ground. Takeoff and landing are greatly dependent on pilot judgment and technique and, therefore, are subject to considerable variation for any given aircraft and set of conditions. Because of this largely unpredictable variable, the pilot, it is neither possible nor practical to make exact prediction or correction of takeoff and landing performance. It is only possible to estimate the approximate capabilities of an aircraft within rather broad limits. For this reason, takeoff and landing performance will be considered from a rather general point of view taking into account only the major variables and making some assumptions concerning the lesser variables."*

Also in January 1973, Volume III of III was revised and republished. The second paragraph on page 5.1 of FTC-TIH-70-1001, *Performance Volume III of III Performance Flight Test Techniques* (reference 39), was:

> *"More than any other tests, takeoffs and landings are affected by factors which cannot be accurately measured and properly compensated for. It is only possible to estimate the capabilities of the airplane within rather broad limits, relying on a statistical average of as many takeoff and landing maneuvers as possible to cancel residual errors."*

The previous excerpt was also published as the opening paragraph of chapter 6 on page 6.1 of the 1982 Flight Test Center, *Flight Dynamics Division Volume I Performance* handbook (reference 40). A list of how a pilot could affect test day takeoff performance was presented on page 6.12:

> *"Individual pilot technique is probably the factor causing the greatest variation in takeoff data. Unfortunately, it cannot be quantified and mathematical corrections are impossible. Some of the factors which can significantly affect takeoff performance are:*
>
> 1. *Speed and sequence of brake release and power application.*
> 2. *The use of nose wheel steering, differential braking or rudder deflection for directional control.*
> 3. *The number and amplitude of directional control inputs used.*
> 4. *Aileron and elevator position during acceleration.*
> 5. *Airspeed at rotation.*
> 6. *Pitch rate during rotation*
> 7. *Angle of attack at liftoff."*

The summary paragraph from page 6.13 of the same document was:

> *"Takeoff and landing tests are an important part of the performance testing of any aircraft. The large number of variables involved, especially the strong influence of individual pilot technique, results in a vast amount of data scatter and a very low degree of repeatability. A large number of data points are required to accurately predict the actual capabilities of the aircraft."*

The July 1987 edition of the USAF Test Pilot School handbook, *Volume I Aircraft Performance* (reference 41), has the first paragraph on page 8.1 copied from the first paragraph from Chapter V of reference 38 and the summary paragraph on page 8.20 copied from the summary paragraph on page 6.13 of reference 40. The two following excerpts are from reference 41 on pages 8.13 and 8.15:

> *"Individual pilot technique is probably the factor causing the greatest variation in takeoff data. Unfortunately, it cannot be quantified and mathematical corrections are impossible."*
>
> *"More than any other tests, takeoffs and landings are affected by factors which cannot be accurately measured and properly compensated for. It is only possible to estimate the capabilities of the airplane within rather broad limits, relying on a statistical average of as many takeoff and landing maneuvers as possible to cancel residual errors."*

Chapter 8, Takeoff & Landing Performance, of the 1993 edition of the USAF Test Pilot School handbook, *Volume I Performance Phase* (reference 42), retains the excerpt from the opening paragraph on page 2 and the summary paragraph on page 19 with one minor exception in the opening paragraph. The 1973 and the 1987 editions use "and operation in close proximity to the ground" in the first sentence. That is replaced by "an operation near the ground" in the 1993 edition (reference 42).

The two sentences from page 8.13 of reference 41 is included unchanged at the top of page 14 of reference 42. The paragraph on page 8.15 of reference 41 is included unchanged in section 8.5, Flight Test, on page 15 of reference 42.

With one minor exception, the four excerpts from the 1987 and the 1993 USAF Test Pilot School handbooks are identical.

The December 2002 edition of the USAF Test Pilot School handbook, *Aircraft Performance* (reference 43), retains the excerpt from the opening paragraph from reference 41 on page 3-1, the two-sentence excerpts from page 8.13 of reference 41 on page 3-13, the paragraph from page 8.15 of reference 41 on page 3-15, and the summary paragraph from page 6.13 of reference 40 on page 3-19. The excerpts from references 40 through 43 were essentially identical.

The Takeoff & Landing Performance, Chapter 3 used by the 2010 classes at the USAF Test Pilot School was the same as in the December 2002 handbook (reference 43).

The two opening paragraphs for section 18.1, Introduction of Chapter 18, Takeoff and Landing Theory and Methods, of Ralph Kimberlin's *Flight Testing of Fixed-wing Aircraft* (reference 44) on page 177 are as presented below:

> *"Takeoff and landing distances are some of the most difficult and costly flight test data to obtain. They are difficult to obtain due to the large number of variables involved with some variables, such as pilot technique, being essentially uncontrollable. They are costly due to the size of the test team required, the amount of specialized test equipment required, and the amount of data reduction involved.*
>
> *Also, takeoff and landing data may only be considered to be ballpark answers due to the large factor that pilot technique plays. This is especially true where less skilled pilots are involved and may be the reason why the FAA in CAR 3 and early FAR Part 23 did not have a regulatory requirement to collect takeoff and landing data for airplanes of less than 6000 lb gross weight."*

These two paragraphs are consistent with the USAF Test Pilot School handbooks.

Don Ward in the 2006 third edition of *Introduction to Flight Test Engineering* (reference 45) published the following in the introduction to Chapter 5 on page 101 and in section 5.2 on page 116:

> *"Every successful flight begins with a takeoff and ends with a landing. An airplane's suitability for many missions may be determined by its performance in this dynamic environment. Since takeoff and landing (TO&L) performance involves accelerations and decelerations, we must concern ourselves with measurement of dynamic conditions, both in flight and on the ground. So, we usually break up takeoff and landing measurements into a ground phase and an air phase. Furthermore, few maneuvers are more difficult to perform consistently. Pilot technique can easily mask important trends in the data. This human variability makes it virtually impossible to exactly compare different data sets and puts the onus on flight test personnel to standardize procedures and techniques as much as possible. Even so, statistical tools are needed to correlate individual measurements and to compare the data to requirements. Average values of distances for number of takeoffs and/or landings are typically used to decide whether or not goals have been met. The large number of variables that affect TO&L performance further complicates these tests. Moreover, many of them are completely uncontrollable."*
>
> *…"The nature of takeoff and landing measurements leaves much to the judgement of the individual flight test team; there is no well-defined "standard" for making these measurements as there is for pitot-static calibrations, climb performance, or cruise performance."*

These excerpts are also consistent with the USAF Test Pilot School handbooks.

Summary:

The cited references were published during the 60 year period between 1946 and 2006. They are all consistent and reflect the opinions of many flight test pilots and flight test engineers. A primary purpose of this handbook is to show that those opinions, while they were valid until approximately 1970-1980, are not valid today. Airframe manufacturers and the government flight test engineers at the Air Force Test Center (AFTC) and the 412th Test Wing have successfully accounted for variations due to pilot technique for the last four decades.

This page was intentionally left blank.

APPENDIX I - TAKEOFF PERFORMANCE HISTORY

This appendix is divided into seven blocks of time based on changes in aircraft performance, flight test instrumentation capabilities, and postflight data analyses capabilities. The divisions are somewhat arbitrary and subjective. Moving a division one way or another by a few years would not significantly change this background.

1900 TO 1927

The time period from 1900 to 1927 featured three significant events:

1. The Wright brother's first flight, 17 December 1903, and the first flights of Alberto Santos-Dumont in September through November 1906
2. World War I (1914-1918)
3. The New York to Paris flight of Charles Lindbergh on 20-21 May 1927

There is some controversy (even a century later) concerning the Wright brothers and Alberto Santos-Dumont. In the United States, the Wright brothers are recognized for the first controllable, sustained flight. In Europe and in Brazil, Santos-Dumont's home country, he is recognized for the first unassisted takeoff and flight on 12 November 1906 in his aircraft, the 14-bis. The Wright brother's aircraft from 1900 through 1908 had no wheels and were catapulted into the air using a rail and the potential energy from a weight raised in a tower behind the rail.

Most airfields were grass fields without runways prior to Lindbergh's flight. The runways that did exist were mostly raised dirt or gravel to minimize standing water and mud during winter operations. Takeoff performance was primarily pass/fail: Could the aircraft takeoff or not? Quantified distances were not as important when the ground roll distance required was a few hundred feet and the available distance was approximately 5,000 feet. Most airfields were located on a level, grass field approximately 1 statute mile by 1 statute mile. In general, there were no runways. The pilot took off and landed into the wind.

Two early aircraft performance documents; *Full Flight Performance Testing* from 1918 (reference 46) and NACA-TR-70, *Preliminary Report on Free Flight Tests* in 1920 (reference 47) did not address takeoffs at all.

The 1923 NACA-TR-154 report, *A Study of Taking Off and Landing an Airplane* (reference 48), is a very early published report on takeoff performance. It looked at two different takeoff techniques: Keeping the tail down in a 3-point attitude or raising the tail to accelerate in a 2-point attitude. The aircraft tested had conventional landing gear: Two main gear ahead of the longitudinal center of gravity and a tailwheel at the back of the aircraft.

The 1925 NACA-TR-216 report, *The Reduction of Airplane Flight Test Data to Standard Atmosphere Conditions* (reference 49) did not address takeoff performance.

Five NACA Technical Memorandums, NACA-TN-381, *Take-off Distance for Airplanes*; NACA-TN-258, *A Warning Concerning the Take-off with Heavy Load*; NACA-TM-77, *Wing Resistance Near the Ground*; NACA-TR-265, *A Full-scale Investigation of Ground Effect*; and NACA-TN-345 *Photographic Time Studies of Airplane Paths* (references 50 through 54) represent the use of the scientific method. They were primarily documenting observed takeoff performance and developing mathematical equations and models describing the physics of the problem. The NACA-TR-249, *A Comparison of the Take-off and Landing Characteristics of a Number of Service Airplanes* (reference 1) presents a graphical solution to correct for headwind variations, page 459 and figure 10 on page 463. A hand fairing was drawn on a plot of wind speed on the y-axis versus ground roll distance on the x-axis. The real data points were for headwinds of zero to 20 statute miles per hour. Another point was added for zero distance and the takeoff airspeed. This was a very early attempt at adjusting test day data to a reference set of conditions. No attempt was documented in reference 1 for approaches to correct for other variables like runway slope, aircraft gross weight, ambient air temperature, or pressure altitude.

Figure 10 in reference 1 had flight test data for nine different aircraft. Data were extracted from figure 10 for the Royal Aircraft Factory S.E.-5A, a British fighter from World War I. The extracted data are presented in tables I1 and I2 and figure I1.

Table I1 Royal Aircraft Factory S.E.-5A Takeoff Ground Roll Distances from NACA-TR-249

Ground Roll Distance (ft)	Headwind (statute miles per hour)
0	53
220	9
230	15
250	11
275	5
325	3

Notes: 1. Data points were extracted from figure 10 of NACA-TR-249 (reference 1).
2. The first "data point" represents the takeoff speed (versus the headwind) and zero ground roll.

The data in table I2 represent the NACA data fairing from figure 10 in reference 1. The fairing shows a ground roll distance of 370 feet for a takeoff with no wind based on the flight test data.

Table I2 Royal Aircraft Factory S.E.-5A Takeoff Ground Roll Distance Data Fairing from NACA-TR-249

Ground Roll Distance (ft)	Headwind (statute miles per hour)
370	0.0
300	4.8
270	10.0
200	13.3
135	20.0
100	24.0
65	30.0
20	40.0
0	53.0

Note: Points were extracted from the data fairing on figure 10 of NACA-TR-249 (reference 1) with the figure enlarged to 400 percent of its original size.

The data points from table I1 and the data fairing from table I2 are presented in figure I1.

The NACA technical note, *A Warning Concerning the Take-off with Heavy Load*, NACA-TN-258 (reference 51) published in July 1927 was an early recognition of what is now known as ground effect.

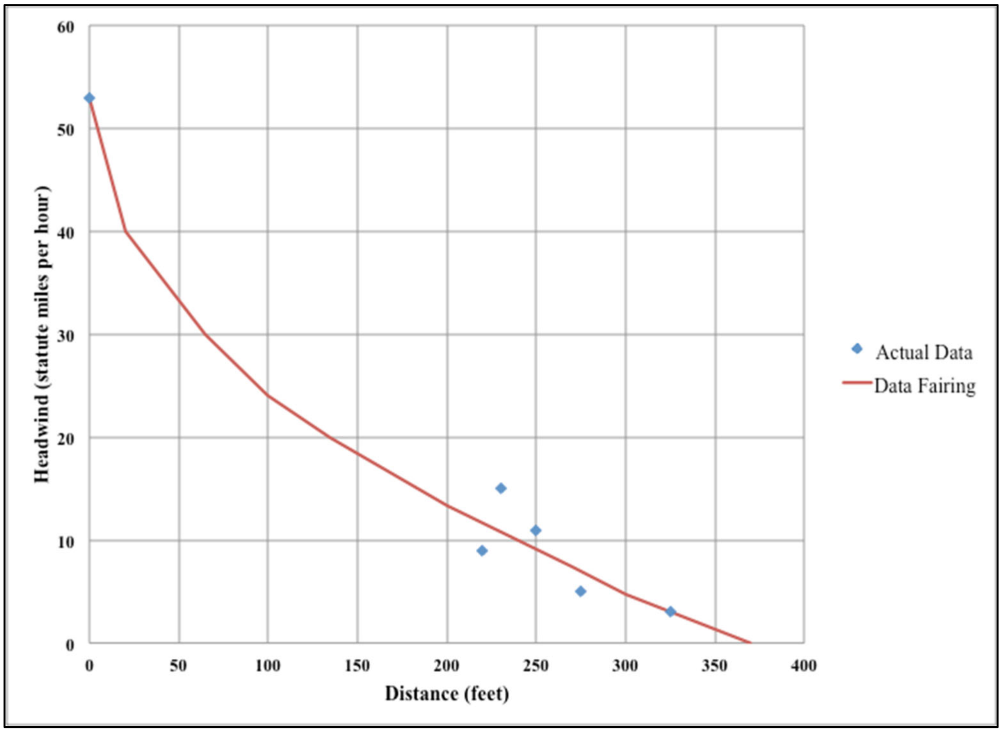

Figure I1 Royal Aircraft Factory S.E. 5A Takeoff Performance

Two earlier NACA documents concerning ground effect are the 1922 technical memorandum, *Wing Resistance Near the Ground*, NACA technical memorandum NACA-TM-77 (reference 52) and the 1927 NACA-TR-265, *A Full-scale Investigation of Ground Effect* (reference 53).

Charles Lindbergh's flight from New York to Paris in May 1927 became a catalyst in the United States that resulted in widespread improvements in airfield facilities, commercial air travel, and in aircraft design. Some of these improvements will be reviewed in the next time period, 1927 through 1935. The review of this time period, 1900 through 1927, concludes with the test results from the takeoff tests performed on the Spirit of St. Louis before the trans-Atlantic flight.

Takeoff performance tests were performed on The Spirit of St. Louis near San Diego prior to the cross-country flight to New York. The results of that testing were published in NACA-TN-257, *Technical Preparation of the Airplane "Spirit of St. Louis"* (reference 55) and in *The Spirit of St. Louis* by Charles Lindbergh (reference 56).

On 4 May 1927, Charles Lindbergh performed seven takeoffs at Camp Kearney, just north of San Diego and south of the current MCAS Miramar, table I3. All of the takeoffs were performed to the west with a downward runway slope of 6 feet vertically for every 1,000 feet horizontally. The runway surface was hard-packed clay and rock with an elevation of 485 feet at the eastern end. The test day ambient air temperatures were not published.

Table I3 Takeoff Performance for the Ryan Spirit of St. Louis

Aircraft Gross Weight (lb)	Headwind (mph)	Ground Roll Distance (ft)
2,600	7	229
2,800	9	287
3,050	9	389
3,300	6	483
3,600	4	615
3,900	2	800
4,200	0	1,023

Notes:
1. These data were extracted from a table on page 10 of NACA-TN-257 (reference 55).
2. The runway slope was downhill at 6 feet vertically for every 1,000 feet horizontally, approximately 0.34 degrees.
3. The field elevation was 485 feet.
4. The ambient air temperatures are not available.
5. mph is statute miles per hour.

The Ryan data fairings for their plot of the takeoff test results are summarized in table I4 and in figure I2. The results were not corrected to a reference set of conditions but the summary plot has two data fairings. One line for no wind and the other for a headwind of 7 statute miles per hour. The data acquired at a field elevation of 485 feet was assumed to be conservative for a takeoff from New York near sea level. With the possible exception of the test day ambient air temperature, all of the key variables for the takeoff performance were addressed. (The takeoffs at Camp Kearney were flown in the afternoon and the New York takeoff was in the early morning, before 0800 local, so the Camp Kearney data were probably conservative for temperature as well.)

Table I4 Ryan Data Fairings for the Ryan "Spirit of St. Louis" Takeoff Test Results

Aircraft Gross Weight (lb)	Ground Roll Distance, (ft)	
	No Wind	7 mph Headwind
0	0	0
1,000	20	20
1,500	50	50
2,000	110	110
2,500	210	210
3,000	370	370
3,500	575	555
4,000	870	790
4,500	1,330	1,060
5,000	2,020	1,390
5,500	3,000	1,800

Notes:
1. These data were extracted from figure 8 on page 20 of NACA-TN-257 (reference 55).
2. The design takeoff gross weight for the New York to Paris flight was 5,135 pounds.
3. mph is statute miles per hour.

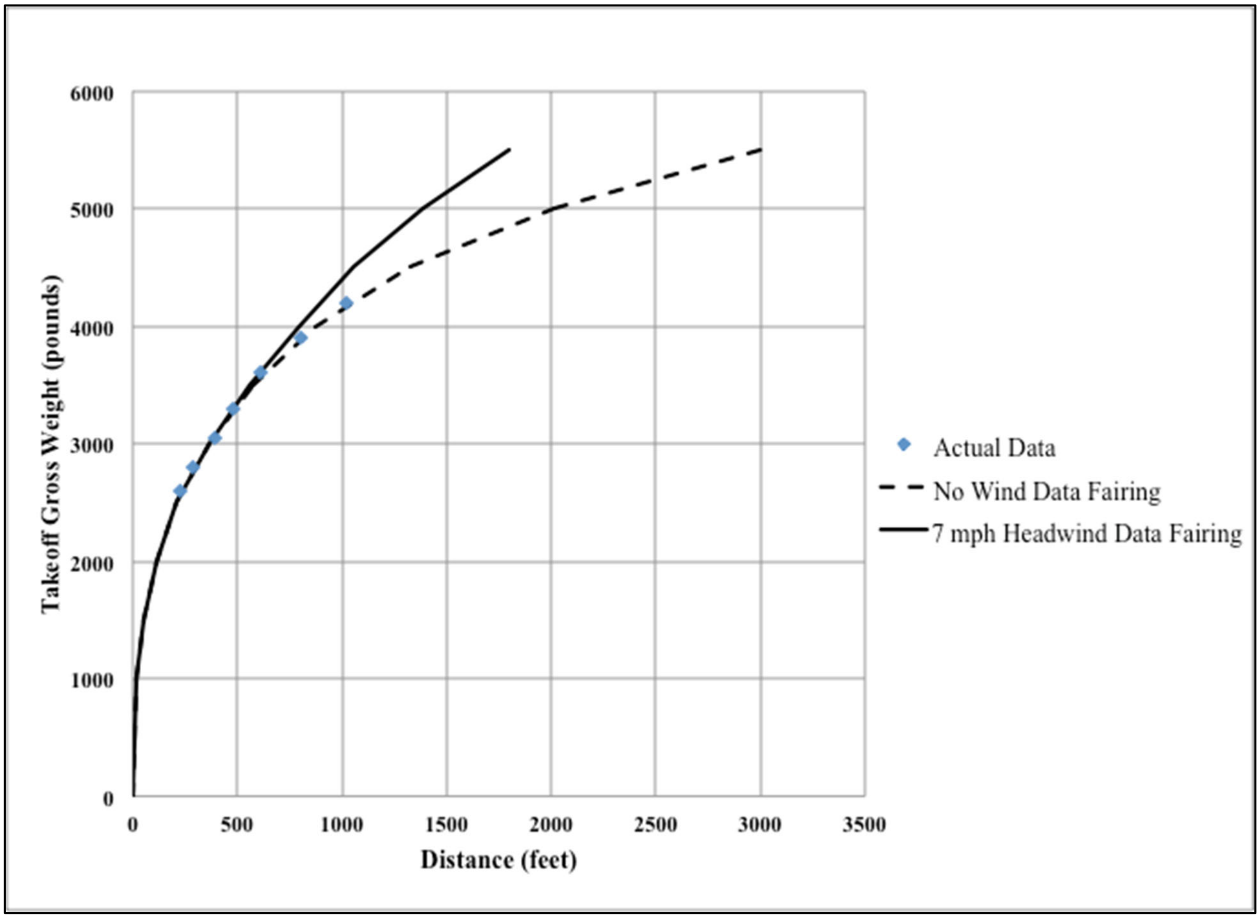

Figure I2 Spirit of St. Louis Takeoff Performance

1927 TO 1935

The time period from Lindbergh's flight from New York to Paris in 1927 until the end of the mid 1930s saw a large number of advances in aircraft design that affected takeoff performance as well as the widespread introduction of paved, either concrete or asphalt, runways. Some of the aircraft improvements included:

1. Leading edge and, more significantly, trailing edge flaps
2. Variable pitch, including constant speed, propellers
3. Retractable landing gear

Paved Runways:

The early airfields were grass fields that were typically 1 statute mile by 1 statute mile. There were no runways. The pilot took off or landed into the wind. Takeoffs and landings were typically not a problem during the dry months. The aircraft had low wing loadings and therefore low takeoff and landing speeds. Ground roll distances of several hundred feet were typical.

Takeoff performance could be significantly degraded during the wet months due to mud or standing water. The solution was to create raised runways. The early raised runways were created using packed dirt, sand, and gravel. The sand and gravel minimized the mud on the runway. Raising the runway surface above the surrounding grass field solved the standing water problem. Paved runways became the logical extension of the airfield evolution when the aircraft tire pressures increased in the 1930s. Table I5 presents some of the early (pre-World War II) airports with raised or paved runways. Hundreds of existing airfields were paved during World War II in addition to the creation of new airports with paved runways.

Table I5 Examples of Early Paved Runways

Date	Airport
1916	Aulnut, France (concrete)
1919	Maynard Field, Winston-Salem, North Carolina (raised runway with packed sand and soil)
1920s	Le Bourget Paris, France
1924	Langley AFB, Virginia
1925	Kelly AFB, San Antonio, Texas
1926	Halle-Leipzig Airport, Germany
1928	Newark Liberty Airport, Newark, New Jersey
1928-1929	Grand Central Airport, Glendale, California
	Ford Airport, Dearborn, Michigan
1929	Floyd Bennett Field, New York, New York
1930	Santa Barbara, California
1928-1933	Cheyenne, Wyoming
	Cincinnati, Ohio
	Louisville, Kentucky

Notes: 1. The information in this table was not acquired from government sources and other conflicting dates have been published.
2. Some of the confusion is due to the date an airport or airfield opened versus when it was upgraded with a paved runway.

Leading and Trailing Edge Flaps:

Aircraft prior to the 1920s typically had relatively low wing loadings and fairly narrow speed ranges, stall speed to maximum speed. The low wing loadings resulted in low stall speeds and therefore low takeoff and landing speeds. The wing loadings increased as the design cruise speeds increased. The higher stall speeds, wider range of airspeeds, and the increase in the aircraft lift-to-drag ratios led to the use of trailing edge flaps and variable pitch propellers. Leading edge devices (fixed slots, moveable slats, and moveable flaps) were initially created and installed on aircraft for stall/spin protection.

Leading Edge Devices.

Leading edge devices were developed independently by a German, Gustav Lachman, in 1918 and by an Englishman, Frederick Handley-Page, in 1919. Both teams applied for patents. Lachmann joined Handley-Page in 1919 thereby avoiding a patent fight. The first aircraft to fly with fixed slots was a modified Airco/deHavilland DH9A, renamed as a Handley-Page H.P.17. It flew in 1919. The first aircraft to fly with slats was a modified deHavilland DH4 renamed a Handley-Page H.P.20. The H.P 20 was a monoplane (the DH4 was a biplane) and flew in 1921.

Table I6 presents examples of some of the early applications of leading edge devices. Several of the examples in table I6, the last four, were developed with leading edge devices to improve their takeoff and landing performance by reducing their stall speeds.

Table I6 Examples of Early Aircraft with Leading Edge Devices

Date	Aircraft
1919	Handley-Page H.P. 17
1920	Dayton-Wright (RB-1) racer
1921	Handley-Page H.P. 20
1923	Handley-Page H.P. 21
1932	Curtiss XF13C-1
1933	Curtiss XF12C-1
1934	Messerschmitt Bf-108A
1935	Messerschmitt Bf-109
1936	Fieseler Fi156 Storch
1939	Stinson model HW-75 (L-5 Sentinel)
1940	Stinson model 74 (L-1/O-49 Vigilant)
1940	Ryan YO-51 Dragonfly

In 1921, NACA published NACA-TN-71, written in part by Lachmann, discussing his work on slotted wing sections, *Experiments with Slotted Wings* (reference 57). He also authored a NACA Technical Memo-282 in 1924, *Results of Experiments with Slotted Wings* (reference 58). A third NACA report (NACA-TR-427) on leading edge devices was published in 1932, *The Effect of Multiple Fixed Slots and a Trailing Edge Flap on the Lift and Drag of a Clark Y Airfoil* (reference 59).

A third leading edge device, the Kruger flap, was invented by a German Werner Kruger in 1943. It was later evaluated on the Boeing 367-80 in 1954. Boeing used Kruger flaps on the 727 (first flight 9 February 1963) and on the 747 (first flight 9 February 1969).

Trailing Edge Flaps.

Initially trailing edge flaps were used to reduce the aircraft's lift-to-drag ratio on landing approach. Prior to using trailing edge flaps, the pilot used a forward slip to reduce the aircraft's lift-to-drag ratio and increase its sink rate. A forward slip was a cross control condition that significantly increased the aircraft's sideslip angle and the aerodynamic drag. The pilot input aileron to create a wing low condition (the left wing for example) and opposite (right, in this case) rudder to maintain the aircraft ground track. Once the slipping approach was established, the pilot controlled the sink rate with bank angle and the ground track with rudder.

The first 10 to 15 degrees of trailing edge flap deflection for a plain flap primarily increased the maximum available lift coefficient with relatively small increases in aerodynamic drag. Those small deflections are now used primarily for takeoffs. Larger deflections, 40 to 50 degrees, resulted in a large drag increase and were used primarily for landing.

Trailing edge flaps are normally described with one of four terms: Plain flaps, split flaps, slotted flaps, or Fowler flaps. Initially, most flaps were plain flaps, similar to an aileron, except that they were extended symmetrically. The first use of a plain flap was by the Royal Air Force on an S.E.4 in 1914, table I7. The Fairey Aircraft Company made extensive use of trailing edge flaps after 1916.

Table I7 Examples of Early Aircraft with Trailing Edge Flaps

Date	Aircraft	Type of Flaps
1914	Royal Aircraft Factory S.E.4	plain
1920	Dayton-Wright (RB-1) Racer	plain
1923	Handley-Page H.P.21	slotted
1925	Supermarine S.4 racer	plain
1931	Lockheed Model 9 Orion	split
1932	Northrup Gamma	split
1932	Curtiss XF13C-1	plain
1933	Curtiss XF12C-1	plain
1933	Douglass DC-1	split
1934	Caudron C.460 racer	split
1934	Boeing P-26A	plain
1934	Northrop XFT-1	plain
1934	Boeing YP-29	plain
1934	Douglas DC-2	split
1934	Messerschmitt Bf108A	Fowler
1935	Boeing Model 299 (B-17)	split
1935	Douglas DC-3	split
1935	Howard Hughes H-1 racer	split
1936	Fieseler Fi156 Storch	slotted
1937	Piaggio Aircraft M-32	double slotted
1937	Lockheed Model 14 Super Electra	Fowler
1939	Consolidated B-24	Fowler
1940	Ryan YO-51	Fowler
1940	Stinson Model 74 (L-1/O-49 Vigilant)	slotted
1942	Boeing B-29	Fowler
1963	Boeing 727-100	triple-slotted Fowler

The slotted flap was developed by G.V. Lachmann in Germany in 1917. The split flap was developed at the United States Army McCook Field in Dayton, Ohio by a team that included Orville Wright and J.M.H. Jacobs in 1920. The Fowler flap was developed by Harlan D. Fowler of the United States Army in 1924. An evaluation of the Fowler flap was published in 1932 by NACA, NACA-TN-419, *Wind-Tunnel Tests of the Fowler Variable-Area Wing* (reference 60). Various trailing edge flaps were evaluated by NACA during this time period. Their results were published in 1936 in NACA-TN-568, *Calculated Effect of Various Types of Flap on Takeoff Over Obstacles (reference 61).*

Operationally, flaps allowed the pilots to change the wing camber to provide additional lift for shorter takeoffs or additional lift and drag to reduce the landing approach speed and increase the approach flightpath angle (to make the approach steeper). The combination of a slower airspeed (less kinetic energy) and a steeper approach resulted in shorter landings with more repeatable touchdown points.

Variable flaps potentially made the takeoff and landing flight test effort more complicated because multiple settings have to be evaluated. Typically, the takeoff flap setting is determined by the runway available, the required climb gradient, the aircraft gross weight, and the atmospheric conditions.

Variable Pitch Propellers:

Propellers can be divided into seven categories:

1. Fixed pitch
2. Ground adjustable
3. Two-position, changeable in flight
4. Controllable pitch
5. Constant speed
6. Full feathering
7. Reversible

Fixed pitch propellers are “fixed”, they are not adjustable. Their most common usage is on low-performance, general aviation aircraft. Ground adjustable propellers can be adjusted on the ground while the engine is not operating. The advantage of a ground adjustable propeller is that it can be adjusted to maximize its low-speed performance for a flight where the takeoff or climb performance is critical. If the low-speed performance is not critical, then it can be adjusted to optimize cruise performance or maximum speed performance.

A two-position, changeable in flight, propeller allows the pilot to select (on the ground) one of two options for inflight use. Typically, the pilot would select a “climb” setting for low-speed operation and a “cruise” setting for high-speed operation.

A controllable pitch propeller is the next logical extension of propeller development for providing pilot flexibility. The pilot can adjust the propeller to any setting between the stops. Controllable pitch propellers cannot normally be feathered or set to produce reverse thrust. A constant speed propeller automatically maintains the pilot selected engine speed by adjusting the orientation of the propeller blades.

The last two options are constant speed propellers with extended ranges of blade angle available. A full feathering propeller’s blades can be moved to an angle that will stop the propeller rotation and significantly reduce its drag following an engine failure. The blades on a reversible propeller can be adjusted by the pilot to allow the propeller to generate drag versus thrust. The reversible feature is used to reduce the aircraft’s landing distance and to reduce wear on the brakes. Conceptually, reverse pitch on a propeller has a similar effect to reverse thrust with a jet engine.

The evolution of the propeller followed the sequence shown above. A number of companies in the United States, Great Britain, and France were working on practical, controllable pitch propellers in the 1920s. The most successful effort was led by Frank W. Caldwell of the Hamilton Standard Division of the United Aircraft Company. His effort won the United States Collier Trophy for 1933. Some of the Hamilton Standard development is summarized in table I8.

Table I8 Hamilton Standard Propeller Development

Date	Development
1925	ground adjustable pitch metal propellers available
1929	inflight adjustable propellers available
1930	controllable pitch propeller flown
1933	controllable pitch propellers available
1934	constant speed propellers available
1937	full feathering on hydromatic, constant speed propeller
1946	reversible propellers used on United Airlines Douglas DC-6 airliners

The adjustable propellers could use a low pitch for takeoff and climb and then change to a high pitch for cruise or for maximum speed. This provided a significant improvement in overall aircraft performance relative to the same aircraft with a fixed pitch propeller. The adjustable pitch propellers provided a 25 percent reduction in ground roll distance for takeoff relative to the same aircraft with a fixed pitch, cruise propeller according to a Hamilton Standard ad from the 1930s. Hamilton Standard adjustable propellers were used for two United States airspeed records in the early 1930s. On 4 September 1933, James R. Wedell set a land plane (versus seaplane) speed record of 305 statute miles per hour with a Hamilton Standard controllable pitch propeller. Howard Hughes raised that record to 352 statute miles per hour on 13 September 1935 with a Hamilton Standard constant speed propeller.

A constant speed propeller with the ability to be feathered significantly improved the engine out climb performance and single-engine service ceilings of twin engine aircraft like the Boeing 247 and the Douglas DC-3 airliners. Feathering also improved the engine out cruise performance of four engine aircraft like the Boeing B-17 and later the Consolidated B-24 in World War II.

Reversible, constant speed propellers had no effect on takeoff performance relative to using constant speed propellers except in the case of an aborted takeoff. According to Hamilton Standard, the United States Navy found that the landing ground roll with reversible propellers and mechanical braking was only 40 percent of that with just mechanical braking. Those tests were probably conducted on a Douglas R6D, the military equivalent of the DC-6A, in the late 1940s.

Table I9 shows some of the rapid propeller development between 1925 with fixed pitch, wooden or metal propellers and the constant speed, metal propellers just 10 years later.

Table I9 Examples of Early Aircraft with Variable Pitch Propellers

Date	Aircraft	Type of Propeller
1926	Curtiss XP-2	ground adjustable
1927	Boeing Model 15 (PW-9C)	ground adjustable
1928	Boeing Model 100 (P-12/F4B)	ground adjustable
1930	Wedell-Williams Model 44 racer	ground adjustable
1933	Boeing 247 airliner	February to May 1933 deliveries were with 3-bladed, fixed pitch propellers. Starting in June 1933, deliveries were with two-bladed, 2-position variable speed propellers. In 1940, the propellers were replaced with constant speed units.
1933	Boeing XF7B-1	controllable
1933	Douglas DC-1	controllable
1934	Caudron C.460 racer	constant speed
1934	deHavilland D.H.88 Comet racer	two position, variable pitch
1934	Boeing YP-29	controllable
1934	Douglas DC-2	controllable
1935	Boeing Model 299 (B-17)	constant speed
1935	Messerschmitt Bf108B	variable pitch
1935	Hughes H-1 racer	constant speed
1935	Douglas DC-3	constant speed
1936	Fieseler Fi156 Storch	adjustable
1936	Amelia Earhart’s Lockheed Electra Model 10E	constant speed

Retractable Landing Gear:

Retractable landing gear were developed in the 1920s, Table I10, to increase the maximum speeds of racing aircraft by reducing their aerodynamic drag. Retractable landing gear had a direct and an indirect effect on takeoff performance. The direct effect was to improve climbout performance through drag reduction. The indirect effect was the need for variable pitch propellers due to the increases in airspeed between stall speed and the higher maximum speeds with the retractable landing gear.

Table I10 Examples of Early Aircraft with Retractable Landing Gear

Date	Aircraft
1920	Dayton-Wright RB-1 racer
1922	Bristol Type 72 racer
1922	Verville-Sperry R-3 racer
1930	Boeing Model 200 Monomail
1930	Lockheed Altair
1931	Lockheed-Detroit YP-24
1931	Boeing Model 215 (XB-901/YB-9)
1931	Lockheed Model 9 Orion
1931	Grumman XFF-1
1932	Martin B-10
1932	Junkers Ju60
1932	Heinkel He70
1932	Curtiss XF13C-1
1932	Beechcraft Model 17 Staggerwing
1933	Boeing 247
1933	Curtiss XF12C-1
1933	Curtiss XF11C-3
1933	Boeing XF7B-1
1933	Grumman XF2F-1
1934	Caudron C.460 racer
1934	Boeing YP-29
1934	Consolidated P-30
1934	Messerschmitt Bf108A
1934	deHavilland D.H.88 Comet Racer
1935	Grumman XF3F-1
1935	Boeing Model 299 (B-17)
1935	Howard Hughes H-1 Racer

NACA Reports:

The NACA reports in the previous section, 1900-1927, references 47 through 53, were primarily initial looks at the challenges associated with takeoff performance and documenting what was observed. The reports from 1928 through 1938 present initial efforts to create models of the observed data, to determine the variables of interest, and to create methodologies for predicting takeoff performance for preliminary designs. References 57 through 75, table I11, are examples of NACA published reports associated with aircraft takeoff performance. Three of those: *The Calculation of Take-off Run* (reference 62), *Considerations of the Take-off Problem* (reference 63), and *The Transition Phase in the Take-off of an Airplane* (reference 64) are good examples of the state of the art in the 1930s.

Table I11 Reference Number and Title

Reference Number	Title
65	*Take-off of Heavily Loaded Airplanes*
66	*On the Take-off of Heavily Loaded Airplanes*
67	*The Reduction of Observed Airplane Performance to Standard Conditions*
68	*Take-off and Propeller Thrust*
69	*The Effect of Trim Angle on the Take-off Performance of a Flying Boat*
70	*Air Conditions Close to the Ground and the Effect on Airplane Landings*
71	*Aerodynamic Characteristics of a Wing with Fowler Flaps Including Flap Loads, Downwash, and Calculated Effect on Take-off*
72	*Ground Effect on the Take-off and Landing of Airplanes*
73	*The Rolling Friction of Several Airplane Wheel and Tires and the Effect of Rolling Friction on Take-off*
74	*General Airplane Performance*
75	*Performance Flight Testing Methods on Jet Propelled Aircraft as used by the Flight Section*

1935 TO 1945

Huge advancements in aircraft performance were made in the years between Charles Lindbergh's flight in 1927 and the period just prior to World War II. The next time period, 1935 through the end of World War II (1945), saw large changes in aircraft size, gross weight, and maximum airspeed. Also, by the end of World War II, almost all major airports had paved runways (either concrete or asphalt). Three takeoff related advances from the decade between 1935 and 1945 were:

1. Tricycle landing gear
2. Jet engines
3. Jet assisted takeoff (JATO) or rocket assisted takeoff (RATO)

Tricycle Landing Gear:

The landing gear for most aircraft can be grouped into one of three categories:

1. Conventional
2. Tricycle
3. Bicycle

Conventional landing gear has the main landing gear forward of the aircraft's center of gravity and a tailwheel in the back. Almost all aircraft built prior to the late 1930s had conventional landing gear and therefore the title. Tricycle landing gear had a nose gear forward of the aircraft's center of gravity and the main landing gear behind the center of gravity. After the late 1930s, most aircraft had tricycle landing gear, table I12. The bicycle arrangement has been used sparingly. Three aircraft that used the bicycle arrangement were the Boeing B-47 and B-52 and the Lockheed U-2.

Table I12 Examples of Early Aircraft with Tricycle Landing Gear

Date	Aircraft
1906	Santos Dumont 14-bis
1908	AEA Red Wing or Aerodrome #1
1908	AEA White Wing or Aerodrome #2
1908	AEA June Bug or Aerodrome #3
1909	AEA Silver Dart or Aerodrome #4
1909	Curtiss Number 1 or Curtiss Gold Bug or Golden Flyer
1909	Curtiss Number 2 or Curtiss Reims racer
1911	1911 Curtiss Model D or “The Curtiss Pusher”
1934	Fred Weick W-1
1937	ERCO Ercoupe
1938	Bell XP-39
1938	Douglas A-20/DB-7/P-70
1939	Lockheed XP-38
1939	Consolidated XB-24
1939	North American NA-40/B-25
1940	Grumman XF5F
1940	Martin B-26
1940	Northrop N-1M
1941	Heinkel He-280
1941	Gloster E.28/39
1941	Douglas XB-19
1941	Arado Ar 232
1942	Douglas DC-4/C-54
1942	Northrop XP-61
1942	Douglas XA-26
1942	Messerschmitt Me-309
1942	Consolidated B-32
1942	Boeing XB-29
1942	Bell XP-59
1942	Bell P-63
1942	Messerschmitt Me 264
1942	Northrop N-9M
1943	Lockheed L-049/C-69
1943	Vultee XP-54
1943	Gloster F.9/40 Meteor
1943	Arado Ar 234
1943	Curtiss-Wright XP-55
1943	deHavilland DH100 Vampire
1943	Messerschmitt Me 262V5

Table I12 Examples of Early Aircraft with Tricycle Landing Gear (Concluded)

Date	Aircraft
1943	Northrop XP-56
1943	Dornier Do-335
1943	Grumman XF7F
1944	Lockheed XP-80
1944	Horton Ho-229
1944	Bell XP-77
1944	Douglas XB-42
1944	Junkers Ju 287
1944	Boeing XC-97
1944	Heinkel He 162
1944	Lockheed P2V/P-2
1945	McDonnell FH-1 Phantom

Jet Engines:

Early jet engine development was conducted independently in England and in Nazi Germany prior to World War II. At least 15 different types of jet-powered aircraft had been flown before the end of World War II, September 1945. They are presented in Table I13.

Early jet-powered aircraft were under powered relative to their contemporary piston-powered, propeller-driven aircraft. That made their takeoff performance more critical. Modeling jet engine performance was generally easier than for their piston-powered, propeller-driven contemporaries. The jet engines did not have propellers and their thermodynamic operation was easier to model and to normalize.

Table I13 Examples of Early Jet-powered Aircraft

Date	Aircraft
1939	Heinkel He 178V1
1940	Heinkel He 280V1
1941	Gloster E.28/39
1942	Messerschmitt Me-262V3
1942	Bell XP-59
1943	Gloster F.9/40 Meteor
1943	Arado Ar 234V1
1943	deHavilland DH-100 Vampire
1944	Lockheed XP-80
1944	Messerschmitt Me 328
1944	Junkers Ju 287V1
1944	Heinkel He 162
1945	McDonnell XFD-1 (FH-1) Phantom
1944	Horton H.IX V2 (Horton Ho 229)

Table I13 Examples of Early Jet-powered Aircraft (Concluded)

Date	Aircraft
1945	Nakajima J8N-1/J9Y
1945	Bell XP-83
1945	Northrop XP-79B
1946	Republic XP-84
1946	MiG-9
1946	Douglas XB-43
1946	North American FJ-1 Fury
1947	MiG-15 (I-310)
1947	McDonnell XF2D-1 (F2H-1) Banshee
1947	North American XB-45
1947	Convair XB-46
1947	Martin XB-48
1947	North American XP-86
1947	Yakovlev Yak-25
1947	Grumman XF9F-2 Panther
1947	Boeing XB-47

Jet Assisted Takeoff (JATO):

The JATO, also known as RATO, was developed independently by the Guggenheim Aeronautical Laboratory, California Institute of Technology (Cal Tech) in Southern California and by Hellmuth Walter in Nazi Germany. The Germans successfully used Walter HWK 500 rockets to assist a heavy weight Heinkel He 111 bomber take off in 1937. The "power kegs" were widely used by the Germans during World War II. Some of the aircraft that used his system were: Arado Ar 234, Heinkel He 111, Junkers Ju 88, Messerschmitt Me-262, Me-321 and Me-323.

The research at Cal Tech started in 1936. In 1938, Mr. Ruben Fleet of the Consolidated Aircraft Company asked the scientists at Cal Tech about using rockets to improve the takeoff performance of heavy weight flying boats. This meeting led to a demonstration in San Diego bay in 1943 with liquid fueled rockets built by Aerojet General Corporation. Prior to the 1943 test, an Engineering and Research Corporation (ERCO) Ercoupe used JATO at March Field in August 1941 and a Douglas A-20A used JATO at Muroc (now Edwards AFB) in April 1942.

These Cal Tech tests led to a large number of operational applications with the United States military including:

1. Boeing B-47
2. Douglas R4D
3. Douglas A3D
4. Grumman TBF
5. Lockheed C-130
6. Lockheed P-2 (P2V)
7. Martin PBM
8. Martin XB-51
9. Republic F-84

The Lockheed C-130s were the last United States aircraft to use JATO. The United States Marine Corps C-130T with the Blue Angels (Fat Albert) last used JATO on 14 November 2009 at NAS Pensacola, Florida. The New York Air National Guard 109th Airlift Wing flies Lockheed LC-130H-2 and LC-130H-3 aircraft to the Antarctic as part of Operation Deep Freeze. At least through 2012, they were still using JATO bottles.

Two NACA documents concerning JATO were published in the 1940s. *Consideration of Auxiliary Jet Propulsion for Assisting Take-off* (reference 76) and *Flight Test of the Aerojet 7KS-6000 T-27 JATO Rocket Motor* (reference 77).

Army Air Forces Takeoff and Landing Test Procedures in 1944:

Performance Flight Testing Methods in Use by the Flight Section, Army Air Forces Technical Report Number 5069 by Paul F. Bikle (reference 26) has an 11-page chapter (Section H) for takeoff and landing tests with piston-powered, propeller driven aircraft. Bikle described three different camera systems that could be used to determine time histories of the aircraft position as a function of time. Bikle also presents four corrections for the observed takeoff performance:

1. Wind correction to the ground roll distance
2. Wind correction to the air phase distance
3. Aircraft gross weight correction to the ground roll distance
4. Aircraft gross weight correction to the air phase distance

The wind corrections were similar to those published by Ken Lush in 1952. The recommended aircraft gross weight corrections were Equation I1.

$$S_2 = S_1 \left(\frac{W_2}{W_1}\right)^n \tag{I1}$$

where:
S_2 = weight-corrected distance
S_1 = wind-corrected distance
W_2 = reference gross weight
W_1 = test day gross weight
n = 2.7 for ground roll distance
n = 2.2 for the total distance to 50 feet AGL

Bikle recommended at least four takeoffs for each aircraft gross weight/flap deflection configuration. The average of the best two of the sets of data becomes the final standardized takeoff results. "Best" most likely implies throwing out the "outliers" and selecting the two most consistent of the remaining sets of data using "engineering judgment". Finally, Bikle recommends: "All tests are run as close as possible to the desired gross weight and weight corrections are held to an absolute minimum."

Discussion of Recent Takeoff and Landing Performance Test Development (reference 78), also published in 1944 by the Army Air Forces in Dayton was based on data from existing test results and from tests of the Boeing B-17E for density altitude effects and the North American P-51B for pilot effects. Some of the other aircraft included:

1. Douglas A-20G
2. Vultee A-31
3. Consolidated B-24D
4. Consolidated XB-24K

5. North American B-25C
6. Martin B-26C
7. Boeing XB-29
8. Douglas C-47A
9. Douglas C-54A
10. Stinson L-1 Vigilant
11. Piper L-4B
12. Lockheed P-38G
13. Bell P-39F
14. Curtiss P-40F
15. Hawker Hurricane
16. Supermarine Spitfire
17. North American AT-6C
18. Lockheed AT-18

The report looked at corrections for winds, aircraft gross weight, and density altitude effects. It recommended the following equation be used to correct the test day ground roll distance for test day winds, equation I2:

$$S_g = S_{gt}\left[\frac{V_g}{V_T}\right]^{1.85} \tag{I2}$$

where:
S_g = wind-corrected ground roll distance
S_{gt} = test day ground roll distance
V_g = groundspeed at liftoff
V_T = true airspeed at liftoff
1.85 = empirically derived constant

Test data were reviewed from a P-38G, a P-39F, and a P-40F aircraft with winds between zero and 30 statute miles per hour to determine the exponent. The Air Force's data showed an exponent between 1.70 and 1.82 for the three aircraft. An exponent of 1.85 was recommended by the Army Air Forces to be consistent with an existing (in 1944) Civil Aeronautics Authority recommended value. Reference 78 retained the equations and the exponents from reference 26 for the aircraft gross weight adjustments. The density altitude adjustments in reference 78 from the B-17E flight test data were equations I3 and I4:

$$S_g = S_{gt}(K_p)\sigma \tag{I3}$$

and

$$S_g = S_{at}(K_p)(\sigma)^{0.5} \tag{I4}$$

where:
S_g = ground roll distance corrected for density altitude
S_{gt} = test day ground roll distance
S_{at} = test day air phase distance
K_p = ratio of (rate of climb at takeoff power at the test day density altitude)/(rate of climb at takeoff power at the reference density altitude (sea level, standard day)
σ = test day ambient air density ratio

The B-17E flight test data were obtained between -1,500 and 8,500 feet density altitude.

The data from the P-51B tests and the data from the other 18 aircraft showed that the relationship between an aircraft's true airspeed (or groundspeed since a wind adjustment has been applied) and its ground roll distance can be approximated by plotting the true airspeed squared on the y-axis and the ground roll distance on the x-axis with a linear curve fit going through the origin of the plot. In hindsight, this should not be surprising. If you assume a constant acceleration, then velocity is equal to acceleration times the incremental time since brake release and distance is equal to one-half the acceleration times the incremental time squared. Once enough flight test data are acquired to create the data fairing, a distance can be picked off the plot for any desired liftoff speed. This engineering "trick" was later used with Ken Lush's equations to adjust the distances for variations in pilot technique (pitch angle at liftoff).

A third reference from 1945, although technically not an Army Air Forces document, used very similar procedures and referenced the government documents. *A Consideration of Calculated Versus Flight Test Take-off Performance* (reference 79), was a Curtiss-Wright Corporation paper documenting their flight test and postflight data analyses procedures used for the C-46 cargo aircraft. The article from the Journal of the Aeronautical Sciences is available through the AIAA.

Reference 79, based on approximately 40 C-46 takeoffs, makes a case for using less flight test dedicated takeoffs and relying more on theoretical methods. (A vote for modeling and simulation from 1944!) The two Curtiss-Wright engineers felt that the industry knowledge concerning takeoff performance had reached a level where the performance could be predicted and just spot-checked with flight test data.

1945 TO 1965

The 20 years after the end of World War II saw developments in jet engine design, data acquisition, data processing, and data analyses. This section is divided into the following subsections:

1. Afterburners/augmentors/reheat
2. Turboprop engines
3. Turbofan engines
4. Data acquisition advances
5. Data processing advances
6. Data analyses advances

Afterburners/Augmentors/Reheat:

The terms afterburner, augmentor, and reheat are synonyms. In the United States, afterburner is the most common and will be used here. Frank Whittle, the Englishman, received patents in 1937 and in March 1940 for both an afterburner and for a turbofan engine. His company, Power Jets (Research and Development) Limited, created the W.2/500 that had an afterburner and W.2/700 that was an afterburning turbofan engine. They were both built under license by the Rover Car Company. Both engines were flight tested but neither engine went into production. The W.2B/700 would have been used in the Miles M.52 supersonic research aircraft that was cancelled by the British government in 1946.

Rolls Royce tested an afterburner on a Rover W.2B/23 engine installed in a Gloster Meteor aircraft in 1943. Additional Rolls Royce flight testing for afterburner development occurred in April 1945 and June 1949 with a Gloster Meteor. Most new fighter aircraft had afterburners after 1949, table I14. The Lockheed F-94C became the first USAF operational jet with an afterburner in July 1951.

Table I14 Examples of Early Jet-Powered Aircraft with Afterburners

Date	Aircraft
1947	Yakovkv YAK-19
1947	Douglas D-558-1
1947	Mikoyan-Gurevitch MiG-9M (I-308)
1948	Douglas X-4
1949	McDonnell XF-88A
1949	Lockheed YF-94A
1949	Lockheed XF-90A
1949	deHavilland FB.1 Venom
1949	Northrop YF-89A
1949	Grumman XF9F-5
1949	North American F-86D (YF-95A)
1949-1950	Mikoyan-Gurevitch MiG-15UTI
1950	Lockheed YF-94C
1950	North American YF-93A/YF-86C
1951	Douglas F4D-1
1951	McDonnell XF3H-1 Demon
1951	Republic F-84F
1951	Mikoyan-Gurevitch MiG-19 (I-350)
1951	Bell X-5
1951	Convair XP-92A
1951	Hawker Hunter (P.1067)
1951	Grumman XF9F-6
1951	deHavilland DH 110
1951	Mikoyan-Gurevtich MiG-17F
1951	Chance Vought F7U-3
1953	Supermarine F.3 Swift
1953	North American YF-100A
1953	Supermarine F.4 Swift
1953	Convair YF-102A
1954	McDonnell F-101A
1954	Fairey F.D.2
1954	Convair XF2Y-1 Sea Dart

Takeoff performance was significantly improved with afterburners. They did, however, introduce a number of flight test and modeling and simulation challenges:

1. Thrust setting at brake release
2. Slowly increase the afterburner segments (sprayrings) or just snap the throttle to maximum afterburner
3. Day- to-day variability in the early afterburner lightoff characteristics

The pilots typically performed pre-takeoff engine health checks prior to brake release. This was not a problem with the early jet engines, but it became a problem with the later jet engines with higher thrust and those with afterburners. One of two aircraft subsystems problems led to changes in the operational procedures. The first problem was that some brake systems could not hold the aircraft when it was producing its takeoff rated thrust. This problem was normally solved for the early jet aircraft with stronger brakes. The second problem was more difficult and was solved by workarounds, changes in pilot procedures. At high thrust settings prior to brake release, the brakes prevented the wheels from rotating. However, the tires rotated out of the wheels. The solution was to perform the engine health checks at a lower power setting and then advance the throttle(s) at or just after brake release. Options for the engine health checks thrust settings included:

1. A core speed percentage
2. A fan speed percentage
3. An engine pressure ratio (EPR)
4. Military power
5. Minimum afterburner

Operationally, most pilots slowly advanced the throttle(s) after brake release while observing the exhaust nozzle(s) open to verify good afterburner lights. The flight test procedure was normally to snap the throttle(s) at brake release. The flight test procedure was selected to reduce the data scatter caused by the day-to-day variability in the afterburner operation and in the pilot's throttle technique.

Two examples of NACA reports on afterburner development at NASA Lewis (now NASA Glenn) are: *Theoretical Investigation of Thrust Augmentation of Turbojet Engines by Tail-pipe Burning* (reference 80) from 1947 and *Theoretical Comparison of Several Methods of Thrust Augmentation for Turbojet Engines* (reference 81) from 1948.

Turboprop Engines:

Metropolitan-Vickers, a British Company, did development work on a turboprop engine, the F.3, in 1942. The Rolls Royce RB.50 Trent engine was first run in June 1944 and was flown for the first time on the left wing of a Gloster Meteor on 20 September 1945. The turboprop engine was popular in the 1940s and the 1950s because its specific fuel consumption was significantly better than the turbojets that were available, Table I15. The turboprop engines are still competitive with the modern turbofan engines at speeds below about 300 KCAS. Current United States military aircraft using turboprop engines include: Beech C-12 family, Beech T-6, Lockheed C-130 family, Grumman C-2, Grumman E-2, and the Lockheed P-3.

Table I15 Examples of Early Turboprop-Powered Aircraft

Date	Aircraft
1945	Gloster Meteor F.1 (Rolls Royce RB.50 Trent)
1945	Convair XP-81
1946	Ryan XF2R-1 Darkshark
1948	Vickers V.630 Viscount
1949	Westland Wyvern
1949	Allison XT38 in the nose of a Boeing B-17
1949	Fairey Gannet
1950	Douglas XA2D-1 Skyshark
1950	Convair XP5Y-1/T40
1950	Pratt and Whitney PT-2 (T34) in the nose of a Boeing B-17
1952	North American XA2J Super Savage
1952	Bristol Type 175 Britannia
1952	Tupolev TU-95 Bear

Table I15 Examples of Early Turboprop-Powered Aircraft (Concluded)

Date	Aircraft
1954	Lockheed YC-130
1953	McDonnell XF-88B
1954	Convair R3Y-1
1954	Lockheed Model 1249A-95-75 Constellation
1954	Convair YC-131C
1955	Convair CV-540
1955	Boeing YC-97J
1955	Republic XF-84H
1955	Fokker F27
1955	Lockheed YC-121F
1956	Douglas C-133
1957	Antonov An-10
1957	Ilyushin Il-18
1957	Tupolev TU-114
1957	Lockheed L-188 Electra
1957	Antonov An-12
1958	Lockheed YP3V-1 Orion
1959	Vickers V.950 Vanguard
1959	Grumman OV-1 Mohawk
1960	Grumman E-2 Hawkeye

Turbofan Engines:

Frank Whittle received a British patent on 4 March 1936 for a turbofan jet engine. Three different aircraft were flying with Rolls Royce Conway turbofan engines in 1959, table I16. All of the aircraft in Table I16 prior to the General Dynamics F-111A with Pratt and Whitney TF30 engines in 1964 were powered by either Rolls Royce Conway engines or by Pratt and Whitney JT3D or TF33 engines.

Table I16 Examples of Early Turbofan-Powered Aircraft

Date	Aircraft
1959	Handley-Page HP.80 Victor B.2
1959	Boeing 707-400
1959	Douglas DC-8-40
1960	Boeing 707-120B
1960	Douglas DC-8-50
1961	Convair 990
1961	Boeing B-52H
1962	Hawker Siddeley DH121 Trident
1963	Lockheed C-141A
1964	Boeing C-135B/KC-135B
1964	General Dynamics F-111A
1965	Ling-Temco-Vought A-7
1968	Lockheed C-5A
1968	Ling-Temco-Vought YA-7D

Table I16 Examples of Early Turbofan-Powered Aircraft (Concluded)

Date	Aircraft
1969	Boeing 747-100
1970	Douglas DC-10-10
1970	Lockheed L-1011
1970	Grumman F-14A

Turbofan engines changed the way installed thrust and fuel flow were modeled for takeoff performance simulation relative to the modeling for turbojet engines. Turbojet engine models used ambient or total air pressure and temperature ratios, freestream Mach number, and engine rotor speed. The controlling variables for turbofan engines were either fan speed or EPR versus rotor speed for the turbojet engine. The more significant changes were the introduction of analog and later digital fuel controllers plus the introduction of variable geometry: movable inlet guide vanes, movable rear compressor guide vanes, and variable exhaust exit area. The rather simple models that were adequate for the early turbojet engines were not valid for the more complex and variable turbofan engines. Fortunately, the introduction of thermodynamic based, electronic cycle decks in the 1960s solved the problem and are still in use today.

Data Acquisition Advances:

Data acquisition advances related to determining aircraft takeoff performance at Edwards AFB in the time period between 1945 and 1965 can be summarized as:

1. Magnetic tape recorders replacing onboard photopanels that had replaced hand-held data
2. Phototheodolite cameras and their associated film development, film reading, and data processing
3. 15,000 x 300 foot concrete runway with a constant slope (21-foot elevation change in a 15,000-foot run)
4. Thrust stand able to measure installed thrust at ground level, static conditions

Early in-flight data were hand recorded by the pilot in a single-place aircraft and normally by an observer in a multi-place aircraft. By the 1930s, some test programs had the pilot radio information to the ground to be hand-recorded there. Maximum (terminal) speed dives are one example that typically used a minimum aircrew and the pilot radioed data to the ground. Telemetry, the logical extension of the pilot using the radio, was not used until World War II. Photopanels were used in the 1930s but were not really common place in flight testing until the 1950s. Photopanels were panels with mechanical instruments installed that were photographed in a controlled lighting environment (a box with a light bulb). The film was developed postflight and the readings for each instrument on each frame of film were read by a technician. The recorded values were corrected for instrument error. The Pitot-static data were also corrected for position errors. The use of inflight magnetic tape recorders and large mainframe digital computers on the ground to read the tapes and process the data resulted in quicker data turnaround and in better quality data.

The acquisition of takeoff distances started with observers and tape measures next to the active runway. In the 1930s, the observers next to the runway were replaced by still cameras. In the 1940s, the still cameras were replaced by movie cameras. The AFFTC main runway, 04R/22L, received an instrumentation upgrade in 1957 with ASKANIA cameras installed in two dedicated towers. The initial tests to check out the system were conducted on 2 November 1957, reference 17. The ASKANIA system used two cameras to triangulate on the aircraft position. Each frame of film from each camera had the aircraft image plus time, azimuth, and elevation. The cameras were run at four frames per second. The nosewheel liftoff or the mainwheel liftoff was assumed to occur one-half of a frame prior to the first frame in which “the tire was clearly off the runway”. The selection of the frame was based on the judgment of the film reader. This system was used by the AFFTC until the end of the Boeing X-32/Lockheed X-35 flights on 6 August 2001. The ASKANIA system was officially retired on 20 December 2005.

A new runway was built at Edwards AFB between 1 December 1953 and October 1954. It is 15,000 feet long and 300 feet wide, plenty of room for a Boeing B-47 or B-52 with outrigger gear near their wingtips. The runway width has come in handy for ground minimum control speed tests. The runway width has also been used to reduce the crosswind component for dedicated takeoff performance tests. The pilot can start on the upwind side of the runway and allow the aircraft to drift towards the downwind side. Otherwise, the pilot would have to use rudder deflection (causing aerodynamic drag) or differential mechanical braking (causing friction drag) to maintain the aircraft ground track parallel to the runway heading. (The pilots are trained to use rudder deflection instead of differential braking.) The other advantage of the runway is that it has a constant runway slope, 0.08 degree or 21-foot change in elevation for a 15,000-foot change in run.

The final data acquisition advance between 1945 and 1965 was the development of a horizontal thrust stand able to measure the installed thrust of an aircraft at ground level, static conditions, reference 11. The stand was operational in October 1958 and was still available in 2020. The data acquired on the stand was used to spot check the installed engine models and to refine them as required. That ensured that the revised thrust model was valid at brake release.

Data Processing Advances:

Digital electronic mainframe computers have been used in support of flight test since the late 1940s. Their capabilities developed very rapidly in the 1940s and 1950s, Table I17. The AFFTC got its first digital computers in the early 1950s. The real advance in data processing came from the combination of onboard tape recorders and the mainframe computers that could read the tapes, process the data, and output the results onto paper. The mid 1950s saw the introduction of magnetic analog recorders. Digital recorders came in the mid-1960s. Many of the tape recorders had 28 tracks, some analog and the others digital.

Table I17 Examples of Early Mainframe Digital Computers

Date	Computer	Comments
1946	ENIAC	The first electronic general purpose computer. It was designed to calculate artillery firing tables for the United States Army.
1949	BINAC	The world’s first commercial digital computer. Developed for the Northrop Corporation.
1951	UNIVAC I	The second commercial computer produced in the United States. The first UNIVAC was accepted by the United States Census Bureau on 31 March 1951. The Pentagon received a UNIVAC in June 1952
1952	IBM 701	IBM’s first commercial computer.
1959	IBM 7090	A second generation computer with transistors versus vacuum tubes. NASA, Caltech/NASA Jet Propulsion Laboratory, the United States Air Force, and the United States Navy used IBM 7090 or 7094 computers.
1959	IBM 1401	The IBM 1401 series could read punch cards or magnetic tape and use high-speed line printers for output.
1964	IBM 360	

Data Analyses Advances:

The most significant data analyses advance related to aircraft takeoff performance during the period of 1945 through 1965 is clearly the introduction of a set of equations created by Ken Lush to adjust test day takeoff distances to a reference set of conditions. The development of the equations are presented in three references, references 82, 2, and 3:

1. Reference 82: *The Reduction to Standard Conditions of Take-off Measurements on Turbo-jet Aircraft*, Reports and Memoranda Number 2890, British Aeronautical Research Council, June 1951 (republished in 1957).
2. Reference 2: *Standardization of Take-off Performance Measurements for Airplanes*, AFFTC Technical Note R-12, 1952.
3. Reference 3: *Standardization of Take-off Performance Measurements for Airplanes* (Corrigendum to AFFTC Technical Note R12), May 1982.

Ken Lush's equations are discussed in greater detail in this handbook. His methods were the preferred approach for takeoff data standardization at the AFFTC from 1953 through 1980.

NACA, NASA, and NATO Takeoff Related Documents:

Four NACA and one National Aeronautics and Space Administration (NASA) documents related to aircraft takeoff performance are presented for the time period of 1945 through 1965.

1. *Wind-Tunnel Investigation of the Horizontal Motion of a Wing Near the Ground*, NACA-TM-1095 (reference 83).
2. *Experimental Verification of Two Methods for Computing the Take-off Ground Run of Propeller-driven Aircraft*, NACA-TN-1258 (reference 84).
3. *An Analytical Investigation of Effect of High-lift Flaps on Take-off of Light Airplanes*, NACA-TN-2404 (reference 85).
4. *Analysis of the Effects of Boundary-layer Control on the Take-off and Power-off Landing Performance Characteristics of a Liaison Type of Airplane*, NACA-TR-1057, (reference 86).
5. *Take-off Distances of a Supersonic Transport Configuration as Affected by Airplane Rotation During the Take-off Run*, NASA-TN-D-982 (reference 87).

The NATO Advisory Group for Aeronautical Research and Development (AGARD) published a report in 1956, *Notes on the Ground-run of Jet-propelled Aircraft During Landing and Take-off*, AGARD Report 82 (reference 88). The report summarized the state of the art for takeoff modeling and simulation 4 years after Ken Lush's AFFTC document (reference 2). The AGARD document relied heavily on graphical methods in this era just prior to the introduction of widespread use of digital computers. The *AGARD Flight Test Instrumentation Series Volume 16 on Trajectory Measurements for Take-off and Landing Tests and Other Short-Range Applications* (reference 89) provides background on phototheodolite systems like the ASKANIA System used at the AFFTC.

1965 TO 1980

The 15-year period between 1965 and 1980 brought improvements in data acquisition, data processing, and aircraft thrust-to-weight ratios for takeoffs. The changes can be grouped into five categories:

1. Introduction of INSs into aircraft
2. Introduction of production avionics into aircraft
3. Introduction of generic aircraft performance software for postflight data processing

4. Introduction of engine thermodynamic based cycle decks for calculating or for predicting installed thrust and fuel flow
5. Introduction of fighter aircraft with installed thrust-to-weight ratios greater than unity.

<u>Inertial Navigation Systems (INSs):</u>

The INSs were developed in the United States in support of two space-related activities: The manned spaceflight programs concluding with the Apollo flights to the moon (reference 90) and the nuclear intercontinental ballistic missile (ICBM) development. The Apollo program was preceded by the Mercury program and the Gemini program, which is shown in table I18. The United States ICBM programs evolved from the German V2 development of World War II. The first successful V2 flight occurred in October 1942 and was followed by operational flights starting in September of 1944. The U.S. Army Redstone first flew in 1953, table I19.

Table I18 Mercury, Gemini, and the Apollo Manned Spaceflight Programs

Launch Date	Mission	Comments
5 May 1961	Freedom 7	First manned Mercury flight with Alan Shepard
20 February 1962	Friendship 7	First U.S. manned orbital flight with John Glenn
15 May 1963	Faith 7	Last Mercury flight
23 March 1965	Gemini III	First manned Gemini flight
11 November 1966	Gemini XII	Last Gemini flight
11 October 1968	Apollo 7	First manned Apollo flight
7 December 1972	Apollo 17	Last Apollo flight

Table I19 Early Ballistic Missiles

First Launch Date	Missile
1953	Redstone
1955	Jupiter
1957	Thor
1957	Atlas
1959	Titan
1960	Polaris
1961	Minuteman I
1964	Minuteman II
1967	Minuteman III

The INSs developed for the space programs became progressively smaller and more accurate. One of the first aircraft applications was a two-axis (horizontal) system used in the Lockheed SR-71 and its predecessors:

1. Lockheed A-12 first flown on 26 April 1962
2. Lockheed YF-12A first flown on 7 August 1963
3. Lockheed SR-71 first flown on 22 December 1964

Four of the next aircraft with production INSs were the Lockheed C-141A and C-5A and the Boeing 747-100 and the KC-135. Those four aircraft had three-axis (north, east, and vertical) systems.

The first flight test use of an INS was probably General Dynamics with their YF-16. The YF-16 first flew on 20 January 1974 (flight zero) and was selected by the USAF as the winner of the YF-16/YF-17 flyoff on 13 January 1975. The first flight of an F-16A was on 8 December 1976. During the 2-year period prior to the first flight of the F-16A, General Dynamics and AFFTC engineers used the YF-16 flight test data to improve their data processing and data analyses techniques. One of the outcomes of their efforts was the use of flight test or production INSs as a data source for aircraft performance and aerodynamic data. Four references publishing their work include: *The Use of a Navigation Platform for Performance Instrumentation on the YF-16 Flight Test Program* (reference 8), *Use of a Navigation Platform for Performance Instrumentation on the YF-16* (reference 9), *F-16 Progress in Performance Flight Testing Using an Inertial Navigation Unit* (reference 10), and *Fighter Aircraft Dynamic Performance*, reference 7).

Avionics Data Buses:

One of the first extensive military uses of avionics data buses was on the F-111A aircraft, first flight on 21 December 1964. Avionics data buses became both a blessing and a curse for the instrumentation engineers and for the data processors. Before the introduction of avionics data buses, an aircraft used to evaluate aircraft performance might have 30 instrumented parameters recorded at 1 to 10 or maybe 20 samples per second. A subsystems aircraft also used by the performance and flying qualities engineers might have 100 parameters recorded at 20 samples per second and another 20 to 30 recorded at 100 samples per second or higher using frequency modulation (FM). A flight test rule of thumb in the early 1980s was that it cost 10,000 dollars to add an analog parameter to an existing instrumentation system. Digital bus parameters were thought to be free. Adding "nice to have" bus parameters increased the size of the data tapes, the postflight computer time required to process the data, the size of the paper output, and ultimately the cost of the flight test program. Some modern flight test programs have more than 10,000 parameters, almost all bus parameters, with data recording rates of 10 to 10,000 samples per second. Most of those parameters are considered "nice to have" just in case something goes wrong.

The avionics buses have data available from a wide variety of onboard electronic systems such as:

1. INS
2. Air data computer
3. Flight control computer
4. Antiskid system
5. Radar altimeter
6. Engine digital fuel controllers
7. Central computer
8. Radar
9. Tactical Air Navigation System (TACAN)
10. Fire control computer

Data from the first six data sources are frequently used for aircraft takeoff performance analyses.

Generic Aircraft Performance Software:

By the late 1960s, the AFFTC aircraft performance engineers were processing the postflight data from onboard digital tapes on a large mainframe digital computer. The one problem with this approach was that each flight test program developed their own software even though most programs were doing very similar calculations. Examples of those calculations included:

1. Sampling the magnetic tape to extract data for selected parameters and converting them from pulse code modulation (PCM) counts to engineering units (EUs)
2. Calculate aircraft mass properties including : gross weight, longitudinal center of gravity, and fuel flow
3. Correct Pitot-static data for position errors

4. Calculate test day gross thrust and propulsive drag using an in-flight thrust deck (IFTD) and measured engine and aircraft parameters
5. Calculate aircraft performance parameters using airspeed and altitude, the energy method
6. Calculate aircraft performance parameters using body-mounted accelerometers
7. Calculate aircraft performance parameters using accelerometers installed in a flight test noseboom and aligned with the local flow
8. Standardize the test day data to a reference set of conditions

Software was added later to take advantage of the introduction of INSs to test aircraft.

The data from the INSs provided:

1. Flightpath and normal acceleration
2. Inertial velocities North, East, and down
3. Pitch, roll, and heading angles
4. Angle of attack
5. Wind speed and direction

In the late 1960s and the early 1970s, generic postflight data processing software was developed at the AFFTC for aircraft performance and flying qualities evaluations. The software, known as the Uniform Flight Test Analysis System (UFTAS) is described in *Performance and Flying Qualities UFTAS Reference Manual* (reference 5). The software was first used for the YA-9/YA-10 flyoff. The Fairchild Republic YA-10 first flew on 10 May 1972. The Northrop YA-9 first flew on 30 May 1972. The YA-10 was announced as the winner on 18 January 1973.

Two additional subroutines (LINKs) were created during the YF-16 data review. LINK 10 used the INS inertial velocities North, East, and vertical to calculate the aircraft displacement along the runway (horizontal) and vertical. LINK 13 used the INS inertial velocities; pitch, roll, and heading angles; and pitch, roll, and yaw rates to calculate lift and drag coefficients; angle of attack; and excess thrust. The UFTAS LINK 13 software is documented in, *Performance and Flying Qualities UFTAS LINK 13 User Guide* (reference 6) and in *Fighter Aircraft Dynamic Performance* (reference 7).

Engine Decks:

An engine thermodynamic cycle deck is a computer simulation that models the thermodynamic properties of a jet engine. The components for an installed afterburning turbofan engine may include the following:

1. Aircraft inlet
2. Fan
3. Compressor
4. Combustor
5. High pressure turbine
6. Low pressure turbine
7. Afterburner
8. Exhaust nozzle
9. Throttle-dependent aircraft boattail effects

A turbojet would not have a fan section to model and a non-afterburning jet would not have an afterburner section. A cycle deck refers back to when the engine decks were stored on a deck of computer cards. A cycle deck could be in one of two forms: A predictive deck using aircraft flight conditions, and an engine power setting or an inflight thrust deck used to calculate gross thrust and propulsive drag using aircraft flight conditions and measured engine parameters.

The “cycle” in cycle deck refers to the computer repeatedly cycling through the software until the model converged. Until the output of the compressor model matched the input to the combustor model for example. Since the flow internal to the engine was subsonic, pressure waves could propagate both forward and aft through the engine core or the bypass duct of a turbofan engine.

The predecessor to the computer based cycle deck was a set of “chase-around charts” in a three-ring binder. An engineer or more likely an engineering technician or a female human computer (A female computer did laborious and repetitious calculations before the introduction of hand calculators and electronic desk computers in the 1970s.) used the charts to predict gross thrust, airflow, propulsive drag, and fuel flow. A simple set of chase around charts might be 20 pages long, while a more complicated (and accurate) one might require 50 charts. The introduction of computer-based cycle decks on large mainframe computers allowed the computer to do in a second for 30 samples of data what a human computer could do for one sample (time) of data in an hour.

The first American engine with an electronic, thermodynamic-based cycle deck was probably the Pratt and Whitney TF30 afterburning turbofan engine. The General Dynamics F-111A (first flight on 21 December 1964) and the Grumman F-14A (first flight on 21 December 1970) both flew with afterburner equipped versions of the TF30 engine. A non-afterburning version was used in the U.S. Navy Ling-Temco-Vought A-7A (first flight on 26 September 1965).

High Installed Thrust-to-Weight Ratios:

The decade of the 1970s introduced a new generation of fighters in the United States, table I20. These aircraft with air-to-air stores (but without external fuel tanks) had installed thrust-to-weight ratios near or greater than unity. This did not fundamentally change how takeoff performance data were acquired or processed, but it did require good instrumentation. The four frames of film per second from the ASKANIA system was no longer adequate. A sample rate of 10 to 20 samples per second from the onboard INS data plus instrumented strut extensions on all three landing gear and wheelspeed sensor data from the antiskid system were highly desired if not required for the higher performance aircraft.

Table I20 New USAF Fighters in the 1970s

First Flight	Aircraft
21 Dec 1970	Grumman F-14
27 Jul 1972	McDonnell F-15
20 Jan 1974 (2 Feb 1974)	General Dynamics YF-16
9 Jun 1974	Northrop YF-17
8 Dec 1976	General Dynamics F-16A
18 Nov 1978	McDonnell F/A-18A

Note: The first flight of the YF-16, flight zero, was on 20 January 1974. The official first flight was on 2 February 1974.

NASA Takeoff Related Document:

The NASA Flight Research Center at Edwards AFB (now NASA Armstrong) published a Technical Note (TN) on their data analyses of flight test takeoff data from the North American XB-70 aircraft, *A Simplified Flight-Test Method for Determining Aircraft Takeoff Performance that Includes Effects of Pilot Technique* (reference 91). The 1974 NASA Technical Note was published only four months after NASA

Ames published their Technical Memorandum (Memo) introducing the NASA TOLAND software. The NASA Technical Note provides the reader with some insight into how some engineers were analyzing aircraft takeoff data just before transitioning to a new (revolutionary) technique using modeling and simulation. The 1974 NASA Technical Note also provides insight into one approach that was used to account for variability's in pilot technique.

1980 TO 1995

The 15 years between 1980 and 1995 saw two significant changes in how the AFFTC collected and standardized aircraft takeoff performance data:

1. Replaced Ken Lush's standardization equations with a computer-based modeling and simulation approach.
2. Used onboard inertial data from INSs replacing phototheodolite (ASKANIA) data as the preferred data source.

NASA TOLAND:

Wayne Olson, who had been part of the YF-16 team, went to graduate school at Stanford in the late 1970s. While there, he met an engineer from NASA Ames who told him about a computer program for estimating aircraft takeoff performance. The program was a design tool that used the required aircraft performance as inputs and output the necessary aerodynamic and propulsive characteristics. When he returned to the AFFTC, he obtained the software and its documentation: *Computer Programs for Estimating Takeoff and Landing Performance* (reference 4). Wayne Olson and Dave Nesst converted the software into a flight test tool. Their version used the following inputs:

1. Pressure altitude
2. Ambient air temperature
3. Headwind component
4. Runway slope
5. Aircraft gross weight
6. Aircraft configuration
7. Engine thrust setting
8. Rolling coefficient of friction
9. Aircraft pitch angle
10. Rotation speed
11. Rotation rate
12. Target pitch angle or climbout speed

The following models were required for each aircraft:

1. In ground effect lift curves
2. In ground effect drag polars
3. Out of ground effect lift curves
4. Out of ground effect drag polars
5. A ground effect interpolation scheme to interpolate between the models
6. Installed gross thrust engine model
7. Installed engine airflow model
8. Installed propulsive drag model
9. Installed fuel flow model
10. Thrust spoolup curve (if required)

The outputs included:

1. Time history data (typically at 10 samples per second) from brake release through 100 feet AGL
2. Ground roll distance and calibrated airspeed at the target rotation speed
3. Ground roll distance, calibrated airspeed, and aircraft pitch angle at mainwheel liftoff
4. Horizontal distance, calibrated airspeed, and aircraft pitch angle with the aircraft at 50 feet AGL

The program typically ran at 100 samples per second. The time history data were output for every tenth sample, at 10 samples per second. The data for rotation, takeoff, and 50 feet AGL were based on the 100 samples per second data.

The onboard INS's inertial data were processed through UFTAS LINK 10 to obtain the test day takeoff performance. The NASA TOLAND simulation was run twice: once for the test day conditions and once for the reference set of conditions. The reference set of conditions for a Northrop T-38C might be:

1. Sea level pressure altitude
2. 15 degrees C (59 degrees F) ambient air temperature
3. No wind (calm)
4. Flat runway (no slope)
5. 12,800 pounds gross weight at brake release
6. Landing gear extended, gear doors closed, and 60 percent (27 degrees) trailing edge flaps
7. Both engines at maximum (full afterburner) thrust
8. 0.015 rolling coefficient of friction
9. 1.0 degree noseup pitch angle from brake release to rotation speed
10. 140 KCAS rotation speed
11. 1.66 degrees per second rotation rate
12. 7.5 degrees pitch angle for climbout

The following data were adjusted to the reference set of conditions for the Northrop T-38C:

1. Ground roll distance from brake release to rotation speed
2. Ground roll distance from brake release to mainwheel liftoff (takeoff)
3. Total horizontal distance from brake release to 50 feet AGL
4. Calibrated airspeed at mainwheel liftoff (takeoff)
5. Calibrated airspeed at 50 feet AGL

The adjustment to the reference set of conditions was made as follows, equation I5:

$$\begin{pmatrix}\text{performance}\\ \text{variable}\\ \text{at the}\\ \text{reference}\\ \text{conditions}\end{pmatrix} = \begin{pmatrix}\text{test day}\\ \text{value}\\ \text{for the}\\ \text{variable}\end{pmatrix} + \left[\begin{pmatrix}\text{TOLAND}\\ \text{predicted}\\ \text{value for the}\\ \text{variable at}\\ \text{the reference}\\ \text{conditions}\end{pmatrix} - \begin{pmatrix}\text{TOLAND}\\ \text{predicted}\\ \text{value for the}\\ \text{variable at the}\\ \text{test day}\\ \text{conditions}\end{pmatrix}\right] \tag{I5}$$

The method described above using the TOLAND software has been the preferred method for adjusting the aircraft takeoff data at the AFFTC since 1980 when it replaced Ken Lush's equations as the preferred method. The first test program at the AFFTC to use this method was the McDonnell F-15C. It was used on data acquired between May 1979 and September 1980. The technical report, *F-15C Limited Takeoff and Landing Evaluation*, AFFTC-TR-81-18 (reference 28) was published in September 1981.

Onboard Data for Takeoff Determination:

Prior to 1980, aircraft takeoff performance at the AFFTC was obtained using:

1. An engineer standing approximately 100 feet off the edge of the active runway recording pressure altitude, ambient air temperature, wind speed and direction, and time using a portable wind kit near the predicted liftoff point.
2. The pilot hand-recording pressure altitude, ambient air temperature, and wind speed and direction from the control tower.
3. The cameras in both ASKANIA towers recorded the takeoff on 35mm film at four frames per second.
4. Data were recorded onboard the aircraft.

Postflight, the ASKANIA film were developed and processed. The processed data from the ASKANIA system included:

1. Ground roll distance from brake release to nosewheel liftoff
2. Ground roll distance from brake release to mainwheel liftoff (takeoff)
3. Horizontal distance from brake release to 50 feet AGL
4. Ground speeds for the three events
5. Elapsed time from brake release to the three events

The three groundspeeds were combined with the runway heading and the assumed wind speed and direction to calculate true airspeeds for the three events. The three true airspeeds were converted to calibrated airspeeds using the ambient air pressure from the pressure altitude and the ambient air temperature.

The aircraft gross weight was determined from the onboard data. The aircraft gross weight, headwind component, runway slope, ambient air pressure and temperature, the ground roll distance for takeoff, and the horizontal distance from brake release to 50 feet AGL were then used with Ken Lush's equations to obtain the standardized ground roll distance and the standardized distance to 50 feet AGL.

Harold Cheney from Douglas Aircraft developed and advocated a different approach based on his work on the YC-15, the re-engined DC-8 (DC-8-70 and DC-8-71), and the DC-9-80 (MD-80):

1. *YC-15 STOL Performance Flight Test Methods and Results* (reference 14)
2. *Takeoff Performance Data Using Onboard Instrumentation* (reference 15)
3. *A Procedure for Determining Flight Path Wind Components During Takeoff and Landing Tests* (reference 16)

His approach to determine the test day performance is summarized below:

1. The runway slope was obtained from an external source (usually a runway survey),
2. Ambient air pressure and pressure altitude were obtained from the onboard air data computer just prior to brake release.
3. Ambient air temperature was obtained from total air temperature and Mach number from the onboard air data computer just prior to rotation.
4. The wind speeds and direction during the takeoff were calculated from the true airspeed from the onboard air data computer and the groundspeed, ground track, and aircraft heading from the onboard INS.
5. Distances from brake release and aircraft pitch angles as a function of time were determined using the onboard INS inertial velocities plus the pitch angle.

6. Takeoff (time) was based on the shape of the antiskid groundspeed time history data (wheelspeed) near the time of the WOW discretes switching
7. The time for 50 feet AGL was based on an onboard radar altimeter and on the integration of the INS vertical velocity.

His approach, with one exception, was used by the AFFTC for the F-15E, F-15S, F-15I, E-8A Joint STARS, and the T-38C evaluations. The one exception was the determination of the test day ambient air temperature. The AFFTC compared the production aircraft total air temperature outputs, the flight test aircraft total air temperature outputs, the production engine fuel controller total air temperature outputs, and the base weather ambient air temperatures. In most cases the AFFTC chose to use the base weather ambient air temperatures as the best data source for takeoff performance evaluations.

A comparison of the phototheodolite ASKANIA system and the onboard production INS in an F-15E aircraft was made at the beginning of the F-15E evaluation in 1988. The evaluation of the results concluded:

1. The onboard INS method required less scheduling of resources and less advanced notice.
2. The onboard INS method required less data turnaround time.
3. The onboard INS method was less expensive.
4. Most of the differences in the distances to nosewheel liftoff, mainwheel liftoff (takeoff), and 50 feet AGL could be reduced by using the ASKANIA time history data with the onboard WOW discretes times versus the human film readers selected times.

The aircraft positions as a function of time were very close for both methods. The differences were caused by assumptions about when the events occurred. The onboard INS method for the F-15E evaluation did not have the wheelspeeds instrumented. The INS method used the WOW discretes to establish the nosewheel and mainwheel liftoff times. The ASKANIA system assumed that the liftoffs occurred one-eighth of a second prior to the first frame of film in which “the tire was clearly off the runway”. (The ASKANIA film rate was four frames per second.) The results of the comparison was published in an AFFTC technical letter report, *Use of On-board Inertial Navigation System Data Instead of ASKANIA Data for Takeoff Performance Determination* (reference 20) and in a Society of Flight Test Engineers paper, *Use of Onboard Data for Takeoff Performance Determination* (reference 21).

1995 TO PRESENT

The AFFTC approach to acquiring, processing, and adjusting aircraft takeoff performance data to a reference set of conditions has not changed since 1995 with one very critical exception. In 1996, Kent Standley published a new version of the NASA TOLAND software that had been previously modified by Wayne Olson and Dave Nesst in the late 1970s: *AFFTC TOLAND User’s Guide*, AFFTC-TIH-96-02 (reference 12). The new version was developed primarily to be more efficient and to add more options for modeling landings, continued takeoffs following an afterburner or actual or simulated (IDLE) engine failure, and aborted takeoffs. However, in hindsight, the most important change was (arguably) the addition of an option for modeling the pitch angle variations from the rotation speed to the aircraft climbing through 50 feet AGL.

In the Wayne Olson/Dave Nesst version, the pitch angle was one value prior to the rotation speed and it then increased at a constant pitch rate until reaching a target pitch angle. The actual test day pitch angle usually increased (noseup) slightly with increasing airspeed prior to the rotation speed. A typical variation for the T-38C aircraft was 0.7 to 0.8 degree just after brake release, increasing to 0.9 to 1.1 degree just prior to rotation. The engineer usually selected the pitch angle just prior to rotation as the input to TOLAND for the entire ground run from brake release to rotation. The selection of an average pitch rate and a final pitch angle was based on engineering judgment. The final pitch angle input was often the pitch angle at takeoff or an average of that angle and the pitch angles through 50 feet AGL. The average pitch rate input was usually equal to the pitch angle at takeoff minus the pitch angle just prior to rotation divided by the elapsed time between the rotation speed and the takeoff. The selection of an average pitch rate and the final pitch angle could significantly change the predicted takeoff and 50 foot AGL results. Some engineers ran TOLAND twice for the test day predictions: Once for the test day takeoff predictions and again for the test day predictions at 50 feet AGL. Obviously a more rigorous method requiring less engineering judgment would have been preferred.

Kent Standley's software offered two options: The Wayne Olson/Dave Nesst one described above or an (arguably) much better choice. The new option allowed the engineer to use a time history (a table) of the actual aircraft pitch angle as a function of elapsed time after the rotation speed was achieved. This relatively simple improvement resulted in a very significant improvement in the comparisons of the predicted and the actual test day aircraft takeoff performance. Equally as important, the new results were much easier to defend. "I used the actual pitch angle time history" was much easier to defend than: "I chose a pitch rate and a target pitch angle that gave me an answer that I liked".

The recommended approach at the AFFTC is to use the table option for the test day predicted TOLAND runs and the pitch rate/pitch angle option for the reference day runs. The pitch rate for the reference day run is chosen as an "average" of all of the test day pitch rates or a flight manual recommended value. The target pitch angle for the reference day run is normally a flight manual recommended value.

This page was intentionally left blank.

APPENDIX J - AIRCRAFT USED TO DEVELOP KEN LUSH'S EQUATIONS

Data from six different aircraft were used to create the equations in *Standardization of Take-off Performance Measurements for Airplanes*, AFFTC Technical Note R-12 (reference 2). They were not identified but Kenneth Lush did provide some clues. The six general categories were:

1. Light aircraft with a fixed pitch propeller
2. Medium-weight aircraft with constant speed propellers
3. Heavy weight aircraft with constant speed propellers
4. A jet fighter identified as "jet fighter number 1"
5. A jet fighter identified as "jet fighter number 2"
6. A medium-weight jet bomber

LIGHT AIRCRAFT WITH A FIXED PITCH PROPELLER

Two clues were given concerning this aircraft in reference 2:

1. The aircraft used a 20-degree flap deflection for takeoff, page 23.
2. The aircraft gross weight was varied between 1,250 and 1,550 pounds, figure 5 on page 88.

This could have been one of many civilian general aviation aircraft or World War II liaison aircraft, table J1. However, most of these aircraft did not have wing trailing edge flaps. The aircraft needed an empty weight of less than approximately 1,050 pounds to take off with a gross weight of 1,250 pounds. That would allow for a 150-pound pilot and 50 pounds, approximately 8 gallons, of fuel.

Table J1 Light Aircraft

Aircraft	Empty Weight (lb)	Gross Weight (lb)
Stinson L-1	2,600	3,350
Taylorcraft L-2	700	1,200
Aeronca L-3	840	1,260
Piper L-4	750	1,220
Stinson L-5 (OY-1)	1,550	2,050
Interstate L-6	1,100	1,650
Universal L-7	970	1,490
Interstate L-8	1,100	1,650
Stinson L-9	920	1,580
Ryan L-10	1,350	2,150
Consolidated L-13	2,070	2,900
Piper L-14	830	1,450
Aeronca L-16	900	1,450
Piper L-18B	850	1,500
Cessna L-19A	1,500	2,430
Piper L-21	900	1,500
Stearman PT-17	1,950	2,700
Fairchild PT-19A	1,820	2,520
Ryan PT-22	1,310	1,860
Fairchild PT-26A	2,020	2,740
Vultee BT-13	3,350	4,400
North American T-6D	4,250	5,160

Table J1 Light Aircraft (Concluded)

Aircraft	Empty Weight (lb)	Gross Weight (lb)
North American T-28A	5,110	6,760
Aeronca Model 7AC	710	1,220
Cessna 140	890	1,450
Cessna 150D (1964)	1,050	1,600
Luscome Model 8 Silvaire	800	1,350
Piper J-3 cub	680	1,100
Piper PA-12	950	1,750
Taylorcraft BC12D-65	750	1,200

Thus the empty weight must be approximately 1,050 pounds and the maximum takeoff gross weight must be at least 1,550 pounds. This eliminates almost all of the aircraft listed in table J1. The remaining aircraft are:

1. Stinson L-9
2. Piper PA-12
3. Cessna 150D (1964)

The Stinson L-9 is the only military aircraft of the three. It was developed from the Stinson Model 10A Voyager that first flew in 1939. Stinson delivered over 3600 Model 105 (L-5) and Model 10A (L-9) aircraft between 1942 and 1945. The L-9 had leading edge slots and slotted trailing edge flaps. The L-9 is the most likely of all of the aircraft in table J1.

The Piper PA-12 Super Cruiser was produced between 1946 and 1948. It was available in the 1952 time period and its empty weight and maximum takeoff gross weights were consistent with the 1,250 and 1,550 pound takeoff weights in reference 92. Wing flaps were available as a factory option. The PA-12 was probably not the aircraft used because it was not a United States Air Force aircraft.

The Cessna 150 was not the aircraft used in reference 92. It did not fly until 1957 and did not have a maximum takeoff gross weight of 1,600 pounds until 1964. However, it did have the required weight range and it did use 20 degrees of wing trailing edge flaps for takeoff.

MEDIUM-WEIGHT AIRCRAFT WITH CONSTANT SPEED PROPELLERS

Reference 2 provides almost no information about this aircraft. The data in figure 6 on page 89 show a weight range from 99,000 to 172,000 pounds. An aircraft could only be described as “medium-weight” at 172,000 pounds when compared to the Boeing B-52, Convair B-36, and XC-99.

Table J2 provides a list of piston-powered, propeller-driven aircraft. Six aircraft from table J2 meet the weight range requirements:

1. Boeing B-50D
2. Douglas C-124
3. Boeing C-97G
4. Douglas C-74
5. Northrop XB-35
6. Northrop YB-35

Table J2 Medium-weight Aircraft with Constant Speed Propellers

Aircraft	Empty Weight (lb)	Gross Weight (lb)
Douglas A-20G	17,000	26,000
Douglas A-26 (B-26)	22,900	35,000
Boeing XB-15	37,700	70,700
Being B-17G	36,000	67,900
Douglas XB-19	84,400	162,000
Consolidated B-24M	36,000	64,500
North American B-25J	19,500	35,000
Martin B-26G	24,000	37,000
Boeing B-29	69,000	140,000
Convair B-32	60,300	120,000
Northrop XB-35	84,000	209,000
Northrop YB-35	89,500	209,000
Douglas XB-42	20,900	35,700
Boeing B-50A	81,000	168,700
Boeing B-50D	80,600	173,000
Curtiss C-46	29,500	50,000
Douglas C-47	18,000	33,000
Douglas C-54G	39,000	82,500
Lockheed C-69	51,000	86,300
Douglas C-74	86,000	172,000
Boeing C-97G	81,300	175,000
Douglas C-118	56,800	129,400
Fairchild C-119G	40,800	72,700
Lockheed C-121G	72,800	145,000
Douglas C-124	101,200	185,000

The two Northrop flying wing aircraft were probably not the aircraft used in reference 2. Only three were built and a limited number of flights were flown. They were also flying wings, which made them non-representative of other aircraft. Only 14 Douglas C-74 aircraft were built and therefore they were probably not the aircraft of choice. Any of the remaining three aircraft (the Boeing B-50D, the C-97G, or the Douglas C-124) are viable candidates. All were available in large numbers in the USAF in 1952.

HEAVY WEIGHT AIRCRAFT WITH CONSTANT SPEED PROPELLERS

Three significant clues were given concerning this aircraft:

1. Gross weight range of 196,000 to 296,000 pounds
2. 3,000 horsepower engines
3. Produced as both an A Model and as a B Model

This aircraft has to be the Convair B-36A and B-36B aircraft, table J3. The B-36A was a trainer version. The B-36B was the first of the operational B-36 bombers.

Table J3 Heavy weight Aircraft with Constant Speed Propellers

Aircraft	Empty Weight (lb)	Gross Weight (lb)	Auxiliary Jet Engines (YES/NO)
Convair XC-99 (original landing gear)	129,900	265,000	NO
Convair XC-99 (new landing gear)	135,200	320,000	NO
Convair XB-36	131,800	278,000	NO
Convair B-36A	155,700	310,400	NO
Convair B-36B	166,200	328,000	NO
Convair B-36D	161,400	357,500	YES
Convair B-36H	168,500	370,000	YES
Convair B-36J	171,000	410,000	YES

Note: The Convair XC-99 was a cargo version of the B-36 bomber. Only one was built.

JET FIGHTERS NUMBERS ONE AND TWO

Reference 2 provides three clues for these aircraft:

1. They both had removable tip tanks.
2. Jet fighter number one had a gross weight range of at least 12,800 to 19,400 pounds.
3. Jet fighter number 2 had a gross weight range of at least 11,400 to 17,200 pounds.

Candidate aircraft are presented in table J4.

Jet fighter number one was probably a Republic F-84. Jet fighter number two might have been either a Lockheed F-80 or a Lockheed F-94 with a higher approved maximum gross weight than those listed in the table.

Table J4 Jet Fighter Aircraft

Aircraft	Empty Weight (lb)	Gross Weight (lb)	Removable Tip Tanks (YES/NO)
Bell XP-59	7,900	12,600	NO
Bell YP-59	7,630	12,600	NO
Bell P-59A	7,950	13,000	NO
Bell P-59B	8,170	13,700	NO
Lockheed XP-80	6,300	8,900	NO
Lockheed XP-80A	7,250	13,750	NO
Lockheed P-80A	7,900	14,500	YES
Lockheed P-80B	8,000	15,350	YES
Lockheed F-80C	8,250	16,850	YES
Bell XF-83	15,000	27,500	NO
Republic XP-84	9,200	19,700	YES
Republic F-84B	10,000	20,000	YES
Republic F-84E	11,000	23,000	YES
Republic F-84F	13,800	27,000	YES
Republic F-84G	11,500	23,500	YES
North American XP-86	9,730	16,400	NO
North American P-86A	10,100	16,400	NO
North American F-86D	13,500	20,000	NO

Table J4 Jet Fighter Aircraft (Concluded)

Aircraft	Empty Weight (lb)	Gross Weight (lb)	Removable Tip Tanks (YES/NO)
North American F-86E	11,000	18,000	NO
North American F-86F	11,000	20,000	NO
McDonnell XF-88	12,100	23,100	NO
Northrop XF-89	25,900	43,900	YES
Northrop F-89A	23,650	36,400	YES
Northrop F-89C	24,600	37,350	YES
Northrop F-89D	24,000	41,000	YES
Lockheed XF-90	18,500	31,000	YES
Lockheed YF-94	9,600	13,000	YES
Lockheed F-94A	9,600	15,500	YES
Lockheed F-94B	9,800	15,700	YES
Lockheed F-94C	12,000	27,000	YES

MEDIUM-WEIGHT JET BOMBER

Reference 2 provides no hints as to the identity of the medium-weight jet bomber. However, there are only a few potential candidates, table J5. Although the Boeing B-47 may be the sentimental choice, this aircraft was almost certainly a North American B-45 aircraft.

Table J5 Medium-Weight Jet Bomber

Aircraft	Empty Weight (lb)	Gross Weight (lb)	Bicycle Landing Gear (YES/NO)
Douglas XB-43	22,900	40,000	NO
North American XB-45	41,900	82,600	NO
North American B-45A	45,500	81,400	NO
North American B-45C	49,000	110,000	NO
Convair XB-46	48,000	95,600	NO
Boeing XB-47	75,000	162,500	YES
Boeing B-47A	73,200	162,500	YES
Boeing B-47B	80,000	185,000	YES
Boeing B-47E	80,800	198,200	YES
Martin XB-48	58,300	102,600	YES
Northrop YB-49	88,500	213,000	NO
Martin XB-51	29,600	62,500	YES

Note: The Northrop YB-49 was a flying wing.

This page was intentionally left blank.

APPENDIX K - T-38C FLIGHT MANUAL TAKEOFF CHARTS

These T-38C Flight Manual charts were extracted from T.O. 1T-38C-1, 1 April 2001, Change 9, 15 May 2006 (reference 92) for an operational T-38C with the propulsion modernization program (PMP) upgrades installed. The thrust model used for the charts had a reduced thrust relative to the AFFTC TOLAND thrust model. The thrust was reduced so the predicted performance would be conservative. It was intended to account for engine-to-engine variability and engine deterioration between scheduled engine overhauls, figures K1 and K2, were extracted from T.O. 1T-38C-1, *USAF Series T-38C Aircraft Flight Manual* (reference 92).

T.O. 1T-38C-1

TAKEOFF DISTANCE

MAX THRUST
FLAPS – 60%
GEAR – DOWN

MODEL: T-38C
ENGINE: (2) J85-GE-5R
DATE: 15 JUNE 2004
DATA BASIS: FLIGHT TEST

NOTES

- DATA BASED ON NORMAL TAKEOFF PROCEDURES:
  AFT STICK APPLIED AT THE ROTATION SPEED SHOWN IN FIGURE B2-2 AND 7.5° PITCH ATTITUDE HELD AFTER ROTATION.
- INCREASE TAKEOFF DISTANCE 3% FOR EACH PERCENT OF UPHILL RUNWAY SLOPE. INCREASE TOTAL DISTANCE TO CLEAR 50-FOOT OBSTACLE 10% FOR EACH PERCENT OF UPHILL RUNWAY SLOPE.
- WITH WSSP INSTALLED, DETERMINE DISTANCES FOR AIRCRAFT PLUS WSSP WEIGHT AND INCREASE TAKEOFF DISTANCE AND TOTAL DISTANCE TO CLEAR A 50-FOOT OBSTACLE BY 1%.

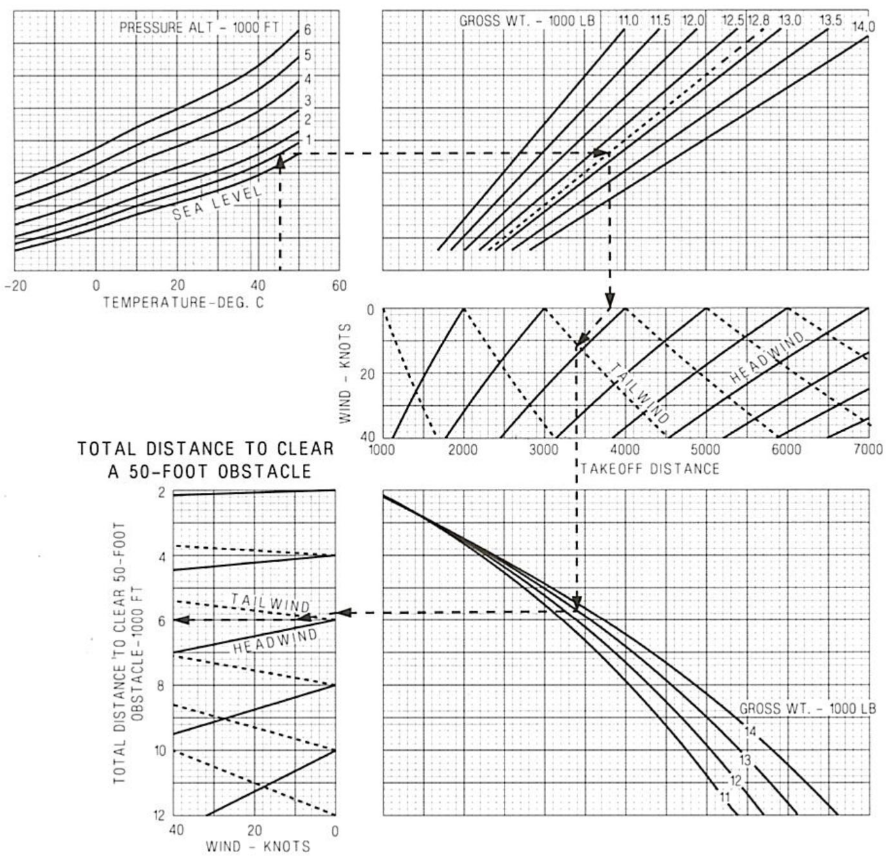

Figure B2-3

Change 6 **B2-7**

Figure K1 Takeoff Distance for T-38C Aircraft

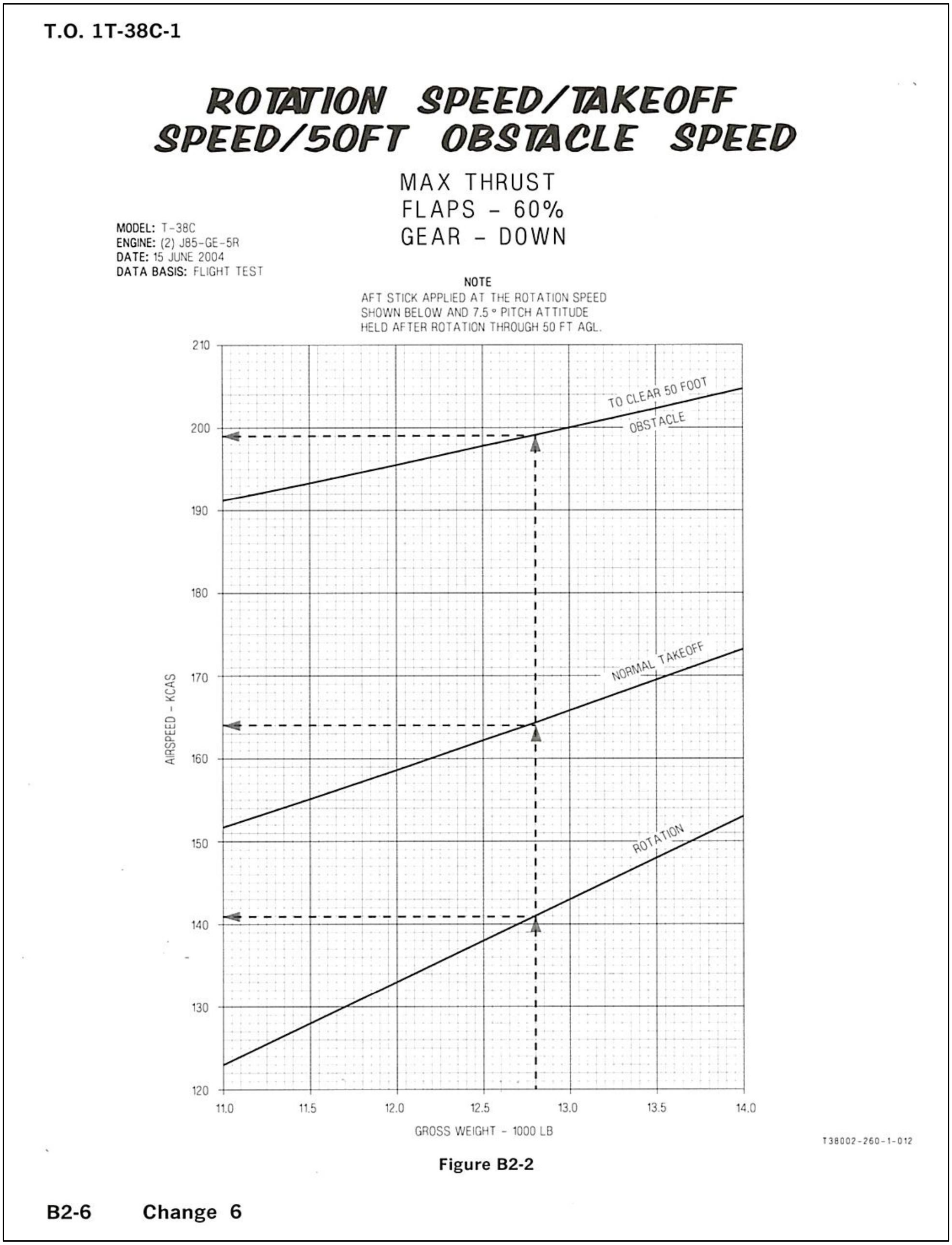

Figure K2 Rotation Speed/Takeoff Speed/50 feet Obstacle Speed

This page was intentionally left blank.

APPENDIX L - LIST OF ABBREVIATIONS, ACRONYMS, AND SYMBOLS

Abbreviation	Definition
AEA	Aerial Experiment Association
AFB	Air Force Base
AFFTC	Air Force Flight Test Center
AFI	Air Force Instruction
AFTC	Air Force Test Center
AFTO	Air Force technical order
AGARD	Advisory Group for Aeronautical Research and Development
AGL	above ground level
AIAA	American Institute of Aeronautics and Astronautics
AKA	also known as
a.m.	midnight to noon
BINAC	Binary Automatic Computer
C	Celsius
Cal Tech	California Institute of Technology
CFR	Code of Federal Regulations
D.C.	District of Columbia
DC	Douglas Commercial
DDMMMYYYY	date/month/year
DDD MM SS	degrees/minutes/seconds
deg	degree
DoD	Department of Defense
DTIC	Defense Technical Information Center
E	east
e.g.	Exempli gratia (for example)
EAR	Export Arms Regulation
EGI	embedded GPS/INS
EGM	Earth Gravity Model
ENIAC	Electronic Numerical Integrator and Computer
EPR	engine pressure ratio
ERCO	Engineering and Research Corporation
EU	engineering units

etc.	et cetera
F	force
Abbreviation	Definition
F	Fahrenheit
FAA	Federal Aviation Administration
FADEC	full-authority, digital engine controls
FAR	Federal Air Regulations
FLIP	flight information publication
FLTS	Flight Test Squadron
FM	frequency modulation
FTC	Flight Test Center
ft	international foot or feet, length exactly equal to 0.3048 of a meter
ft-lb	foot-pounds
$ft/(sec)^2$	feet per second squared
g	reference value for the acceleration due to gravity, equal to 9.80665 meter per second squared
GPS	global positioning system
Hg	mercury
HAGL	height above ground level
HH:MM	hours:minutes
HUD	head-up display
IATA	International Air Transport Association
IAW	in accordance with
IBM	International Business Machines
ICAO	International Civil Aviation Organization
ICBM	intercontinental ballistic missile
IFTD	inflight thrust deck
in	inch, length of exactly 0.025 400 of a meter
in Hg	inch of mercury
Inc.	incorporated
INS	inertial navigation system
JATO	jet-assisted takeoff (also known as RATO)
Joint-STARS	Joint Surveillance Target Attack Radar System
JP	jet propellant
JRB	Joint Reserve Base

KCAS	knots calibrated airspeed
lb	pound
Abbreviation	Definition
LINK	a major subroutine in the Uniform Flight Test Analysis System (UFTAS)
M&S	modeling and simulation
MAX	maximum
McAir	McDonnell Aircraft Company
MCAS	Marine Corps Air Station
MIN	minimum
MIT	Massachusetts Institute of Technology
MITO	minimum-interval takeoff
mph	statute miles per hour
N	north
N/A	not applicable, or not assigned, or not available
NACA	National Advisory Committee for Aeronautics
NAS	Naval Air Station
NASA	National Aeronautics and Space Administration
NATO	North Atlantic Treaty Organization
PC	personal computer
pct	percent
p.m.	after midday
PMP	propulsion modernization program
RATO	rocket-assisted takeoff, also known at JATO
S	south
sec	second
SETP	Society of Experimental Test Pilots
SFTE	Society of Flight Test Engineers
SRATIO	ground effect interpolation factor
St.	Saint
T	ambient air temperature
TIH	technical information handbook
TLR	technical letter report
TM	technical memo
TN	technical note

T.O.	technical order
TR	technical report
<u>Abbreviation</u>	<u>Definition</u>
TOLAND	takeoff and landing
TW	Test Wing
UFTAS	Uniform Flight Test Analysis System
U.S.	United States
USA	United States of America
USAF	United States Air Force
U.S.C.	United States Code
USFS	United States Forest Service
UNIVAC	Universal Automatic Computer
V	true airspeed
W	west
WGS	World Geodetic System
WOW	weight-on-wheels, weight-off-wheels
x	variable
δ	mean thrust
σ	ambient air density ratio

APPENDIX M - DISTRIBUTION LIST

Onsite	Number of Copies E-mail	Digital	Paper
Edwards AFB Technical Research Library Attn: Darrell Shiplett 307 E Popson Ave Edwards AFB CA 93524	0	0	2
AFTC/HO Email: jeannine.geiger@us.af.mil 305 E Popson Ave Edwards AFB CA 93524	1	0	0
775 TS/CL E-mail: daniel.stevenson.5@us.af.mil 307 E Popson Ave Edwards AFB CA 93524	1	0	0
773 TS/CL E-mail: john.kok@us.af.mil 307 E Popson Ave Edwards AFB CA 93524	1	0	0
773 TS/ENFB E-mail: reagan.woolf@us.af.mil 307 E Popson Ave Edwards AFB CA 93524-6630	0	50	50
412 TENG/CL E-mail: charles.staley.1@us.af.mil 307 E Popson Ave Edwards AFB CA 93524	1	0	0
412 OG/DT E-mail: christopher.klug@us.af.mil 195 E Popson Ave Edwards AFB CA 93524	1	0	0
412 EWG/DD E-mail: mark.crawford@us.af.mil 20 Hoglan Ave Edwards AFB CA 93524	1	0	0
412 TENG/DD E-mail: gary.wagner@us.af.mil 307 E Popson Ave Edwards AFB CA 93524	1	0	0

Onsite (Concluded)	Number of Copies E-mail	 Digital	 Paper
412 TW/CT E-mail:412 TW Distribution Box 195 E Popson Ave Edwards AFB CA 93524	1	0	0
Offsite			
Defense Technical Information Center Submit per DTIC procedures Attn: DTIC-O 8725 John J. Kingman Rd, Ste 0944 Ft Belvoir VA 22060 Email: Jackie.L.Rike.civ@dtic.mil	1	0	0
Total	9	50	52